The impact of centrally and systemically administered TNFα on CNS inflammation and function

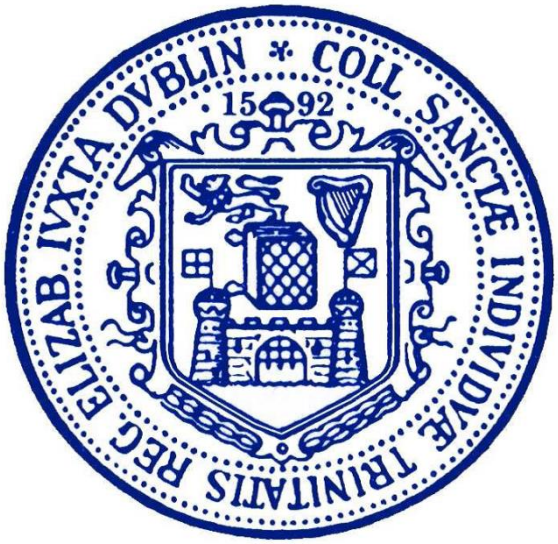

by

Edel Hennessy

Thesis submitted for the degree of Doctor of Philosophy at the University of Dublin, Trinity College

Submitted April 2015

School of Biochemistry and Immunology and Trinity College Institute of Neuroscience, Trinity College Dublin, Dublin 2

I Declaration

I declare that this thesis is entirely my own work, except elements of figures (3.15-3.22, 4.12-4.17 and 5.8-5.13) where labelling was performed by students under my tutelage and supervision, and that it has not been previously submitted as an exercise for a degree at this or any other University. I give my permission to the library to lend or copy this thesis.

_____

Edel Hennessy

II Summary

Inflammation has long been recognised as a driver of dementia. However, the pathways by which inflammation alters neuronal function and causes neuronal death remain under investigation. Microglia are primed by chronic neurodegeneration such that toll-like receptor agonists, such as lipopolysaccharide (LPS), drive exaggerated pro-inflammatory cytokine responses on this background. The data presented in this thesis show that endogenous cytokines can also activate primed microglia. Furthermore this thesis describes the novel finding of primed astrocytes in the ME7 prion disease model of neurodegeneration and the APP/PS1 amyloid aggregation model. The astrocyte population showed exaggerated production of the chemokines CXCL1 and CCL2 in response to exogenous LPS or endogenous IL-1β or TNFα challenges in ME7 animals compared to NBH animals. In the ME7 model we examined downstream effects of exaggerated chemokine expression, which resulted in markedly increased neutrophil, T-cell and monocyte infiltration and astrocyte proliferation in the diseased brain. These data have significant implications for acute sterile inflammatory insults such as stroke and traumatic brain injury occurring on a background of aging or neurodegeneration.

Systemic infection has been shown to exacerbate progression of neurodegeneration in AD cohorts, this was found to be significantly correlated with levels of systemic circulating TNFα. In mice a single acute dose of systemic TNFα (250μg/kg) exacerbated features of sickness behaviour; including core body temperature changes, open field activity and body weight, in ME7 compared to NBH. A lower dose (50μg/kg) can induce a transient cognitive deficit in a hippocampal dependent task in ME7 animals but not in NBH animals. However these changes are independent of any changes in features of pathology examined. While there was no TNFα effect we discovered a novel feature of pathology; a robust aggregation of APP varicosities in the posterior (PO) and Ventroposteromedial (VPM) nuclei of the thalamus, overlapping with significant neuronal loss in the PO and significant synaptic loss in the VPM. Given systemic TNFα administration did not significantly alter ME7 pathology we utilised systemic administration of XPRO1595 a dominant negative TNFα inhibitor prior

to systemic administration of LPS. This showed that the exacerbation of ME7 pathology by LPS was independent of TNFα actions. The timepoint used in the ME7 model is one with severe and widespread pathology, the mild inflammation caused by systemic TNFα in comparison to systemic LPS was not sufficient to alter this severe pathology. It would be of great interest to examine the effects of TNFα on a less severe model of pathology.

Elevated systemic TNFα has been shown to be associated with significantly more rapid cognitive decline across 6 months in an AD patient cohort. It is not clear whether this might constitute a causal relationship. A repeated systemic TNFα challenge model was used to examine consequential behaviour and pathology in female APP/PS1 mice. This showed that repeated TNFα did not significantly alter learning of the hippocampal dependent Y maze. Repeated systemic TNFα induced significant deficits in rearing behaviour in W+TNFα but not APP/PS1+TNFα animals. Progressive weight loss was observed in the WT mice but this was not apparent in the APP/PS1 mice. A significant decrease was observed in the hippocampal Amyloid β burden with a concurrent increase in aggregations of APP in both the hippocampus and thalamus. Microglia were increased in APP/PS1, however there was no alteration following repeated systemic TNFα. There were elevated numbers of T cells in the APP/PS1 animals. Following repeated TNFα there was a further increase in the T cells in APP/PS1s this did not occur in the WT+TNFα group. Repeated TNFα in APP/PS1 animals also diminished the levels of ongoing cell proliferation, a similar decrease did not occur in the WT+TNFα group. These results indicate that repeated systemic TNFα administration has differential effects in aged APP/PS1 and WT animals, suggesting important implications for cognitive and functional decline with systemic inflammation.

The data presented here significantly contributes to the study of inflammatory processes in neurodegeneration. The importance of chronic sterile inflammatory co-morbidities is highlighted by this data and perhaps lends evidence to an alternative hypothesis of neurodegeneration, rather than the amyloid beta focused hypothesis that remains prevalent in the field.

III Table of contents

IV Acknowledgements

First of all thank you to my supervisor Colm Cunningham for being incredibly kind to me while I was so ill for so long! Your endless enthusiasm and passion for science is a source of great inspiration to me and I hope that you continue to enthuse people to do great science for years to come.

No thanks to my gallbladder, lungs and immune system (oh, the irony). But to everyone who was there for me when I was sick, thank you! Shane, you are the best possible flatmate I could have hoped for through this entire process, great for a moan, a hug or bringing things to me in the hospital!

To the ladies of the Cunningham lab, Eadaoin, Carol and Niamh, I most definitely could not have done this without you guys. Eadaoin, as well as being a great friend you were a constant source of great advice and support, best of luck with your new endeavours. Carol, thank you for all of your time, always there for any help I needed and always a good friend. Niamh, I love our conversations, science and otherwise, and I hope that we never stop having them! Donal, Rob and Marc, working with you guys was a pleasure! To all of the students that I have worked with, I always enjoyed getting to know you however special thanks go to Caoimhe, Renata, Michael and last but definitely by no means least the hilarious Conor!

To all of my Carlow crew, Amy, Cait, David, Eamonn, Lisa and Sinead, well we have certainly been through it these last few years but I'm so glad we're all still friends, no matter what continent we're on. Roisin you deserve a medal for how supportive you have been over the last few months, thank you so much! Also to Phil, you have been absolutely brilliant to have in Dublin these last few years, here's to another fifteen years of talking crap and trying to figure out how to save the world!

Finally I want to thank my family, my brothers Padraic and Mark, and especially mam and dad for their constant, unwavering emotional support and interest throughout my entire education. I don't think I would have come this far without you both behind me, you are my motivation. This thesis is dedicated to you.

V List of Abbreviations

6-OHDA	6 Hydroxydopamine
Aβ	Amyloid beta
ABC	Avidin biotin complex
ACTH	Adrenocorticotropin hormone
AD	Alzheimer's disease
ADAS-COG	Alzheimer's Disease Assessment Scale-cognitive subscale
AICD	App intracellular domain
ALS	Amyotrophic lateral sclerosis
AMPAR	α-amino-3-hydroxy-5-methyl-4-isoxazolepropionic acid receptor
ANOVA	Analysis of variance
APOE	Apolipoprotein E
APP	Amyloid precursor protein
Aβ	Amyloid beta
BACE1	Beta-site amyloid precursor protein cleaving enzyme 1
Bad	Bcl-2-associated death promoter
Bak	Bcl-2 homologous antagonist/killer
Bax	Bcl-2–associated X protein
BBB	Blood brain barrier
Bmf	Bcl-2-modifying factor
C57BL/6	C57 black 6
CA1	Cornu ammonis area 1
CA3	Cornu ammonis area 3
CatD	Cathepsin D
CCL2	Macrophage chemoattractant protein (MCP-1)
CD	Cluster of differentiation
CDK5	Cell division protein kinase 5
CFAS	Cognitive function and aging studies
CFC	Contextual fear conditioning
CNS	Central nervous system
COX	Cycloxygenase
CRF	Corticotrophin releasing factor
CSF	Cerebrospinal fluid
CTF	C terminal fragment
CXL1	Neutrophil chemoattractant chemokine (CINC1, GROα, KC)
CXCL10	Chemokine (IP-10)
DAB	3,3'-Diaminobenzidine
DAMP	Damage associated molecular pattern
dH_2O	Distilled water

DNA	Deoxyribonucleic acid
dNTP	Deoxyribonucleotide triphosphate
E-coli	Escherichia coliform
ELISA	Enzyme linked immosorbant assay
ERK	Extracellular signal-regulated kinases
FAM	6-carboxyfluorescein
FRET	Fluorescence resonance energy transfer
GABA	Gamma amino butyric acid
GAPDH	Glyceraldehyde-3-phosphate dehydrogenase
GFAP	Glial fibrillary associated protein
GSK3β	Glycogen synthase kinase 3 beta
IAP	Inhibitor of apoptosis
IBA-1	ionized calcium-binding adapter molecule 1
IC	Intracerebral
ICAM	Intercellular adhesion molecule
ICV	Intracerebroventrticular
IFN	Interferon
IHC	Intrahippocampal
IL-10	Interleukin ten
IL-1Ra	Interleukin one receptor antagonist
IL-1β	Interleukin one beta
IL-6	Interleukin six
iNOS	Inducible nitrogen oxide synthase
IP	Intraperitoneal
IP3	Inositol triphosphate
IRAK	Interleukin one receptor associated kinase
JNK	c-Jun N-terminal kinases
LD	Lateral dorsal nucleus
LP	Lateral posterial nucleus
LPS	Lipopolysaccharide
LTP	Long term potentiation
MAP	Microtubule associated protein
MCAO	Middle cerebral artery occlusion
MCI	Mild cognitive impairment
MCP-1	Macrophage chemoattractant protein one
ME7	ME7 prion disease
MemTNF	Membrane bound Tumour necrosis factor
MHC	Major histocompatibility complex
MMP9	Matrix metalloproteinase 9
MPO	Myeloperoxidase
MPTP	Mitochondrial permeability transition pore

MRC	Medical research council
MS	Multiple sclerosis
NALP3	NACHT, LRR and PYD domains-containing protein three
NBH	Normal brain homogenate
NeuN	Neuronal nucleus
NFH	Neuronal filament heavy chain
NFT	Neurofibrillary tangle
NF-κb	Nuclear factor kappa b
NIH	National institutes of health
NMDAR	N-methyl-D-aspartate receptor
NO	Nitric oxide
NSAID	Non steroidal anti-inflammatory drug
PAMP	Pathogen associated molecular pattern
PBS	Phosphate buffered saline
PD	Parkinson's disease
PO	posterior complex
Poly I:C	Polyinosinic:polycytidylic acid
PPARγ	Peroxisome proliferator-activated receptor gamma
PrP^{SC}	Prion protein scrapie
PTX3	Pentraxin three
PUMA	p53 upregulated modulator of apoptosis
RAGE	Receptor for advance glycation end products
RANK	Receptor activator Nuclear factor κ B
RANTES	Regulated on Activation, Normal T cell Expressed and Secreted
RIPK1/3	Receptor-interacting protein kinases
RNA	Ribonucleic acid
ROS	Reactive oxygen species
RT	Reticular nucleus
RT	Reverse transcriptase
Rt-PCR	Real time polymerase chain reaction
SEM	Standard error of the mean
SIE	Systemic inflammatory event
SMAC	Second mitochondria derived activator of caspases
SNpc	Substantia nigra pars compacta
SOD1	Super oxide dismutase 1
SolTNF	Soulble tumour necrosis factor
STEAP4	six transmembrane epithelial antigen of prostate
TACE	Tumour necrosis factor alpha-converting enzyme
TAMRA	Tetramethylrhodamine
TB	Tuberculosis
TBI	Traumatic Brain Injury

TEM	Transendothelial migration
TGF-β	Transforming growth factor beta
Tg	Transgenic
TIMP1	Tissue inhibitor of metalloprteinases 1
TLR	Toll like receptor
TNFR	Tumour necrosis factor receptor
TNFα	Tumour necrosis factor alpha
TRAF6	TNF receptor associated factor six
TUNEL	Terminal deoxynucleotidyl transferase dUTP nick end labeling
uPAR	Urokinase-type plasminogen activator receptor
VCAM	Vascular adhesion molecule
VM	Ventral medial nucleus
VPL	Ventral posterolateral
VPM	Ventral posteromedial
WHO	World health organisation
WT	Wild type

Vi List of figures and tables

Chapter 1

Introduction

1.1 - Dementia

The National Institute on Aging of John Hopkins University recently charged a working group with redefining the 1984 definitions of dementia. What this group defined as the core characteristics of dementia covers all types of dementia and all severities. These include an inability to function in everyday life and a decline from previous levels of functioning and performance (not being explained by delirium or major psychiatric illness). These cognitive and behavioural impairments will involve an impaired ability to acquire and remember new information, impaired reasoning and handling of complex tasks, decreased visuospatial abilities, limited language functions and altered personality and behaviours (McKhann et al., 2011). Alzheimer's disease (AD) is thought to account for 50% of all demented patients. To ascertain that a patient is suffering from Alzheimer's disease they say that the patient must meet these additional symptoms; gradual onset, history of worsening cognition and amnestic, visuospatial or language presentation, or executive dysfunction.

In Ireland dementia is a problem that is coming to the fore with increased lifespans and thus increasing numbers of cognitively impaired elderly patients entering our health care system. Dementia affects 1 in 20 people over 65 and 1 in 4 over 80 in Ireland; this ranks dementia as the 4th leading cause of death in people over 65. In 2006 the cost of dementia was estimated to be €400m with cases expected to triple from 2002 to 2036. Globally this issue is no different to Ireland, in the USA it is thought that 5.4 million people are suffering from Alzheimer's disease and the annual cost is $183 billion (Moschetti et al., 2012). The American prevalence of AD is expected to triple and the costs to total more than $1.1 trillion by 2050 (Thies and Bleiler, 2011).

While Alzheimer's disease is often used as a synonym for dementia, dementia is not Alzheimer's disease alone. Dementia accounts for more than the specific pathologies attributed to Alzheimer's disease. Dementia is contributed to by a spectrum of pathologies. A recent large epidemiological study CFAS, run by the MRC in the UK has taken stock of some of the main "attributable factors" to dementia at time of death. What this study showed was that the amyloid beta and tau lesions primarily

associated with Alzheimer's disease occur in similar proportions of the demented and the non-demented oldest old population. It showed that age determined the strength of the connection between Aβ and tau pathology with dementia. There was a stronger connection between the Aβ and tau pathology with dementia at younger ages. In older individuals that had the same pathology there was a much lower association with dementia. This would indicate that the Aβ and Tau pathologies affect different individuals with differing outcomes. Cortical atrophy, the third classical hallmark of dementia pathology, is an indicator of synaptic and neuronal loss. Atrophy was a marker of degeneration that remained a significant indicator of dementia irrelevant of age (Wharton et al., 2011). This is an important factor in aiding future research in dementia fields. The presence of Aβ and Tau pathologies in non-demented individuals makes neuronal loss a more relevant pathological marker of dementia. This is not something that is being taken into consideration with the current animal models of Alzheimer's disease. Transgenic mice designed to alter the APP or Tau processing pathways produce plentiful neuritic plaques or neurofibrillary tangles however minimal neuronal degeneration occurs. It has now become clear that there is more to Alzheimer's disease than amyloid beta and tau.

Over the past decade, genome wide association studies (GWAS) have revealed a large number of common variants that are associated with a small increased risk of Alzheimer's disease, these include a number of genes involved in innate immunity such as CLU, CR1 and PICALM (Jun et al., 2010). In addition there are loci of much more significant risk such as TREM2, a macrophage gene, involved in phagocytosis and suppression of pro-inflammatory phenotype in microglia (Neumann and Daly, 2013). These AD loci all suggest altered macrophage phagocytic function. In addition to this, a genome wide scan of affected versus non-affected siblings with late onset AD showed an associated haplotype of TNFα which results in higher levels of TNFα (Collins et al., 2000). These results indicate that the innate immune system is important in progression of cognitive decline.

1.2 - The immune system

There are two branches of the immune system, the innate and the adaptive. The innate immune system is the body's first line of defence; it manifests a non-specific defence to pathogens but confers no long lasting immunity. If this defence is insufficient the innate immune system can recruit the adaptive system which can perform more specific and targeted defences of the body, these two systems while technically separate are highly interdependent. The adaptive immune system also confers immunity against pathogens. I will predominantly focus upon the innate immune system here.

Cells of the immune system (commonly known as leukocytes) derive from pluripotent hematopoietic stem cells (see Figure 1.1). Cells of the adaptive system are derived from the lymphoid lineage; this includes B, T and NK cells, while cells of the innate system are derived from the myeloid lineage. Some of the cells of the myeloid lineage are phagocytic in nature and the three main types of phagocytes are; dendritic cells, granulocytes (neutrophils, eosinophils and basophils) and monocytes/macrophages. I will focus my attention now upon neutrophils and macrophages.

Granulocytes are so called due to numerous densely stained granules in their cytoplasm. Neutrophils are the most numerous cells in innate immune system and are also known as polymorphonuclear leukocytes (PMNs) due to their multi-lobed nuclear bodies. They are short lived cells that can phagocytose a wide variety of microorganisms efficiently and destroy them in intracellular vesicles using anti-microbial enzymes stored in their granules.

The other main phagocytic cell is called a monocyte while circulating in the blood stream and as a macrophage when it migrates into tissue, differentiates and becomes resident there. Macrophages are long lived cells and as they are resident in tissue rather than circulating like neutrophils they are often the first immune cells to come in contact with a pathogen. They perform many duties such as orchestrating the immune response, recruiting other immune cells, aiding the adaptive response and scavenging cellular debris.

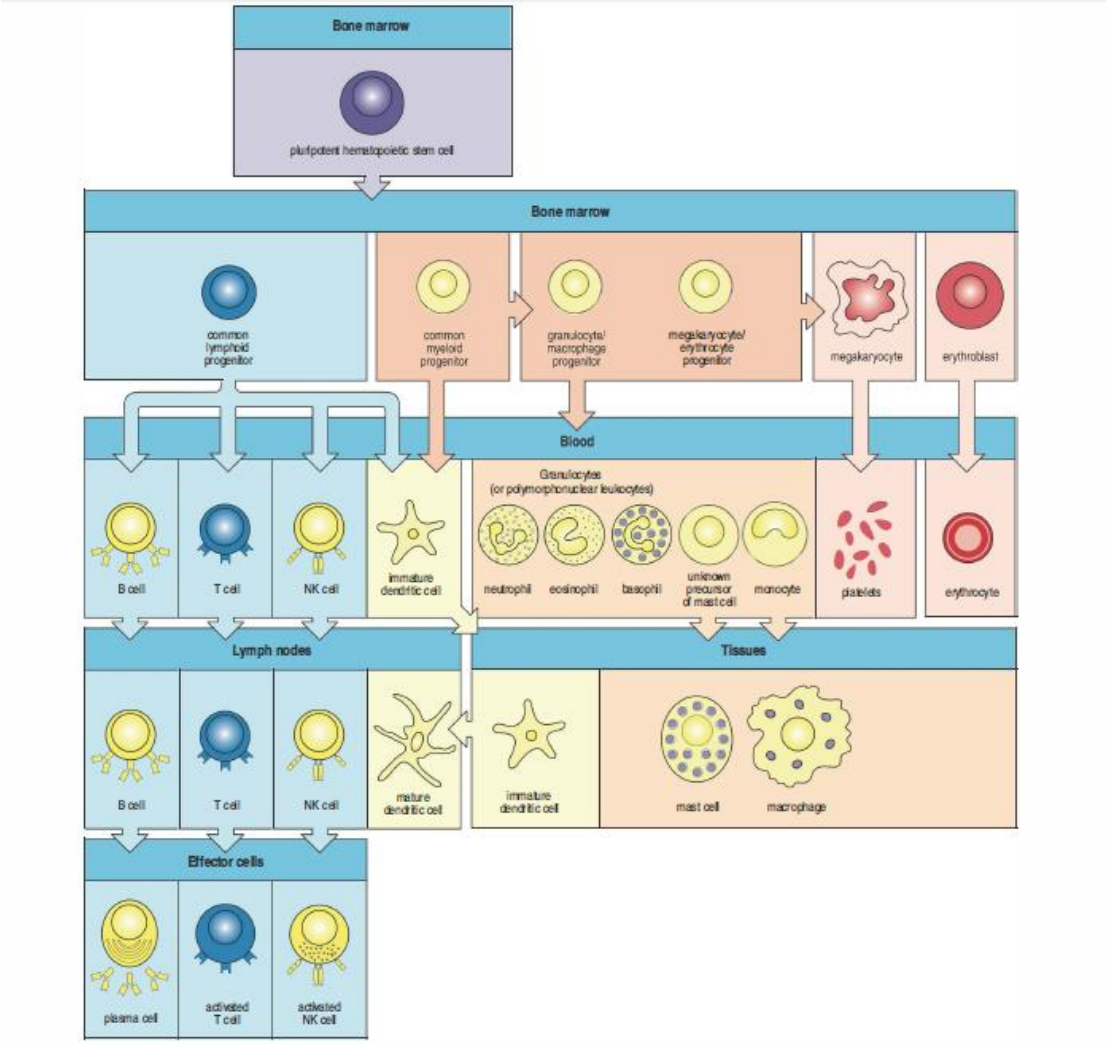

Figure 1.1 Immune cell lineages

Both lymphoid and myeloid cell lines originate from the same common progenitor, a pluripotent haematopoietic stem cell (Murphy, 2011).

Inflammation was described by Celsus in AD300 as heat, pain, redness and swelling. These 4 symptoms are generally beneficial to the defence against a micro-organism and they are mediated by proteins released by affected immune cells. One key class of these proteins are known as cytokines. When a tissue resident macrophage encounters a Pathogen Associated Molecular Pattern (PAMP) such as the bacterial Lipopolysaccharide (LPS) or viral nucleic acid *via* its Pattern Recognition Receptors (PRRs) it releases cytokines. Some of the basic functions of cytokines include induction of increased blood flow, vasodilation and altering the permeability of the endothelium. These changes allow recruitment of other immune cells by chemokines,

chemoattractant proteins which can also be produced by activated tissue resident immune cells.

The main pro-inflammatory cytokines include TNFα, IL-1β and IL-6. When these cytokines are released systemically in response to an infection they have wide ranging and diverse effects (see figure 1.2). To begin with they activate the acute phase response in the liver, recruit neutrophils from the bone marrow, increase body temperature and can initiate the adaptive response via dendritic cells. I will now examine TNFα and IL-1β in more detail.

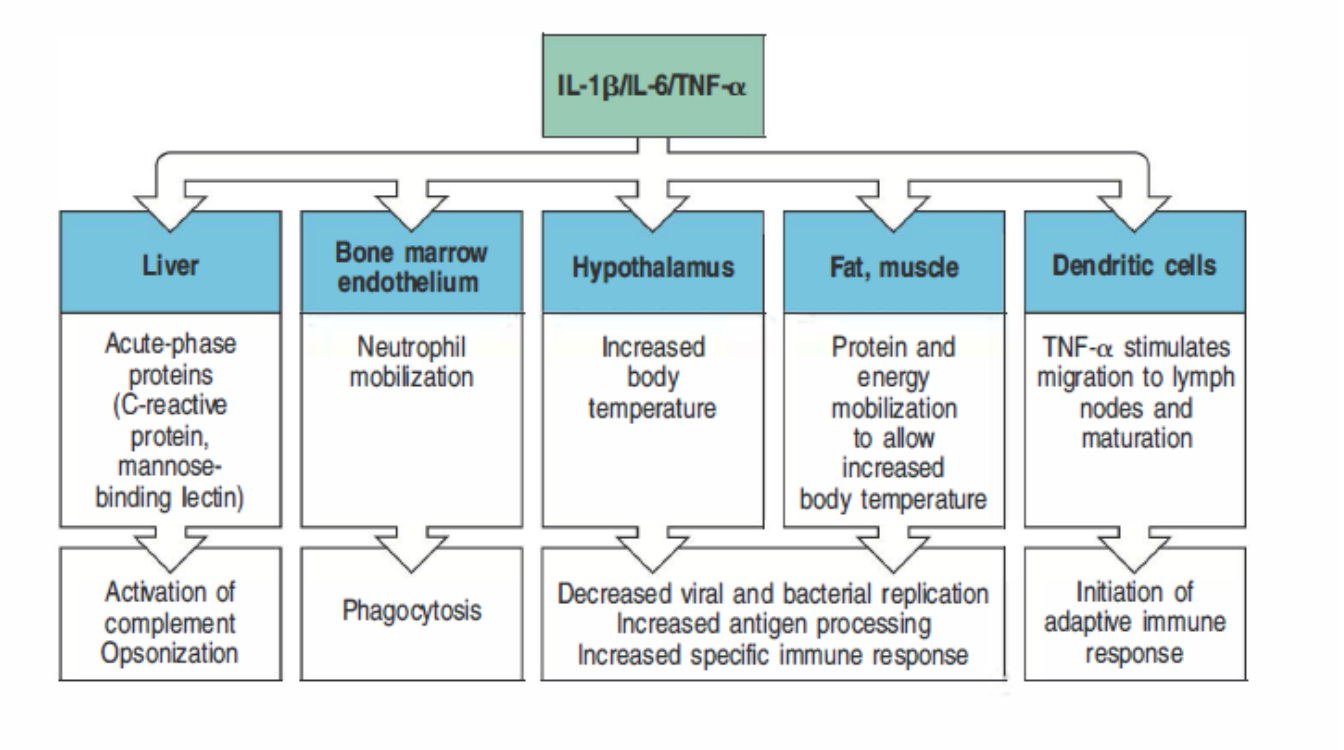

Figure 1.2 Cytokine effects

Examples of the diverse effects of systemic elevation of the pro-inflammatory cytokines IL-1β, IL-6 and TNFα on various tissue types (Murphy, 2011).

1.2.1 - TNFα

Tumour Necrosis Factor Alpha (TNFα) is produced in response to PAMPs or DAMPs. TNFα exists as both soluble and membrane bound versions. The membrane bound

form is a type II membrane protein which self assembles into trimers. The soluble form is a trimer that derives from the membrane form via TACE proteolysis (Rauert et al., 2010). Soluble TNF is thought to mediate inflammatory diseases while membrane TNF mediates host immunity to infectious diseases (Garcia et al., 2011). Two TNFα receptors exist, TNFR1 (p55) and TNFR2 (p75) which are type I transmembrane receptors. TNFR1 is constitutively found on most cell types while TNFR2 is usually found on immune and endothelial cells. The structure of the receptors determines their function. TNFR1 contains a cytoplasmic death domain where TNFR2 does not; this means that TNFR1 can mediate both cellular survival and cell death while TNFR2 can only mediate cell survival signalling, see figure 1.3 (Gupta, 2002). The different forms of TNF differentially activate the two TNF receptors. Membrane bound TNF (memTNF) can strongly activate both TNF receptors. Soluble TNF (solTNF) acts robustly on only TNFR1 (Hehlgans and Mannel, 2002).

Studies of the bacterial mimetic lipopolysaccharide (LPS), indicates that systemically TNFα is the first cytokine synthesised. It then goes on to induce IL-1β which can in turn induce IL-6 production (Dantzer et al., 1998). These cytokines alter behaviour to fight invading pathogens, inducing a febrile response, hypophagia, anhedonia and insomnia (Wang et al., 1997; Dantzer, 2001; Palin et al., 2009). TNFα has been found to directly cause sickness behaviours such as decreased social exploration or activity (i.c.v. 50ng/mouse) (Palin et al., 2009). TNFα also suppresses feeding on systemic administration (Dantzer, 2001). TNFα induces a short lived decrease in murine core body temperature followed by a small increase (Wang et al., 1997). Anti-TNFα completely abolishes the cryogenic phase, initiating the pyrogenic phase at an earlier time-point (Kozak et al., 1995). TNFα is implicated in the hypophagic effect (Porter et al., 1998).

TNF is integral to the innate immune response in many ways and it has been shown that deficiencies in TNFα signalling lead to impairments in host defence (Hehlgans and Pfeffer, 2005). TNFα has been shown to orchestrate the early induction of chemokines and leukocyte recruitment; it has also been shown to be responsible for organising aggregation of leukocytes into a functioning granuloma to fight infection (Roach et al., 2002). Mice lacking TNFR1 signalling are more susceptible to *Listeria monocytogenes* infection. There are higher mortality levels in TNFR1$^{-/-}$ mice challenged with *Listeria monocytogenes* and 1000 fold greater bacterial titres in TNFR1$^{-/-}$ mice 6 days post infection versus WT animals (Pfeffer et al., 1993). A later study showed that it was the lack of TNFR1 on cells of haematopoietic origin that induced the increased susceptibility to *Listeria monocytogenes* infection. It was shown that phagocytes lacking the TNFR1 were incapable of confining and eradicating

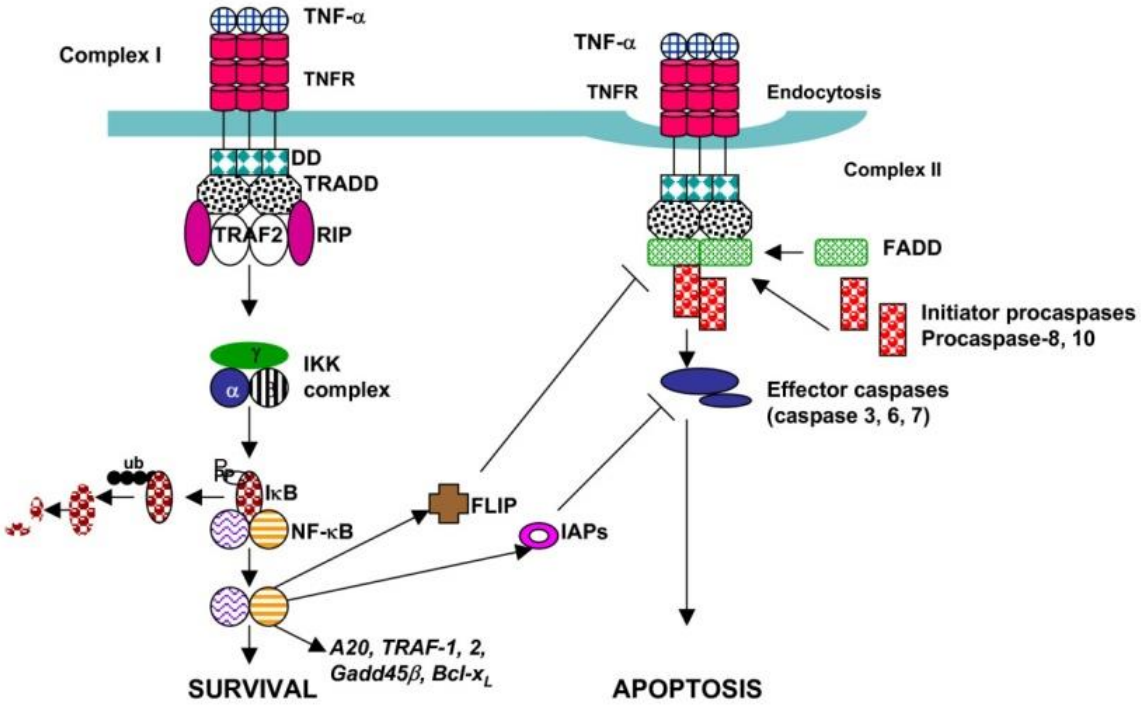

Figure 1.3 TNFα Receptor signalling

This figure shows the diverging pathways of TNFR1 towards apoptosis, and TNFR2 towards survival (Gupta et al., 2006).

Listeria monocytogenes inside of phagolysosomes (Endres et al., 1997). Wild type mice can restrict and control the growth of Mycobacterium tuberculosis within

around 14 days thus surviving infection, however TNFR1-/- mice could not control the spread of this bacterium and succumbed to infection around day 30 (Ehlers et al., 2003). TNFRI$^{-/-}$ mice also show increased susceptibility to intracellular parasite infections such as *Leishmania major* or *Trypanosoma cruzi*, TNFR1$^{-/-}$ mice showed higher parasitaemia and mortality than control mice (Castanos-Velez et al., 1998; Nashleanas et al., 1998).

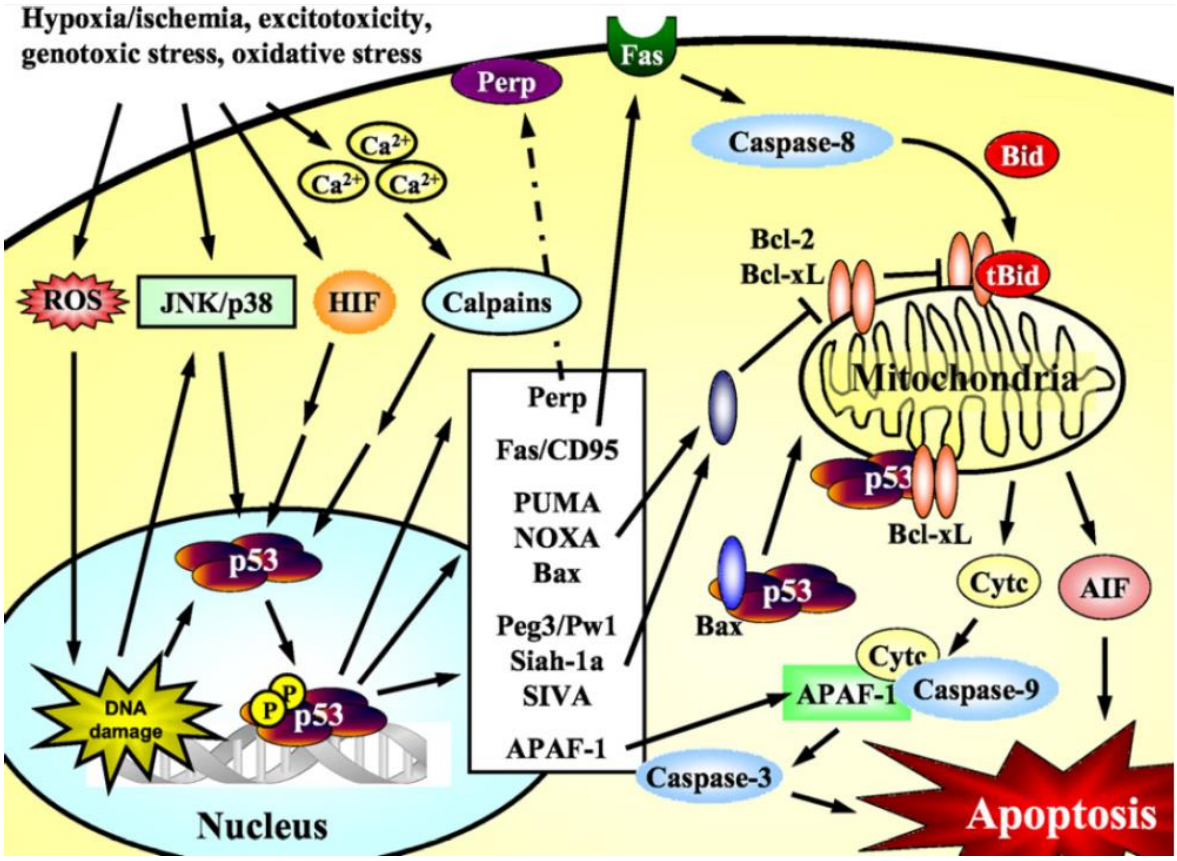

Figure 1.4 Opening of the Mitochondrial Permeability Transition Pore
Apoptosis can be initiated by many different factors however they all converge to open the Mitochondrial Permeability Transition Pore, which initiates the caspase cascade (Culmsee and Mattson, 2005).

An important function of TNFα is regulating the balance between pro and anti-apoptotic signals. TNFR2 signalling through NF-κB can induce anti-apoptotic proteins of the Bcl-2 family such as Bcl-2 and Bcl-Xl (Patel and Brewer, 2008). TNFR1 signalling induces pro-apoptotic signalling through a variety of pathways. The transcription factor p38-JNK phosphorylates the pro-apoptotic Bcl-2 family proteins

Bim and Bmf which go on to activate Bad, Bax and Bak (Varfolomeev and Ashkenazi, 2004; Czabotar et al., 2009). Receptor internalisation on binding TNF causes formation of a complex which activates caspase 8/10. Caspase 8/10 activates Bid, this displaces the anti-apoptotic Bcl-2 and Bcl-Xl and allows Bax and Bak to form a Mitochondrial Permeability Transition Pore (MPTP) (Yin, 2000; Chen et al., 2007b). The MPTP allows release of second mitochondria-derived activator of caspases (SMAC) and Cytochrome C (Crompton, 2000). SMAC removes the cIAP inhibition of Caspases 3 and 7 which allows cytochrome C and APAF 1 to activate these effector caspases, initiating apoptosis (Gupta, 2002). See figure 1.4 for a schematic depiction of some of these pathways. TNF may also activate the transcription factor p53 (Wu and Lozano, 1994; Piguet et al., 1998). This initiates production of more Bcl-2 pro-apoptotic proteins such as PUMA, NOXA and Bax all directly involved in the formation of the MPTP. p53 also activates APAF-1 a necessary co-factor of Cytochrome C in the activation of effector caspases. p53 can also inhibit NF-κb production of Bcl-2 and Bcl-Xl tipping the balance towards a pro-apoptotic state (Culmsee and Mattson, 2005). Changes in transcription of genes such as PUMA, NOXA, Bax and Bak would indicate a pro-apoptotic profile induced by TNF signalling.

1.2.2 - IL-1β

Interleukin 1 Beta (IL-1β) is a potent pro-inflammatory cytokine and is believed to produce the majority of the effects of LPS (Wang et al., 1997; Swiergiel and Dunn, 1999). IL-1β transcription is known to be regulated by transcription factors induced by LPS, TNFα and IL-1β. LPS is known to increase IL-1β mRNA stability (Allan et al., 2005). IL-1α and IL-1Ra are also active members of the interleukin 1 family. IL-1Ra is the IL-1 receptor antagonist, a highly selective competitive antagonist for the IL-1 receptors (Gibson et al., 2004). IL-1α has a significant role in sterile inflammation, it is primarily intracellular and locally acting with a slower time frame than that of IL-1β which is more rapidly expressed and is extracellularly active (Chen et al., 2007a). IL-1β is produced in a Pro-IL-1 form which requires cleavage by an activated inflammasome (a multi protein scaffold). Toll Like Receptor (TLR) signalling activates the inflammasome allowing Pro-IL-1 to be cleaved by caspase 1 producing mature IL-1β. There are two IL-1β receptors, IL-1R1 and IL-1R2. IL-1R2 is thought to be a decoy

receptor for IL-1β. IL-1β elicits most of its effects through the IL-1R1 receptor. On binding IL-1R1, IL-1β induces recruitment of IRAK which binds TRAF6 causing activation of IKK. IKK activation induces phosphorylation of IκB releasing NFκB's p50/p65 heterodimer. NFκB signalling induces COX2, iNOS, IL-1, TNF and interferon signalling (O'Connor and Coogan, 1999).

IL-1β is reported as an endogenous pyrogen affecting the hypothalamic thermoregulatory centre. It induces infiltration of lymphocytes and directs macrophages and microglia by production of chemokines and adhesion molecules. It also induces astrogliosis and proliferation of microglia. IL-1β produces proinflammatory cytokines (IL-1β, TNFα, IL-6, IL-8), prostaglandins and Nitric Oxide. Intraperitoneal IL-1β has been found to induce typical aspects of sickness behaviour such as lethargy, hypophagia, adipsia and reduced social activity as well as activating the HPA axis (Dantzer et al., 1998; Dunn, 2006). IL-1β inhibited spatial learning in rats (Dantzer, 2001). As well as significantly altering murine core body temperature, decreasing it and then increasing it (Wang et al., 1997), IL-β is known to be associated with alternative avenues of cell death including pyroptosis (Sanz et al., 2014).

1.2.3 - Chemokines

Work from the Cunningham group shows that the cytokines IL-1β and TNFα can induce hepatic and hippocampal chemokines (CCL2 and CXCL1) when normal animals are challenged intraperitoneally (Skelly et al., 2013b). CCL2 can be produced by TNFα acting on a variety of different cell types, this can occur through the MAPK or NF-κB pathways (Chen et al., 2004; Ho et al., 2008). CCL2 has been shown to be responsible for recruitment of circulating monocytes to sites of infection or injury. CCL2 is also thought to polarise macrophages to become more phagocytic and pro-inflammatory to aid in recovery from injury (Moreno et al., 2014; Morganti et al., 2015). IL-1β has been shown to induce CXCL-1 via the NF-κB pathway in multiple cell types (Souza et al., 2005; Ribaux et al., 2007). CXCL1 has been shown to induce recruitment of neutrophils to the site of injury (Zhang et al., 2001). Cytokine production from tissue injury thus induces chemokines that regulate the recruitment and extravasation of leukocytes to the site of injury.

1.3 - Glia

For years the brain was considered an immune privileged organ. It was thought to be separate from the rest of the body in terms of how pathogens could affect it and also how the body's immune system could act within it. It is now clear that the brain is not entirely privileged, but has a tightly regulated immune response that differs from the periphery in some respects, most likely in order to limit damage to essential nervous tissue. Entry and exit of cells, such as peripheral immune cells, to the CNS is highly regulated by the blood brain barrier (BBB). Other tissue types mediate immunity by dendritic cells presenting antigens to B and T cells in the local lymph nodes. Until recently limited lymph drainage was known to occur via channels in the cribriform plate. These antigens are delivered to cervical lymph nodes but not by dendritic cells (Galea et al., 2007). In 2015 lymph drainage was discovered in the meninges of the mouse brain, indicating that there may be more significant lymph drainage from the brain than previously thought (Louveau et al., 2015). Once antigen specific T cells have been directed to the CNS by the cervical lymph nodes they must survive Fas ligand apoptotic signals and find their specific antigen presented by Major Histocompatibility Complex (MHC). MHC is only upregulated in the central nervous system (CNS) when inflammation has been established. It is however now clear that the innate immune system is mediated in the brain via its glial cell population. When we think of the brain we generally think of neurons, the cells responsible for decision making and control of the body. However glial cells vastly outnumber neurons in some regions of the brain. Glial cells are known to have a wide range of functions in the CNS. Astrocytes are the most abundant cells in the CNS and microglia constitute 15% of the cells in the CNS, I will describe the functions of these cells below. There are other less abundant but no less important glial cells; Oligodendrocytes provide the myelin sheath that insulates neuronal axons, Ependymal cells line the ventricles of the CNS producing cerebrospinal fluid (CSF) and forming the blood-CSF barrier, Radial glia are integral to CNS development functioning as neuronal progenitor cells and providing a scaffold along which neurons can migrate. Two cells types make up the BBB, endothelial cells with tighter gap junctions than the same cells in other tissue types comprise the walls of the blood vessels in the brain, Pericytes are

contractile cells that surround the endothelial cells of blood vessels and control blood flow and permeability of these vessels (see figure 1.5).

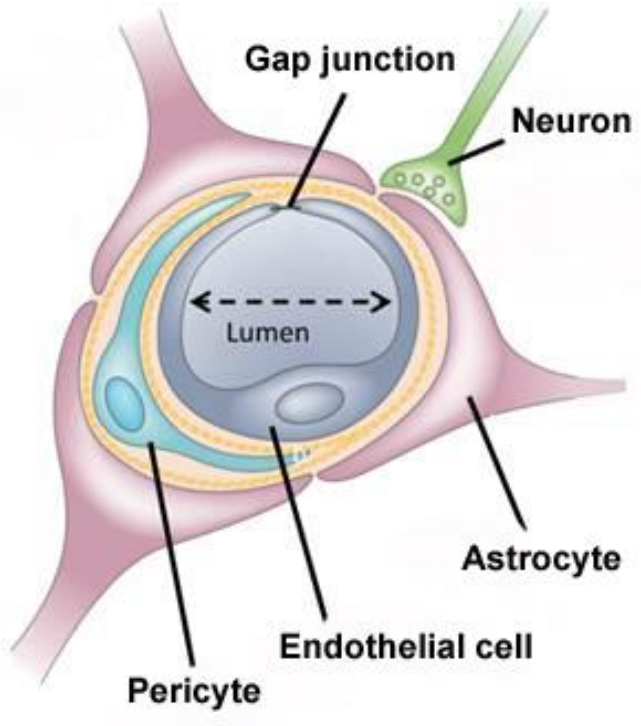

Figure 1.5 Structure of the Blood Brain Barrier

Cell types that maintain the structure of the blood brain barrier. Image taken from (Konofagou, 2012), modified.

1.3.1 - Astrocytes

Astrocytes are ubiquitous star shaped cells with many unbranched processes. They are extremely important, functioning mainly as a support system for neurons. However, much recent work has focussed on their role in the tri-partite synapse between the pre-synaptic neuron, post-synaptic neuron and astrocytic end feet. At the tri-partite synapse they provide metabolic support for neurons, regulate synaptic levels of glutamate, synthesise and release glutathione and regulate extracellular ion concentrations. Astrocytes can also release "Gliotransmitters" with a wide variety of functions, the most commonly known is calcium, however there are many such as glutamate, D-serine, ATP or BDNF (Parpura and Zorec, 2010). They also form and

maintain the structure of the BBB and perform many immune functions. Astrocytes can express cytokines such as TGF-β, IL-10, IL-1β and TNFα and chemokines such as CXCL-1, CCL2 and RANTES. Astrocytes are also found to express TLR2, TLR3, TLR4 and RAGE. These receptors allow them to react to a wide range of pathogens or damage associated molecular patterns (DAMPs) (Fuller et al., 2009).

1.3.2 - Microglia

Microglia are derived from the myeloid lineage, this differs from all other cells in the brain which derive from neuroectodermal cells. Myeloid lineage cells migrate into the developing brain at an early stage and this forms the basis of the microglial population. Microglia are responsible for maintaining immune homeostasis in the CNS, they continually survey and monitor their environment determining the best course of action from the signals they receive (Davalos et al., 2005; Nimmerjahn et al., 2005). When there is a disturbance in the environment microglia respond rapidly via a variety of mechanisms. They can express pro-inflammatory cytokines such as TNFα (to kill infected cells), IL-1β (to upregulate pro-inflammatory cell activity) and chemokines which can attract other immune cells. They can release a cytotoxic burst of H_2O_2 or NO to kill micro-organisms or they can phagocytose debris, foreign objects, micro-organisms and dying cells. Microglia can also act as antigen presenting cells (APCs) to activate cells of the adaptive immune system such as T cells. They are however poor APCs unless they have been activated to upregulate their levels of MHC II (Wlodarczyk et al., 2014).

Microglia exist in a variety of morphological states. It was believed that different morphological states related to the activity status of the cell. The typical microglial cell in a non-activated scenario exists as a ramified cell. Ramified microglia are highly branched with these branches being elongated to allow for extensive surveillance of the surrounding environment. Non-phagocytic activated microglia have been shown to retract their branches to form a condensed or “bushy” morphology. Activated phagocytic microglia are typically described as having an amoeboid morphology. Microglia are highly regulated by their presence in the brain and always strive to return to homeostasis as rapidly as possible to produce as little damage to the CNS as

possible. Neurons express CD200 and fractalkine. These ligands induce an anti-inflammatory response in microglia aiding the return to homeostasis from a pro-inflammatory status. As neurons degenerate, these signals are lost as is the anti-inflammatory effect (Cameron and Landreth, 2010).

1.4 - CNS Inflammation

The majority of modern studies into CNS inflammation have utilised LPS, a bacterial protein which can induce a response similar to the initial stages of a bacterial infection. Toll Like Receptors (TLRs) are one of the main PAMP receptor families and TLR4 is the receptor for LPS. Within the CNS, TLR4 is only expressed on microglial cells and TLR4 activation of microglia has been shown to be necessary for astrocytic cells to respond to LPS (Holm et al., 2012). Exogenous stimuli such as LPS activate microglial cells to produce cytokines such as IL-1β or TNFα (Lee et al., 1993; Kong et al., 1997). These cytokines in turn induce the astrocytic cells to produce chemokines such as CCL2 or CXCL-1 (Oh et al., 1999) and upregulate cell adhesion molecules or integrins on the BBB (Ballestas and Benveniste, 1995; Yu et al., 1998; Kyrkanides et al., 1999).

In the early 90s Andersson et al described the effect of administering LPS directly into the hippocampus, compared to other tissue types it was realised that in normal brain tissue there is a muted recruitment of innate immune cells and many of these cells do not undergo diapedesis across the endothelium into the parenchyma (Andersson et al., 1992a). This study was followed up with intrahippocampal injection of the cytokines TNFα, IL-1β and CXCL-1 which showed similar results, recruitment to the ventricles and meninges but minimal extravasation into the CNS parenchyma of normal animals (Andersson et al., 1992b). There are many factors to take into account when we discuss the infiltration of peripheral immune cells into the CNS following an elevation of central cytokines. A lot of early studies compared IL-1β and TNFα, finding that TNFα induced a limited response in comparison to IL-1β. However some of these studies ended at a 24h time-point, unaware of the differential dynamic cellular responses displayed by the different cytokines. At 24h the main IL-1β response is over but the main response to TNFα may only be beginning (Quagliarello

et al., 1991). There are also many different compartments within the CNS, all of which react in varied ways to elevations in cytokines. Intracerebroventricular TNFα has been shown to recruit T lymphocytes into the CSF and leukocytes to the perivascular areas, however in the same study intracerebral TNFα did not induce similar cellular recruitment (Seabrook and Hay, 2001). The parenchyma of the CNS reacts with a more restrained and limited cellular infiltration following an inflammatory challenge in comparison to the CSF filled ventricles; this is a dynamic process that alters with aging (Campbell et al., 2007).

Although inflammatory cell infiltration to the CNS is very limited upon intrahippocampal LPS challenge (Andersson et al., 1992a) both IL-1β and TNFα are induced following CNS LPS challenge and the resulting cellular infiltrate comprises both neutrophils and monocytes. Intrastriatal injection of these cytokines shows preferential induction of individual chemokines and differential patterns of cellular infiltration. IL-1β has a neutrophil led infiltration with neutrophils outnumbering monocytes 10 to 1; TNFα has a monocyte dominated infiltrate with monocytes outnumbering neutrophils 20 to 1 (Schnell et al., 1999a). What is apparent from the literature is that in normal animals when these cytokines are placed directly into the CNS parenchyma, IL-1β may recruit both neutrophils and monocytes to marginate to the lumen of the vessels however the main cell type to diapedese will be neutrophils. Similarly with TNFα, both neutrophils and monocytes may be recruited to the lumen of vessels however the main cell to undergo transendothelial migration will be the monocytes. It is generally accepted that IL-1β induces CXCL1 and thus neutrophil infiltration (Campbell et al., 2002) and TNFα induces CCL2 and thus monocyte infiltration (Campbell et al., 2005) and that these pathways do not significantly cross-over. There is *in vitro* evidence for TNFα induction of CXCL1 (Wang et al., 2007; Lee et al., 2012; Zhang et al., 2013b) and IL-1β induction of CCL2 (Jing et al., 2010; An et al., 2011; Fouillet et al., 2012). *In vivo*, intrahippocampal IL-1β increased CCL2 mRNA but CCL2 protein was not measured (Moore et al., 2004), and while intrathecal TNFα induced spinal cord CXCL1 (Zhang et al., 2013b) demonstrations of this in the brain are lacking.

Given that both cytokines can induce the recruitment of both cell types, IL-1β and TNFα must both be producing both chemokines. In that case what limits diapedsesis to predominantly one cell type? TNFα and IL-1β have both been shown to regulate

many other factors related to the BBB structure and cell signalling molecules. Intracerebral TNFα has been shown to increase the permeability of the BBB via decreases in claudin 5 (Aslam et al., 2012) or redistribution of F-actin filaments (Deli et al., 1995). IL-1β has been shown to alter the structure of the BBB by loss of occludin or redistribution of Vinculin (a cell-cell junction protein) (Bolton et al., 1998). Both TNFα and IL-1β have been implicated in Endothelin 1 production which increases BBB permeability (Didier et al., 2003). Transendothelial migration of peripheral immune cells into the CNS parenchyma involves a multitude of dynamic molecular steps. Chemokines induce increases of E-selectin on the endothelium of blood vessels (Gerszten et al., 1999), this induces rolling of neutrophils and macrophages (Sumagin et al., 2010). Rolling cells are then able to recognise chemokines expressed on the endothelium, this induces upregulation of specific integrins necessary for adhesion to the endothelium and transendothelial migration. Neutrophils adhere to the endothelium via LFA-1 (αLβ2 Integrin) and cross the endothelium using Mac-1 (αMβ2 Integrin). Macrophages adhere to the endothelium using VLA-4 (α4β1 Integrin) and use LFA-1 or Mac-1 to cross the endothelium. ICAM and VCAM are cellular adhesion molecules which are upregulated in inflammatory scenarios and control transendothelial migration (Gorina et al., 2014). Integrins allow the inflammatory cells to move to regions of vessels with high adhesion molecule expression; these regions are also areas with lower expression of basement membrane proteins (Wang et al., 2006a). Endothelin 1 has been found to aid monocyte diapedesis (Reijerkerk et al., 2012) while neutrophils are known to utilise degranulation of intracellular vesicles to release membrane digesting enzymes such as MMP9 or Neutrophil elastase (Allen et al., 2012). Given the many steps involved in inflammatory cell migration into the CNS parenchyma there are a multitude of steps at which the cytokine pathways could differentiate between which cells are recruited and remain at the endothelium and which cells are recruited and diapedese.

Study	Cytokine	Animal model	Injection site	Dose	Parenchymal neutrophils	Parenchymal monocytes	Ventricular neutrophils	Ventricular monocytes
(Campbell et al., 2005)	TNFα	Wistar rat	Striatum	1μg	-	↑	↑	↑
(Blond et al., 2002)	TNFα	Wistar rat	Striatum	330ng	-	↑	-	↑
	IL-1β	Wistar rat	Striatum	1μg	↑	-	↑	-
	LPS	Wistar rat	Striatum	1μg	↑	↑	↑	↑
(Schnell et al., 1999a)	IL-1β	Wistar rat	Striatum	1ng	↑	↑	↑	↑
	TNFα	Wistar rat	Striatum	300ng	↑	↑	↑	↑
(Andersson et al., 1992b)	IL-1β	BALB/c	Hippocampus	1-100U	↑	-	↑	↑
	TNFα	BALB/c	Hippocampus	10^4U	-	-	↑	↑
(Andersson et al., 1992a)	LPS	BALB/c	Hippocampus	20ng - 2μg	↑	↑	↑	↑

Table 1.1 Parenchymal cytokine administration

As discussed earlier in this text cytokines are known to control sickness behaviour via certain areas of the brain, some of the main effects of elevated cytokines in normal animals are modulation of behaviours associated with sickness. It has been shown that IL-1β and TNFα are responsible for the majority of the effects of LPS induced sickness behaviour, with one compensating when the other is missing (Bluthe et al., 2000). ICV TNFα has been shown to increase mean arterial blood pressure (Zera et al., 2008), promote sleep (Dickstein et al., 1999), weight loss (Yoshida et al., 1999), increase plasma cortisol (Warren et al., 1997) and elicit a febrile response (Cao et al., 1998). ICV IL-1β has been shown to induce anorexia (Plata-Salaman et al., 1988), promote sleep (Shoham et al., 1987), reduce novel object investigation (Spadaro and Dunn, 1990), induce adipsia (Sonti et al., 1997), hypertension (Zou et al., 2001) and a febrile response (Dinarello, 1984). There is doubtless much overlap between the pathways of both of these two cytokines and it has been shown that TNF can compensate for IL-1β loss and that IL-1Ra can attenuate the effects of TNFα (Bluthe et al., 1994; Bluthe et al., 2000).

Central IL-1β has been shown to be integral in traumatic brain injury (TBI) and stroke models (Relton and Rothwell, 1992; Toulmond and Rothwell, 1995; Gibson et al., 2004) and in the last year 2 separate groups have conducted phase II studies on the effectiveness of IL-1Ra in TBI and subarachnoid haemorrhage patients. A Cambridge group showed that subcutaneous IL-1Ra in TBI patients induced significant modification of potential inflammatory targets (Helmy et al., 2014). A Manchester group conducted a phase II trial on IL-1Ra in cerebral subarachnoid haemorrhage, while this study was not powered to assess efficacy, only safety, there was a significant reduction in plasma and CSF IL-6 following IV IL-1Ra which is a promising indicator (Singh et al., 2014). Central TNFα has been shown to be elevated in human ischaemic brain injury. Glial TNFα was shown to be elevated in the acute phase while parenchymal TNFα peaked 2 to 3 days post injury and expression persisted up to 18 days post injury (Sairanen et al., 2001). Central TNFα has been shown in many animal models to contribute to the severity of ischemia and TBI, blocking TNFα using ICV or IP anti-TNF biologics was shown to reduce infarct volume and to improve neurological functional outcomes (Barone et al., 1997; Chio et al., 2013; King et al., 2013; Lei et al., 2013; Clausen et al., 2014a). The use of TNFα inhibitors in human TBI and stroke is complicated somewhat by controversy surrounding the group conducting experiments on this

and their erratic methodologies. Their publications with perispinal Etanercept (TNF decoy receptor) show a surprisingly rapid amelioration of neurological functional deficits following both TBI and stroke, however these studies are neither randomised nor controlled, and have very small N numbers with no long term follow up (Tobinick et al., 2012).

1.5 - Amyloid Beta & Tau - CNS inflammatory stimuli

Alzheimer's is a disease characterised by very specific hallmarks of pathology (Figure 1.6). Neurofibrillary tau tangles (NFT), senile plaques of amyloid beta (Aβ) and neuronal death are all obvious post mortem indications of the disease (Marchesi, 2012). These standout hallmarks prompted the most prevalent theory of disease for Alzheimer's known as the 'amyloid cascade hypothesis' whereby the aggregations of the amyloid beta protein cause the associated memory loss and neuronal death. George Glenner the chief pathologist of a NIH research institute in the 1960s first isolated what later became known as amyloid beta. With the advent of genetic technologies in later years the precursor of Aβ, amyloid precursor protein (APP) was discovered.

The physiological function of APP is not fully understood. It is thought that it may be involved in neurite outgrowth and synaptogenesis, neuronal protein trafficking along the axon and transmembrane signal transduction. Cleavage of APP determines its impact upon the brain. Normally APP is cleaved by α-secretase producing sAPPα which has an important role in neuronal plasticity and survival. It is protective against excitotoxicity, regulates neural stem cell proliferation and is important for early CNS development. Alternative cleavage of APP by β-secretase produces sAPPβ thought to function as a death receptor ligand, mediate axonal pruning and neuronal cell death. However, it is the C Terminal Fragment (CTF) following secretase cleavage that is most important. Following α secretase cleavage CTFα is cleaved by a γ-secretase producing p83 which is rapidly degraded, and APP intracellular domain (AICD). Following β secretase cleavage CTFβ is also cleaved by γ-secretase. In this case Aβ and AICD are produced. Depending on the γ secretase cleavage either Aβ1-40 or Aβ1-42 is produced. 1-40 is the majority Aβ species however the 1-42 Aβ is a more amyloidogenic species

(Zhang et al., 2011). This entire process is shown in figure 1.6 below. Early onset Alzheimer's disease has been found to be associated with mutations in the main players in APP processing. Mutations on chromosome 21 cause abnormal APP to form, this causes preferential β secretase cleavage. Two mutations occur on chromosome 14 in the subunits of γ-secretase known as presenilins. These mutations cause familial AD, however this is a tiny proportion of the total AD population and the rarity of these mutations showed that sporadic Alzheimer's was more complex.

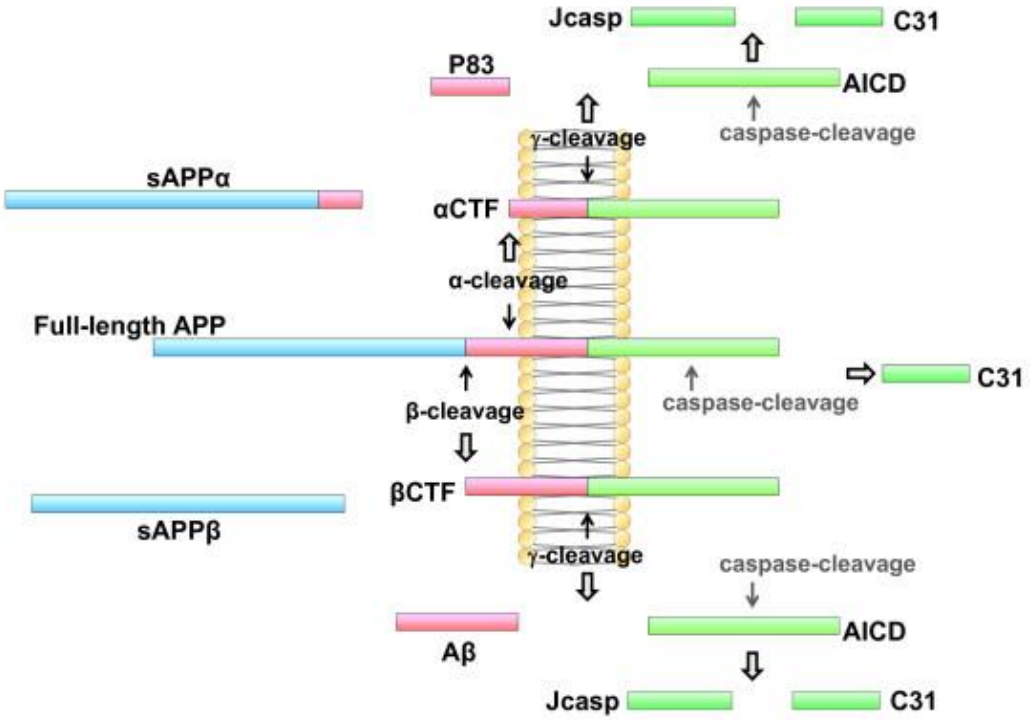

Figure 1.6 APP processing

The alternative cleavage pathways of APP, cleavage by β-secretase followed by γ-secretase results in Amyloid β production (Zhang et al., 2011).

Tau is a Microtubule Associated Protein (MAP). MAPs act to stabilize microtubules, a part of the cell structure formed by tubulin. This is integral to cell structure and cellular transport. Tau is involved in the pathology of numerous neurodegenerative diseases. Filamentous tau pathology occurs in Pick's disease, Corticobasal Degeneration, Progressive Supranuclear Palsy and Frontotemporal dementia and Parkinsonism linked to chromosome-17. Tau is normally a soluble monomer. When Tau becomes phosphorylated it forms non-soluble polymers. Tau can be phosphorylated by many kinases however current research is focusing mainly on GSK3β, CDK5 and ERK1/2. Upon phosphorylation, tau has been shown to lose its affinity for microtubules and increasingly aggregate (Himmelstein et al., 2012). In a hyper-phosphorylated state it forms paired helical filaments which then aggregate into tangle form (Figure 1.7) (Binder et al., 2005). Tau is essential in stabilising cell structure, perturbations can lead to axonal transport deficits causing synapse dysfunction and ultimately neuronal loss (Ballatore et al., 2011). It is also thought that the neurofibrillary tangles formed by the paired helical filaments are themselves toxic to cells (Himmelstein et al., 2012).

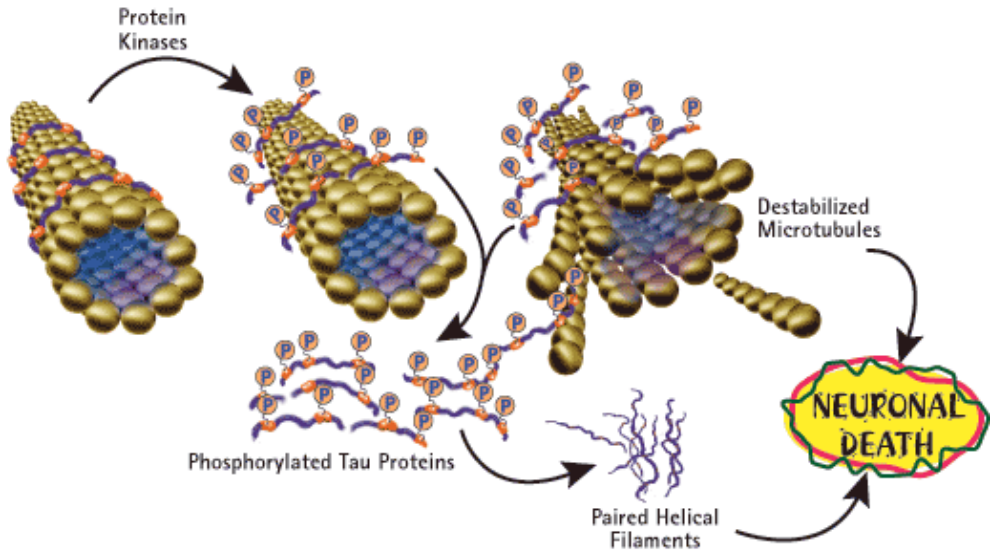

Figure 1.7 Tau aggregation

Tau becomes hyper-phosphorylated which induces aggregation of paired helical filaments, destabilising microtubules and contributing to neuronal death.

In the neurodegenerative brain morphological changes as well as gliosis occur; this means the numbers of microglia and astrocytes are increasing. It has commonly been thought that increased numbers of these microglia with an

"activated" appearance caused large increases in the amounts of pro-inflammatory cytokines released into the brain parenchyma. Recent studies on human AD patients have, however, shown limited or no increases in levels of the main markers of microglial activation such as IL-1β, iNOS and CD45 (Colton et al., 2006).

In AD, Aβ and aggregated Tau appear to stimulate the immune system of the CNS. Amyloid β can bind the RAGE receptor on microglia causing activation and on neurons causing cellular stress and release of inflammatory factors. Microglia aggregate on senile plaques and display a condensed morphology (McGeer and McGeer, 2003). Amyloid plaques in the parenchyma are surrounded by microglial cells which display upregulated MHC class II. (Wyss-Coray and Mucke, 2002) Neurofibrillary tangles (NFTs) show a parallel distribution with activated microglia in AD. The microglial upregulation of MHC II correlates with the amount of NFTs in AD. It also appears that the APOE genotype can influence the link between NFTs and activated microglia. (Zilka et al., 2012) When Aβ oligomers and fibrils are phagocytosed by microglia they induce lysosomal damage. This triggers NALP3 activation causing formation of the inflammasome. This activates caspase 1 and produces mature IL-1β (Glass et al., 2010).

1.6 - Effects of central TNFα in neurodegeneration

TNFα is a cytokine known to modulate fundamental processes of the CNS such as synapse formation, neurogenesis and regeneration and maintenance of the CNS (Montgomery and Bowers, 2012). During chronic neurodegenerative states evidence suggests that aberrant TNFα production is responsible for cell death, gliosis, demyelination, inflammation and BBB deterioration (Montgomery and Bowers, 2012). In a neurodegenerative state the two most important regulatory mechanisms of TNFα are the balance of pro and anti-apoptotic pathways and the production of further pro-inflammatory molecules.

TNFα is also a driver of glutamate excitotoxicity. TNFα rapidly increases AMPAR expression and insertion in the neuronal membrane. TNF also increases NMDAR localisation to cell membranes via activation of the sphingomyelinase pathway. Through its activation of the JNK pathway TNFα influences IP3 receptors. IP3

receptors control the cells internal calcium stores in the endoplasmic reticulum. This is the mechanism by which TNF can influence LTP. However when there are apoptotic levels of TNFα it induces release of calcium from the IP3 mediated stores which initiates glutamate exocytosis, this, combined with TNF-induced increases in AMPAR and NMDAR cell membrane localisation causes excitotoxicity (Montgomery and Bowers, 2012).

TNFR1 has been found to be expressed on the dopaminergic neurons of the human substantia nigra *pars compacta* (SNpc). Blockade of the TNFR1 in the 6OHDA model of PD attenuated the death of DA neurons. In the MPTP model of PD TNFα was detectable in the SNpc of monkeys 14 years after the MPTP infection. This displays a link between chronic levels of TNFα and progressive dopaminergic neurodegeneration (Collins et al., 2012).

Fronto Temporal Dementia is associated with a loss of function mutation in progranulin. The normal function of progranulin is binding of TNFR1 and inhibiting TNFα inflammation (Czirr and Wyss-Coray, 2012). Loss of progranulin function would allow excess TNFα activity in the CNS (Sjogren et al., 2004). In Multiple Sclerosis (MS) TNFα is detected upon post mortem examination of MS lesions. Levels of TNFα are increased in the CSF of patients and are shown to correlate with disease severity and progression. TNFα has been implicated in myelin and oligodendrocyte damage, lymphocyte infiltration, astrocyte activation and upregulation of MHC class I and II molecules on CNS cells in MS (Montgomery and Bowers, 2012).

In AD TNFα is elevated in both CSF and serum of patients. The level of upregulation was found to correlate with disease severity and progression (Paganelli et al., 2002). Mild cognitive impairment (MCI) patients who later went on to develop AD were found to have elevated levels of TNFR1 and TNFR2 that correlated with BACE1 activity compared to controls. The levels of TNFRs were correlated with plasma levels of Aβ and with CSF levels of the axonal damage marker tau (Buchhave et al., 2010). Tarkowski found that MCI patients with elevated CSF levels of TNFα were more likely to progress to AD (Tarkowski et al., 2003). Overall these results indicate that the more elevated an individual's levels of TNFα are, the more likely they are to progress to MCI and then onto AD.

Daily intracerebroventricular injections of the monoclonal anti-TNF antibody, Infliximab in APP/PS1 mice showed decreased amyloid plaques and decreased tau

phosphorylation (Shi et al., 2011). Medeiros et al showed that administering an anti-TNF antibody ICV 15 minutes before ICV Aβ prevented the learning and memory impairments seen in the Morris water maze following ICV Aβ. Similar effects were produced in a TNFR1 knock-out (Medeiros et al., 2007). Systemic imipramine, showed a protective effect against $A\beta_{25-35}$ induced deficits in the water maze and the y maze, concurrent with a frontal cortex reduction in elevated TNFα due to $A\beta_{25-35}$ (Chavant et al., 2010).

In another water maze study PD/APP animals were either given weekly i.p. injections of anti-TNF monoclonal antibody or were crossed with a TNFα knockout mouse. In this case the chronic treatment with anti-TNF prevented an abnormal behaviour, stereotyped circling at 6 months however the stereotyped circling appeared by 15 months. TNFα negative mice did not develop the circling behaviour at 6 or 15 months however they displayed a larger amyloid load after 15 months (Giuliani et al., 2009). A study using 3xTg-AD mice crossed with a TNFR1/TNFR2 knockout showed exacerbated amyloidogenic and tau pathologies. Microglia derived from these animals display reduced phagocytic abilities indicating TNFα may be necessary in this process (Montgomery et al., 2011). These studies indicate that while TNFα is probably detrimental to the brain in neurodegenerative situations it may be deleterious to block TNFα function entirely.

1.7 - Effects of central IL-1β in neurodegeneration

In the normal brain IL-1β is involved in regulating neuronal and glial survival and growth during neonatal development (Giulian et al., 1988; Ma et al., 2014). It is also thought that IL-1 is involved in modulating synaptic plasticity (Chapman et al., 2010). This effect is dependent on both location and concentration. At low concentrations IL-1 has been shown to inhibit LTP, block calcium currents in hippocampal neurons and enhance GABA currents in cortical neurons. High concentrations have been shown to release NO and Arachidonic acid, increase intracellular calcium concentrations (Zhao and Schwartz, 1998). IL-1β has been shown to have a potent effect in control of seizures. IL-1β can prolong a

pharmacologically induced seizure while intrahippocampal IL-1Ra can significantly inhibit seizures (Vezzani et al., 2000).

Central IL-1β has long been seen as a leading cause of much of the damage to the brain following ischaemia or TBI: administering ICV IL-1β following transient ischaemia increased infarct size and the numbers of infiltrating neutrophils (Yamasaki et al., 1995). While central infusion of IL-1Ra significantly ameliorated the effects of transient ischaemia and TBI (Relton and Rothwell, 1992; Toulmond and Rothwell, 1995; Yang et al., 1998). Central overexpression of IL-1Ra in another model of TBI showed delayed cytokine induction and a greater neurological recovery again implicating central IL-1β in causing neurological deficits following CNS injury (Tehranian et al., 2002).

IL-1β has been implicated in production of spatial impairment following secondary challenge with Bacillus Calmette-Guérin (BCG). Two challenges with BCG, the first in the hippocampus and the second subcutaneously induces impairment in spatial memory and was observed to elevate hippocampal IL-1β concurrently. The spatial impairment was rescued using subcutaneous IL-1Ra (Palin et al., 2004).

Intrahippocampal (IHC) IL-1β can produce memory deficits in contextual fear conditioning (CFC) while also down regulating hippocampal BDNF production (Barrientos et al., 2004). Bilateral IHC injections of IL-1β into young and aged animals showed an exaggerated inflammatory response in the aged animals. Cytokine mRNA was increased in both young and aged animals however the mRNA was only translated into the active protein form in the aged animals (Hopp et al., 2014).

Use of an IL-1R1 knockout model with a murine prion disease showed that IL-1β is a driver of prion associated gliosis. The IL-1R1$^{-/-}$ mouse showed reduced gliosis and prion protein depositions compared to wild type infected with PrP^{Sc}. This resulted in prolonged survival times (from 172±4 days in C57 B6 to 197±7 in IL-1R1$^{-/-}$) and delayed disease onset (Schultz et al., 2004).

In the 6-hydroxydopamine (6-OHDA) model of Parkinsons disease intra-striatal injection of LPS exacerbated neurodegeneration and increased motor signs of disease. These symptoms were ameliorated by increasing striatal expression of IL-1Ra. Increased IL-1Ra prevented the majority of the neurodegeneration seen in the striatum following LPS administration (Pott Godoy et al., 2008).

Post mortem brain samples from Alzheimer's disease and vascular dementia (VD) showed that levels of IL-1β were significantly increased in the frontal cortex and hippocampus of AD patients compared to both VD patients and controls (Cacabelos et al., 1994). Increased IL-1β receptor activity was also found in post mortem AD tissue compared to both PD and control tissue (Araujo and Lapchak, 1994).

IL-1β requires activation of the NLRP3 inflammasome and Caspase 1 to be cleaved into its mature form. Amyloid β has been shown to activate the NLRP3 inflammasome and produce mature IL-1β (Parajuli et al., 2013). Human MCI and AD brains show elevated Caspase 1 activity, implicating ongoing IL-1β processing. APP/PS1 mice lacking in NLRP3 or Caspase 1 showed decreased deposition of Aβ and were protected against loss of spatial memory in the Morris water maze (Heneka et al., 2013). Chronic dosing of 3xTg-AD mice with an IL-1R blocking antibody showed significant effects on both pathology and behaviour. Decreasing IL-1β activity in the 3xTg-AD model alleviated cognitive deficits in the Morris water maze and CFC, it also decreased both Tau and Aβ pathology (Kitazawa et al., 2011).

1.8 - Systemic inflammation in neurodegeneration

It is obvious to anyone that has had a systemic infection, that it can affect your mood, motivation, emotion and cognition. However, we also know that once an infection has been resolved we return to normal. That is to say, the CNS changes brought about by systemic inflammation are adaptive. These changes constitute a motivational state known as sickness behaviour. Sickness behaviour reprioritises an organism's activity to make conditions optimal for recovery from an infection. Sickness behaviour is characterized by decreased social interaction, decreased activity, hypophagia, a febrile response, fatigue, poor concentration, hypersomnia, anhedonia and irritability. Sickness behaviour removes an organism from the environment and makes them rest; this reduces energy expenditure which allows the highly energetic febrile response to take place. The febrile response aids recovery by creating an inhospitable environment for microbial reproduction, while removing an animal from social settings and inputs such as food which can

prevent exposure to more infections (Dantzer and Kelley, 2007). These behaviours are adaptive; they may not be pleasant but they must occur in order to fight an infection.

Systemic inflammation must be monitored by the CNS in order for the brain to induce the set of sickness behaviours necessary to aid recovery. Systemic inflammation can signal to the CNS via four routes. Infections are detected by the immune system by PAMPs or by cytokines released by other immune cells; firstly both of these signals can communicate with the CNS via vagal afferents in the thoracic-abdominal cavity. The vagus nerve signals directly to the nucleus of the solitary tract in the medulla oblongata and from the medulla these tracts signal to the hypothalamus. The hypothalamus is a major control centre for most of the aspects of sickness behaviour (feeding, drinking, and thermoregulation). Secondly, the presence of cytokines in the circulatory system brings them in direct contact with the sensory circumventricular organs (CVOs), the organum vasculosum of the laminae terminalis (OVLT), the subfornical organ (SFO) and the area postrema. The CVOs are areas of the brain with an incomplete BBB, this does not mean that cytokines can freely enter the brain at these regions but they can signal via these CVOs to relevant areas of the brain (Quan, 2008). Thirdly, the BBB has a host of receptors which aid in transmitting systemic inflammatory signals into the CNS. Circulatory cytokines can transmit signals via their receptors on the BBB and brain endothelium, IL-1β and TNFα have both been shown to be transported across the BBB via a specific and saturable transporter (Banks et al., 1991; Gutierrez et al., 1993) . Fourthly, there are also pathogen receptors on the BBB by which micro-organisms or their PAMPs can signal directly into the CNS, inducing molecules such as prostaglandins (Quan and Banks, 2007).

The immune system is highly regulated and has evolved to be adaptive to a wide variety of pathogens. In recent years it has been realised that what is adaptive in a normal person may be maladaptive in an aging person. In adults the immune system has evolved to scavenge cell debris and to be activated by DAMPs. In an aging or diseased person as signs of cellular damage escalate so does the activation in the immune system. This system that was adaptive and scavenged debris in a normal person could now be maladaptive and cause more inflammatory damage than it prevents in an aging or diseased person. This has been shown in many scenarios.

It has become clear over the past two decades that there is a significant inflammatory component in dementia and indeed all chronic neurodegenerative diseases. It was 1990 when McGeer and McGeer published their epidemiological findings on the impact of NSAIDs (non-steroidal anti-inflammatory drugs) in lowering an individual's predisposition to dementia (McGeer et al., 1990). Long term NSAIDs were prescribed for inflammatory conditions such as rheumatoid arthritis. McGeer and McGeer developed a hypothesis based on observations of microglia and astrocytes centred on Alzheimer's disease lesions, and the associated presence of numerous immune molecules such as cytokines, activated complement proteins and acute phase reactants. In 1995 the McGeers published a paper describing what they called the autotoxic loop, a process by which the pathology associated with Alzheimer's disease initiated a small amount of neuronal death. They believed that the resulting inflammatory response to this process then amplified the neuronal death.

Numerous papers appeared from 1995 onwards on the effects of long term systemic NSAIDs, such as ibuprofen and indomethacin, on risk of AD (1994; Breitner et al., 1994; Andersen et al., 1995; Haruda, 1995; Rich et al., 1995). Epidemiological studies showed a clear protection of NSAIDs against subsequent development of AD. Studies using NSAIDs in AD patients however have not had significant ameliorative effects against existing disease (Aisen, 2002; Martin et al., 2008). NSAIDs act as inhibitors of cycloxygenase (COX). COX is a mediator of inflammatory signals inducing production of prostaglandins upon activation. It is thought that COX is an essential component in transduction of systemic inflammatory signals to the CNS parenchyma (Laflamme et al., 1999).

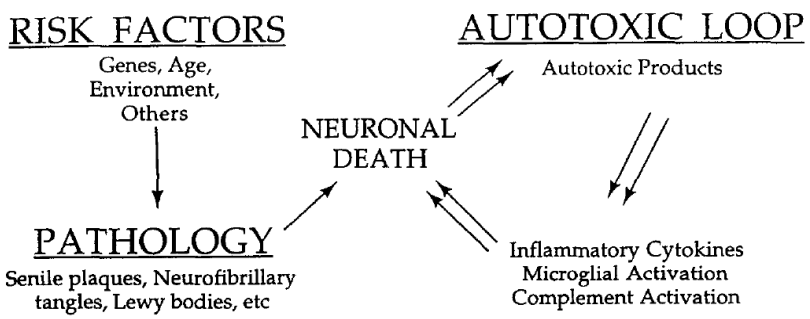

Figure 1.8 McGeer & McGeer Autotoxic Loop

Initial pathology causes neuronal death, which can then initiate a toxic loop via inflammatory cytokines and cell activation. (McGeer and McGeer, 1995)

Sepsis shows an extreme example of how systemic inflammation can affect the brain. One study showed that the odds of developing moderate to severe cognitive impairment following an episode of sepsis were 3.3 times higher than patients with a non-septic hospitalisation (Iwashyna et al., 2010). A study in children found that 44% of those that survived septic shock had cognitive scores 25% lower than the normal population (Bronner et al., 2009).

Epidemiology shows a link between systemic inflammatory events (SIEs), chronic neuroinflammation and the aetiology of the progressive nature of Parkinson's disease. Following the 1918 H1N1 influenza A pandemic, people affected by the virus displayed a dramatic increase in post-encephalitic-parkinsonism. 90 years later we can see that people born at the time of the pandemic are 2 to 3 fold more likely to have Parkinson's disease. The fact that the H1N1 virus preferentially targets the SNpc is thought to be a factor in this increase. H5N1, Coxsackie virus, Japanese encephalitis B, St. Louis virus, West Nile virus and HIV are all associated with secondary Parkinsonism. In the 6-OHDA lesion model of PD in rats low dose systemic LPS increased SNpc dopaminergic neuronal loss (Collins et al., 2012).

Individuals with prior cognitive decline are more susceptible to the cognitive effects of systemic infection (Jackson et al., 2004; Fong et al., 2009; Witlox et al., 2010). This can induce a state of delirium. Delirium is an acute neuropsychiatric state of inattention with a fluctuating course and related features of altered arousal, disorganised thinking, psychosis with perceptual and sleep-wake cycle disturbances (Lipowski, 1989; Inouye, 2006). Episodes of delirium are associated with further cognitive decline, increased subsequent institutionalisation, loss of independence and death (Witlox et al., 2010; Cunningham and Maclullich, 2012). However milder systemic inflammation not resulting in delirium can also precipitate further cognitive decline. Data from a six month study of mild to severe cases of AD showed that some patients had raised serum levels of TNFα. Patients in the lowest quartile of TNFα showed no cognitive decline over the study period. Those in the highest TNFα category who also had one or more systemic inflammatory event (SIE) displayed almost a 10 fold increase in cognitive decline compared to the lowest TNFα group (Holmes et al., 2009a). It is also known that

risk factors for AD such as smoking, obesity, diabetes, atherosclerosis and periodontitis are all associated with low grade systemic inflammation (Perry, 2010).

1.9 - A model of neurodegeneration and systemic inflammation

Findings from our laboratory studying microglia in prion disease have proven informative for the study of the interaction between systemic inflammation and neurodegeneration. ME7 prion is a modified form of the ovine prion scrapie used in mice. ME7 initiates a disease that is characterised by aggregations of a misfolded protein, microglial activation and a gradual progression of the disease through the brain causing synaptic loss and neuronal death. These features are consistent with many of those of Alzheimer's disease. To replicate what had been seen in clinical settings, systemic injections of LPS were used in ME7 mice to investigate the impact of systemic inflammation on a degenerating brain. Similarly to a mechanism discovered in macrophages in 1983 (Pace et al., 1983), it was found that microglial cells are primed by prior neurodegeneration to react in an exaggerated manner to a subsequent stimulus(Cunningham et al., 2005b).

Cunningham et al in 2005 showed an altered response of ME7 prion animals to central and peripheral LPS. Microglial cells were producing exaggerated levels of IL-1β and iNOS protein following intracerebral (i.c.) LPS in the ME7 model. i.c. LPS also induced an exaggerated neutrophil infiltration in the degenerating brain. 18 and 24 hours post-central LPS challenge there was no marked alteration of morphology of microglia in ME7 animals (19 weeks post-innoculation) compared to saline challenged animals (Cunningham et al., 2005b; Hughes et al., 2010). This exaggerated microglial response was not limited to direct i.c. challenges. Following intraperitoneal (i.p.) LPS, central levels of both IL-1β and TNFα mRNA were increased compared to control (normal brain homogenate, NBH)+LPS and the microglia in the vicinity of the hippocampal and thalamic vasculature express significant IL-1β protein 3 hours post-challenge with LPS (Cunningham et al., 2005b). It is important to note that the systemic inflammatory response to peripheral immune challenge is equivalent in diseased and normal animals (Murray et al., 2012).

In a Wallerian degeneration model of optic nerve crush, a similar priming of microglia was found with exaggerated IL-1β and iNOS production following peripheral LPS challenge. However, in this study it was also observed that there was prolonged elevation of pro-inflammatory transcripts following inflammatory challenge. Microglial cells primed by prior Wallerian degeneration also displayed a more phagocytic phenotype following LPS challenge (Palin et al., 2008).

There are many functional consequences to the exaggerated levels of pro-inflammatory cytokines in a degenerating brain following a second inflammatory stimulus. TUNEL staining revealed that apoptosis was 2 fold higher in ME7 animals following LPS challenge than in saline challenged or unchallenged ME7 animals and 7 fold higher than the same challenge in NBH animals. Staining for activated caspase 3 (an apoptotic protein) and neurofilament H showed that these dying cells were neurons. These data demonstrate that intraperitoneal LPS can induce acute neurodegeneration in ME7 animals but not in NBH animals (Cunningham et al., 2005b). The increased sensitivity of the CNS in this neurodegenerative model exacerbates neuronal degeneration induced by inflammatory stimuli.

The exaggerated reactions of primed microglia to inflammatory stimuli leading to increased levels of apoptosis of neurons is associated with a more rapidly progressing disease state and exacerbated functional deficits. Cunningham et al demonstrated this by training animals on the horizontal bar and inverted screen task between 12 weeks and 15 weeks post-inoculation. This task is a neurological examination of motor skills involving timing how long a mouse can stay on the horizontal bar or inverted screen. At 15 weeks post-innoculation all animals were performing well on the task. Upon challenge with LPS, ME7 animals showed a decrease in performance compared to NBH animals. Following this single challenge the animals' performance on the bar, the screen and in the open field was monitored for 5 weeks. These data showed that ME7 animals challenged with a single LPS dose scored progressively lower than all other groups on all three of these neurological tests (Cunningham et al., 2009a). This indicates that a single episode of systemic inflammation in a vulnerable animal can induce both acute and long lasting effects on the acceleration and progression of disease. This is evident not only late in disease but also quite early in disease progression.

A novel behavioural task, the paddling alternation T maze task was used to assess working memory deficits. These tests were designed to elucidate the parallels between delirium in humans and working memory deficits in vulnerable animals administered an acute systemic inflammatory challenge. Animals were trained for several weeks until they achieve a consistent performance of about 80% correct choices on the alternation T maze. At 16 weeks post-inoculation all animals were challenged with i.p. LPS and tested in the T maze. The NBH+LPS group showed no impairments whereas the ME7+LPS group had a significant impairment in this task. All groups recovered to baseline at 26 hours. These data showed that a single dose of LPS produced a transient working memory deficit in animals with prior neurodegeneration. NBH animals were tested with twice the dose of LPS to ascertain whether inflammation alone could cause a working memory deficit (Murray et al., 2010). LPS in a normal animal was not sufficient to induce a working memory deficit. The interplay of both prior neurodegeneration and systemic inflammation is required to induce a working memory deficit in these mice. This may explain why elderly patients are more susceptible to delirium.

In 2002 Combrinck showed that ME7 animals displayed an exaggerated response to systemic LPS. The animals displayed a heightened hypothermic response and profound hypo-activity at 19 weeks post inoculation, together with raised levels of IL-1β protein in the brain (Combrinck et al., 2002). In 2009 Cunningham et al assessed animals at 12 weeks post-inoculation. In the study, multiple evaluations of behaviour were shown to be modified by ME7 at 12 weeks. Burrowing behaviour was still impaired at 24 hours post ME7+LPS where NBH+LPS had recovered. Open field activity was inhibited to 80% in ME7+LPS but only to 50% in NBH+LPS. Core body temperature showed a significant hypothermia in ME7+LPS with no observable alteration in NBH+LPS (Cunningham et al., 2009a). Hence, the ME7 model of neurodegeneration displays an exaggerated sickness behaviour response upon inflammatory stimulation.

Another paper from the Cunningham lab in 2010 demonstrated that this phenomenon was not specific to the bacterial endotoxin, LPS. Polyinosinic : polycytidylic acid (Poly I:C) is a viral mimetic that interacts with TLR3. CNS mRNA transcripts of cytokines were acutely increased following Poly I:C. Microglial activation was visualised using IBA-1, COX-1 and IL-1β following Poly I:C in ME7

animals. Similarly to LPS, a single dose of Poly I:C at 12 weeks post-innoculation with ME7 had negative consequences for ME7 mice on the bar (from 6 to 24 hours) and screen (from 6 to 14 hours). These animals showed progressively worse performance than ME7+saline or NBH + Poly I:C groups for 7 weeks afterwards. A subset of animals were repeatedly dosed with Poly I:C at 3 fortnightly intervals, demonstrating that repeated doses increased the progression of disease with increasingly worse performance on the bar and screen. ME7+Poly I:C animals also had significantly higher levels of apoptosis than NBH+Poly I:C or ME7+saline animals (Field et al., 2010).

What are the consequences of primed microglia for vulnerable individuals? So far not much has been demonstrably attributed to the activation of primed microglia. However, work by Griffin et al showed that with progression of disease from 12 to 16 weeks in the ME7 model, the severity and duration of cognitive dysfunction is significantly increased following a systemic challenge (Griffin et al., 2013). This indicates that during neurodegenerative disease individuals may be increasingly susceptible to, and increasingly affected by, the detrimental cognitive effects of systemic inflammation. This prediction was supported by results from the Vantaa 85+ study which showed that with every Mini Mental State Exam (MMSE) point lost there was an increase of 5% in risk of incident delirium (Davis et al., 2014).

These experiments have demonstrated that there is an exaggerated and prolonged response from primed microglia in the degenerating CNS, this may be linked to decreased functional outcomes following infection in a vulnerable patient. The process of phenotypic switching by primed microglia appears to be integral to the interaction of the systemic immune system and the neurodegenerating brain. The ME7 model has shown the effects of microglial priming in the neurodegenerative brain very well. However, microglial priming is not a phenomenon specific to ME7 prion disease. It appears to be a generic phenomenon of CNS aging and pathology.

1.10 - Other models of systemic inflammation and neurodegeneration

When we study the effects of systemic inflammation and neurodegeneration we can look at two separate indicators of an altered CNS. We can use elevated

cytokine and iNOS production or microglial phagocytosis to show evidence of activation of primed microglia. Or we can study exacerbation of disease features following activation of a primed microglial population. Activation of primed microglia has not been definitively demonstrated to exacerbate disease features, however it is highly likely that the increased inflammation following activation of primed microglia is contributing to declining function in disease.

Phenotypic switching of primed microglia was displayed by Palin et al in a model of Wallerian degeneration using optic nerve crush model of axonal injury. In this model, crushing of the optic nerve induces anterograde degeneration of axons separated from their cell bodies. Upon degeneration, microglia proliferate and display an activated morphology. On inspection, these microglia that appear "activated" are not producing pro-inflammatory cytokines. Following LPS challenge to animals with Wallerian degeneration, microglia display rapid phenotypic switching to a more pro-inflammatory and phagocytic profile (Palin et al., 2008). Therefore, the microglia were primed by the primary axonal pathology to produce exaggerated responses to acute inflammatory stimulation with elevated levels of IL-1β, IL-6 and iNOS, and increased phagocytic markers. In a midline fluid percussion model of TBI, mice later exposed to systemic LPS showed exaggerated microglial IL-1β and TNFα indicating priming of the microglial population as well as increased social withdrawal, immobility and anhedonia; indicating exacerbation of injury following TBI (Fenn et al., 2014).

Aging has also been shown to contribute to altered response profiles of microglia. In aged vs. adult mice treated with LPS i.p., levels of TNFα, IL-1β and IL-6 mRNA increased in aged mice compared to younger cohorts indicating priming of microglia. Aged mice also displayed a greater decline in spatial tasks, social exploration, locomotor activity and food consumption following LPS challenge indicating exacerbation of age-associated memory impairments (Godbout et al., 2005; Chen et al., 2008). Peripheral LPS administration was also shown to induce atrophy of pyramidal neurons in the CA1 of aged but not adult mice (Richwine et al., 2008). Using *Bacillus Calmette-Guérin* to induce a chronic infection in aged animals induced a prolonged set of sickness behaviours, with aged mice not regaining weight lost due to sickness, decreased locomotor activity and rearing compared to adult mice similarly challenged (Kelley et al., 2013). Using both contextual fear conditioning and the Morris water maze, Barrientos et al displayed

an *E. coli* infection-induced impairment of hippocampal dependent memory in aged rats, exacerbating features of aging. The aged rats also displayed significantly elevated levels of IL-1β in the hippocampus 4 days after *E. coli* infection, indicating activation of primed microglia (Barrientos et al., 2006). The same group later found that multiple types of long term potentiation (LTP), increased levels of synaptic strength linked to memory formation, were adversely affected in aged animals following an infection (Chapman et al., 2010). In two separate studies blocking central IL-β using ICV IL-1Ra has been shown to attenuate the exaggerated effects of systemic inflammation produced by aging (Abraham and Johnson, 2009; Frank et al., 2010). This implicates primed microglia in the exaggerated responses to subsequent immune stimuli observed in aged animals.

Models of AD and PD have also presented evidence for priming of microglia. Sly et al in a model of age related Aβ accumulation found evidence of microglial priming. LPS induced cortical and hippocampal IL-1β protein in aged Tg2576 mice but not in younger Tg2576 animals or in similarly aged non transgenic littermates. In young and old Tg2576 mice Aβ1-40 levels were raised following LPS. Aβ1-42 levels were raised only in aged Tg2576 following LPS. Microglia in this model appear to be primed by the Aβ accumulation allowing phenotypic switching on LPS challenge (Sly et al., 2001). Pott Godoy et al used the 6-hydroxydopamine (6-OHDA) model of Parkinson's to display the effect of a systemic chronic adenoviral vector expressing IL-β. They showed that chronic systemic il-1β exacerbated the neurodegenerative effects of 6-OHDA with significantly less dopaminergic cells present following il-1β treatment (Pott Godoy et al., 2008).

The majority of these studies utilise exogenous pathogens and measure resultant increases in endogenous cytokines. Many studies have examined the levels of endogenous cytokines in at risk populations and drawn correlations between progression of cognitive decline and cytokine levels. However, very few people have directly studied the effects of elevated levels of cytokines in neurodegenerative models. Let's examine the evidence for elevated endogenous cytokines contributing to neurodegeneration in human populations and animal models.

1.11 - Chronic systemic inflammation exacerbates cognitive decline

Many chronic co-morbidities such as rheumatoid arthritis, atherosclerosis, obesity and diabetes have now been associated with elevated incident risk of dementia. These co-morbidities have all been revealed to have a significant inflammatory component. However, the impact of an inflammatory co-morbidity on an individuals likelihood to develop cognitive decline appears to be highly dependent upon that individuals baseline inflammatory status (Yaffe et al., 2004). Here I examine some of these co-morbidities and their likely effects upon cognitive decline.

1.11.1 - Rheumatoid arthritis

Epidemiological studies showing that rheumatoid arthritis (RA) patients were protected against the subsequent development of AD lead some to suggest that arthritis may actually protect against AD (Boyd et al., 2010). More recently, a population-based study identified RA as an important risk factor for subsequent dementia generally (risk ratio (RR) 2.77) or AD specifically (RR 2.45) (Wallin et al., 2012). Therefore it is likely that RA patients take anti-inflammatory treatments for their condition, which in turn protect against the development of AD. Anti-TNF therapies are an effective treatment for RA (Aaltonen et al., 2012), and recent conference proceedings from the American College of Rheumatology have reported that they significantly reduce the risk of development of AD. This is consistent with prior data demonstrating that the TNFα level in the serum of AD patients is predictive of accelerated cognitive decline (Holmes et al., 2009b). In spite of these epidemiological indications, there are few studies on the interaction between RA and AD using animal models of disease or indeed the impact of RA on the aged, non-transgenic, brain. One recent study reported decreased Aβ, but increased vascular damage and mortality in RA APP/PS1 double transgenic mice

(Park et al., 2011). Another study assessed the impact of osteoarthritis on AD pathology in APP/PS1 mice. Since IL-1β is known to contribute to osteoarthritis pathology, the Col1-IL1β^{XAT} Cre inducible model was used to model osteoarthritis and when these animals were crossed with APP/PS1 mice and injected with Cre to induce chronically elevated IL-1β expression, there were significant exacerbations of Aβ deposition and associated microglial activation (Kyrkanides et al., 2011). No one, to our knowledge, has assessed its impact on cognitive decline and other features of neuropathology and this should be investigated.

1.11.2 - Metabolic Syndrome

Obesity, diabetes and atherosclerosis fall under the umbrella of Metabolic syndrome (MetS), which is the name given to the grouping of at least 3 of the following features; abdominal obesity, hypertension, hyperglycaemia, hypertriglyceridemia and low levels of high-density lipoprotein (HDL). Metabolic syndrome is a significant risk factor for development of AD but it is significant that this association was limited to those MetS cases with elevated serum pro-inflammatory markers (Yaffe et al., 2004) indicating that inflammatory processes associated with, or even underpinning, MetS may contribute to dementia progression. Here we briefly review the impact of these co-morbidities on brain ageing in animal models and examine possible inflammatory mechanisms, while recognising that non-inflammatory mechanisms, also may be important.

1.11.3 - Atherosclerosis

A meta-analysis of epidemiological studies showed a correlation between mid-life serum cholesterol levels and dementia (Anstey et al., 2008). Atherosclerosis is characterised by elevated Low Density Lipoprotein (LDL) which becomes oxidised (oxLDL) and activates macrophages via the scavenger receptor CD36, producing IL-1β via the NLRP3 inflammasome (Napoli and Palinski, 2005; Sheedy et al., 2013). This leads to a state of chronic systemic inflammation (Libby et al., 2013). The acute reactant CRP is most readily measureable and it has been shown that

high CRP levels are associated with increased microglial activation in human PET imaging studies (Drake et al., 2011).

There are numerous rodent models combining Atherosclerosis (ATH) and Alzheimer's disease (AD) risk factors in an effort to discern common aetiologies. The addition of a high cholesterol (atherogenic) diet leads to alterations in APP processing and exacerbated spatial learning impairment in the Tg2576 human APP-overexpressing mouse (Li et al., 2003). Apolipoprotein E is a lipid binding protein integral to the metabolism of cholesterol via Low Density Lipoprotein Receptor (LDLR) and the Apoε4 allelle is a major risk factor for both Atherosclerosis and Alzheimer's disease. Removing or overexpressing LDLR modulates cholesterol up or down and can increase or decrease Aβ respectively, suggesting that cholesterol has direct effects on amyloid deposition and/or clearance. Expression of Apoε4 versus Apoε3 in mice resulted in impairments in spatial and avoidance memory (Bour et al., 2008; Segev et al., 2013). ApoE deficient animals (that show a similar phenotype to Apoε4 allele carrying mice) show elevated inflammation and gliosis associated with their deficient phagocytosis of apoptotic bodies (Grainger et al., 2004) and APP23 mice negative for ApoE fed an atherogenic diet also showed increased endothelial activation and increased vascular pro-inflammatory markers but no alteration in Aβ deposition (Tibolla et al., 2010). Statins have long been used to regulate peripheral cholesterol and meta-analysis shows that these drugs reduced dementia risk (Song et al., 2013). Statins are now recognised to have anti-inflammatory actions (Niessner et al., 2006) and they significantly enhanced memory and reduced Aβ plaque deposition without altering serum lipid levels in an APP overexpression model (Kurata et al., 2012). These data indicate atherosclerosis affects cognitive ageing and has a robust inflammatory aetiology but precise pro-inflammatory mechanisms contributing to accelerated cognitive decline and AD risk require elucidation

1.11.4 - Obesity and type 2 Diabetes

Obesity, and the frequently associated complication type 2 diabetes (T2D) are associated with functional deficits in learning, memory and executive functions

and with increased risk of dementia (Biessels et al., 2006; Miller and Spencer, 2014). Excessive nutrient intake is key in the genesis of obesity and T2D: adipocytes and macrophages in the white adipose tissue respond to molecules such as free fatty acids, advanced glycation end products and reactive oxygen species with the production of TNFα, IL-1β, IL-6, CCL2 and adipokines like leptin (Gregor and Hotamisligil, 2011). The cytokines TNFα and IL-1β can phosphorylate insulin receptor substrate (IRS)-1 to induce insulin resistance (Shoelson et al., 2006), while the Islet amyloid polypeptide (IAPP) deposited in the pancreas can activate the NLRP3 inflammasome to drive IL-1β secretion (Masters et al., 2010; Sheedy et al., 2013). Thus inflammation has key aetiological roles in obesity and diabetes.

Exposure to a High Fat Diet (HFD) can induce both obesity and a diabetic (insulin resistant) state in rodents, which means that models of obesity and diabetes are highly overlapping: consumption of HFD or use of leptin deficient (ob/ob) or leptin receptor deficient (db/db) mice, which do not respond appropriately to this satiety hormone. Consumption of HFD in normal mice increases hippocampal pro-inflammatory markers IBA-1, TNFα, GFAP, reduces BDNF and dendritic complexity and decreases long term potentiation (LTP), learning ability and impaired working and spatial memory (see (Miller and Spencer, 2014) for review). Chronic HFD also exacerbated peripheral and brain inflammatory responses to LPS (Andre et al., 2014), indicating a priming of macrophage and/or microglial cells, and when superimposed on the ageing brain showed exacerbated systemic inflammation, BBB disruption, oxidative damage, hippocampal micro-vascular rarefaction and hippocampal dependent cognitive decline (Morrison et al., 2010; Tucsek et al., 2013; Tucsek et al., 2014). Alzheimer transgenic models fed HFD show exacerbated memory impairment as well as increased levels of Aβ oligomers and deposition (Maesako et al., 2012; Barron et al., 2013). Memory deficits induced by HFD in the 3xTg AD model were independent of alterations in Aβ or Tau pathology but did drive exacerbated neuro-inflammation (Knight et al., 2014).

The obese/diabetic leptin receptor deficient db/db mouse exhibits synaptic dysfunction, microglial priming and impaired spatial and object recognition memory (Stranahan et al., 2008). Combination of APP transgenics with db/db mice showed increased inflammation, amyloid angiopathy, increased brain

atrophy, cortical Tau pathology and exacerbated cognitive deficits but no additional effect on β-amyloid deposition (Takeda et al., 2010; Ramos-Rodriguez et al., 2013; Niedowicz et al., 2014). Insulin resistance in this model also chronically elevates corticosterone, which, like chronic stress (Frank et al., 2012), contributes to microglial priming, increasing brain IL-1 and TNF responses (Dey et al., 2014). Intrahippocampal administration of IL-1Ra was protective against obesity-induced neurophysiological dysfunction, indicating that leptin deficiency promotes a pro-inflammatory environment in the brain and may contribute directly to cognitive decline (Erion et al., 2014).

Use of Glucagon like peptide 1 (GLP-1), which stimulates insulin can reverse deleterious effects of HFD on learning and memory, CA1 LTP and hippocampal GFAP, mTOR and VEGF (Lennox et al., 2014) and this is now a promising therapeutic target for AD (Holscher, 2014). There are many ways in which reduced efficacy of the Insulin Receptor (IR) pathway may contribute to AD-associated changes and the primary aetiological role of inflammatory mediators in driving insulin resistance places inflammation at the centre of the obesity/diabetes-associated AD risk.

A more recent development is the finding that increased adiposity, altered adipokines and/or inflammatory mediators (but not body weight per se) induce microgliosis (Gao et al., 2014), cytokine secretion (De Souza et al., 2005) and neuronal dysfunction and death in the hypothalamus (Thaler et al., 2012). The hypothalamus is a key site of action of insulin and leptin and is the CNS regulator of appetite control and energy expenditure. These pathological changes contribute to furthering the metabolic dysfunction and once again underline the key role of inflammation in metabolic syndrome. Perhaps of even more significance, inflammatory signalling in the hypothalamus (IKK-β and NFκB) also drives frailty

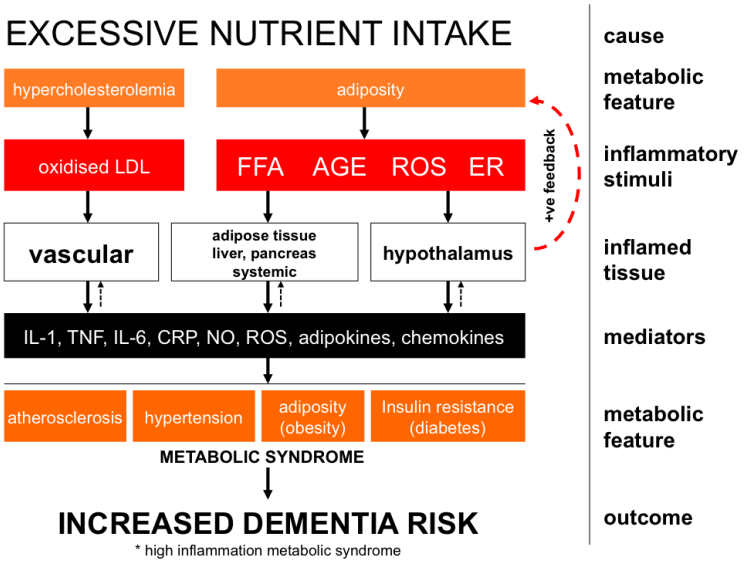

and decreases neurogenesis, effectively accelerating aging (Zhang et al., 2013a). This places inflammation in the hypothalamus as a key determinant of rates of cognitive and function decline.

Figure 1.9 Inflammatory Metabolic Syndrome mediators

Excessive nutrient intake results in induction of inflammatory mediators, this is associated with an increased risk of dementia (Cunningham and Hennessy, 2015).

1.12 - The role of systemic TNFα in neurodegeneration

It has been shown that chronic low grade inflammatory conditions that result in persistently elevated TNFα levels such as atherosclerosis, arthritis, diabetes, periodontitis and obesity are risk factors for Alzheimer's disease (Cechetto et al., 2008). Following an epidemiological study of infections in aging cohorts, chronic TNFα has been implicated in the progression of neurodegeneration and cognitive decline (Holmes et al., 2009a). The coincidence of Systemic Inflammatory Events (SIEs) and the levels of TNFα in peripheral blood were used to determine the effect of TNFα on the cognitive outcome of an elderly cohort. It was found that baseline levels of TNFα correlated with scores on cognitive tests such as the ADAS-COG, i.e. the higher the baseline TNFα levels the lower the cognitive score was. Over 6 months the rate of cognitive decline as shown by change in ADAS-COG score was found to be 4 fold higher in those with higher baseline TNFα levels, however, changing scores did not correlate with changing TNFα serum levels. The occurrence of SIEs and an increase in serum TNFα levels caused a 2 fold increase in the rate of cognitive decline. The combination of high baseline TNFα and the occurrence of a SIE resulted in a 10 fold increase in cognitive decline compared to those with low baseline TNFα and no SIEs (C. Holmes). This may indicate that while acute systemic elevations in TNFα are important in a cognitive context, chronically elevated levels of TNFα are more relevant to cognitive decline over time.

Tan et al (2007) examined the levels of spontaneous production of cytokines from PBMCs in a large cohort of cognitively intact community dwelling participants.

TNFα levels were divided into tertiles. It was found that the participants within the highest TNFα tertile were at a significantly greater risk of developing dementia (Tan et al., 2007). Another study found that serum TNFα levels were significantly higher in AD and MCI cases than in control cases. In the AD cases there was found to be a significant age associated increase in TNFα levels that did not occur in MCI or control cases. However, there was found to be no correlation between TNFα serum levels and age of onset, disease severity, sex or APOE4 status (Alvarez et al., 2007). Paganelli et al (2002) found that comparing within demented groups of patients, TNFα levels are predictors of the severity of cognitive decline. Paganelli compared mild to moderate AD with severe AD and found that severe AD was predicted by higher serum TNFα levels (Paganelli et al., 2002).

Studies of Cerebrospinal Fluid (CSF) have found altered levels of TNFα present prior to development of Alzheimer's disease. Patients with MCI displayed significantly greater levels of TNFα in the CSF compared to healthy controls. When this group of MCI patients were followed up 9 months later those that had progressed to Alzheimer's disease displayed significantly higher levels of TNFα in the CSF compared to controls, where those MCI patients that had not progressed to AD did not have significantly different levels of TNFα in the CSF (Tarkowski et al., 2003). In another paper by Tarkowski, CSF levels of TNFα in AD patients were found to be 25 fold higher than controls where serum levels of TNFα were not significantly different from controls (Tarkowski et al., 1999). The reason why serum levels of TNFα may not have been found to be different in this study as in the previously mentioned studies may be due to their low numbers and possibly less sensitive ELISA techniques. However this may also be explained by concurrent systemic inflammation in patients with MCI which contributed to progression to AD. The finding of hugely elevated levels of TNFα in the CSF implies that increasing levels are possibly linked with progression from MCI to AD. Preliminary data from a study of patients on anti-TNFα therapy for rheumatoid arthritis has shown a dramatically reduced risk of Alzheimer's (Chou, unpublished). Given this evidence there is a surprising lack of investigations into the effects of systemic TNFα on the vulnerable CNS.

Recent work on anti-TNFα therapies has shown that selective inhibition of solTNFα is a better option than complete blockade of TNFα (Zalevsky et al., 2007;

Olleros et al., 2009). Using therapies blocking both soluble and membrane bound TNF, have shown that rheumatoid arthritis and psoriatic arthritis patients were more susceptible to severe infections, especially TB due to TNFα blocking treatments (Gardam et al., 2003; Hamilton, 2004; Wallis et al., 2004). Patients on Etanercept (TNFα receptor fusion protein) were shown to have a 22.6% incidence rate of severe adverse events (SAEs). Patients taking Infliximab (monoclonal antibody against TNFα) show a SAE incident rate of 28.3% while control groups showed an incident rate of only 6.8% (Nacci and Matucci-Cerinic, 2011). Completely blocking TNFα can allow latent infections to take hold. It is now common practice prior to treatment to thoroughly screen for tuberculosis and hepatitis. However the WHO believe that one third of the population carry latent tuberculosis (Nacci and Matucci-Cerinic, 2011) and worldwide 400 million and 170 million carry Hepatitis B and C respectively (Vigano et al., 2012). Selective blockade of solTNFα would allow memTNFα to continue to function with no preferential receptor activation. SolTNF blockade can treat illnesses such as arthritis, psoriasis or Crohns disease while the memTNFα can still perform its duties in host immunity preventing opportunistic infections while not causing inflammation (Olleros et al., 2010).

1.13 - The role of systemic IL-1β in neurodegeneration

While there is extensive evidence for systemic inflammation in general contributing to cognitive decline it is often very difficult to determine which molecule is the root cause of this decline. IL-1β is an extremely potent cytokine; this means that miniscule amounts are required to have a dramatic effect. Many clinical studies find elevated levels of IL-6 or acute phase proteins in dementia patients however some people now believe that these molecules are not the root cause of any exacerbation but instead markers of IL-1β activity which is more likely to be behind exacerbated cognitive decline (Simi et al., 2007). Contributing to this idea genome analysis has shown that alleles which overexpress IL-1β and IL-1α increase incident risk of Alzheimer's disease (Nicoll et al., 2000).

Multiple studies have shown increased levels of systemic IL-1β in patients with pre-existing dementias compared to controls (Licastro et al., 2000; Zuliani et al.,

2007; Veryard et al., 2013). However there is very limited information on systemic levels of IL-1β prior to development of overt cognitive decline. A study comparing controls, MCI and AD showed that all variants of MCI and AD had significantly increased IL-1β compared to controls. In this study the most severe form of MCI showed IL-1β levels comparable to the AD cohort and was significantly elevated compared to not just controls (three fold), but also to the less severe MCI cohorts (Forlenza et al., 2009).

A Japanese group describes an "agitation state" which aggravates cognitive decline; this includes episodes of aggression and altered circadian rhythms. Patients who had an elevated level of systemic IL-1β concurrent with an episode of agitation were shown to be more significantly associated with AD (Higuchi et al., 2010; Honma et al., 2013).

Patients in a community dwelling cohort were examined for IL-1β levels and systemic inflammatory events (SIEs). This study though small showed that following an SIE systemic levels of IL-1β were elevated and this was associated with a greater cognitive decline over the following 2 months regardless of another SIE (Holmes et al., 2003).

In a post-ischemic stroke study the numbers of peripheral blood mononuclear cells (PBMCs) expressing IL-1β was found to correlate to the degree of neurological impairment at multiple timepoints post-ischemia (Kostulas et al., 1999). Intravenous IL-1Ra has been shown to ameliorate CNS injuries, as this is a very large molecule with very little crossing into the CNS, these results indicate a role for systemic IL-1β in neurological outcomes post-ischemia (Emsley et al., 2005).

1.14 - Advancing the priming story

Macrophage priming was first described in the early eighties. IFNγ can sensitise macrophages to subclinical doses of LPS producing exacerbated pro-inflammatory effects (Pace et al., 1983; Williams et al., 1992). It wasn't until 2005 that this same priming effect was found in the macrophages of the CNS, microglial cells. Microglial cells can be primed by a variety of stimuli to react in an exaggerated pro-inflammatory manner to a subsequent stimulus (Cunningham et al., 2005b).

Primed microglia react to secondary stimuli to produce exaggerated levels of IL-1β and NO. Astrocytic cells are also an important source of inflammatory mediators in the brain. Astrocytes are a significant cellular source of chemokines and given the response of primed microglial cells to acute stimulation, we hypothesized that the astrocytes in the degenerating brain would also respond in an exaggerated manner to acute cytokine stimulation.

Astrocytes present in neurodegeneration also undergo many alterations in the disease process. Neurons rely on astrocytes to provide a homeostatic microenvironment but in neurodegeneration astrocytes become hypertrophic (gliosis) or dystrophic. Knockdown of astrocytic NF-Kb has been shown to be neuroprotective in ischaemic and spinal cord injury (Brambilla et al., 2005; Brambilla et al., 2009; Dvoriantchikova et al., 2009). It has been shown that CCL2 present at amyloid plaques induces chemotaxis of astrocytes around the plaques (Khandelwal et al., 2011). There is some evidence that astrocytes produce cytokines in response to the presence of Aβ, primarily TNFα and IL-1β (Medeiros, 2013). Astrocytes surrounding amyloid plaques are also found to secrete large amounts of iNOS and astrocytes stimulated with Amyloid beta produce nitric oxide (NO) (Hu and Van Eldik, 1999; Wong et al., 2001; Haas et al., 2002). Neurons carrying NFTs are also found to be associated with activated astrocytes (Fuller et al., 2009). Post mortem PD brains show increases in astroglial cells and an increase in dystrophic astrocytes (Glass et al., 2010).

While astrocytes primarily act as support for neurons they are also important players in any immune response. This may be especially important in an aging or degenerating brain. Both CCL2 and CXCL-1 have been shown to be produced in vitro by astrocytes in response to many stimuli such as E-coli, LPS, IL-1, TNF, flagellin, endothelins and spinal crush injury (Kim et al., 2005; Wang et al., 2007; Thompson and Van Eldik, 2009; McKimmie and Graham, 2010; Pineau et al., 2010; van Neerven et al., 2010; An et al., 2011; Choi et al., 2011; Fouillet et al., 2012; Lee et al., 2012; Koyama et al., 2013). In many cases this chemokine induction has been shown to be Nf-κb dependent (Kim et al., 2005; Khorooshi et al., 2008; Thompson and Van Eldik, 2009; Lee et al., 2012). However p38/JNK has also been implicated in cytokine induced astrocytic chemokines (Wang et al., 2006b; Thompson and Van Eldik, 2009; Le Dreau et al., 2010). If the astrocytic population of the degenerating CNS is primed, could this priming be manifested in altered

chemokine profiles, thus altering the cellular infiltrate in response to elevated CNS cytokines.

1.15 - Aims and Objectives

We must understand the actions of systemic inflammatory cytokines such as TNFα and IL-1β on a neurodegenerating brain if we are to understand how co-morbidities may affect our aging population. Systemic and central inflammation have both been shown to exacerbate neurodegeneration however the mechanisms behind this remain unclear. In the western world we are facing an aging population replete with multiple systemic inflammatory co-morbidities and IL-1β and TNFα are factors that unify many systemic inflammatory diseases and conditions.

Neurodegeneration has been shown to prime the microglial population of the CNS to react in an exaggerated manner to subsequent inflammatory stimuli. Prior studies of glial priming predominantly use the exogenous PAMP LPS. Centrally occurring LPS is however a rare pathophysiological scenario. It is unknown whether primed microglia can also be activated by the endogenous cytokines TNFα and IL-1β.

The studies described in this thesis were designed to address two key questions:

1) What is the nature of glial priming in neurodegenerative diseases?

2) What are the consequences of further stimulation of a degenerating brain with the proinflammatory cytokines TNFα and IL-1β?

We hypothesised that the cytokines IL-1β and TNFα would be able to activate primed microglia in a similar manner to LPS. We believe that there would also be an altered activation state in the astrocytic cells of the neurodegenerating brain. We hypothesised that exaggerated acute microglial and astrocytic responses to inflammation would have long term consequences for cellular infiltration into a degenerating brain.

It was our intention to address these hypotheses in the following manner; in the third chapter we pathologically examined whether the cytokines TNFα and IL-1β administered intrahippocampally activated primed microglia in a manner similar

to central LPS, i.e. can induce microglia to produce exaggerated levels of IL-1β in ME7 animals. These animals were then examined at 2, 24 and 72 hours post challenge. We examined the effects of these centrally administered cytokines on other cell types in the neurodegenerating brain, such as astrocytes. Peripheral immune cell recruitment and extravasation, specifically neutrophils, macrophages and T-cells were also investigated. The effects of intrahippocampal LPS and IL-1β in the APP/PS1 model were also considered.

Systemic inflammation has been shown to accelerate and exacerbate neurodegeneration; human studies have shown that elevated levels of systemic TNF are a driver of this decline. Thus we hypothesised that elevated systemic TNFα will be detrimental to neurodegenerative models such as ME7 prion disease or APP/PS1 transgenic mice.

In the fourth chapter we sought to establish the effects of systemic TNFα on normal animals with a time course experiment examining inflammatory markers in blood plasma, and inflammatory and apoptotic markers in hippocampal and hypothalamic mRNA. Using information from this time-course we then examined the most salient time-points following systemic TNFα in the ME7 prion disease model of neurodegeneration. We investigated inflammatory mediators in the CNS, sickness behaviour and cognitive alterations at acute time-points. We also examined neurodegenerative and pathological effects at later time points. The effects of a Dominant Negative Sol-TNF inhibitor (XPRO1595) were investigated on levels of apoptosis following LPS. We also examined the effects of systemic TNFα in the APP/PS1 model of Alzheimer's disease, especially the effects of chronic TNFα on cognition.

Chapter 2

Methods

2.1 - Animals

Female C57BL/6 mice (Harlan, Bicester, United Kingdom) or female B6.Cg-Tg(APPswe,PSEN1dE9)85Dbo/Mmjax (MMRRC, Jackson Laboratories, California, USA) were housed in cages of 5 at 21°c with a 12:12 light, dark cycle. Food and water access was *ad libitum*. All animal experimentation was performed under a license granted by the Minister for Health and Children, Ireland, with approval from the local ethical committee and in compliance with the Cruelty to Animals Act, 1876 and the European Community Directive, 86/609/EEC, and every effort was made to minimize stress to the animals.

2.1.2 - ME7 Surgery

Mice were allowed to adjust to the animal unit for a 2-3 weeks before surgery. Avertin (2, 2, 2-tribromoethanol) was used at approximately 0.1ml per 5g body weight + 0.1ml. The mouse was prepped by shaving its head and administering local anaesthetic (lidocaine) to the ear canal. Using a stereotaxic frame a stable position was achieved using ear bars and an incisor bar (David Kopf Instruments, Tujunga, CA, USA). The scalp was incised allowing removal of the pericranial membrane, exposing the skull. Bregma was ascertained to find precise coordinates for injection. Holes were drilled at anteroposterior -2.0mm from bregma and lateral ±1.6mm either side of the midline, 1µl 10% w/v ME7 infected C57/BL6 brain homogenate is injected through a Hamilton microsyringe (Reno, Nevada, USA) to a depth of -1.7mm. The needle was left in situ for 2 minutes before slow withdrawal. Mice were placed in an incubator at ~25°c for recovery. When returned to their home cage they were administered Sucrose (5% w/v) and Carprofen (0.05% v/v; Rimadyl, Pfizer, Ireland) for 2 days post surgery. Animals were monitored for recovery from surgery. Control animals were administered 1µl 10% w/v normal brain homogenate (NBH).

2.1.3 - Treatment Administration

2.1.3.1 - Intraperitoneal TNFα

For intraperitoneal TNFα mice were injected with recombinant mouse TNFα (Peprotech, Rocky Hill, NJ, USA) at a dosage of 50 μg/kg or 250μg/kg prepared in sterile saline (Sigma, Poole, UK). Control animals were injected using sterile saline (Sigma, Poole, UK) 200μl per 20g body weight.

2.1.3.2 - Intrahippocampal TNFα

Intrahippocampal TNFα was prepared using sterile saline (Sigma, Poole, UK) to a dose of 300ng/μl. The animal is anaesthetized (Avertin) and placed in the stereotaxic frame (David Kopf Instruments, Tujunga, CA, USA) A hole was drilled and 1μl was administered unilaterally (coordinates from bregma: anteroposterior, -2.0mm; lateral, -1.6mm; depth -1.6mm) using a microcapillary left in place for 1 minute.

2.1.3.3 - Intrahippocampal IL-1β

Intrahippocampal IL-1β was prepared using sterile saline (Sigma, Poole, UK) to a dose of 10ng/μl. The animal is anaesthetized (Avertin) and placed in the stereotaxic frame (David Kopf Instruments, Tujunga, CA, USA) A hole was drilled and 1μl was administered unilaterally (coordinates from bregma: anteroposterior, -2.0mm; lateral, -1.6mm; depth -1.6mm) using a microcapillary left in place for 1 minute.

2.1.3.4 - Intrahippocampal LPS

Intrahippocampal LPS was prepared using sterile saline (Sigma, Poole, UK) to a dose of 1μg/μl. The animal is anaesthetized (Avertin) and placed in the stereotaxic frame (David Kopf Instruments, Tujunga, CA, USA) A hole was drilled and 1μl was administered unilaterally (coordinates from bregma: anteroposterior, -2.0mm; lateral, -1.6mm; depth -1.6mm) using a microcapillary left in place for 1 minute.

2.1.3.5 - Intraperitoneal XPRO1595

Intraperitoneal XPRO1595 (Xencor, Monrovia, CA, USA) was prepared in sterile PBS to a dose of 30mg/kg. Control animals were injected using sterile PBS 200μl per 20g body weight. XPRO1595 was used 1 hour prior to subsequent stimuli.

2.1.3.6 - Intraperitoneal MC21

Mc21 was a gift from Steffen Jung (Weizmann Institute, Rehovot, Israel). Depletion of systemic macrophages was achieved using a two dose administration, 14 hours prior to central challenge and 20 hours post central challenge. 200µl was administered i.p. independent of body weight.

2.1.4 - Behavioural Tests

2.1.4.1 - Open Field

The open field consisted of a plastic base (58 cm x 33cm) surrounded by walls of 19 cm. The floor of the box is divided into a grid of equal sized squares. Measurement was made of distance travelled (in terms of grid squares crossed) and total number of rears (frequency with which the mice stood on their hind legs in the maze). An animal's baseline activity is measured prior to experimentation. Animals were scored on 2 minutes in the Open Field.

2.1.4.2 - Core Body Temperature

A thermocouple rectal probe (Thermalert TH5, Physitemp; Clifton, NJ, USA) was used to measure core body temperature. The mice were acclimatised to measurement of rectal temperature for 2 days prior to experimentation to minimise stress effects. Baseline temperature was usually taken at time of challenge, followed by various timepoints.

2.1.4.3 - T Maze alternation task

Hippocampal-dependent working memory was assessed in mice by observing alternation behaviour in a novel water T-maze task (Murray et al., 2012). The T-maze, constructed from black perspex, was of the following dimensions (cm); long axis 67, short axis 38, depth 20 and arm width 7. Single 4 cm diameter holes were at the end of each choice arm, 2 cm from the floor and black exit holes were placed into these holes. These exit holes could be blocked to prevent escape from the maze. A "guillotine" door was inserted to prevent access to one or other choice arm. Water to a depth of 2 cm at a temperature of 20°C was poured into the maze; at this height a mouse must paddle and thus is motivated to leave the maze through an exit tube. Animals were taken with their cage mates to a holding cage. Each mouse was individually placed in the start arm of the maze with 1 arm

blocked, such that they were forced to make a left or right turn. The arm sequences were chosen in a pseudo-random manner, with equal numbers of left and right turns in any one session; moreover, there were no more than 2 consecutive runs to the same arm. On making the turn the mouse could escape from the water by entering the exit hole into small tube, and then a transit tube, in which it was carried to another holding cage. The animal remained in this holding cage for a 30 second intra-trial interval, in which the guillotine door was removed and exit tube switched to the opposite arm. The mouse was then replaced in the start arm and could choose either arm. Since the exit hole which it had escaped through was blocked, the mouse must alternate from its original turn to escape. On choosing correctly the mouse escaped to the transit tube and was returned to its home cage. On choosing incorrectly the mouse was allowed to self-correct to the correct exit arm. Animals were typically trained for 14 blocks of 10 trials (inter-trial interval of 20 minutes) before other experimental manipulations are performed.

Most animals reached alternation of greater than 80%. No animals were experimentally challenged unless they performed at 70% or above for consecutive days. Furthermore, no animals that performed at lower than 80% in the last block of 5 trials or displayed evidence of a side preference on the day prior to experimental challenges were included. Some animals developed a side preference in the course of training. In such a situation a correction strategy was employed. The side preference was broken in some cases, but not all, by not allowing mice to self-correct: i.e. instead of an animal being allowed to cross the T from the incorrect arm to the correct arm, the entrance to the correct arm was closed at the moment that the incorrect arm was chosen. The animals thus returned to the start arm and once again had the option to choose the correct arm. This was repeated until the animal finally chose the correct body turn when starting from the start arm. This correction strategy was only employed for animals displaying a complete side preference (i.e. always turning in one direction if that arm was open to them), was discontinued once their side preference was broken and was never employed within 2 days of administration of substances to examine effects on working memory.

2.1.4.4 - Y-maze reference memory task

The Y-maze is a hippocampal dependent reference memory task. A clear perspex Y-shaped-maze mounted on a white plastic base was filled with 2 cm of water at 20°C to 22°C, sufficient to motivate mice to escape the maze by paddling to an exit tube at the distal end of one arm, 2 cm above the floor. The location of the escape arm was fixed for each animal. Burrowing tubes were placed over the false exit tubes and the correct exit tube so that, from the centre, all arms looked identical. Mice were placed in one of the two possible start arms in a pseudorandomized sequence for 6 trials and the groups were counterbalanced with respect to the location of the exit. An arm entry was defined as entry of the whole body, excluding the tail. The mouse exits to a burrowing tube in which it is returned to its home cage. An incorrect trial is when a mouse explores the arm that is not the escape arm.

2.2 - Molecular Work

2.2.1 - Real-time Polymerase Chain Reaction (PCR)

2.2.1.1 - Tissue for quantitative PCR

Animals were terminally anaesthetised using ~200µl Sodium Pentobarbital i.p (Euthatal, Merial Animal Health, Essex, UK) and transcardially perfused with heparinised saline using a peristaltic pump (Anachem, Luton, UK). Brains were rapidly removed and the left and right hippocampus and the hypothalamus were dissected out. The tissue was snap frozen in Eppendorfs on liquid nitrogen before being stored at -80°c.

2.2.1.2 - RNA Isolation

Prior to work, the RNA area and all equipment was sterilised using 70% ethanol. The tissue was removed from the -80, but kept on dry ice. All samples were weighed to ensure they were within the required weight. An RNeasy Plus Mini Kit (Qiagen, Crawley, UK) was used for the procedure. Manufacturer's instructions were followed with minor alterations for optimisation. Lysis Buffer was made up from 10µl β-Mercaptoethanol to 1ml Buffer RLT Plus. 600µl of the Lysis Buffer was added to the sample tube and a pestle and mechanical homogeniser were

used to disrupt the tissue to a homogenous solution. The solution was placed in Qiashredder tubes and centrifuged in the IEC MicroCL 21R Centrifuge (Thermo Electron Corporation) for 6 minutes at 14,800rpm. The supernatant was transferred to Genomic DNA Eliminator tubes which were spun for 30 seconds on full speed. 550µl of 70% ethanol was added to the flow through of the Genomic DNA Eliminator tubes. This solution was added to RNeasy Spin Columns which were spun at 14,800rpm for 15 seconds. This allowed the RNA in the solution to bind to the column. The flow through from the RNeasy columns was discarded. The RNeasy columns were washed using 350µl of RW1 buffer and then spun for 15 seconds at 14,800rpm. The flow through was discarded. To ensure complete removal of all DNA a solution of DNase and buffer RDD (10µl:70µl respectively) was made up and added to the column for 15 minutes. The RNeasy columns were washed using 350µl of RW1 buffer and then spun for 30 seconds at 14,800rpm. The flow through was discarded. 500µl of Buffer RPE was added to the column and it was spun for 15 seconds at 14,800rpm. The flow through was discarded. 500µl of Buffer RPE was added to the column and it was spun for 2 minutes at 14,800rpm. The flow through was discarded. These steps wash the column and dry it. The column was placed in a new tube and spun for 1 minute at 14,800rpm to eliminate any carryover of Buffer RPE. The column was placed in a new tube. 30µl of RNase free water was added and the column was spun for 1 minute at 14,800rpm. The water in this step draws down the RNA from the Spin Column membrane. The samples were placed on dry ice to be quantified by the nanodrop.

2.2.1.3 - RNA Quantification

Using the Nanodrop ND1000 Spectrophotometer (Thermo Fisher Scientific) the total concentration and purity of the RNA in each sample was quantified. Using 1µl of RNase free water the machine was blanked. 1µl of each sample was then pipetted onto the fibre optic pedestal. The pedestal was wiped down between each quantification. Absorbance of each sample was measured at wavelengths of 260nm and 280nm. This gives the concentration of RNA using Beers Law and the formula A=eCl, where A is absorbance at 260nm, e is the RNA extinction coefficient (25µl/µg/cm), C is RNA concentration and l is the pathlength of the spectrophotometer (0.05mm - 0.1mm). The ratio of 260:280 determines the purity of the RNA. A ratio of 1.8 to 2.1 indicates pure RNA. The RNA was stored in the -80 until required for cDNA synthesis.

2.2.1.4 - cDNA synthesis

A High Capacity cDNA Reverse Transcriptase Kit (Applied Biosystems, Warrington, UK) was used for cDNA synthesis. All calculations were based on a reaction using 400ng of RNA per 20µl. Using the yields from the nanodrop the amount of sample required to have 400ng/20µl was calculated. This was then made up to 10µl using RNase free water. The other 10µl in the reaction was Master Mix. Master Mix was made up using; 2µl 10X RT Buffer, 0.8µl 25X dNTP mix, 2µl 10X RT random primers, 1µl Multiscribe Reverse Transcriptase, 4.2µl RNase free water to a final 10µl. In practice this Master Mix was made up in bulk. Two negative controls were prepared, the first contained no RNA and the second contained no Reverse Transcriptase, these were replaced with RNase free water. The 10µl of sample and 10µl of master mix were placed in a PCR mini tube. The samples were then placed in the thermocycler (Peltier Thermal Cycler PTC-200) at 25˚c for 10 minutes, 37˚c for 120 minutes and 85˚c for 5 minutes and 4˚c until collection. The samples were then centrifuged and stored at 4°c and used within 2 weeks or stored at -20°c for long term storage.

2.2.1.5 - Real Time PCR

The StepOne™ Real-Time polymerase chain reaction (PCR) system was supplied by Applied Biosystems (Warrington, UK) and used in 96-well format with a 25µl reaction volume per well for quantitative (Q)-PCR. Primers and probes used are shown in table 1 these were obtained from publications or designed using Primer Express software (Applied Biosystems, Warrington, UK). Probes were designed to cross introns such that they were cDNA specific. Where no probe was available SYBR green a fluorescent DNA binding probe was used. All primer pairs were checked for specificity following standard RT PCR using gel electrophoresis to produce a discrete band of the expected amplicon size.

PCR Master Mix of 24µl per well was made up. This consisted of 12.5µl TaqMan Universal PCR Master Mix (Applied Biosystems), 10µl RNase free water, 0.5µl forward primer, 0.5µl reverse primer and 0.5µl of the probe. 1µl of the template cDNA was then added to each well and mixed thoroughly. The plate was then sealed using the ABI Prism Optical Adhesive Cover and centrifuged to ensure there are no bubbles in the mix.

Real Time Quantitative Reverse Transcriptase PCR works by measuring fluorescent emission from each well. The plate was placed in the Applied

Biosystems 7300 Real Time PCR machine. PCR cycles have four stages; the first stage was at 50˚c for 2 minutes, the second stage was at 95˚c for 10 minutes, the third and fourth stages are then repeated a minimum of 40 times at 95˚c for 15 seconds and 60˚c for 1 minute. Quantification occurred at the end of each cycle during the 60˚c stage. Fluorescence is determined by the 5` to 3` activity of the Taq Polymerase in the Master Mix, on the probe. The probe which binds to the template cDNA is labelled with the reporter dye FAM and the quenching dye TAMRA. In the sample the probe binds to a specific sequence in the gene to be amplified. While the probe is intact, TAMRA quenches all fluorescence from FAM by means of Fluorescence Resonance Energy Transfer (FRET). However once the Taq Polymerase is activated by the PCR process the enzyme proteolytically cleaves the probe as it polymerases a new DNA strand, separating FAM and TAMRA. This allows FAM to fluoresce freely and this amount of fluorescence is directly related to the amount of the gene of interest present.

Assays were quantified using a relative standard curve. This was constructed using total RNA from a naive mouse brain 6 hours post Intrahippocampal LPS which produces a large reaction. CDNA is created using higher levels of mRNA. This ensures that the samples being tested will fall within the range of the standard curve. The curve is constructed using 1 in 4 serial dilutions from 1 to 1/1024. A curve is plotted of the Ct value (cycle threshold - the cycle number at which the fluorescence of the product of transcribed gene crosses the threshold of detection) versus the log of the concentration (assigned an arbitrary value since the absolute concentration of cytokine transcripts is not known). Verification that this curve is a straight line using the Pearson Coefficient confirms the efficiency of the PCR reaction across the entire concentration range and the equation of this line can then be used to calculate the relative concentrations of the experimental samples. Since the top standard has been assigned an arbitrary value, it follows that the calculated concentrations of all experimental samples will also have arbitrary values, but these values will be directly related to the equation of the line. All PCR data were normalised to the expression of the housekeeping gene glyceraldehyde-3-phosphate dehyrdrogenase (GAPDH).

Table 2.1 Mouse PCR Taqman probes and primers

Target	Accession Number	Oligonucleotide	Sequence	Amplicon Size (bp)
GAPDH		*Forward* *Reverse*	*5'-GACGGCCGCATCTTCTTGT-3'*	*65*

	XM_001473623.1	Probe	5'-CACACCGACCTTCACCATTTT-3' 5'-CAGTGCCAGCCTCGTCCCGTAGA-3'	
TNF α	M11731	Forward Reverse Probe	5'-CTCCAGGCGGTGCCTATG-3' 5'-GGGCCATAGAACTGATGAGAGG-3' 5'-TCAGCCTCTTCTCATTCCTGCTTGTGG-3'	149
IL-1β	M15131	Forward Reverse Probe	5'-GCACACCCACCCTGCA-3' 5'-ACCGCTTTTCCATCTTCTTCTT-3' 5'-TGGAGAGTCTGGATCCCAAGCAATACCC-3'	69
IL-6	NM_031168	Forward Reverse Probe	5'-TCCAGAAACCGCTATGAAGTTC-3' 5'-CACCAGCATCAGTCCCAAGA-3' 5'-CTCTGCAAGAGACTTCCATCCAGTTGCC-3'	72
IFN β	X14455	Forward Reverse Probe	5'-CCATCATGAACAACAGGTGGAT-3' 5'-GAGAGGGCTGTGGTGGAGAA-3' 5'-CTCCACGCTGCGTTCCTGCTGTG-3'	67
CCL2	NM_011333.3	Forward Reverse Probe	5'-GTTGGCTCAGCCAGATGCA-3' 5'-AGCCTACTCATTGGGATCATCTTG-3' 5'-TTAACGCCCCACTCACCTGCTGCTACT-3'	81
CXCL-1	NM_008176	Forward Reverse Probe	5'-CACCCAAACCGAAGTCATAGC-3' 5'-AATTTTCTGAACCAAGGGAGCTT-3' 5'-TCGCGAGGCTTGCCTTGACCC-3'	82
Inos	U43428	Forward Reverse Probe	5'-CAGCTGGGCTGTACAAACCTT-3' 5'-CATTGGAAGTGAAGCGTTTCG-3' 5'-CGGGCAGCCTGTGAGACCTTTGA-3'	95
Upar	NM_011113.3	Forward Reverse Probe	5'-TGCAATGCCGCTATCCTACA-3' 5'-TGGGCATCCGGGAAGACT-3' 5'-CCCTCCAGAGCACAGAAAGGAGCTTGAA-3'	116
CD68b	NM009853	Forward Reverse Probe	5'-CAAGGTCCAGGGAGGTTGTG-3' 5'-CCAAAGGTAAGCTGTCCATAAGGA-3' 5'-CGGTACCCATCCCCACCTGTCTCTCTC-3'	75
PTX3	X83601	Forward Reverse Probe	5'-ACAACGAAATAGACAATGGACTTCAT-3' 5'-CTGGCGGCAGTCGCA-3' 5'-CCACCGAGGACCCCACGCC-3'	62
CD11b	NM_001082960.1	Forward Reverse	5'-CTCCAACCTCCAGATCCGAG-3' 5'-TCCACAGTCTTTACCACGATG-3'	90
TNFR1	X57796	Forward Reverse	5'-GATGTAAAAGGAAAAGAACATAACAAGAAC-3' 5'-GATGGCAGGTATTACCAAGGAAGA-3'	132
Fas	M83649	Forward Reverse	5'-CTGCGATGAAGAGCATGGTTT-3' 5'-CCATAGGCGATTTCTGGGAC-3'	208
FasL	U58995	Forward Reverse Probe	5'-AAGAAGGACCACAACACAAATCTG-3' 5'-CCCTGTTAAATGGGCCACACT-3' 5'-TGCAGAAGGAACTGGCAGAACTCCG-3'	234
P53	NM_011640	Forward Reverse Probe	5'-CCACAGCGTGGTGGTACCT-3' 5'-TGTACTTGTAGTGGATGGTGGTATACTCA-3' 5'-AGCCACCCGAGGCCGGCT-3'	71
PUMA	NM_133234	Forward Reverse	5'-GCGGCGGAGACAAGAAGA-3' 5'-AGTCCCATGAAGAGATTGTACATGAC-3'	75
RIPK1	NM_009068	Forward Reverse Probe	5'-GAACTATTCGCTGGTGATGGAGTA-3' 5'-CACGATTATCCTTCCTTTCAATGA-3' 5'-TGCACGTGCTAAAGACCCAGATAGATGTCC-3'	103
NOXA	NM_021451	Forward Reverse	5'-CCTGGGAAGTCGCAAAAGAG-3' 5'-GAGCACACTCGTCCTTCAAGTCT-3'	79
Bax	L22472	Forward Reverse	5'-GCCAGACGATGGATTCTGTGA-3' 5'-TGAACTCTGGTCCCCAATGAC-3'	238
Bim	NM_207680.2	Forward Reverse	5'-GGCCAAGCAACCTTCTGATG-3' 5'-GCCTTCTCCATACCAGACGG-3'	326
Bid	NM_007544.3	Forward Reverse	5'-AGCACATCACAAACCTGCTG-3' 5'-CTGGCAATGTTGTGGATGAC-3'	223
Bcl-Xl	NM_009743.3	Forward Reverse	5'-GACTTTCTCTCCTACAAGC-3' 5'-CGAAAGAGTTCATTCACTAC-3'	365
Bcl-2	NM_177410.2	Forward Reverse	5'-GCTACCGTCGTGACTT-3' 5'-GCCGGTTCAGGTACTC-3'	231
Caspase 6	NM_009811.3	Forward Reverse	5' -CAACGCAGACAGAGACAACCT-3' 5' -TCGACACCTCGTGAATTTTGAG-3'	113

2.2.2 - Plasma ELISA

ELISA uses specific antibodies to bind and quantify proteins or antigens of interest. Animals were terminally anaesthetised with sodium pentobarbital

(~200µl per mouse i.p., Euthatal, Merial Animal Health, Essex, UK). The thoracic cavity was opened and blood collected in heparinised tubes directly from the right atrium of the heart. This whole blood was spun at 1.5 x *g* for 15 minutes to remove cells; the plasma was then aliquoted and stored at -20 °C. These samples were then analysed for IL-1β, TNF-α, IL-6, CXCL1 and CCL2.

A standard protocol was followed. Maxisorp (Nunc Immuno, Thermo Fisher Scientific) plates were used. The Maxisorp plate was coated with 100µl primary (capture) antibody. This was sealed and incubated over night at room temperature. In the morning the plate was washed 4 times using 100µl of a 0.05% Tween 20 PBS Wash Buffer per well, this was repeated between each step. 250µl 1% Bovine Serum Albumin blocked any non-specific binding sites on the surface of the ELISA plate. This was incubated on a rocker for 1 hour. Serial dilutions of both samples and standards were used. Different dilutions were used depending on the expected concentrations of the protein. All samples and standards were diluted using HPE (High Performance Elisa Buffer, Sanquin, Amsterdam, Netherlands) to 100µl, the plate was sealed and incubated on the rocker for 2 hoursat room temperature. 100µl of the secondary (detection) antibody was added to the plate for 1.5 hours. The antibody is biotinylated as part of the detection mechanism. Streptavidin – HRP (100ng/ml, 100µl per well; Sanquin, Amsterdam, Netherlands) was added to the plate. Streptavidin formed an avidin-biotin complex with the biotinylated detection antibody. The plate was incubated at room temperature out of direct light for 20 minutes. TMB and H_2O_2 were used as substrate solution. The substrate solution reacted with the HRP attached to the avidin-biotin complex to turn blue. The plate was incubated for ~20 minutes at room temperature out of direct light. 50µl of the stop solution (Sulfuric Acid) was added to each well turning the wells yellow. A plate reader was used to quantify the absorbance of the plate at 450nm with correction at 570nm determining protein quantity by colour density after extrapolation from the standard curve.

Table 2.2 ELISA Antibody concentrations

	IL-1β	TNFα	IL-6	CCL2	CXCL-1
Capture	4µg/ml	0.8µg/ml	2µg/ml	0.2µg/ml	2µg/ml
Detection	600ng/ml	150ng/ml	200ng/ml	50ng/ml	200ng/ml

2.2.3 - Immunohistochemistry

2.2.3.1 - Tissue Preparation

Animals were terminally anaesthetised with sodium pentobarbital (~200µl i.p, Euthatal, Merial Animal Health, Essex, UK) and transcardially perfused with heparinised saline for approximately 3 minutes followed by 10 % formalin (Sigma, Poole, UK) for approximately 15 minutes. Brains were then removed post-fixed in 7ml sterilin flasks over 2 days in formalin and then placed in PBS until embedding.

2.2.3.2 - Paraffin wax embedding and sectioning of tissue

Brains for embedding were placed in plastic cassettes (Thermo Fisher Scientific, Dublin, Ireland) and transferred to a container of 70% alcohol for 20 minutes to begin the dehydration process. This was followed by 1.5 hourly changes in successively increasing alcohols: 70% alcohol II, 80%, 95%, 100% I, 100% II. Cassettes were then placed in 100% alcohol III overnight. The following day cassettes went through two five hour periods in the clearing agent Histoclear II (National Diagnostics, Manville, NJ, USA) followed by a final overnight in Histoclear. The cassettes were then transferred to and put through two changes of molten paraffin wax (McCormick Scientific, St Louis, MO, USA), heated to 60°C, each for 2 hours. Embedding moulds were filled with wax, placed on a cooling stage and brains were removed from their cassettes and placed in the mould. Cassettes were placed on top of the mould and more wax was placed on top. The wax was allowed to solidify on a cooling stage. Coronal sections (10 µm) of brains were cut on a Leica RM2235 Rotary Microtome (Leica Microsystems, Wetzlar, Germany) at the level of the hippocampus and floated onto electrostatically charged slides (Menzel-Glaser, Braunschweig, Germany) and dried at 37°C overnight.

2.2.3.3 - General immunohistochemistry protocol

Sections were dewaxed in xylene and Histoclear and rehydrated through alcohols of decreasing concentration immediately before beginning a staining protocol. Immunohistochemistry was performed for the microglia marker IBA-1 (Abcam, Cambridge, UK), IL-1β (Peprotech, NJ, USA), TNFα (R&D Systems, Minneapolis, MN, USA), P65 (Santa Cruz Biotechnology, Heidelberg, Germany), CCL2 (R&D

Systems, Minneapolis, MN, USA), GFAP (DakoCytomation, Glostrup, Denmark), CXCL-1 (R&D Systems, Minneapolis, MN, USA), 6E10 (Covance, Princeton, NJ, USA), APP (Invitrogen, Dublin, Ireland), CD68 (AbD Serotec, Oxford, UK) , Pu.1 (Cell Signalling, Beverly, MA, USA), MBS-1 (A gift from Professor Daniel Anthony, Oxford, UK), MPO (Abcam, Cambridge, UK), CD3 (Dako,Cytomation, Glostrup, Denmark), NeuN (Chemicon/Millipore, Billerica, MA, USA) , Sy38 (Chemicon/Millipore, Billerica, MA, USA), PrP (Santa Cruz Biotechnology, Heidelberg, Germany), CatD (Santa Cruz Biotechnology, Heidelberg, Germany), Ubq (DakoCytomation, Glostrup, Denmark), AT8 (Pierce antibodies, Loughborough, UK), SMI-31 (Abcam, Cambridge, UK), SMI-32 (Novus Bio/Abcam, Cambridge, UK) and markers of apoptosis (TUNEL, Promega, Southampton, UK). Tissue sections were dewaxed in xylene for 30 minutes and passed to two separate vessels of Histoclear II for 10 minutes each to total clearance of wax from the tissue. Sections were then rehydrated through a series of ethanols of decreasing concentration: 100 % II, 100 % I, 95 %, 85 %, and 70 %. Following rehydration, non-specific endogenous peroxidase activity was eliminated (quenched) by incubating sections in 1 % v/v hydrogen peroxide in methanol (1 ml H_2O_2 per 100ml methanol) for 20 minutes. For some immunohistochemical reactions, heat based antigen retrieval was performed by incubation in citrate buffer, pH 6, and microwaving twice for 5 minutes followed by 5 minutes of cooling after incubation. Slides were cooled to room temperature by the slow addition of cold tap water. Sections were washed three times in PBS for 5 minutes, encircled with a ring of wax using a liquid blocking PAP pen (Sigma, Poole, UK), and the appropriate blocking serum applied (10 % in PBS - 40 µl) and incubated at room temperature for 40 minutes. Serum was tapped off and sections were incubated in 30 µl of primary antibody. Primary antibodies were prepared in PBS unless otherwise stated. Following primary antibody incubation, sections were washed three times in PBS for 5 minutes and incubated with secondary antibody. All biotinylated secondary antibodies were supplied by Vector Laboratories (Peterborough, UK). Three 5 minute washes with PBS followed and staining was then visualized using the ABC method using peroxidase as enzyme, 0.05% v/v hydrogen peroxide as substrate, and diaminobenzidine (DAB) as chromogen. Sections were incubated in ABC solution (1 drop reagent A and 1 drop reagent B added to 5 ml PBS as per the manufacturers instruction; Vector Laboratories,

Peterborough, UK) for 45 minutes followed by three washes in PBS, and finally developed in DAB solution (250 ml 0.1 M phosphate buffer, 5ml DAB, 125 µl hydrogen peroxide). All sections were counterstained with haematoxylin for 20 – 60 seconds depending on intensity desired, acidified in 1 % acid alcohol (1 % v/v hydrochloric acid in 70 % ethanol) for 5 seconds, and differentiated in Scott's tap water (500 ml distilled water, 15 g magnesium sulfate, 1 g potassium bicarbonate). Sections were dehydrated through a series of ethanols of increasing concentration for 5 minutes each (70 %, 80 %, 95 %, 100 % I, 100 % II), followed by two changes of Histoclear II for 10 minutes each, and a final incubation in xylene for 15 minutes. Slides were finally mounted in DPX (Sigma, Poole, UK) and coverslips applied.

2.2.3.14 - TUNEL

Immunohistochemistry for apoptotic cells was performed using the "Dead End" TUNEL staining kit (Promega, Southampton, UK) Non-specific peroxidase activity was eliminated as described above. Sections were then washed in 0.85% NaCl for 5 minutes before pretreatment with proteinase K (20 µg/ml) for 5 minutes. Sections were preincubated with equilibration buffer for 10 minutes at 37°c and then with TUNEL buffer (25 µl per section: 22 µl equilibration buffer, 2.5 µl nucleotide mix, 0.5 µl TdT enzyme) for 2 hours at 37 °C, labelling apoptotic cells with flourescein. The reaction was stopped by addition of a 2X sodium citrate solution to sections for 15 minutes. Sections were then blocked with 10% normal goat serum for 30 minutes. The secondary biotinylated anti-flourescein antibody (5 µg/ml) was incubated at room temperature for 30 minutes. The normal Avidin-Biotin-Complex method for visualisation as described above was then used. Cells that were TUNEL-positive and also showed evidence of nuclear condensation were counted in the hippocampal and thalamic regions of 10µm coronal sections. Two sections were counted and summed for each animal and groups of n = 4 or n = 5 animals were grouped to calculate average numbers of cells per treatment.

Table 2.3 Immunohistochemical conditions used

Antibody	Marker	Pretreatments	Block	Incubation	Secondary
IBA-1	Microglia	Citrate Pepsin (20mins)	10% Rabbit	1/2000 Overnight @ 4°C	Rabbit anti goat
P65	NF-κB P65	1% Triton (15mins)	10% Horse	1/1000 Overnight @ 4°C	Horse anti mouse
TNFα	TNFα	Citrate	10% Rabbit	1/1000 Overnight @ 4°C	Rabbit anti goat
IL-1β	IL-1β	Citrate	20%	1/50 in 20%	Goat anti

			Goat	Goat serum Overnight @ 4°C	rabbit
CCL2	CCL2	Citrate Pepsin (20mins)	10% Rabbit	1/100 Overnight @ 4°C	Rabbit anti goat
CXCL1	CXCL1	Citrate	10% Rabbit	1/50 in 10% Rabbit serum Overnight @ 4°C	Rabbit anti goat
GFAP	Astrocytes	Citrate	10% Goat	1/2000 Overnight @ 4°C	Goat anti rabbit
6E10	Amyloid beta	70% formic acid (20mins)	10% Horse	1/1000 Overnight @ 4°C	Horse anti mouse
APP	Amyloid precursor protein	PBS-T washes Citrate	10% Horse	1/100 90mins @ RT	Horse anti mouse
CD68	Microglia	0.5% Pronase (20mins)	10% Rabbit	1/50 Overnight @ 4°C	Rabbit anti rat
Pu.1	Microglia	Citrate 1% Triton (20mins)	10% Goat	1/400 Overnight @ 4°C	Goat anti rabbit
MBS-1	Neutrophils	PBS-T washes Citrate	10% Goat	1/5000 Overnight @ 4°C	Goat anti rabbit
MPO	Myeloperoxidase	Citrate 1% Triton (15mins)	10% Goat	1/50 Overnight @ 4°C	Goat anti rabbit
CD3	T-cells	Citrate Pepsin (20mins) 1% Triton (15mins)	10% Goat	1/250 in 10% Goat serum Overnight @ 4°C	Goat anti rabbit
NeuN	Neurons	Citrate	10% Horse	1/5000 Overnight @ 4°C	Horse anti mouse
Sy38	Synaptophysin	0.2M Boric acid, pH 9, 65°c (30min)	10% Horse	1/2000 Overnight @ RT	Horse anti mouse
PrP	Prion protein	90% formic acid (5min) 50µg/ml Proteinase K (30min)	10% Horse	1/100 Overnight @ 4°C	Horse anti mouse
Cat D	Cathepsin D	Citrate Pepsin (20min)	10% rabbit	1/500 Overnight @ 4°C	Rabbit anti goat
Ubq	Ubiquitin	90% formic acid (5min)	10% Goat	1/300 Overnight @ 4°C	Goat anti rabbit
AT8	Hyperphosphorylated Tau	Citrate	10% Horse	1/200 Overnight @ 4°C	Horse anti mouse
SMI-31	Phosphorylated neurofilament H	Citrate	10% Horse	1/1000 Overnight @ 4°C	Horse anti mouse
SMI-32	Un-phosphorylated Neurofilament H	Citrate	10% Horse	1/200 Overnight @ 4°C	Horse anti mouse

2.2.3.15 - Double labelling and confocal microscopy

Slides were dewaxed and rehydrated as per above. Slides are washed repeatedly between each step using PBS. Any pretreatments specific to either antibody is performed at this point. Slides were blocked with a serum compatible with both antibodies to be colocalised. The first primary antibody is applied and incubated overnight if necessary. The first fluorescent secondary is applied on day two and incubated for 90 minutes. From application of the first fluorescent antibody the slides are protected from light. Following the secondary a second block can be applied if compatible. The second primary is then applied and allowed to incubate

overnight if necessary. On day three the second secondary is applied for 90 minutes. This is washed off and the slides are washed using dH_2O. Hoechst stain is applied at 0.5µg/ml for 10 minutes. The slides are washed in dH_2O prior to coverslipping. Coverslips were washed in alcohol to remove any auto-fluorescence. Prolong Gold (Sigma) is used as an aqueous mounting solution. Cover slips are sealed using nail polish. Slides are allowed to dry overnight and cleaned using water prior to visualisation on an Olympus FV 1000 confocal microscope using FV10 ASW 3.0 software. Images were captures using sequential excitation of the fluorophores. Images were captured at 1024 pixels at 10µs per pixel. The Kalman filter was applied to each image to reduce background noise. Most images were obtained at 60x oil with optional digital zoom (numerical aperture 1.35).

Table 2.4 Fluorescent secondaries absorption spectra

Alexa Fluor Dye	Absorption Maxima (nm)	Emission Maxima (nm)
Hoechst	350	461
488	495	519
546	556	573
568	578	603
594	590	617
633	632	647

2.3 - Statistical Analysis

Statistical analyses were performed using Graphpad Prism or GB Stat. Graphpad Prism was used for One way and Two way ANOVAs. GB Stat was used for Three way ANOVAs. Bonferroni multiple comparison *post hoc* was used where appropriate. In all cases data are expressed as mean ± SEM.

Chapter 3

Central inflammation in neurodegeneration

The majority of the work in this chapter forms a manuscript which has been accepted for publication by the *Journal of Neuroscience*.

3.1 - Summary

Microgliosis and astrogliosis are standard pathological features of neurodegenerative disease. Microglia are primed by chronic neurodegeneration such that toll-like receptor agonists, such as lipopolysaccharide (LPS), drive exaggerated cytokine responses on this background. However, sterile inflammatory insults are more common than direct CNS infection in the degenerating brain and these insults drive robust IL-1β and TNFα responses. It is unclear whether these pro-inflammatory cytokines can directly induce exaggerated responses in the degenerating brain. We hypothesised that glial cells in the hippocampus of animals with chronic neurodegenerative disease (ME7 prion disease or APP/PS1 transgenic (TG) mice) would display exaggerated responses to central cytokine challenges. TNFα or IL-1β were administered intrahippocampally to ME7-inoculated mice and normal brain homogenate-injected (NBH) controls. Both IL-1β and TNFα produced much more robust IL-1β synthesis in ME7 than in NBH animals and this occurred exclusively in microglia. However, there was strong nuclear localisation of the NF-kB subunit p65 in the astrocyte population, associated with marked astrocytic synthesis of the chemokines CXCL1 and CCL2 in response to both cytokine challenges in ME7 animals. Conversely, very limited expression of these chemokines was apparent in NBH animals similarly challenged. Thus, astrocytes are primed in the degenerating brain to produce exaggerated chemokine responses to acute stimulation with pro-inflammatory cytokines. We also administered IL-1β or LPS intrahippocampally to APP/PS1 mice, this model also showed priming of microglia with an exaggerated IL-1β response and priming of astrocytes with exaggerated chemokine response in the APP/PS1 compared to WT. In the ME7 model we examined downstream effects of exaggerated chemokine expression, which resulted in markedly increased neutrophil, T-cell and monocyte infiltration and astrocyte proliferation in the diseased brain. These data have significant implications for acute sterile inflammatory insults such as stroke and traumatic brain injury occurring on a background of aging or neurodegeneration.

3.2 - Introduction

Microgliosis and astrogliosis are hallmarks of neurodegeneration. Microglia in the degenerating brain show a 'primed' response to LPS stimulation (Cunningham et al., 2005b). When first described, the term priming was used to convey that microglia responded to acute stimulation with the Pathogen Associated Molecular Pattern (PAMP) LPS by producing an exaggerated IL-1β response and robust synthesis of inducible nitric oxide synthase (iNOS), similar to the original description of peripheral macrophage priming (Pace et al., 1983). Microglial priming was first demonstrated in the ME7 model of prion disease but has been replicated in multiple models of brain pathology including aging (Chen et al., 2008), Tg2576 model of AD (Sly et al., 2001) and models of PD (Pott Godoy et al., 2008).

Godbout et al showed that older mice contained increased levels of IL-1β protein in the brain post systemic LPS compared to young animals (Godbout et al., 2005). Sly et al showed that 16 month old Tg2576 mice showed a greater production of cortical and hippocampal IL-1β protein in response to i.v. LPS than age matched non transgenic mice (Sly et al., 2001). Pott Godoy et al used the 6-OHDA model of Parkinson's to show that neurodegeneration in the substantia nigra in this model also primes microglia to produce exaggerated levels of IL-1β protein in response to central LPS (Pott Godoy et al., 2008). These studies indicate that aging, amyloid aggregation and neurodegeneration can also prime microglia which can then be activated in an exaggerated manner by LPS.

There is not specific evidence that primed microglia have a discrete molecular identity. Rather, one may use the term 'primed' to describe the propensity of a particular cell type to make an exaggerated response to a typical stimulus and therefore this terminology may also be applied to other CNS cell types in situations where they show exaggerated production of secretory products typical to that cell population. In the case of primed microglia they show an exaggerated IL-1/iNOS response to LPS (Cunningham et al., 2005b). However, all prior studies of microglial priming examine responses to LPS, the appearance of which inside the CNS is a rare pathological event. It is unclear whether microglia in the degenerating brain show differential responses to sterile inflammatory insults such as the pro-inflammatory cytokines IL-1β and TNFα and this was investigated

in the current study. Elevated levels of these cytokines are known to occur in the CNS following elevated systemic inflammation (Skelly et al., 2013b), over the course of a systemic illness or injury (Bromander et al., 2012; Granger et al., 2013) and these cytokines can also be elevated following stroke or traumatic brain injury (TBI) (Liu et al., 1993; Mathiesen et al., 1997; Hayakata et al., 2004; Hutchinson et al., 2007). Therefore the reaction of primed microglia to IL-1β and TNFα may be of more general relevance than previously described reactions to LPS.

It is also of considerable interest to interrogate whether astrocytes may also be primed to show exaggerated responses to typical stimulators of astrocyte activation. These cells support metabolic functions of neurons and maintain CNS homeostasis but they also have immune functions in the CNS. Stimuli such as Aβ, E.coli, Poly I:C, LPS and Flagellin induce production of chemokines such as CCL2 and CXCL1 in astrocytes in vitro (Kim et al., 2005; McKimmie and Graham, 2010) and both TNFα and IL-1β can also induce astrocyte CCL2 and CXCL1 in vitro (Thompson and Van Eldik, 2009; An et al., 2011; Choi et al., 2011; Lee et al., 2012). Thus, the hypothesis that both microglia and astrocytes in the degenerating brain may respond in an exaggerated manner to acute cytokine stimulation and that chemokine synthesis might be a significant feature of any such exaggerated response was examined. To investigate the reactions of both microglial and astrocytic cells to acutely elevated cytokines, intrahippocampal TNFα or IL-1β was administered to normal and ME7 prion-diseased animals and cytokine and chemokine expression was examined at 2 hours post-challenge. To investigate the cellular consequences of acute cytokine and chemokine secretion, neutrophil infiltration was examined at 24 hours and immune cell infiltration and proliferation at 72 hours was examined, predicting more robust infiltration and proliferation in animals with prior disease.

It is reported that IL-1β induces CXCL1 and neutrophil infiltration (Campbell et al., 2002) and TNFα induces CCL2 and monocyte infiltration (Campbell et al., 2005) and that these pathways only cross-over to a limited extent (Schnell et al., 1999a; Blond et al., 2002). However, experiments on the extent, and the cell-type selectivity, of immune cell infiltration after intracerebral inflammatory insult have generally been performed in young healthy animals. The degree to which inflammatory cell infiltration remains tightly regulated during acute insults to the

degenerating brain has been little studied and, therefore, patterns of immune cell infiltration after TNFα or IL-1β challenge in animals with existing neurodegeneration (ME7), compared to normal healthy animals was examined.

The ME7 prion disease model functions as a useful model of gradual and progressive neurodegeneration. However; it is also of great use to examine these features in models of Alzheimer's disease that utilise Amyloid beta aggregation such as the transgenic APP/PS1 model. Therefore to further examine the effects of neurodegeneration on microglial populations the APP/PS1 transgenic mouse model of Alzheimer's disease was utilised. To investigate the status of the microglial and astrocyte populations in the APP/PS1 model intrahippocampal LPS or IL-1β were administered at 3 and 2 hours post-challenge respectively and IL-1β, CCL2 and CXCL1 production was interroggated.

Thus the activation of primed microglia in response to central LPS or the cytokines IL-1β or TNFα in ME7 prion disease or the APP/PS1 transgenic model was investigated, and the response of primed microglia to systemic LPS in the APP/PS1 model.

Secondly the activation state of astrocytes in ME7 prion disease and the APP/PS1 model, and their response to central and systemic inflammatory activation was also investigated.

3.3 - Results

3.3.1 - Hippocampal inflammatory transcripts in NBH and ME7 animals 2 hours post intrahippocampal TNFα or IL-1β

Given the prediction of both microglial and astrocyte priming in the diseased brain, and exaggeration of cytokine and chemokine responses post-IL-1β (10ng) or TNFα (300ng), it was important to interrogate whether there was exaggerated or differential transcription of these genes and others that might confirm the further activation of astrocytes. Unilateral intrahippocampal injections of 1μl of TNFα or IL-1β were performed at the following coordinates from bregma: anteroposterior, -2.0mm; lateral, -1.6mm; depth -1.6mm. These injections were performed using a microcapillary, which was left in place for 1 minute. Animals were then terminally anaesthetised at 2 hours and transcardially perfused with heparinised saline. Hippocampal mRNA transcripts of cytokines, chemokines and markers of astrocytic activation were examined. PCR results were analysed by two-way ANOVA followed by Bonferroni *post hoc* tests.

Both IL-1β and TNFα treatment lead to significant transcription of IL-1β (figure 3.1a; main effect of treatment $P<0.001$, $F_{(2,18)}=13.05$). There were also main effects of disease and an interaction between disease and treatment ($P<0.05$, $F_{(2,18)}=3.65$) and levels were significantly increased in ME7 animals compared to NBH animals following both TNFα (Bonferroni *post-hoc*, $p<0.01$) and IL-1β ($p<0.001$) challenge.

There was a main effect of treatment on TNFα mRNA levels (figure 3.1b; $P<0.05$, $F_{(2,21)}=3.53$) but IL-1β was the more robust driver of TNFα transcription: ME7+IL-1β animals were significantly different to NBH+IL-1β animals (Bonferroni, $p<0.01$), while TNFα induced TNFα transcription equally in both NBH and ME7 animals.

CXCL1 analysis, in particular, showed a robust phenotypic switch between ME7+saline and ME7+IL-1β or TNFα (figure 3.1c). There was no expression in saline-treated animals (NBH or ME7) and no effect of disease but a main effect of treatment ($P<0.001$, $F_{(2,17)}=22.93$). CXCL1 transcription was induced by TNFα and IL-1β approximately equally in both NBH and ME7 animals.

CCL2 (figure 3.1d) was robustly induced by cytokine treatment ($P<0.001$, $F_{(2,21)}=10.46$), but also showed a main effect of disease ($P<0.001$, $F_{(1,21)}=24.23$). Importantly there was an interaction between these two effects ($P<0.05$, $F_{(2,21)}=4.303$) and CCL2 mRNA was significantly higher in ME7+TNFα and ME7+IL-1β compared to NBH groups similarly challenged (Bonferroni *post-hoc* tests, $p<0.01$).

RANTES (figure 3.1e) is a T-cell chemoattractant chemokine, and is significantly elevated by disease ($P<0.001$, $F_{(1,18)}=58.03$) but is also increased by TNFα, showing a significant effect of treatment ($P<0.05$, $F_{(2,18)}=5.904$) and an interaction between treatment and disease ($P<0.05$, $F_{(2,18)}=4.463$), with no obvious effect of TNFα in NBH animals. IL-1β appeared to have no effect on RANTES expression.

CXCL10 is a chemokine responsible for attracting monocytes and T-cells and was significantly induced by both IL-1β and TNFα (figure 3.1f). There was a main effect of treatment ($P<0.001$, $F_{(2,22)}=10.95$), of disease ($P<0.001$, $F_{(1,22)}=48.26$) and an interaction between these factors ($P<0.01$, $F_{(2,22)}=7.276$), which indicates much more robust acute induction in ME7 animals than in NBH. Bonferroni *post-hoc* tests indicate that CXCL10 (figure 3.1f) is significantly elevated following both TNFα and IL-1β treatment in ME7 versus NBH animals ($p<0.001$).

ICAM and VCAM are cell adhesion molecules necessary for peripheral cell infiltration into the CNS. ICAM (figure 3.1g) is robustly elevated by IL-1β ($p<0.001$) and TNFα ($p<0.001$) in ME7 animals compared to NBH animals. ICAM is significantly elevated by disease ($P<0.001$, $F_{(1,22)}=49.27$) and treatment ($P<0.001$, $F_{(2,22)}=11.17$), and there is a significant interaction between disease and treatment ($P<0.01$, $F_{(2,22)}=7.443$).

VCAM (figure 3.1h) is significantly elevated by disease ($P<0.05$, $F_{(1,22)}=4.519$) but was not significantly altered by either TNFα or IL-1β. There is a trend towards elevation following IL-1β and TNFα challenge however this time-point may be too early for significant alterations in VCAM transcription.

Astrogliosis is a significant feature of the ME7 strain of murine prion disease and GFAP mRNA (figure 3.2a) was significantly elevated in all ME7 animals (main effect of disease: $P<0.001$, $F_{(1,18)}=147.2$) but was not altered 2 hours after intra-hippocampal cytokine treatment. Other genes indicative of astrocyte activation such as PTX3, STEAP4 and TIMP1 were assessed, these have been shown in a microarray study to be upregulated in astrocytes following Middle Cerebral Artery

Occlusion (MCAO) or central LPS administration (Zamanian et al., 2012). Astrocytic pentraxin 3 (PTX3) has also been shown to be neuroprotective in a rat seizure model (Ravizza et al., 2001). STEAP4 (six-transmembrane protein of prostate 4) in the brain has not been studied however in the periphery it is responsible for metabolic regulation (Cheng et al., 2011). Tissue Inhibitor of Metalloproteinases 1 (TIMP1) has been shown to be responsible for controlling tissue remodelling post-CNS injury (Zhang et al., 2006).

PTX3 (figure 3.2b) is significantly increased by disease ($P<0.001$, $F_{(1,18)}=52.72$). However it was very robustly induced by cytokine treatment ($P<0.01$, $F_{(2,18)}=9.521$) and there was a significant interaction between disease and treatment ($P<0.01$, $F_{(2,18)}=8.245$) demonstrating that PTX3 is robustly increased by TNFα and IL-1β in ME7 but this is barely discernible in NBH animals similarly challenged (Bonferroni *post-hoc*, $p<0.001$). This strongly supports an exaggerated astrocyte response to cytokine stimulation.

STEAP4 (figure 3.2c) was significantly elevated by disease ($P<0.01$, $F_{(1,18)}=12.36$). Treatment also had a significant effect on expression ($P<0.001$, $F_{(2,18)}=13.05$) and while TNFα had more robust effects on STEAP4 in ME7 than in NBH animals (Bonferroni *post-hoc*, $p<0.001$), IL-1β treatment had equivalent effects on STEAP4 in both NBH and ME7. There was an interaction between disease and treatment ($P<0.05$, $F_{(2,18)}=5.516$) indicating more robust effects of TNFα in ME7 animals with respect to NBH. TIMP1 (figure 3.2d) was significantly elevated by disease ($P<0.001$, $F_{(1,22)}=56.62$) but was not altered by either treatment.

Generally these data show more robust effects of cytokine treatment on cytokine, chemokine and astrocyte transcripts in ME7 than in NBH animals. While many markers are already elevated somewhat in ME7, others such as CXCL1 are not. PTX3 and STEAP4 both indicate exaggerated astrocytic activation in ME7 animals following intrahippocampal challenges. Exaggerated induction of astrocytic transcripts and chemokine proteins in astrocytes, were demonstrated in this study in the degenerating brain compared to the normal brain following central sterile inflammatory insult.

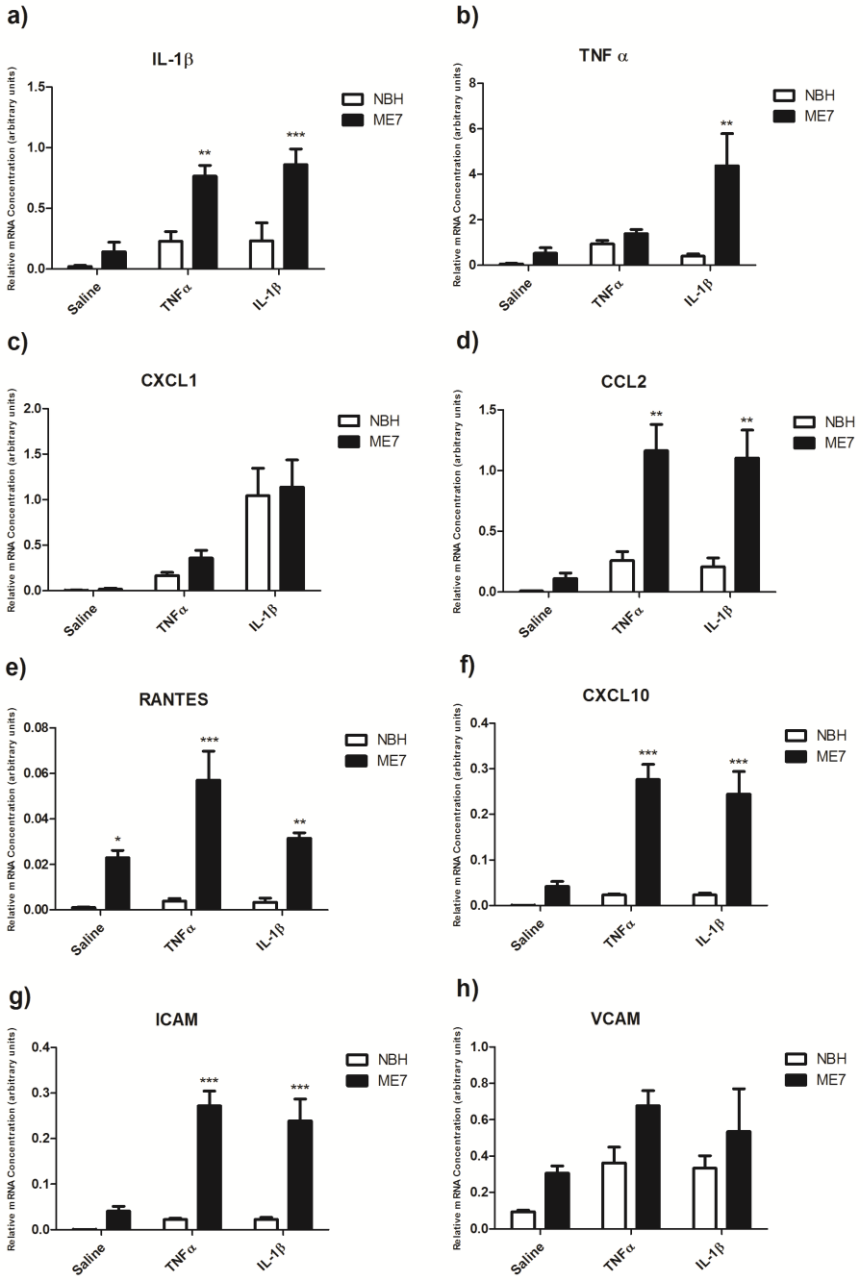

Figure 3.1 Impact of i.h.c TNFα and IL-1β on hippocampal inflammatory transcripts

Measures of hippocampal inflammatory transcripts 2 hours post TNFα (300ng) or IL-1β (10ng) i.h.c in ME7 animals 18 weeks post inoculation. Data were analysed using a Two Way ANOVA followed by a Bonferroni multiple comparison test comparing NBH to ME7. Statistical significance is denoted by * (P<0.05), **(P<0.01), ***(P<0.001). All data are represented as the mean ±SEM, n=3-6 for all groups.

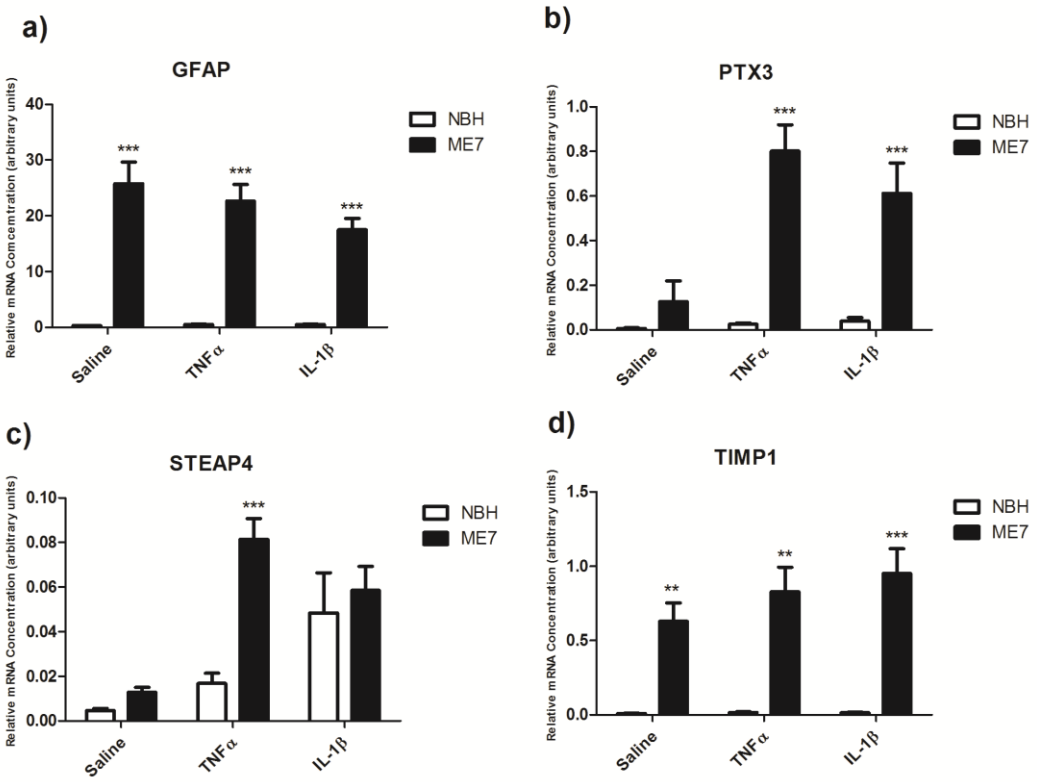

Figure 3.2 Impact of i.h.c TNFα and IL-1β on hippocampal astrocyte transcripts

Measures of hippocampal astrocyte transcripts 2 hours post TNFα (300ng) or IL-1β (10ng) i.h.c in ME7 animals 18 weeks post inoculation. Data were analysed using a Two Way ANOVA followed by a Bonferroni multiple comparison test comparing NBH to ME7. Statistical significance is denoted by * ($P<0.05$), **($P<0.01$), ***($P<0.001$). All data are represented as the mean ±SEM, n=3-6 for all groups.

3.3.2 - Immunohistochemical analysis of inflammatory changes 2 hours post-intrahippocampal TNFα or IL-1β

Microglial labelling with IBA-1 was examined 2 hours after IL-1β and TNFα challenges. There were no apparent morphological alterations in microglia in normal animals 2 hours post cytokine challenge (figure 3.3a, b, c). As previously described microgliosis occurs in ME7 animals, increasing microglial numbers and altering morphology (3.3a, b, c versus d, e, f). Using the higher power images g, h and i, it is possible to discern a robust alteration in microglial morphology occurring in ME7 animals following cytokine challenge. Following both cytokine challenges, microglia in ME7 animals display a more condensed cell body with retracted processes compared to the less dense cell body and more ramified processes displayed in vehicle injected ME7 animals (figure 3.3g).

These sections were also labelled with antibodies against IL-1β or TNFα. The injected TNFα is apparent in the hippocampus of both NBH (figure 3.3l) and ME7 (3.3o), owing to the relatively large amount injected (300 ng) and it is not possible to establish whether there is any *de novo* TNFα production in these animals. There is a robust upregulation of TNFα mRNA at 2 hours post-IL-1β in the ME7 animals. However figure 3.3k and n show that intrahippocampal IL-1β does not induce any TNFα protein at 2 hours post-injection. This would indicate that production of TNFα protein is at least to some degree under translational control.

Unlike TNFα, injected IL-1β could not be observed due to the small amounts of this potent cytokine injected (10 ng). Reliably detectable IL-1β production in NBH animals; whether saline- or cytokine-injected was not found (figure 3.3p, q, r). Vehicle-injected ME7 animals (figure 3.3s) show a small amount of detectable IL-1β adjacent to the needle track, however both IL-1β (3.3t) and TNFα (3.3u) robustly induce IL-1β throughout the hippocampus of ME7 animals at 2 hours post challenge. Without exception, the morphology of IL-1β-positive cells was microglial. Bright-field microscopy was sufficient to discern IL-1β produced exclusively by cells with branched processes and small elongated nuclei (microglial) alongside large, rounded astrocytic nuclei devoid of IL-1β protein labelling (figure 3.3u inset). Double labelling was performed for the microglial marker IBA-1 and IL-1β following both challenges in order to confirm this observation. Figure 3.4c shows co-localisation of IL-1β production (green) with

IBA-1 (red) following IL-1β challenge in ME7. Figure 3.4f shows co-localisation of IL-1β production with IBA-1 following TNFα challenge in ME7. Thus these microglia are primed to produce exaggerated IL-1β production upon challenge with either IL-1β or TNFα. Furthermore they show evidence of morphological change as soon as 2 hours post-cytokine challenge.

Figure 3.3 Microglial priming, activation and IL-1β synthesis.

Microglial activation status was examined at 2 hours post-intrahippocampal IL-1β (10ng) or TNFα (300ng) challenge in NBH and ME7 animals. Hippocampal CA1 IBA-1 microglial labelling x20 (a-f), x100 (g-i). Hippocampal TNFα labelling x5 (j-o). Inset (n) shows TNFα labelling after i.h.c LPS with and without preabsorption of the antibody with excess TNFα. Hippocampal IL-1β labelling is shown at x20 (p-u). Inset (u) shows IL-1β positive microglia adjacent to unlabelled astrocytic-like nucleus.

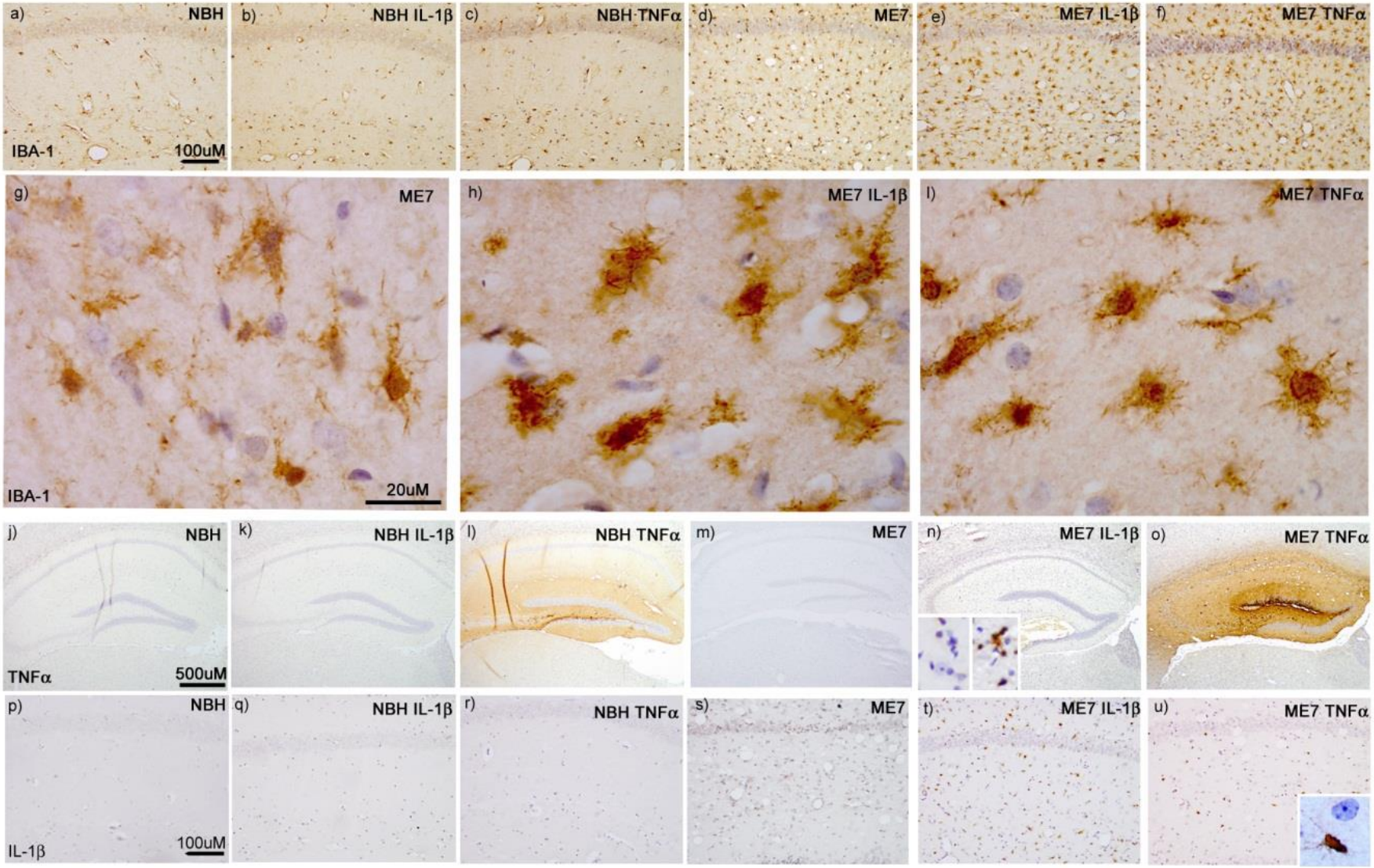
a) NBH
b) NBH IL-1β
c) NBH TNFα
d) ME7
e) ME7 IL-1β
f) ME7 TNFα
IBA-1
100uM
g) ME7
h) ME7 IL-1β
l) ME7 TNFα
IBA-1
20uM
j) NBH
k) NBH IL-1β
l) NBH TNFα
m) ME7
n) ME7 IL-1β
o) ME7 TNFα
TNFα
500uM
p) NBH
q) NBH IL-1β
r) NBH TNFα
s) ME7
t) ME7 IL-1β
u) ME7 TNFα
IL-1β
100uM

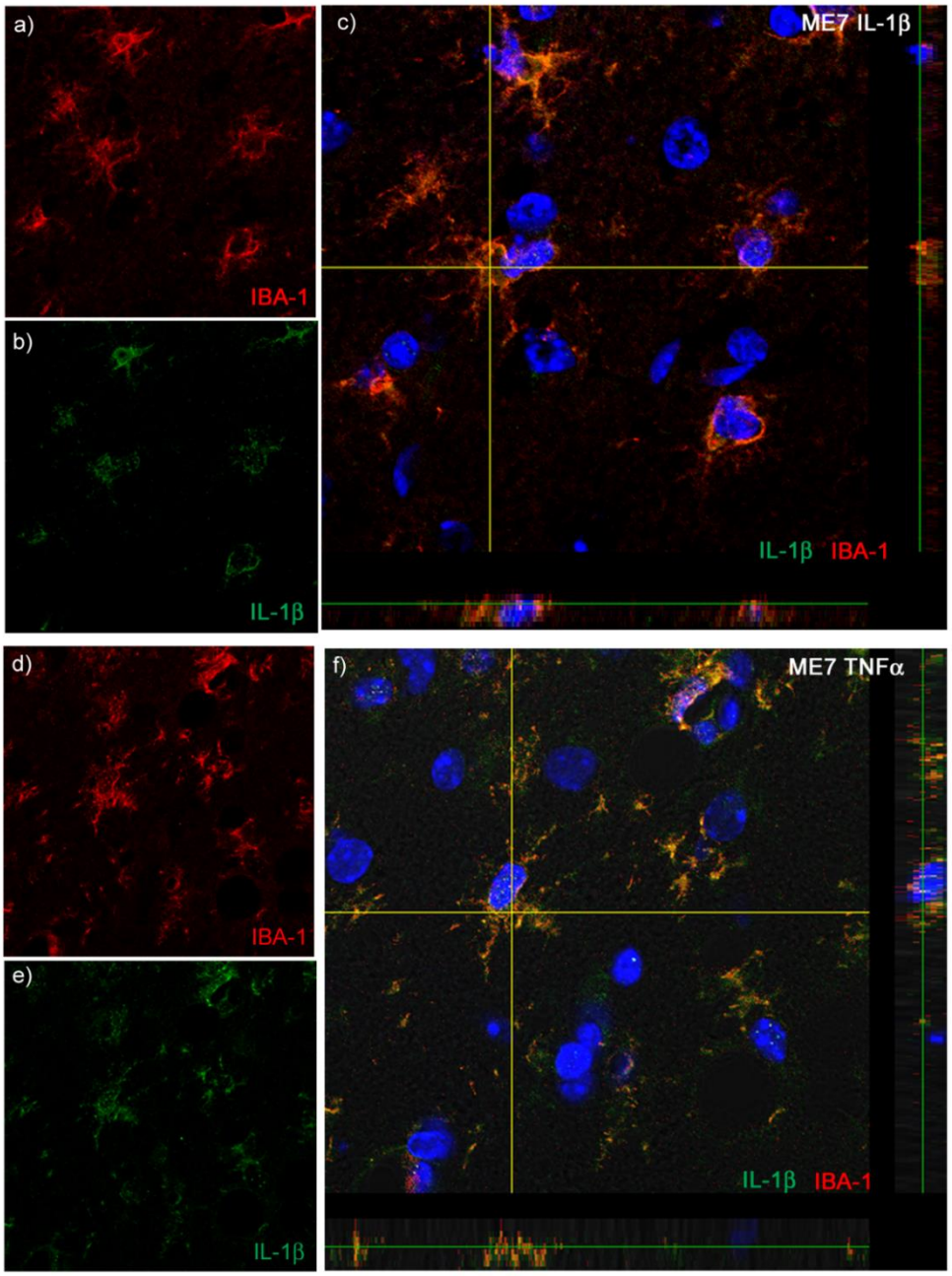

Figure 3.4 Colocalisation of microglial marker IBA-1 and IL-1β

Microglial production of IL-1β was examined 2 hours post-intrahippocampal IL-1β (10ng) or TNFα (300ng) challenge in NBH or ME7 animals. Overlap of the two signals indicates the microglial cells are producing IL-1β. (a-f) fluorescent double labelling of IBA-1 (594 nm) with IL-1β (488 nm) and Hoecsht 33258 (blue) in ME7 animals 2 hours post IL-1β (a-c) or TNFα (d-f).

Based on the well-described activation of NF-κB by IL-1β and TNF, the p65 subunit of NF-κB was examined. Nuclear localisation of p65 indicates activation of NF-κB and will generally lead to initiation of transcription of NF-κB-dependent genes in that cell. Nuclear localisation of p65 was not readily apparent in NBH and ME7 animals. However following both IL-1β and TNFα challenge there was clear nuclear localisation of p65 in both NBH and ME7 animals. These cells, positive for nuclear localised p65, were more frequent in ME7 animals challenged with IL-1β (Figure 3.5e) or TNFα (3.5f) than in NBH animals challenged with IL-1β (3.5b) or TNFα (3.5c) and included nuclei resembling those of both astrocytes (large and round, white arrow, figure 3.5f) and microglia (small and often somewhat elongated, black arrow, figure 3.5f).

Immunolabelling for the chemokine CCL2 (macrophage chemoattractant protein, MCP-1) was assessed and found no readily detectable parenchymal CCL2 in NBH (Figure 3.5g) and very few cells, adjacent to the injection track in vehicle-injected ME7 (3.5j) animals (but not sham-operated). NBH animals challenged with TNFα (3.5i) showed barely discernible, levels of parenchymal CCL2 induction while ME7 animals challenged with TNFα (3.5l) showed a very robust induction of CCL2. ME7 animals challenged with IL-1β (3.5k) also showed a very robust induction of CCL2, but once again there was little or no detectable parenchymal induction of CCL2 in NBH animals treated with IL-1β (3.5h). Thus, ME7 animals show an exaggerated induction of CCL2 expression following both IL-1β and TNFα challenges. The vast majority of the CCL2 protein appears clustered in granules surrounding large round nuclei resembling those of astrocytes while small elongated microglial-like cells remain negative (Inset in figure 3.5l).

Immunolabelling for the neutrophil chemoattractant CXCL1 (CINC-1, KC, GROα) was also performed. There was no detectable parenchymal CXCL1 induction in either NBH (3.5m) or ME7 (3.5p) animals. NBH+IL-1β (3.5n) animals showed a low level induction of CXCL1 that is barely discernible even at 100X magnification. However, ME7+IL-1β (3.5q) animals showed a robust and clearly demonstrable CXCL1 induction. ME7+TNF (3.5r) showed a large induction of CXCL1 similar to ME7+IL-1β (3.5q). NBH animals showed no induction of CXCL1 following TNFα challenge (3.5o). Once again, CXCL1 appeared clustered around astrocytic-like

nuclei but not microglial-like nuclei (inset 3.5r). Thus, ME7 animals show exaggerated induction of CXCL1 and CCL2 following both IL-1β and TNFα. This is not because there are more astrocytes: not a single cell in any of the NBH animals shows an equivalent response to what is observed in a large number of the astrocytes in the ME7 brain.

Although our lab has previously described exaggerated responses of primed microglia to acute LPS challenge (Cunningham et al., 2005b) and here show that this is also true for exaggerated IL-1β responses to acute IL-1β or TNFα challenge, the labelling patterns with NFκB p65, CCL2 and CXCL1 were all suggestive of a predominantly astrocytic localisation. That is to say, the labelling was manifest as a 'cloud' of vesicles proximal to large rounded nuclei resembling astrocytes rather than small elongated nuclei resembling microglia. This was a consistent feature and it was difficult to identify any chemokine labelling reliably associated with microglial-like nuclei. Astrogliosis is known to occur in ME7. This is evident in the glial fibrillary acidic protein (GFAP)-labelled sections of ME7 animals (Figure 3.5v), compared to NBH (3.5s). The ME7-associated astrogliosis is prominent in the stratum radiatum of the hippocampus, which is the region of the most intense chemokine production in the current study. Thus both morphology and location suggested that the astrocytes were the source of chemokines.

To confirm our observations from light microscopy, double-labelling of p65, CCL2 and CXCL1 with GFAP was performed. Figure 3.6 (a-i) shows double labelling of these markers in an ME7 animal following TNFα challenge. It is clear that p65 (red) labelling is within the nucleus of the GFAP (green)-positive astrocytic cells (Figure 3.6c). There is some limited evidence of microglial p65 nuclear localisation in smaller more elongated nuclei but this is not as robust by confocal imaging as was the case by light microscopy, perhaps due to generally weaker p65 labelling by confocal. Figure 3.6f shows the presence of CCL2-positive (red) vesicles inside a GFAP-positive astrocyte (green), while figure 3.6i shows the presence of CXCL1 (red) in the cell body of an astrocyte. There was very limited chemokine labelling that was not associated with astrocytes or the vasculature arguing against a significant contribution from microglia. These images indicate that ME7 animals challenged with TNFα show activation of astrocytes resulting in production of the

chemokines CCL2 and CXCL1. This astrocyte localisation of the cytokine-induced chemokine was also true of IL-1β challenged animals: CCL2 (red) co-localised with astrocytic GFAP (green) following IL-1β challenge in ME7 animals (Figure 3.7d). Collectively the data from figures 3.5 to 3.7 indicate that astrocytes in the degenerating brain are primed by the primary pathology of ME7 to show exaggerated chemokine responses to subsequent stimulation with cytokines. Under these neurodegenerative conditions, acutely administered IL-1β robustly induced CCL2 and TNFα robustly induced CXCL1 as soon as 2 hours post-challenge with these cytokines. While in normal animals IL-1β does not produce significant CCL2 and TNFα does not produce significant CXCL1.

Peripheral immune cell infiltration is influenced by events at the cerebral endothelium. Figure 3.8 (a-d) shows representative images of CCL2 and CXCL1 expression at the major blood vessels of the hippocampus and at the glia limitans that separates the hippocampus from the CSF in ME7 animals challenged with IL-1β and TNFα. Unlike astrocytic labelling, vascular labelling with CXCL1 and CCL2 was always detectable in both NBH and ME7 animals. Figure 3.8e shows the colocalisation of the astrocytic marker GFAP with CCL2 proximal to a blood vessel and CCL2 on the luminal surface of the vessel, where it can stimulate circulating macrophages.

Figure 3.5 Astrocyte priming, activation and chemokine synthesis.

NF-κB activation and chemokine expression 2 hours post-intrahippocampal IL-1β (10ng) or TNFα (300ng) challenge of NBH and ME7 animals. NF-κB p65 labelling (x100) in the hippocampus (a-f) with astrocytic-like nucleus indicated by white arrow and microglial-like nucleus indicated by black arrow in 2f. Hippocampal CCL2 labelling at x100 magnification (g-l). CXCL1 labelling at x100 magnification (m-r). Insets show CCL2 and CXCL1 labelling (l,r respectively) associated with an astrocyte-like nucleus adjacent to a microglia-like nucleus devoid of labelling. Hippocampal CA1 GFAP astrocyte labelling in NBH and ME7 animals is shown at x20 (s-x).

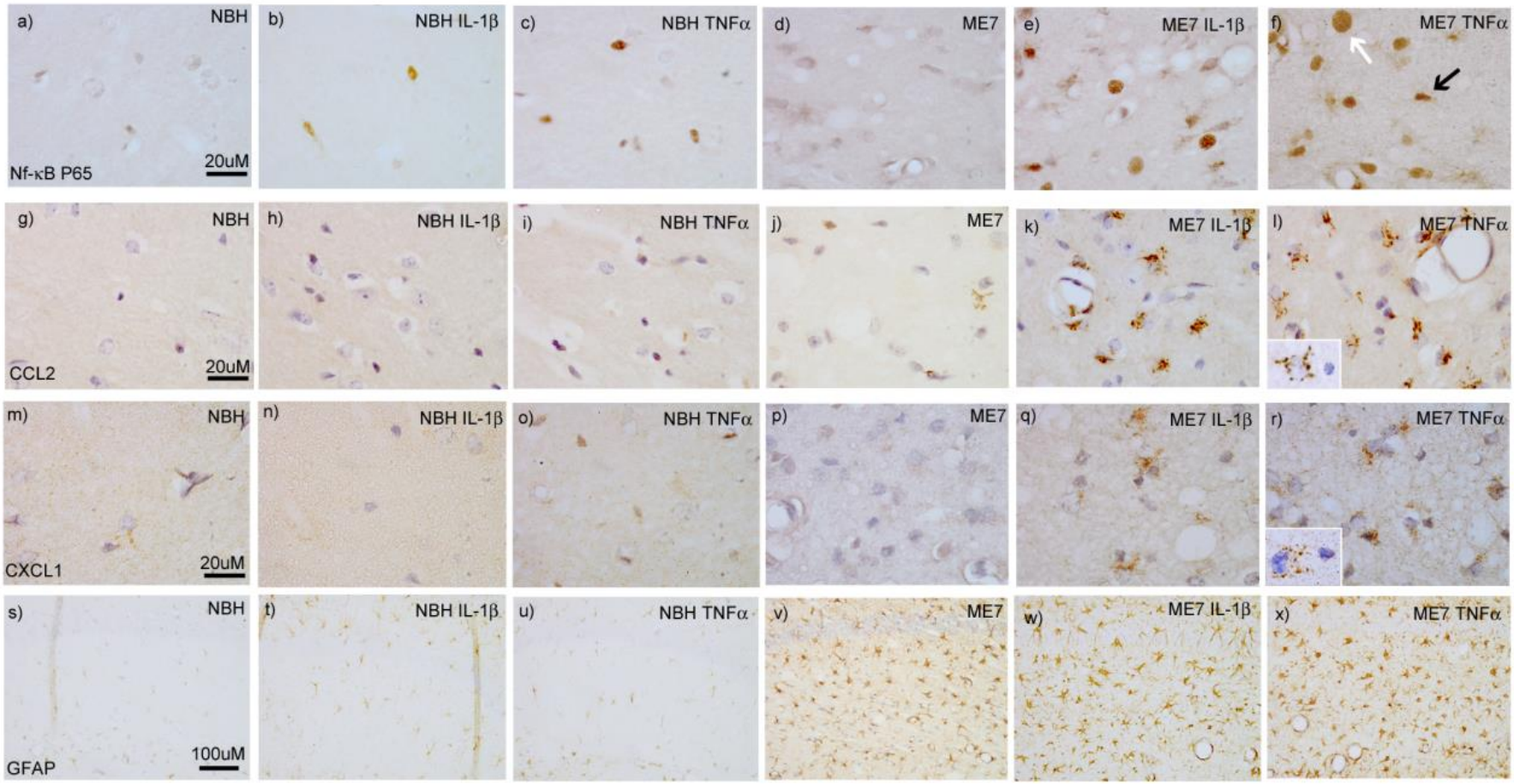
a)
NBH
Nf-κB P65
20uM
b)
NBH IL-1β
c)
NBH TNFα
d)
ME7
e)
ME7 IL-1β
f)
ME7 TNFα
g)
NBH
CCL2
20uM
h)
NBH IL-1β
i)
NBH TNFα
j)
ME7
k)
ME7 IL-1β
l)
ME7 TNFα
m)
NBH
CXCL1
20uM
n)
NBH IL-1β
o)
NBH TNFα
p)
ME7
q)
ME7 IL-1β
r)
ME7 TNFα
s)
NBH
GFAP
100uM
t)
NBH IL-1β
u)
NBH TNFα
v)
ME7
w)
ME7 IL-1β
x)
ME7 TNFα

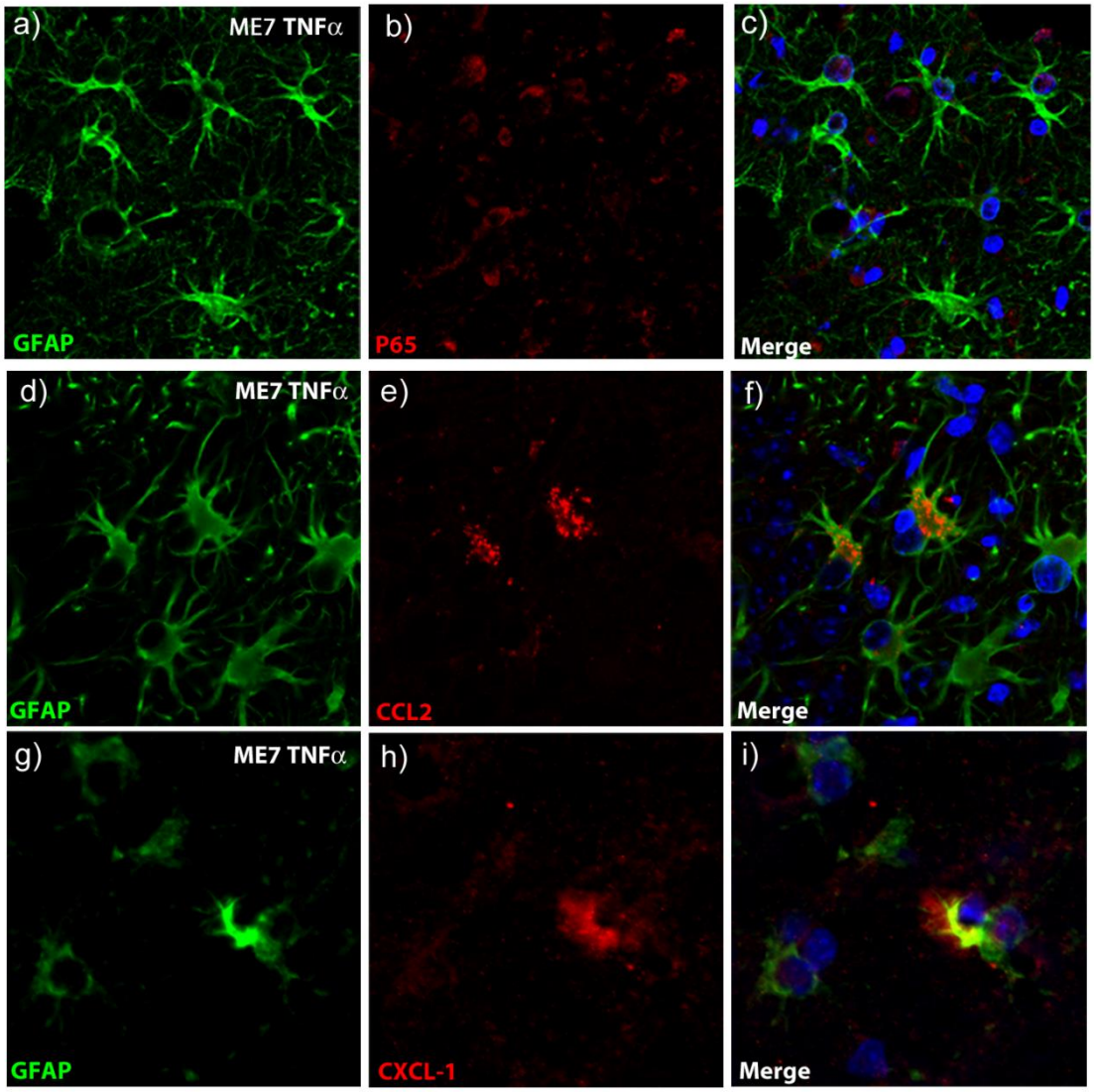

Figure 3.6 Colocalisation of GFAP with P65, CCL2 or CXCL-1 following intrahippocampal TNFα

Hippocampus region of 18 weeks ME7-inoculated animals, treated with TNFα (300ng), 2 hours post challenge. (a-i) fluorescent labelling of GFAP (488 nm) with either (c) p65 (633 nm), (f) CCL2 (594 nm) and (i) CXCL1 (594 nm) 2 hours post TNFα challenge.

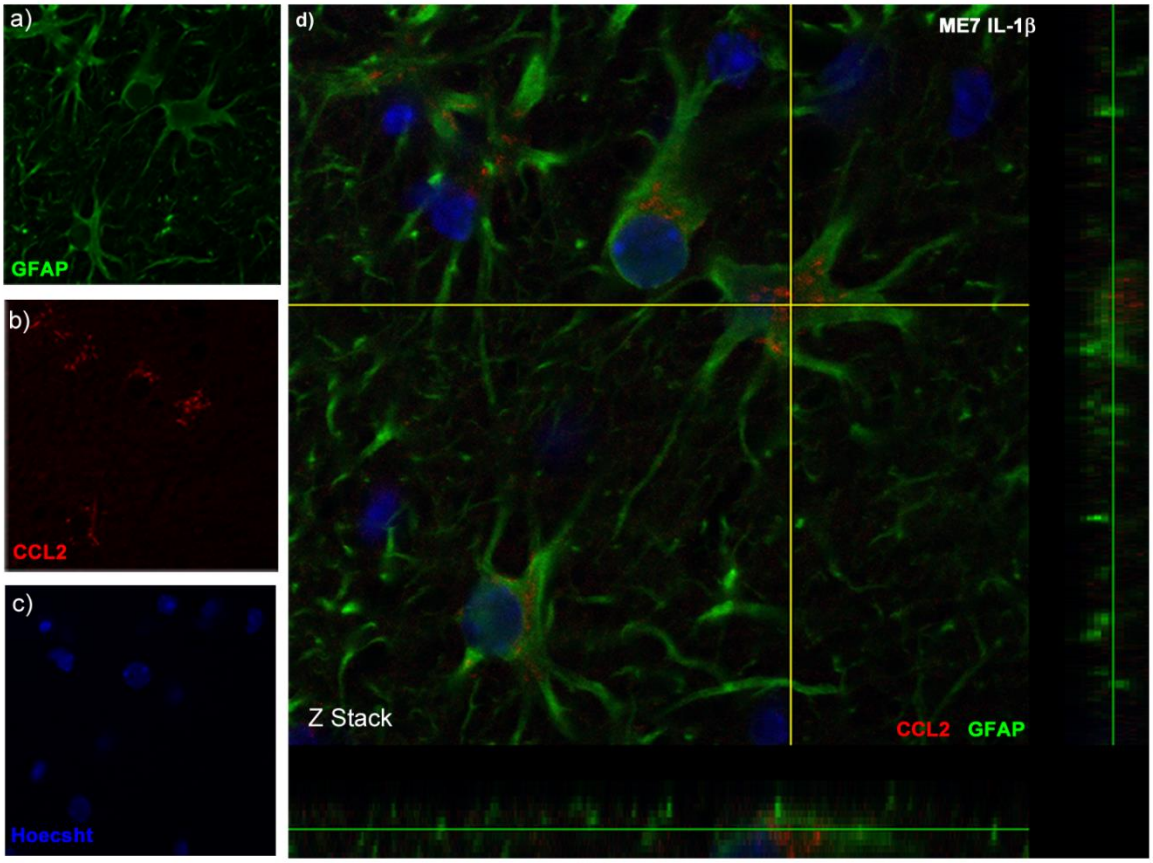

Figure 3.7 Colocalisation of GFAP with CCL2 following intrahippocampal IL-1β

Hippocampus region of 18 weeks ME7-inoculated animals, treated with IL-1β (10ng), 2 hours post challenge. (a-d) fluorescent labelling of GFAP (488 nm) and CCL2 (594 nm) 2 hours post IL-1β challenge.

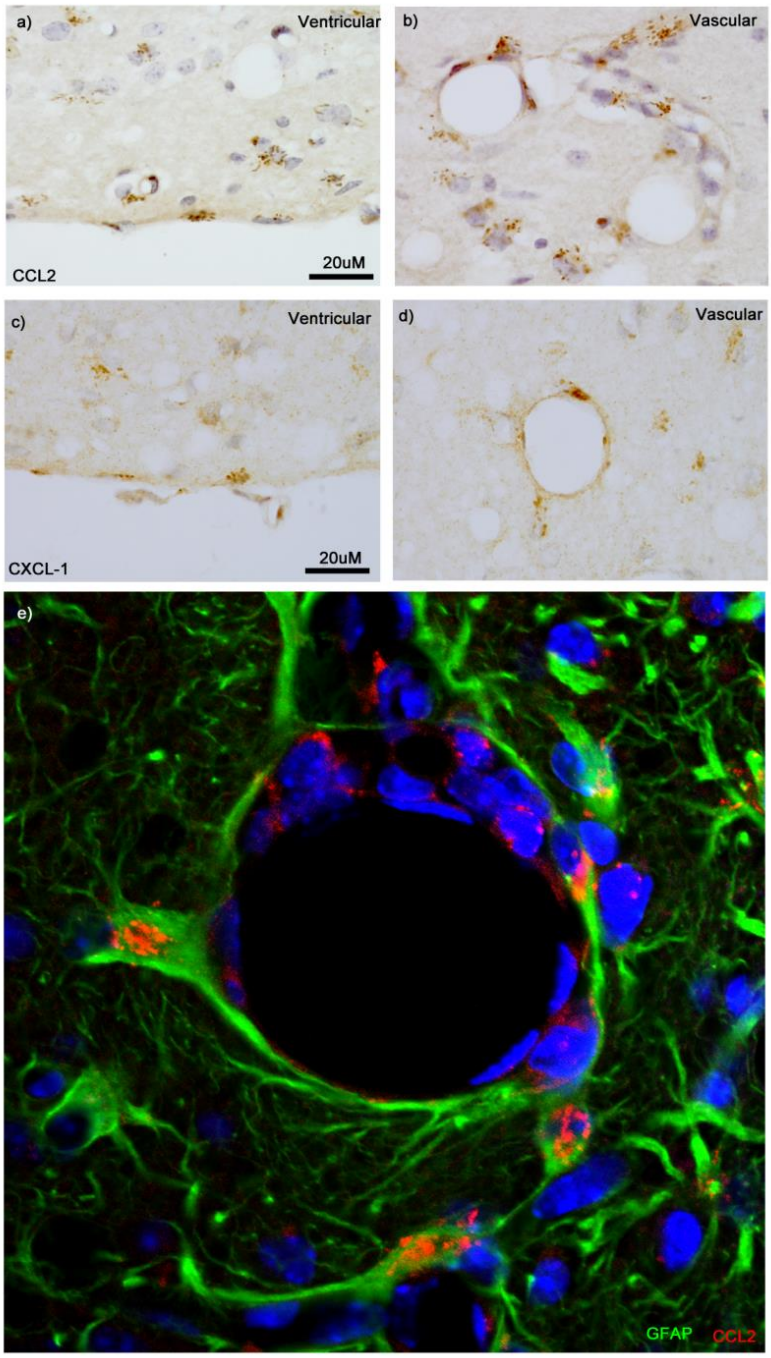

Figure 3.8 Ventricular and vascular expression of CCL2 and CXCL1

Ventricular and vascular expression of CCL2 and CXCL1 in the hippocampal region of ME7 animals 18 weeks post inoculation, treated with (a-d) IL-1β (10ng) and (e) TNFα (300ng), 2 hours post challenge. Representative images of CCL2 at the ventricular (a) and vascular (b) membranes x100 at 2 hours. CXCL-1 at the ventricular (c) and vascular (d) membranes x100 at 2 hours. GFAP and CCL2 colocalisation at a vessel at 2 hours (e). Production of CCL2 within astrocytic cells was visualised with fluorescent antibodies GFAP (488nm - green) and CCL2 (594nm - red).

3.3.3 - ME7 Intrahippocampal TNFα or IL-1β at 24 hours

The exaggerated levels of the neutrophil chemoattractant protein CXCL1 induced in response to TNFα and IL-1β in the ME7 brain (Figure 3.3) predicted significant effects on cellular infiltration. Neutrophil infiltration at 24 hours post-cytokine challenge was assessed using MBS-1, a polyclonal anti-neutrophil anti-serum. Neutrophils were not found in the parenchyma of NBH+saline (figure 3.9a) or ME7+saline animals (figure 3.9d). There was some neutrophil infiltration following both IL-1β and TNFα in the NBH animals (3.9b and c respectively), although this was limited to the injection site with TNFα. ME7+IL-1β animals (3.9e) showed exaggerated neutrophil infiltration throughout the hippocampus compared to NBH+IL-1β-treated animals (3.9b). Quantification (3.9g) and two-way ANOVA of this comparison shows that there was a main effect of IL-1β ($P<0.001$, $F_{(1,11)}=67.94$), a main effect of disease ($P<0.01$, $F_{(1,11)}=12.15$) and an interaction between treatment and disease ($P<0.01$, $F_{(1,11)}=12.13$). Similarly quantification of neutrophil numbers in ME7+TNFα animals (3.9f) showed an exaggerated infiltration compared to NBH+TNFα (3.9c). Following TNFα in ME7 animals infiltration occurred throughout the parenchyma of the injected hemisphere in rather than being limited to the injection site, as was the case in NBH animals. Following TNFα challenge (Figure 3.9h) there was a main effect of treatment ($P<0.001$, $F_{(1,10)}=29.15$), a main effect of disease ($P<0.05$, $F_{(1,10)}=6.707$) but also an interaction between disease and treatment ($P<0.05$, $F_{(1,10)}=6.67$). These data demonstrate that infiltration of neutrophils is exaggerated in the ME7 brain challenged with either IL-1β or TNFα compared to NBH animals similarly challenged.

Neutrophil infiltration is also influenced by events at the cerebral endothelium. Figure 3.8 shows significant expression of CCL2 and CXCL1 in the ME7 animals challenged with IL-1β and TNFα at the major blood vessels of the hippocampus and at the glia limitans. At 24 hours post-challenge there is a differential recruitment of cells to these surfaces by IL-1β and TNF. The neutrophil marker MBS-1 shows a large number of neutrophils in the parenchyma of the ME7+IL-1β group but few, if any, cells, remaining at the glia limitans (3.10h). However, in the NBH+IL-1β group there remains a significant build-up of neutrophils at the glia

limitans (3.10b), suggesting more successful extravasation of neutrophils in ME7 animals with respect to NBH animals. Thus neutrophils were recruited in both NBH and ME7 but extravasated more readily in those animals with robust CXCL1 expression in the brain parenchyma (Figure 3.5).

In the ME7+TNFα (3.10i) group there is a large recruitment of cells to the ventricular space between hippocampus and thalamus, which is greatly exaggerated compared to the NBH+TNF group (3.10c), however only a small number of these are MBS-1 positive. Most are positive for the macrophage marker CD68. Although this cannot distinguish between peripheral macrophages and microglia, here in the ventricular space, its presence in abundance indicates that the majority of cells recruited to the glia limitans in the ME7+TNF group are monocytes (3.10l), There is some recruitment of CD68-positive cells following IL-1β challenge however the recruitment is much larger in the TNF groups indicating that there remains a different profile of recruitment between ME7+TNFα and ME7+IL-1β: even though TNFα does induce robust neutrophil infiltration, it still appears to recruit monocytic cells more effectively than does IL-1β.

Myeloperoxidase (MPO) is typically thought of as a neutrophil marker due to its constitutive presence in neutrophil granules (Prokopowicz et al., 2012). However, in recent years MPO has been found in macrophages activated by varying disease states (Sugiyama et al., 2001; Karakas and Koenig, 2012; Stefanova et al., 2012). When Myeloperoxidase (MPO) expression at the glia limitans was examined following IL-1β it can be seen that the cells remaining at the glia limitans (in the NBH animal) have a stronger MPO signal than those that have transmigrated into the tissue. Following TNFα in ME7 animals there is a large number of MPO positive cells in the ventricle at 24 hours, and cells that have transmigrated have a visibly diminished MPO signal.

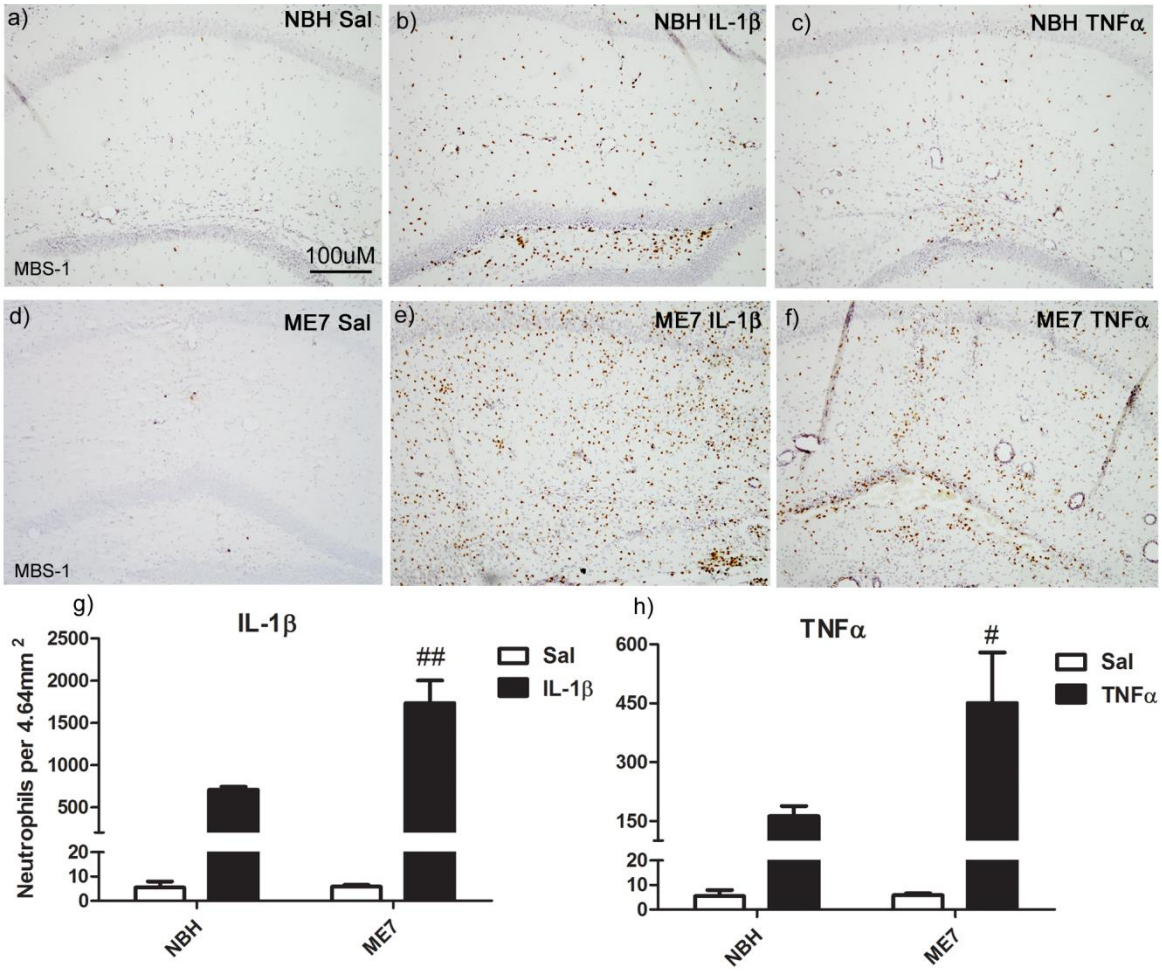

Figure 3.9 Neutrophil infiltration 24 hours post IL-1β or TNFα

Hippocampus of NBH-inoculated (a,b,c) and ME7-inoculated (d,e,f) animals at 18 weeks post inoculation, treated with saline, TNFα (300ng) or IL-1β (10ng) at 24 hours post challenge. Neutrophil infiltration at 24 hours was visualised using MBS-1 labelling at x20 magnification (a-f). Quantification of neutrophils in an area of 4.64mm^2 centred on the injected dorsal hippocampus following IL-1β (g) and TNF (h) injection. Data were analysed using a two-way ANOVA followed by Bonferroni post-hoc test. Interaction between treatment and disease is denoted by # ($p<0.05$) or ## ($p<0.01$). All data are represented as the mean ±SEM, n=3-5 for all groups.

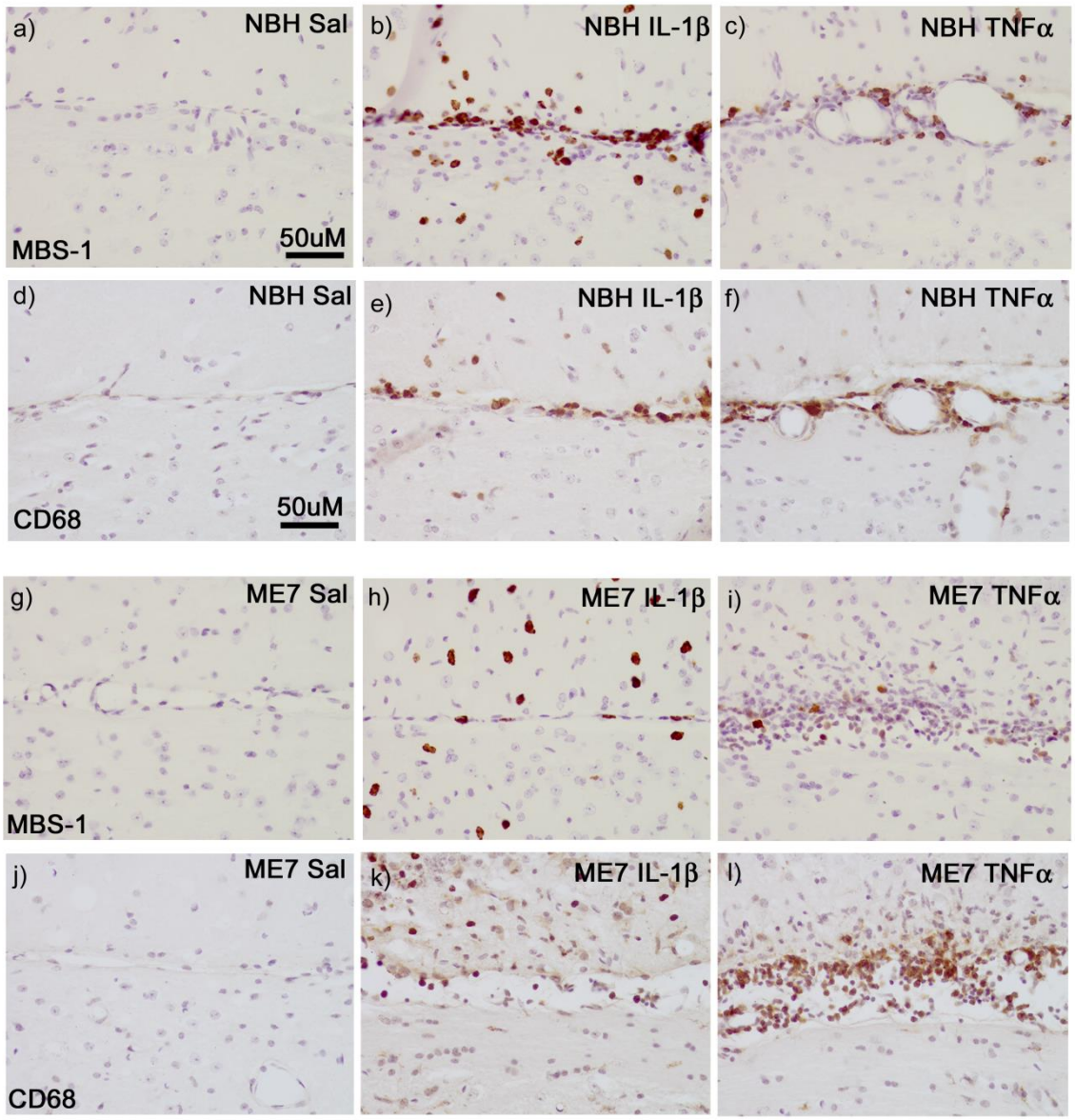

Figure 3.10 Cell recruitment and extravasation at the glia limitans 24 hours post IL-1β or TNFα

Glia limitans of NBH-inoculated and ME7-inoculated animals at 18 weeks treated with Saline, TNFα (300ng) or IL-1β (10ng) at 24 hours post challenge. MBS-1 neutrophil labelling at the ventricular membrane at 24 hours post challenge x40 NBH animals (a-c), ME7 animals (g-i). CD68 monocyte labelling at the ventricular membrane at 24 hours post challenge x40 NBH animals (d-f), ME7 animals (j-l).

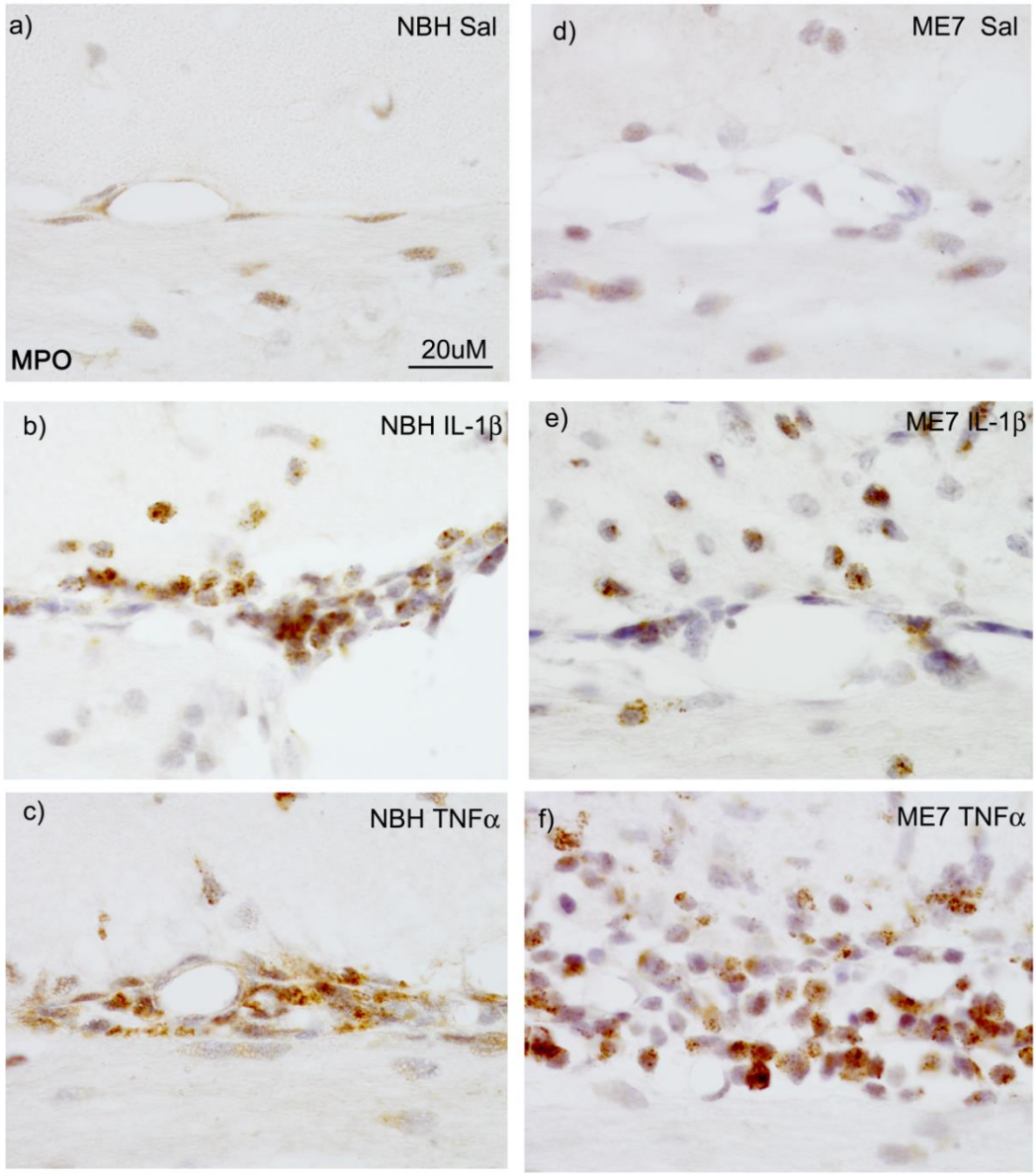

Figure 3.11 MPO expression on cells recruited to the Glia limitans 24 hours post IL-1β or TNFα

Glia limitans of NBH-inoculated and ME7-inoculated animals at 18 weeks treated with saline, TNFα (300ng) or IL-1β (10ng) at 24 hours post challenge. Representative images of Myeloperoxidase labelling at the Glia limitans are shown.

3.3.4 - ME7 Intrahippocampal TNFα or IL-1β at 72 hours

Having demonstrated robust neutrophil infiltration at 24 hours, and observed significant CD68-positive monocytes at the glia limitans in TNFα-treated animals (both NBH and ME7) TNFα-treated animals at 72 hours was examined to assess whether NBH and ME7 showed differential cellular infiltration. Based on our earlier observations, the hypothesis that exaggerated astrocytic CCL2 production at 2 hours in ME7 animals would exert a differential impact on macrophage infiltration in ME7 versus NBH animals was investigated.

It is immediately apparent by assessing Haematoxylin counterstain, that ME7 animals are hypercellular in the hippocampus compared to NBH (Figure 3.12e versus 3.12a), due to disease-associated astrocytosis and microgliosis. TNFα further exaggerated the ME7 induced hypercellularity (figure 3.12g versus 3.12e). Multiple perivascular cuffs were observed in each field examined in ME7+TNF animals, indicative of cellular infiltration from the periphery. To assess the contribution of neutrophils to the increased cell numbers seen at 72 hours MBS-1-positive cells in the hippocampus of these animals were examined. Occasional neutrophils could be seen in NBH+TNF (3.13b) and ME7+TNF (3.13d) animals, however there were few neutrophils remaining in the hippocampus of these groups at 72 hours (figure 3.13m) compared to their peak at 24 hours. There was no significant effect of treatment or disease by 2 way ANOVA. Thus, neutrophils account for an insignificant proportion of the increased cellularity at 72 hours.

T-cell infiltration was also examined. Consistent with prior studies, there were some CD3-positive cells in the hippocampus of ME7 animals (3.13g) however these were somewhat variable in number. CD3 labelling (3.13 e-h) revealed TNFα-induced T-cell infiltration and this was heightened in ME7+TNFα (3.13h) animals compared to NBH+TNFα (3.13f). Quantification of CD3 positive T-cells (figure 3.13n) showed a main effect of both treatment ($P<0.01$, $F_{(1,18)}=11.20$) and disease ($P<0.001$, $F_{(1,18)}=27.38$) with an interaction between these two factors ($P<0.05$, $F_{(1,18)}=4.757$). Thus T-cells are more readily recruited to the ME7 brain than to the normal brain, however this is still a relatively minor contribution to the hypercellularity observed after TNFα challenge.

At the 72hour timepoint alterations in IBA-1 labelling made it difficult to quantify cell numbers (figure 3.12h). Therefore the readily quantifiable myeloid lineage marker Pu.1 was utilised to label both macrophage and microglial nuclei to assess macrophage/microglial contribution to the observed hypercellularity. This marker shows both the ME7 disease-associated microgliosis (figure 3.13k versus 3.13i) and TNFα-induced focal increases in macrophages. Quantification was performed in an area close to the injection track to avoid 'diluting' the infiltrating cells among the considerable resident Pu.1-positive microglial population of the ME7 brain (figure 3.13o) and 2 way ANOVA showed significant effects of disease ($P<0.001$, $F_{(1,24)}=24.53$) and treatment ($P<0.01$, $F_{(2,24)}=6.100$). Bonferroni *post-hoc* shows that Pu.1 labelled cells are significantly greater in number in ME7+TNFα versus NBH+TNFα ($p<0.001$). To interrogate whether these Pu.1 positive cells originate outside the brain the Mc21 CCR2 antibody was used, Mc21 depletes systemic monocytes (Bruhl et al., 2007; Yona et al., 2013). Administration of Mc21 prior to intra-hippocampal TNFα administration significantly decreased Pu.1-positive macrophages in the hippocampus (effect of treatment $P<0.05$, $F_{(1,18)}=6.313$; Bonferroni *post-hoc* comparison of ME7+TNFα versus ME7+TNFα+Mc21: $p<0.05$). This indicates that infiltrating monocytes are contributing significantly to the increased cell numbers seen at 72 hours post TNFα administration. The number of monocytes infiltrating the brain, rather than the fold increase from baseline (ME7+saline), is the most relevant parameter and this number is considerably higher in ME7+TNFα than in NBH+TNFα (Figure 3.13o).

Ki67 is a marker of cellular proliferation. There were elevated numbers of Ki67-positive cells in the ME7+TNFα (3.14d) animals compared to the ME7+saline (3.14c) treated animals, indicating increased proliferation present in the hippocampus following intrahippocampal TNFα. This exaggerated proliferation in ME7 animals 72 hours post TNFα i.h.c. was quantified (3.14e), there was a main effect of treatment ($P<0.001$, $F_{(1,8)}=34.84$), a main effect of disease ($P<0.001$, $F_{(1,8)}=144.7$) and an interaction between treatment and disease ($P<0.01$, $F_{(1,8)}=23.03$) in Ki67-positive cell numbers. A number of different Ki67-positive nuclear morphologies were observed in the brain parenchyma, predominantly in ME7 animals, and examples of those observed and quantified are shown in figure

3.14 (f, g). The most frequently observed morphology in ME7+TNFα animals was that shown in figure 3.14g, i.e. large rounded nuclei consistent with astrocytic nuclei. Ki67 was double labelled with both astrocytic (GFAP) and microglial markers (IBA-1 and Pu.1). This failed to find any significant co-localisation of Ki67 and microglial markers. The vast majority of the Ki67 positive cells at 72 hours post-TNFα were GFAP positive astrocytes (figure 3.15).

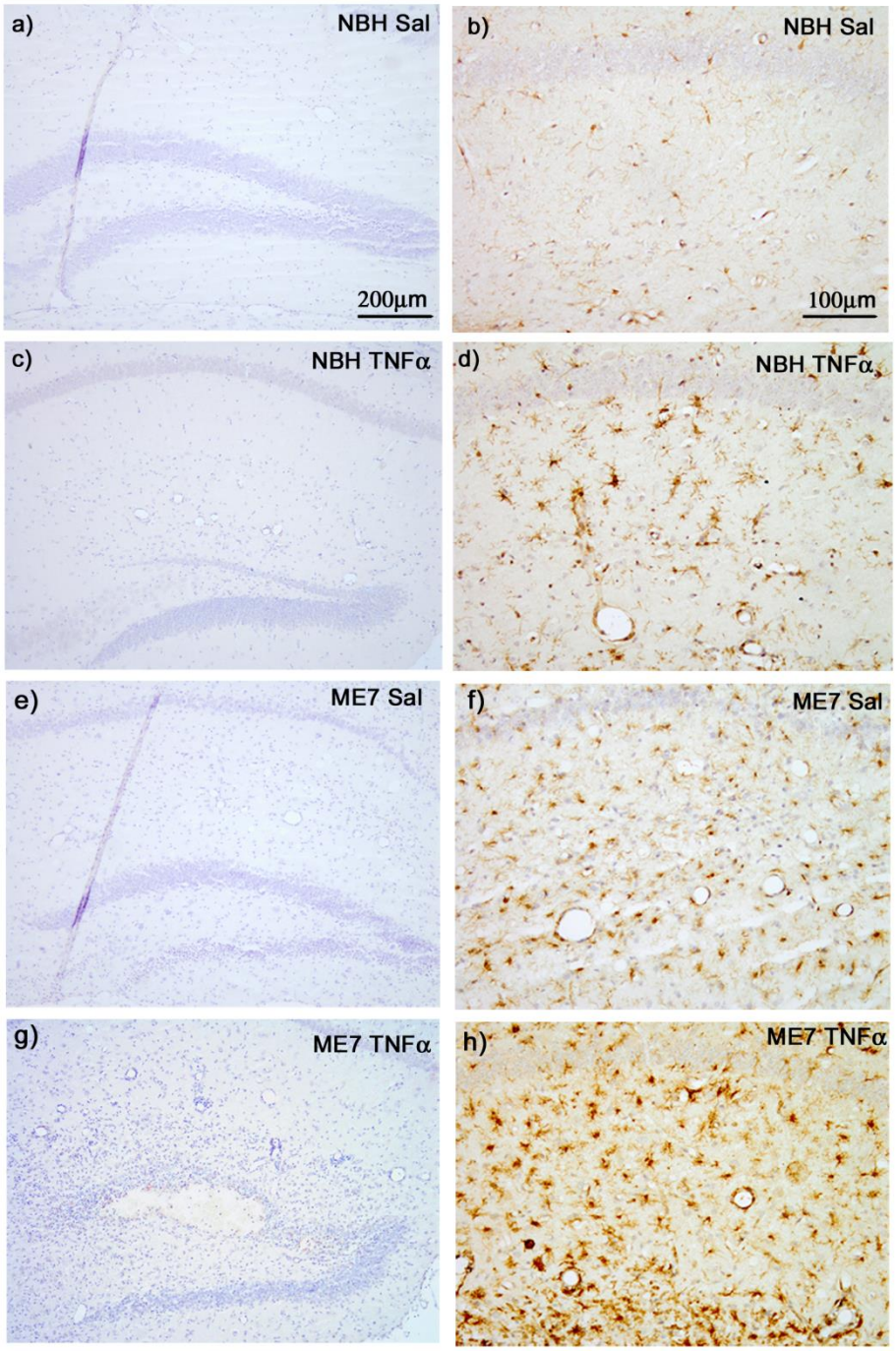

Figure 3.12 Hypercellularity at 72 hours

Cellular infiltration at 72 hours post intrahippocampal TNFα (300ng) challenge. Hypercellularity was visible using Haematoxylin staining. Using IBA-1 immunolabelling it was not possible to differentiate individual cells in order to quantify total hippocampal myeloid cell numbers. Hippocampus shown at x10, scale bar = 200µm for haematoxylin and at x20, scale bar = 100µm for IBA-1.

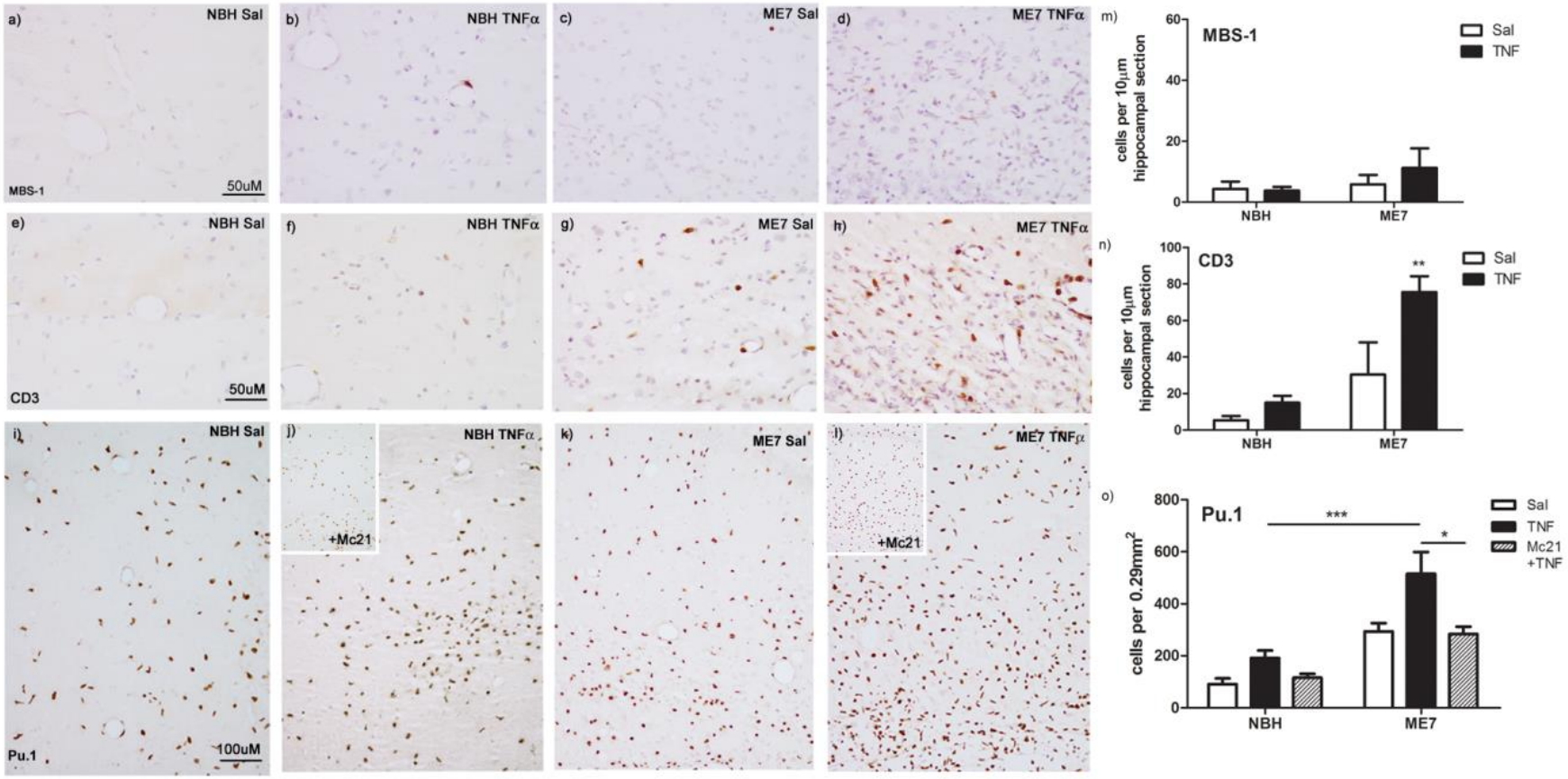
a)
NBH Sal
MBS-1
50uM
b)
NBH TNFα
c)
ME7 Sal
d)
ME7 TNFα
e)
NBH Sal
CD3
50uM
f)
NBH TNFα
g)
ME7 Sal
h)
ME7 TNFα
i)
NBH Sal
Pu.1
100uM
j)
NBH TNFα
+Mc21
k)
ME7 Sal
l)
ME7 TNFα
+Mc21
m)
MBS-1
cells per 10μm hippocampal section
Sal
TNF
NBH
ME7
n)
CD3
cells per 10μm hippocampal section
**
Sal
TNF
NBH
ME7
o)
Pu.1
cells per 0.29mm2
***
*
Sal
TNF
Mc21 +TNF
NBH
ME7

Figure 3.13 Immune cell infiltration at 72 hours.

Cellular infiltration at 72 hours post intrahippocampal TNFα (300ng) challenge. Hippocampal MBS-1 neutrophil labelling, x40 (a-d), CD3 T-cell labelling, x40 (e-h) and Pu.1 macrophage/microglial labelling, x20 (i-l). Quantification of MBS-1-positive neutrophils (m) and CD3 positive T cells (n) in the injected hippocampus at 72h. Pu.1-positive macrophages and microglia were quantified per 0.29mm^2 of the injected hippocampus (o). The latter were quantified in the presence and absence of peripherally administered Mc21 to deplete circulating monocytes. Data were analysed using two-way ANOVA (full analysis in main text) followed by Bonferroni post hoc test. Selected statistically significant pairwise comparisons are denoted by * $p<0.05$. All data are represented as the mean ±SEM, n=3-7.

Figure 3.14 Immunohistochemical detection of proliferation marker Ki67 at 72 hours

Ipsilateral hippoccampus of NBH-inoculated and ME7-inoculated animals at 18 weeks treated with saline or TNF (300ng) at 72 hours post challenge. Representative images of the ipsilateral hippocampus are shown at x40, scale bar = 50μm, (a-d). Proliferating cells were quantified at 72 hours using the Ki67 immunolabel. Data was analysed using two way ANOVA followed by Bonferroni post hoc test. Statistical significance is denoted by *** ($P<0.001$). All data are represented as the mean ±SEM, n=3 for all groups. Images f and g are examples of the varying morphology of Ki67 (x100). (h-i) shows representative images of GFAP and Ki67 co-localisation following both double fluorescent immunolabelling and double light immunolabelling. The majority of Ki67 positive cells 72 hours post-TNFα in ME7 animals were GFAP positive astrocytes.

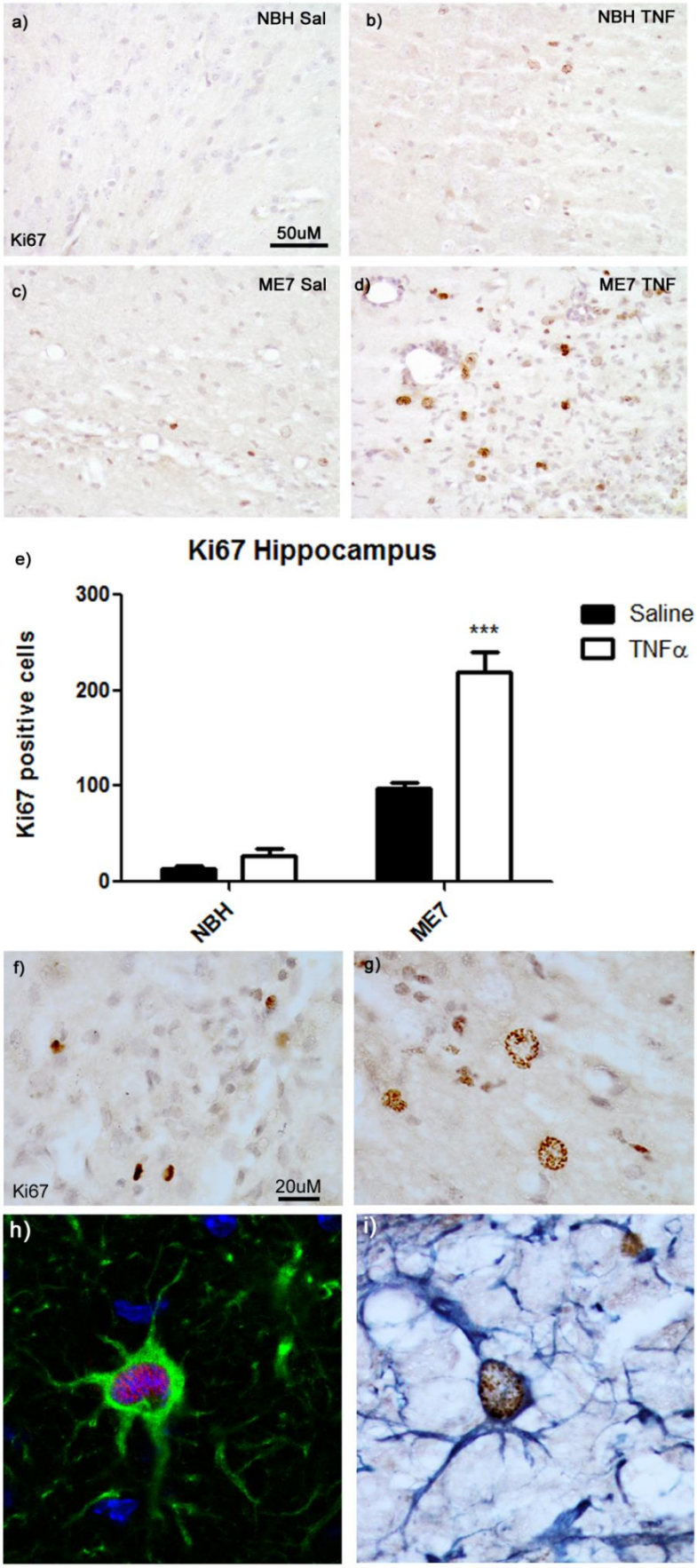
a)
NBH Sal
Ki67
50uM
b)
NBH TNF
c)
ME7 Sal
d)
ME7 TNF
e)
Ki67 Hippocampus
Ki67 positive cells
300
200
100
0
***
Saline
TNFα
NBH
ME7
f)
Ki67
20uM
g)
h)
i)

3.3.5 - Intrahippocampal LPS or IL-1β in the APP/PS1 transgenic mouse model of Alzheimer's disease

It was predicted that these features of microglial and astroglial priming would not be restricted to the ME7 model. This prediction was investigated with the commonly used APP/PS1 double-transgenic mouse model of Alzheimer's disease. To investigate the effect of intrahippocampal IL-1β (10ng) or LPS (1μg) on hippocampal markers of inflammation, unilateral intrahippocampal (i.h.c) injections of 1μl were performed at the coordinates from bregma: anteroposterior, -2.0mm; lateral, -1.6mm; depth -1.6mm. These injections were performed using a microcapillary, which was left in place for 1 minute. Animals were then terminally anaesthetised and transcardially perfused with heparinised saline followed by 10% neutral buffered formalin at 2 hours (Saline and IL-1β) and 3 hours (LPS) post-challenge before embedding the brains in paraffin wax. Sections were cut at 10μm. Various markers of inflammation were visualized using immunohistochemistry.

To verify the genotype of animals amyloid beta (Aβ) plaques were visualised using 6e10 immunolabelling of amino acids 1-16 of the Aβ protein. The typical hippocampal distribution of Aβ plaques in APP/PS1 animals is shown in figure 3.15a, 3.15b shows a more detailed view of an individual plaque. IBA-1 immunolabelling was used to visualise microglial numbers and morphology. WT microglia display a standard elongated and highly branched morphology (figure 3.16a), there is very little morphological difference in WT microglia following IL-1β (3.16c) or LPS (3.16e) administration. Microglia in APP/PS1+Saline (3.16b) show a more condensed morphology and retraction of processes than WT+Saline particularly around apparent plaques. When the percentage area of IBA-1 positive labelling in a 0.29mm^2 area is quantified (figure 3.16g) there is significantly more IBA-1 labelling in APP/PS1 animals than WT ($P<0.0007$, $t=4.348$, $df=14$). This indicates microgliosis in the APP/PS1 animals. Given the aggregation of microglia on the amyloid beta plaques it is difficult to distinguish numbers of cells and both increased density and increased cell numbers may be contributing to the difference between WT and APP/PS1. Following IL-1β (3.16d) or LPS (3.16f) in the APP/PS1 groups there appears to be a greater condensation of the microglial population and retraction of microglial processes.

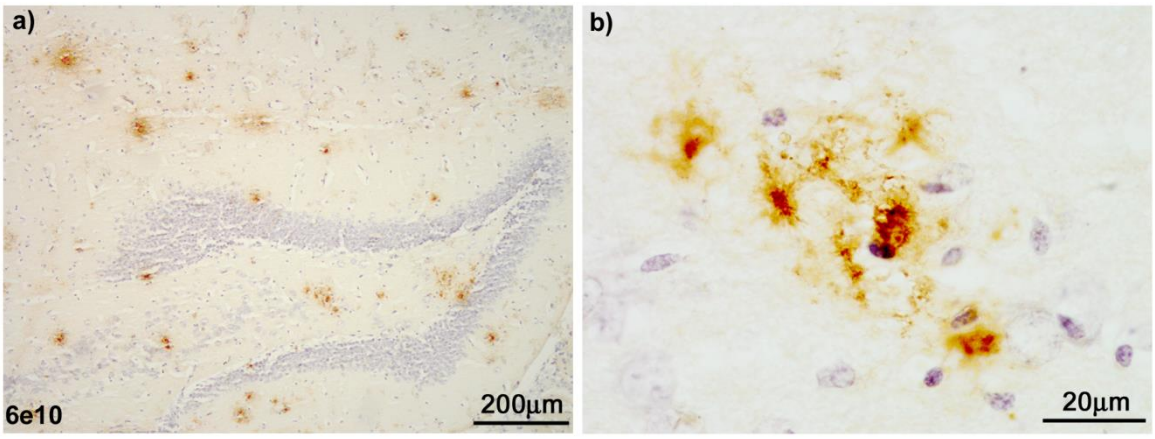

Figure 3.15 Immunohistochemical detection of amyloid β plaques

Representative image of hippocampal 6e10 positive amyloid beta plaques of an APP/PS1 animal at 18 months (x10, scale bar = 200µm, x100, scale bar = 20µm).

Figure 3.16 Immunohistochemical detection and quantification of IBA-1 labelling

Ipsilateral hippocampus of wild type and APP/PS1 animals at 18 months. 2 hours post i.h.c. saline or IL-1β (10ng) and 3 hours post i.h.c. LPS (1µg) challenge. Microglial cells are immunolabelled using IBA-1 (x100, scale bar = 20µm). (g) Image J was used to quantify the percentage area covered by IBA-1 labelling in a x20 section (per 0.29mm^2). Data were analysed using Student's t test. Statistically significance is denoted by ** $p<0.01$. All data are represented as the mean ±SEM, WT n=9, APP/PS1 n=7.

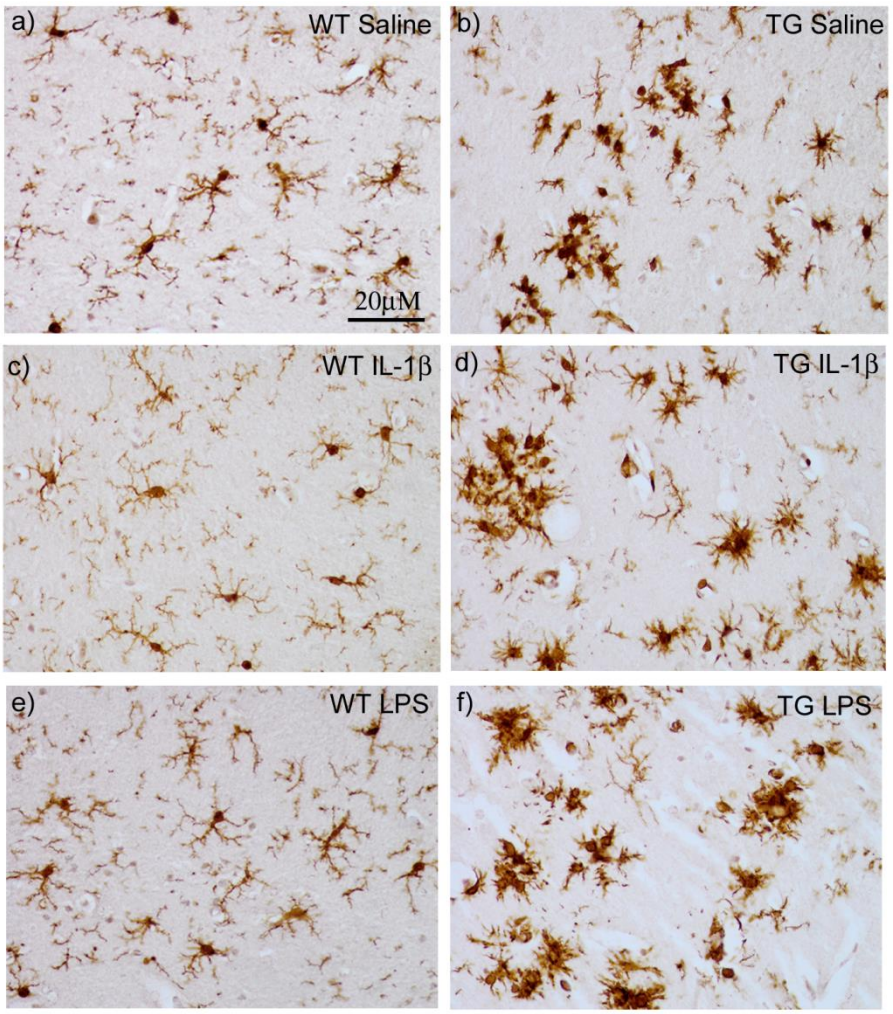
a)
WT Saline
20μM
b)
TG Saline
c)
WT IL-1β
d)
TG IL-1β
e)
WT LPS
f)
TG LPS

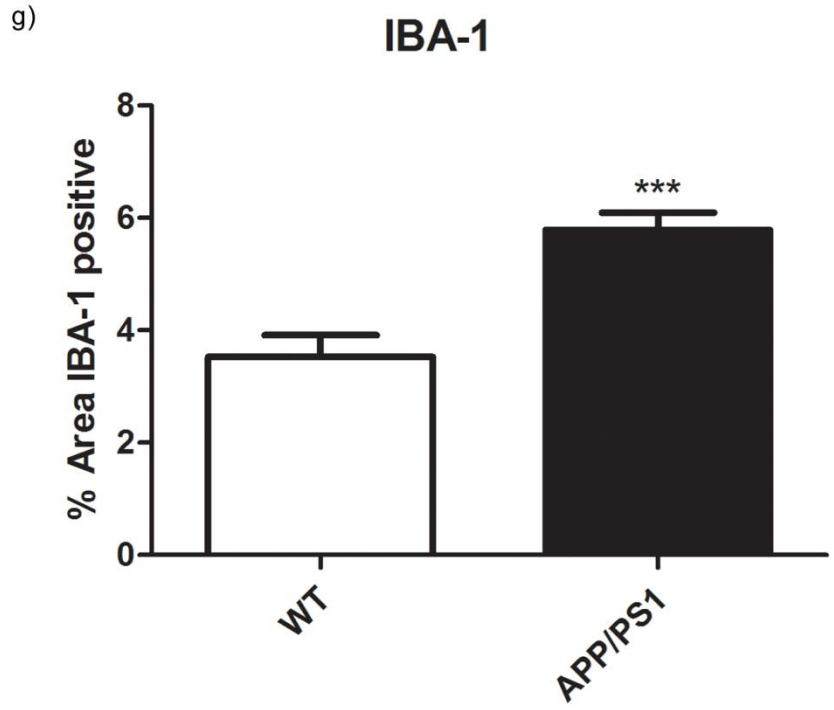
g)
IBA-1
% Area IBA-1 positive
0
2
4
6
8
***
WT
APP/PS1

There is no IL-1β protein in WT (figure 3.17a) or APP/PS1 (3.17b) animals treated with saline at 2 hours. IL-1β does not induce detectable levels of IL-1β protein in WT animals at 2 hours (3.17c). 2 hours post IL-1β in APP/PS1 animals however there is significant production of IL-1β by cells that appear microglial in morphology (3.17d). WT animals treated with LPS also show production of IL-1β by microglial like cells (3.17e). This production is however greatly exaggerated in the microglial cells of the APP/PS1 animals (3.17f). These results indicate that the aggregation of amyloid beta in the APP/PS1 transgenic model can prime microglial cells to produce exaggerated levels of IL-1β when activated, compared to the same cells present in WT animals. These primed microglia can react in an exaggerated manner compared to WT microglia when activated with either the endogenous cytokine IL-1β or the exogenous TLR ligand LPS.

Having confirmed the presence of primed microglia in the APP/PS1 model it ws investigated whether there was an altered activation state in the astrocyte population. To do this production of both CCL2 and CXCL-1 in the parenchyma and at the vascular membranes of the injected hippocampi was examined. CCL2 is found at the vasculature of both WT and APP/PS1 animals treated with IL-1β (3.18 h and k) and LPS (3.18 i and l). However levels of parenchymal CCL2 differ between WT and APP/PS1. APP/PS1 animals treated with IL-1β (3.18e) and LPS (3.18f) display a robust induction of CCL2 protein while in WT animals LPS (3.18c) produces a limited peri-nuclear production of CCL2 and IL-1β (3.18b) produces no detectable CCL2 protein.

Similarly CXCL-1 is found at the vasculature of WT animals post IL-1β (3.18t) and LPS (3.18u) as well as APP/PS1 animals post IL-1β (3.18w) and LPS (3.18x). In the parenchyma of WT animals there is minimally detectable CXCL-1 protein post IL-1β (3.18n) or LPS (3.18o). There is some plaque associated CXCL1 in APP/PS1 animals treated with saline. However APP/PS1 animals treated with both IL-1β (3.18q) and LPS (3.18r) show production of CXCL-1 by astrocyte like cells. These results indicate that the astrocyte population of the APP/PS1 transgenic model is also primed by the amyloid beta deposition, to produce an exaggerated chemokine response to subsequent inflammatory stimulation.

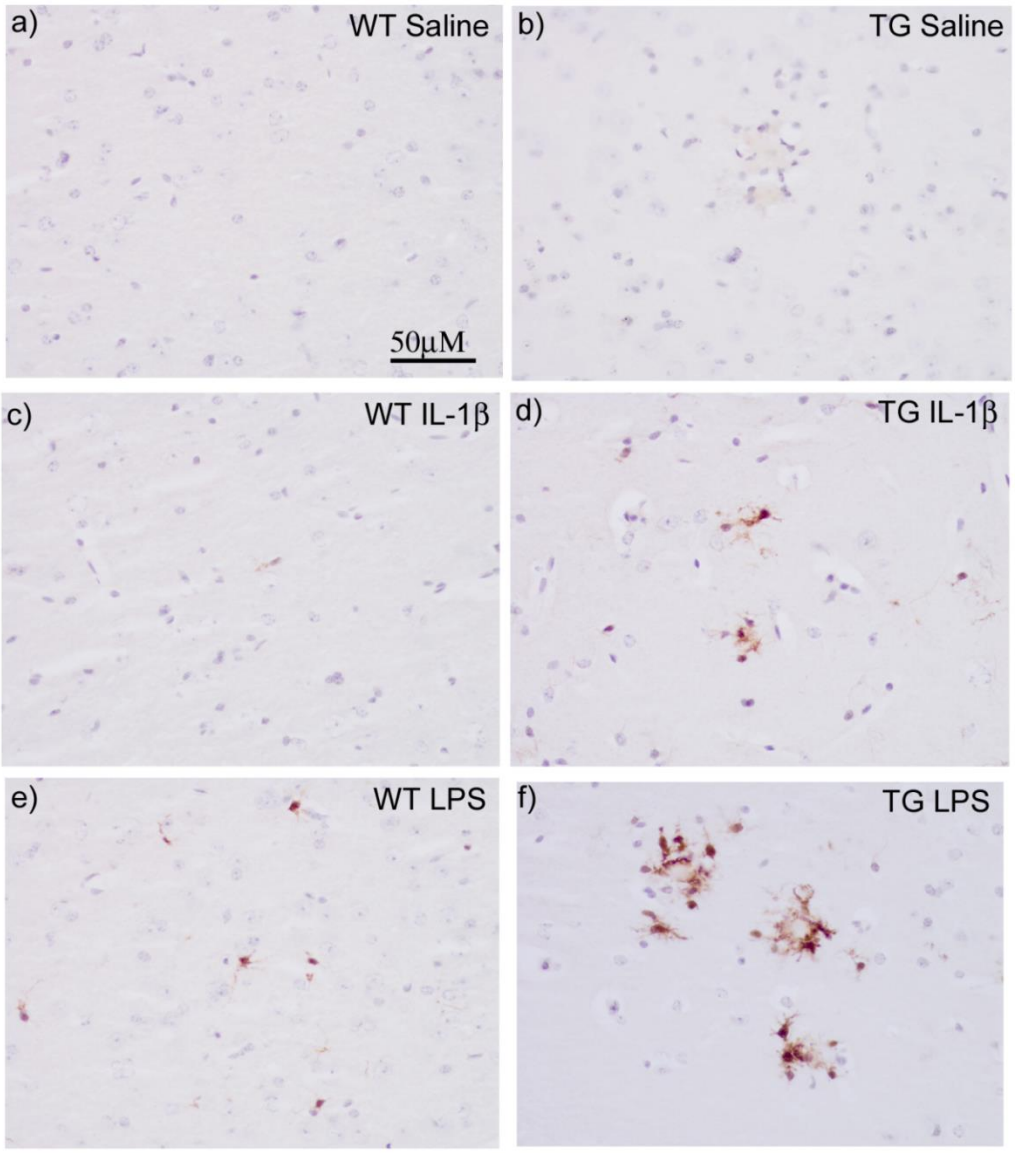

Figure 3.17 Immunohistochemical detection of IL-1β

Ipsilateral hippocampus of wild type and APP/PS1 animals at 18 months, 2 hours post i.h.c. saline or IL-1β (10ng) and 3 hours post i.h.c. LPS (1µg) challenge. De novo IL-1β production was visualised (x40, scale bar = 50µm).

Figure 3.18 Immunohistochemical detection of CCL2 and CXCL-1

Ipsilateral hippocampus of wild type and APP/PS1 animals at 18 months, 2 hours post i.h.c. saline or IL-1β (10ng) and 3 hours post i.h.c. LPS (1µg) challenge. Macrophage chemoattractant protein CCL2 and neutrophil chemoattractant protein CXCL-1 were immunolabelled (x100, scale bar = 20µm). Parenchymal CCL2 is shown (a-f), vascular CCL2 (g-l), parenchymal CXCL1 (m-r) and vascular CXCL1 (s-x), (x100, scale = 20µm).

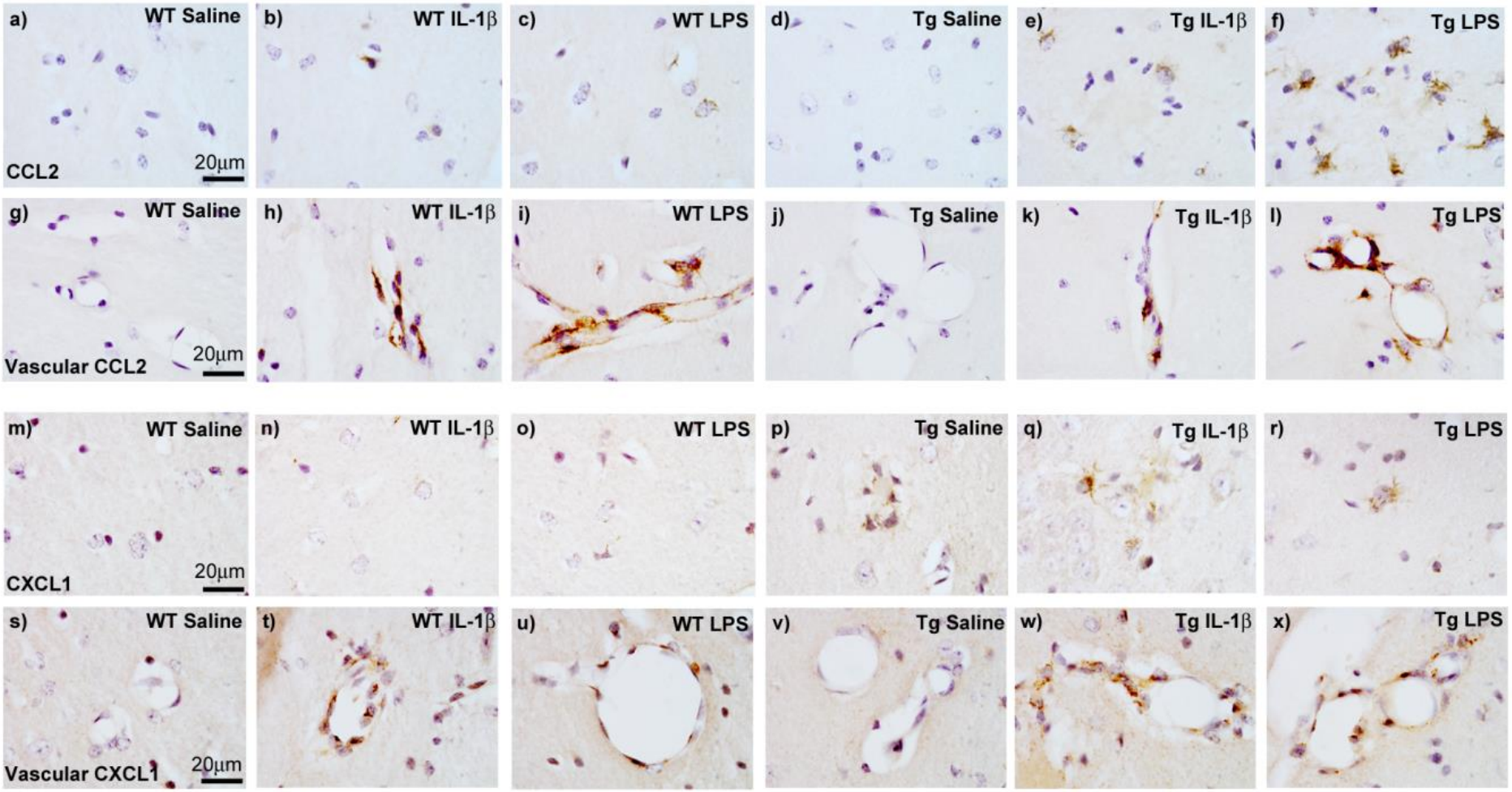
a) WT Saline
b) WT IL-1β
c) WT LPS
d) Tg Saline
e) Tg IL-1β
f) Tg LPS
CCL2
20μm
g) WT Saline
h) WT IL-1β
i) WT LPS
j) Tg Saline
k) Tg IL-1β
l) Tg LPS
Vascular CCL2
20μm
m) WT Saline
n) WT IL-1β
o) WT LPS
p) Tg Saline
q) Tg IL-1β
r) Tg LPS
CXCL1
20μm
s) WT Saline
t) WT IL-1β
u) WT LPS
v) Tg Saline
w) Tg IL-1β
x) Tg LPS
Vascular CXCL1
20μm

3.3.6 - Intraperitoneal LPS in the APP/PS1 transgenic mouse model of Alzheimer's disease

Given that the APP/PS1 model of Alzheimer's disease showed activation of primed microglia and astrocytes in response to intrahippocampal LPS and IL-1β it was predicted that it would also show activation of primed microglia in response to peripheral LPS, similar to that previously described in the ME7 model following peripheral LPS (Cunningham et al., 2005b). To investigate the effect of intraperitoneal LPS (500μg/kg) on hippocampal markers of inflammation, 9 month old APP/PS1 animals were terminally anaesthetised and transcardially perfused with heparinised saline followed by 10% neutral buffered formalin 3 hours post saline or LPS challenge. The brains were then embedded in paraffin wax and sections were cut at 10μm. Various markers of inflammation were visualized using immunohistochemistry.

There is significant condensation of microglia at the amyloid beta plaques of APP/PS1 animals (3.19 c and d), however there is no alteration of microglial morphology following i.p. LPS administration in either WT or APP/PS1 animals. There is however a differential reaction of these microglial cells with regards to IL-1β production. When the hippocampal parenchyma was examined we can see that microglial-like cells are producing detectable IL-1β in the APP/PS1 animals (3.20l) where there were minimally detectable levels of IL-1β in the WT microglia (3.20f). The distribution of these IL-1β positive microglia is not as widespread as the distribution following an intrahippocampal challenge, however there are still IL-1β positive microglia in the parenchyma in the APP/PS1 animals. This would indicate that the primed microglia of the APP/PS1 transgenic model can be activated by systemic LPS similarly to the ME7 model. When IL-1β protein in WT and APP/PS1 animals was visualised post-systemic LPS it can see that the stromal macrophages of the choroid plexus (3.20 d and j) and the endothelial cells of the vasculature (3.20 e and k) react similarly in both strains, producing detectable IL-1β protein, indicating that other compartments of the CNS react similarly and are not primed.

When the production of the chemokines CCL2 and CXCL1 was assessed following systemic LPS in the WT and APP/PS1 animals the answer is not as clear. In the case of CCL2 there is increased CCL2 in stromal macrophages of the choroid

plexus following LPS in both WT (3.23d) and APP/PS1 (3.21j), and also in the endothelial cells of the vasculature following LPS in both WT (3.21e) and APP/PS1 (3.21k). In the hippocampal parenchyma are low levels of CCL2 in the APP/PS1+Saline (3.21i). It is difficult to determine whether levels are significantly higher in APP/PS1+LPS vs WT+LPS.

It is difficult to determine in this circumstance whether there is elevated CXCL1 in the choroid plexus following systemic LPS. There is evidence of increased CXCL1 expression at the vasculature following systemic LPS in both WT (3.22c) and APP/PS1 (3.22g) animals. In the case of the hippocampal parenchyma there is some evidence of CXCL1 protein expression in WT+LPS (3.22d). However in comparison this appears to be increased in the APP/PS1+LPS group in the areas surrounding the amyloid beta plaques (3.22h). This may indicate some activation of the primed astrocyte population.

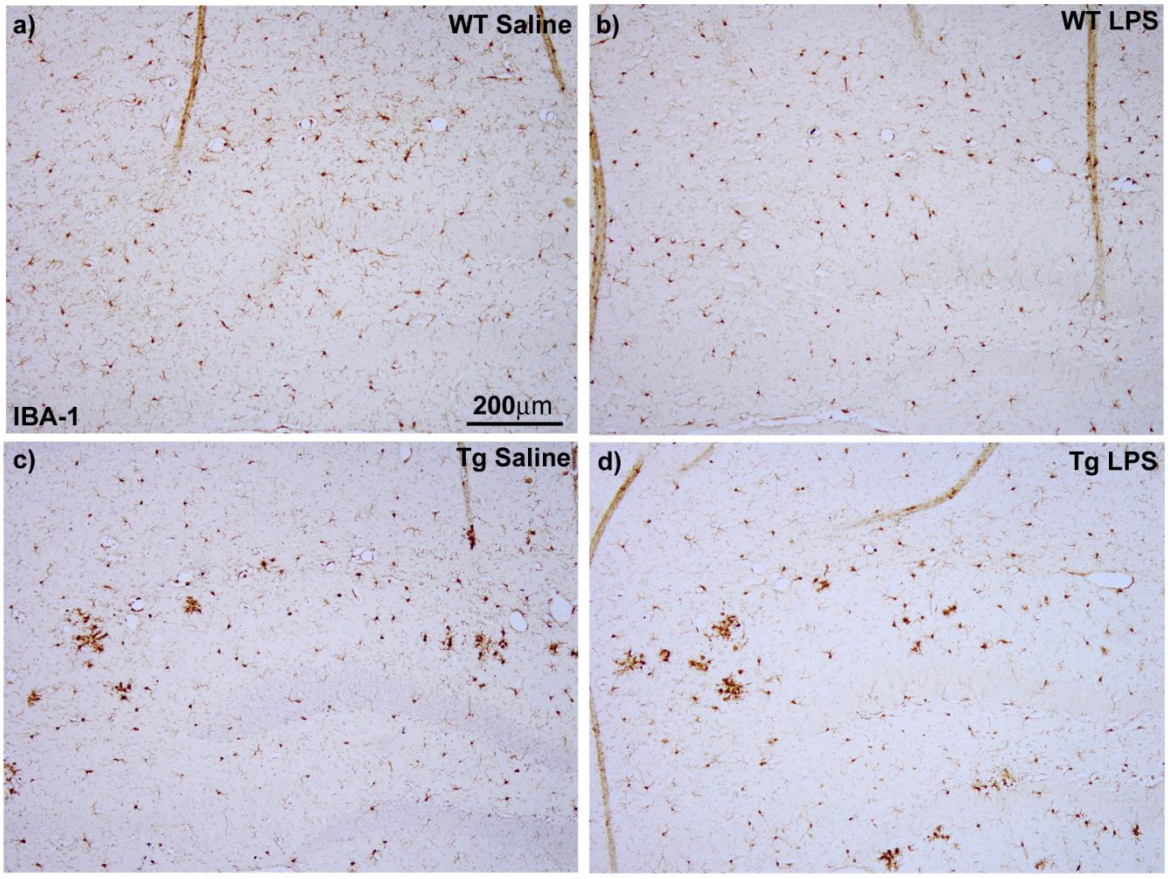

Figure 3.19 IBA-1 immunolabelling of microglia

Hippocampus of wild type and APP/PS1 animals at 9 months, 3 hours post saline or 500µg/kg LPS i.p. Microglial marker IBA-1 was immunolabelled (x10, scale bar = 200µm).

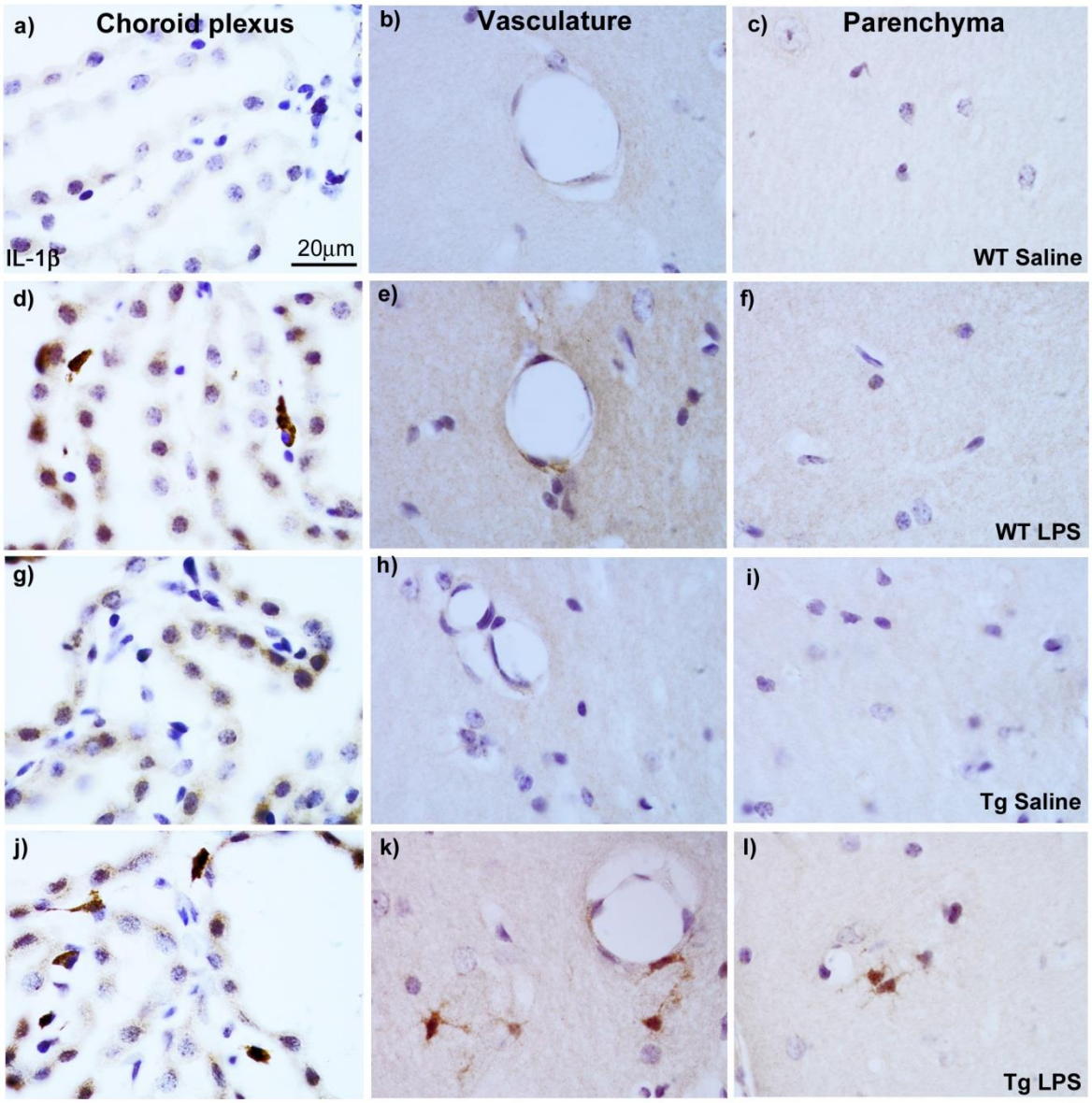

Figure 3.20 Immunolabelling of IL-1β

Choroid plexus, vasculature and hippocampal parenchyma of wild type and APP/PS1 animals at 9 months, 3 hours post saline or 500μg/kg LPS i.p. Cytokine IL-1β was immunolabelled (x100, scale bar = 20μm).

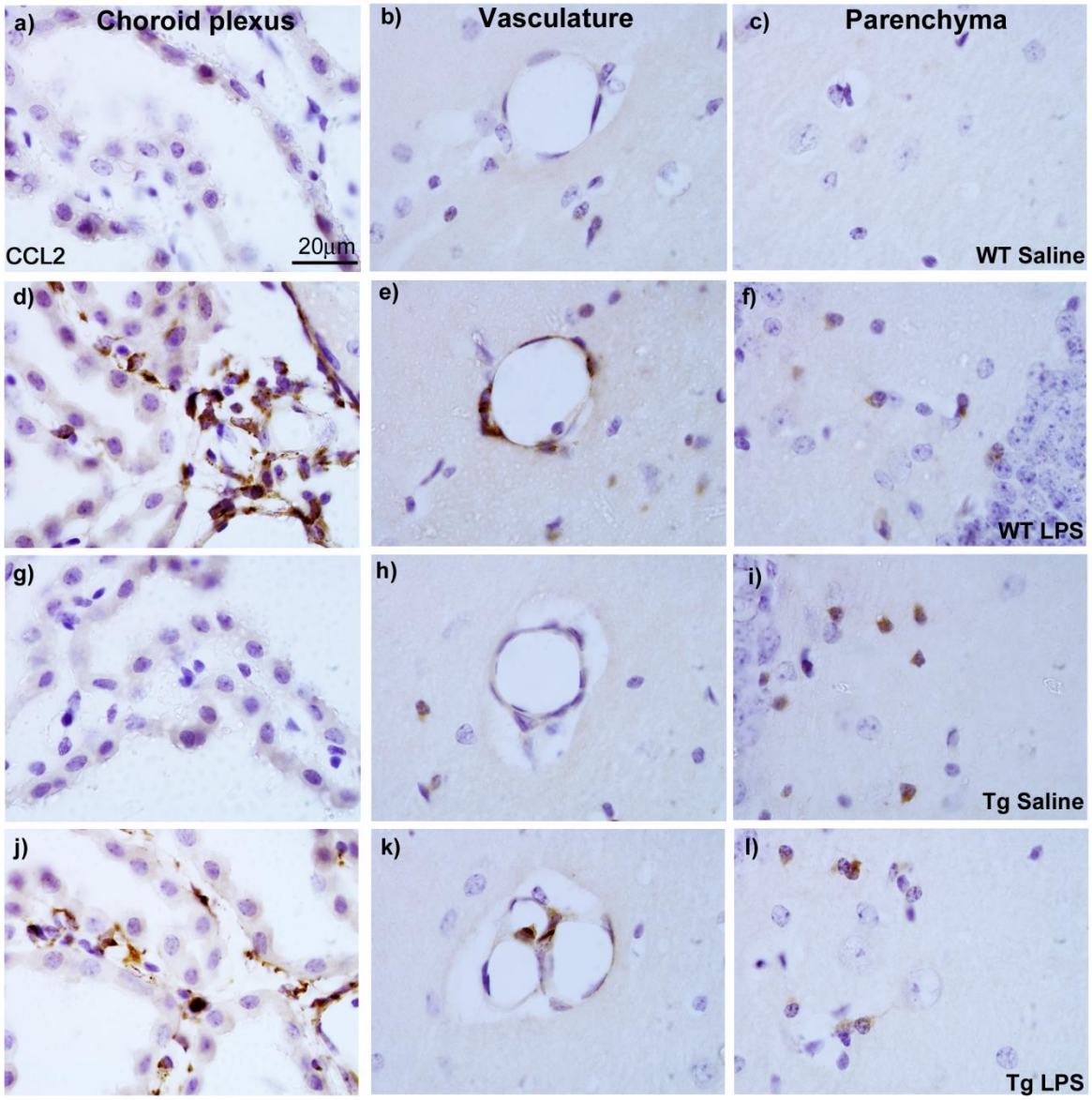

Figure 3.21 Immunolabelling of CCL2

Choroid plexus, vasculature and hippocampal parenchyma of wild type and APP/PS1 animals at 9 months, 3 hours post saline or 500μg/kg LPS i.p. Chemokine CCL2 was immunolabelled (x100, scale bar = 20μm).

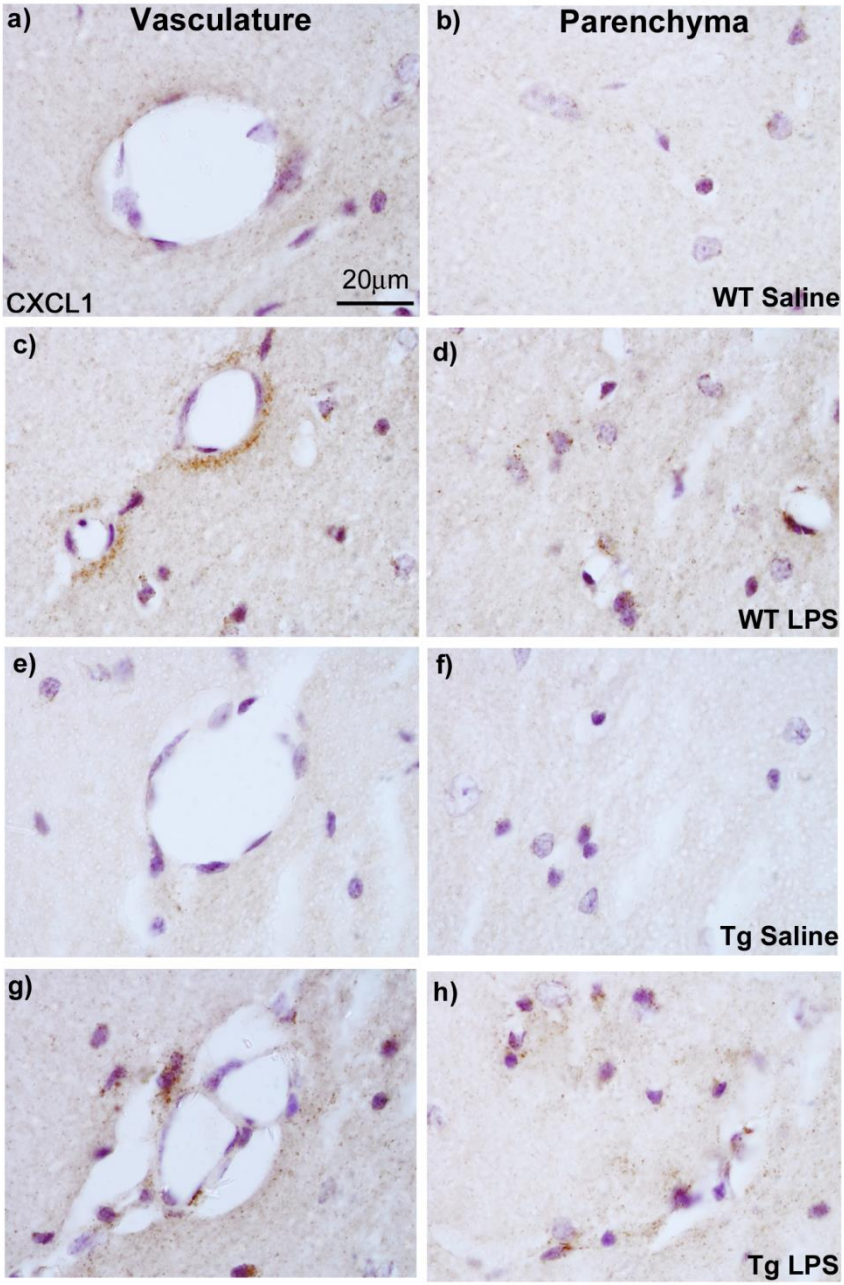

Figure 3.22 Immunolabelling of CXCL1

Choroid plexus, vasculature and hippocampal parenchyma of wild type and APP/PS1 animals at 9 months, 3 hours post saline or 500µg/kg LPS i.p. Chemokine CXCL1 was immunolabelled (x100, scale bar = 20µm).

3.4 - Discussion

Across two models of neurodegeneration, ME7 prion disease and APP/PS1 transgenics. It has been shown that microglia produce exaggerated IL-1β production in response to acute sterile inflammation induced by IL-1β or TNFα. It has also been shown that astrocytes are similarly primed to produce exaggerated chemokine responses to acute cytokine challenge. This markedly heightened chemokine response, in ME7 animals has been shown to induce exaggerated neutrophil, T cell and macrophage infiltration in the diseased brain.

3.4.1 - Primed Microglia

Microglia in ME7 animals switch their phenotype upon central challenge with LPS, robustly producing iNOS and IL-1β (Cunningham et al., 2005b; Hughes et al., 2010). Here, both IL-1β and TNFα induce robust IL-1β, cell soma condensation and process retraction, likely reflecting a more phagocytic phenotype (Hughes et al., 2010). Both IL-1β and TNFα can trigger this phenotypic change and this occurs as soon as 2 hours post-cytokine. Moreover, since both cytokines robustly induced these changes only in ME7 animals (at 2 hours), one can say that microglia in the ME7 animals are primed to produce exaggerated responses to the inflammatory cytokines IL-1β and TNFα. Part of this finding was also replicated in the APP/PS1 model, demonstrating that APP/PS1 microglia are also primed to react in an exaggerated manner to not only LPS but also IL-1β. This expands the repertoire of inflammatory molecules to which primed microglia are demonstrated to respond in an exaggerated fashion, and is significant since molecules such as LPS are rarely experienced in the brain parenchyma. The data with APP/PS1 animals provides the clearest demonstration to date that Aβ plaque is sufficient to prime microglia. Thus the phenomenon of primed microglia is not specific to ME7 prion disease and is a generic phenomenon which can be caused by multiple features of neuropathology.

3.4.2 - Astrocyte priming and chemokine production

Central IL-1β and TNFα induced exaggerated astrocyte synthesis of both CXCL1 and CCL2 in the ME7 brain with respect to NBH, while central LPS and IL-1β induced exaggerated synthesis of both CXCL1 and CCL2 in the APP/PS1 brain with

respect to wild type. This indicates a priming of the astrocyte population that may be analogous to microglial priming (Cunningham et al., 2005b) suggesting generally heightened sensitivity of the degenerating CNS to subsequent inflammatory stimulation. This necessitates a clear definition of the priming concept. We employ the term priming to convey the propensity of a particular cell type to make an exaggerated response to a typical stimulus. Therefore, priming has a general use but not a specific molecular or cellular identity. In the case of primed microglia they show an exaggerated IL-1β response to LPS (Cunningham et al., 2005b; Godbout et al., 2005) and to IL-1β and TNFα (in the current study). Conversely, primed astrocytes show exaggerated CCL2 and CXCL1 responses to IL-1β, TNFα or LPS challenge. Astrocyte priming has long been suggested from *in vitro* studies: IFN-γ sensitized astrocytes to exaggerated responses to subsequent LPS or IL-1β (Chung and Benveniste, 1990). More recently, astrocytes were primed by IL-1β, TNFα or LPS-stimulated microglial conditioned media to produce exaggerated chemokine and cell adhesion molecule synthesis upon TLR2 stimulation (Henn et al., 2011). Following i.p. LPS administration in the APP/PS1 model there was significant activation of primed microglia but not greatly exaggerated astrocyte chemokine synthesis. However, there may be a few reasons as to why a greatly exaggerated astrocyte response to systemic stimulation in these animals was not yet seen as was observed with the intrahippocampal challenge. These animals were at a younger time-point in disease (9 months) than the intrahippocampal cohort (18months). The differential routes of administration may also require different time-points for examination of the astrocyte response. This study has now demonstrated astrocyte priming *in vivo*, both with and without exogenous TLR ligands, which would rarely appear in the brain. Microglial priming proved to be generic across multiple animal models of brain pathology and the replication of these effects in APP/PS1 suggests that astrocyte priming behaves similarly.

Astrocyte priming may reduce selectivity of chemokine responses. It is reported that IL-1β induces CXCL1 and neutrophil infiltration (Campbell et al., 2002) and TNFα induces CCL2 and monocyte infiltration (Campbell et al., 2005) and that these pathways do not significantly cross-over (Schnell et al., 1999a; Blond et al., 2002). Despite this there is *in vitro* evidence for TNFα induction of CXCL1 (Wang

et al., 2007; Lee et al., 2012; Zhang et al., 2013b) and IL-1β induction of CCL2 (Jing et al., 2010; An et al., 2011; Fouillet et al., 2012). Intrathecal TNFα induced spinal cord CXCL1 (Zhang et al., 2013b) but demonstrations of this in the brain are lacking. Here both IL-1β and TNFα robustly induced both CXCL1 and CCL2 in astrocytes of the degenerating brain. It cannot be said whether the failure to observe this in normal animals reflects chemokine class-restricted expression or simply much lower chemokine expression. While exaggerated induction of microglial IL-1β by TNFα could potentially explain the robust TNF-α-induced CXCL1 observed here, we think this unlikely since it would require transcription, translation, maturation, secretion and action of IL-1β, followed by transcription and translation of CXCL1 all to be achieved in 2 hours (although increased microglial IL-1β will likely contribute to events that occur after 2 hours). One might argue that the degree to which IL-1β/CXCL1 and TNFα/CCL2 are discrete pathways has been overstated and that given a sufficient dose both cytokines can induce both chemokines. Regardless, the data presented here suggests that chemokine induction and cellular infiltration are tightly regulated in the healthy brain but these restraints are loosened in the diseased brain, leading to more robust chemokine synthesis in response to both IL-1β and TNFα stimulation. The mechanisms are currently unclear. IL-1RI and TNF-R p55 expression are elevated in the ME7-diseased brain (Murray et al., 2012), likely increasing sensitivity to these immune activators. Similarly, astrocytic NF-κB inhibition decreases chemokine expression (Brambilla et al., 2014) and it is plausible that increased astrocytic expression of NF-κB subunits, and consequent increased transcriptional activation, may underpin exaggerated astrocyte responses to acute stimulation. That astrocytic NF-κB activation is a key event in these exaggerated responses could be tested using selective inactivation of astroglial NF-κB via expression of dominant negative IκBα under astrocyte-specific promoter control (Brambilla et al., 2005). Nonetheless, evidence of post-transcriptional control in the current study has been shown: despite similar transcription of CXCL1 mRNA in IL-1β-challenged ME7 and NBH animals, ME7 astrocytes translated CXCL1 to a much greater extent than those of NBH animals.

3.4.3 - Consequences of chemokine induction

Intrahippocampal LPS recruits a mixed brain infiltrate, via induction of both IL-1β and TNFα but intraparenchymal IL-1β and TNFα, given separately, are reported to

more effectively recruit neutrophils and macrophages respectively (Schnell et al., 1999a; Blond et al., 2002). The robust CXCL1 expression observed after both IL-1β and TNFα in ME7 animals leads to considerable neutrophil infiltration proportionate to the exaggerated CXCL1-expression. TNFα can induce neutrophil recruitment to the meninges and choroid plexus but these cells failed to infiltrate the parenchyma (Andersson et al., 1992b; Campbell et al., 2005). In the current study, the unexpected TNFα-induced CXCL1 production leads to robust neutrophil infiltration, indicating a weakening of regulation of extravasation in the diseased brain. Chemokine expression at the brain endothelium contributes to neutrophil recruitment (Thornton et al., 2010) and many neutrophils were recruited to the glia limitans in NBH+IL-1β animals. However, very few of these extravasated into the tissue compared to ME7+IL-1β, with most remaining at the glia limitans at 24 hours. Thus, the increased neutrophils reaching the parenchyma may be facilitated both by increased numbers recruited but also by their success in extravasating into the tissue. The dramatic neutrophil infiltration observed upon primed microglial responses to LPS in this model (Cunningham et al., 2005b) may have been the result of both an exaggerated microglial IL-1β production after LPS challenge and an exaggerated response of astrocytes to that IL-1β, producing even more exaggerated CXCL1 secretion and neutrophil recruitment.

The robustly elevated parenchymal chemokine expression seen in this study undoubtedly strongly drives the resulting cellular infiltration however there may be other factors which contribute to the differential cell infiltration. Chemokine expression on the brain endothelium contributes to extravasation of neutrophils and monocytes in that the recognition of chemokines by rolling leukocytes induces their expression of the integrins, LFA (CD11a/CD18) and Mac-1 (CD11b/CD18). ICAM on the endothelium binds the integrins LFA and Mac-1 causing adhesion. LFA induces shear resistant arrest on the endothelium initiating diapedesis across the endothelium via Mac-1 for neutrophils (Gorina et al., 2014). Concurrent degranulation of neutrophils releases myeloperoxidase (MPO), neutrophil elastase and matrix metalloproteinase 9 (MMP9) which participate in the breakdown of the extracellular matrix to facilitate transendothelial migration (TEM) (Stowe et al., 2009; Bao Dang et al., 2013). Post IL-1β in ME7 mice cells seen in the parenchyma are mildly positive for MPO, suggesting MPO positive granules

were used to facilitate TEM. LPS and IL-1β have both been shown to increase expression of ICAM on endothelial cells (Allen et al., 2012; Gorina et al., 2014). Inhibition of CXCL1 has been shown to block neutrophil TEM (Lee et al., 2002) and anti Mac-1 antibodies have also been shown to block neutrophil TEM (Chen et al., 1994; Chopp et al., 1994; Weaver et al., 2000). Myeloperoxidase (MPO) is typically thought of as a neutrophil marker due to its constitutive presence in neutrophil granules (Prokopowicz et al., 2012). However, in recent years MPO has been found in macrophages activated by varying disease states (Sugiyama et al., 2001; Karakas and Koenig, 2012; Stefanova et al., 2012). At 24 hours there is an aggregation of cells at the glia limitans that have not undergone TEM following TNFα in ME7 animals that is not seen following IL-1β in ME7 animals. The majority of the cells reaching the *glia limitans* following TNFα challenge are macrophages which are MPO positive. Post-TNFα cells which are in the process of TEM are less strongly positive for MPO, indicating MPO may be facilitating macrophage TEM. Macrophage MPO has been shown to alter endothelial cell layers and activate matrix-metalloproteinases which would aid with TEM (Fu et al., 2001; Sugiyama et al., 2004). However the majority of aggregated cells post-TNFα are not undergoing TEM. It is likely that while the secondary signal required for neutrophil degranulation and consequent TEM is present on the *glia limitans,* the secondary signal required for macrophages to release their MPO is not yet present on the *glia limitans* and this is delaying their infiltration into the CNS, causing them to aggregate at the glia limitans at 24 hours (Sugiyama et al., 2001). In the case of monocyte infiltration LFA1 and MAC1 binding of ICAM is necessary for adhesion to the membrane. However, transmigration across the membrane appears to be dependent on VCAM interaction with the integrin VLA4 in certain situations (Meerschaert and Furie, 1995). As seen in the mRNA alterations at 2 hours, ICAM was significantly upregulated rapidly by both TNFα and IL-1β in ME7 animals compared to NBH animals. This could contribute to facilitation of transmigration of any neutrophils that arrived at the CNS membranes in ME7 animals from that point onwards. However at the 2 hour timepoint there is no significant increase in VCAM mRNA expression following TNFα or IL-1β treatments. There is perhaps a trend towards elevated VCAM following TNFα and IL-1β in ME7 animals. It has been shown that VCAM elevation was delayed in comparison to that of ICAM (Schnell et al., 1999b), therefore the monocytes

adherent to the ventricular membrane may not yet have the secondary signal VCAM, that they require for transmigration across the membrane. It has previously been shown that VCAM is induced in a spinal cord injury model, and that inhibiting TNFα in this model can prevent infiltration of monocytes to the injury site, suggesting TNFα can induce VCAM (You et al., 2013). Antibodies against VCAM have also been shown to decrease MPO activity, this suggests that if VCAM is the signal necessary for monocyte infiltration into the CNS it may induce release of the MPO visualised on the adherent monocytes at 24 hours (Altavilla et al., 1996). MPO can aid in transmigration across membranes.

The CD68-positive cells recruited by TNFα to the glia limitans of ME7 animals at 24 hours appeared to have migrated into the TNFα-injected hippocampus by 72 hours. The TNFα treated ME7 hippocampus showed significantly increased Pu.1-positive macrophages, which were blocked by systemic depletion of monocytes using Mc21. Thus, when CCL2 expression is exaggerated, more monocytes are recruited to brain barriers and more also extravasate. Although T-cells were somewhat increased in the hippocampus at 72 hours, the large increase in Pu.1-positive cells is the major contributor to the observed hypercellularity in the ME7+TNFα hippocampus at 72 hours. This robust monocyte infiltration indicates clear downstream effects of astrocyte priming and exaggerated CCL2 expression, which may be important for outcomes. Astrocytic NF-κB leads to expression of CCL2 in axonal injury (Khorooshi et al., 2008) and ablation of astrocytic CCL2 reduces CNS accumulation of macrophages, clinical deficits and axon loss in EAE, (Experimental Autoimmune Encephalitis – an animal model of demyelinating disease) (Moreno et al., 2014). CCL2 has also been shown to increase BBB permeability by redistributing tight junction proteins (Stamatovic et al., 2006; Yao and Tsirka, 2011). Our data indicate that TNFα induction of exaggerated CCL2 in the degenerating brain facilitates significant monocyte infiltration and may have significant deleterious consequences.

There is significant CSF-1/IL-34-dependent microglial proliferation in the ME7 model (Gomez-Nicola et al., 2013) and increased Ki67-positive proliferating cells were apparent at 72 hours after TNFα in the current study. Little Pu.1/Ki67 double-labelling was observed but this cannot exclude the possibility of increased

proliferation of microglia. The vast majority of Ki67 positive cells were also GFAP positive astrocytes. This indicates a significant alteration in astrocyte population activity at 72 hours post TNFα in the ME7 model. It has previously been shown that intracranial TNFα and IL-1β downregulate FOXO3a nuclear expression in vivo, dysregulating astrocytic cell cycles and inducing astrocyte proliferation, as verified by BrdU integration and Ki67 expression (Cui et al., 2011). Blocking reactive gliosis in a spinal cord injury model was shown to ameliorate function (Toyooka et al., 2011). It has also been shown that aged mice show more reactive astrocytes following ischemic stroke, with more rapid induction of an exaggerated glial scar and concurrently show greater deficits in motor function tests than younger animals (Badan et al., 2003). Greater astrogliosis following a CNS injury may be detrimental to long term functional recovery post-injury.

It is also known that the chemokines CCL2 and CXCL-1 have other functions in the brain. Systemic administration of CXCL-1 has been shown to inhibit rears, open field activity and burrowing in rats. However, central administration of CXCL-1 in that study had no effects on sickness behaviour (Campbell et al., 2010). It has been shown that Traumatic Brain Injury (TBI) elevates CCL2 at 24 hours rising to a peak at 72 hours post injury. Using a CCL2 antagonist reduced neuronal apoptosis and also improved performance of spatial memory in the Morris water maze (Liu et al., 2013).

It has been postulated that CCL2 acts as a neuromodulator. It has been shown to alter cognition both *in vivo* and neuronal activity *in vitro*. In APP PS1 mice lacking the CCL2 gene there is impaired memory acquisition and retention and impaired neurogenesis (Kiyota et al., 2013). Animals chronically overexpressing CCL2 in astrocytes have been shown to have altered basal synaptic function and excitability in the hippocampus (Nelson et al., 2011). In APP mice overexpressing the CCL2 gene there are accelerated memory impairments, synaptic dysfunction and an increase in Aβ oligomer formation (Kiyota et al., 2009; Nelson et al., 2011). Another relevant function of CCL2 is its ability to increase the permeability of the blood brain barrier in vivo (Stamatovic et al., 2005). CCL2 can induce BBB permeability by redistributing tight junction proteins, via PKC, and by reorganising the actin cytoskeleton in a CCR2 dependent manner (Stamatovic et

al., 2006; Yao and Tsirka, 2011). To perform this function CCL2 must first be truncated by plasmin (Sheehan et al., 2007; Yao and Tsirka, 2011). It has previously been shown that uPA the plasmin activator is highly elevated in ME7 prion disease (Cunningham et al., 2009b). This may also contribute to the exaggerated cell infiltration observed after exaggerated chemokine expression.

3.4.4 - Consequences of primed microglia and astrocytes

It has been shown in this chapter that both astrocytes and microglia are 'primed' by chronic neurodegeneration to produce exaggerated responses to central IL-1β and TNFα but also to peripheral LPS and IL-1β. A generalised heightened inflammatory sensitivity of multiple cell populations in the degenerating brain is highly significant since sterile CNS inflammatory insults such as stroke and TBI are common in the aging and neurodegenerating brain. However elevated systemic inflammation on a neurodegenerative background is also an extremely common scenario and these results show that exaggerated chemokine production and resulting cellular responses could have extremely deleterious consequences for the vulnerable brain in any of these scenarios.

In a model of closed head injury ablation of CXCR2 the CXCL1 cognate receptor significantly attenuated neutrophil infiltration at 12 hours and 7 days post-injury. This resulted in reduced tissue damage, neuronal loss and cell death. However, attenuation of CXCL1 signal did not ameliorate motor function deficits post-injury (Semple et al., 2010a). When normal and diabetic mice were compared post-ischemia and reperfusion, diabetic mice displayed significantly greater neutrophil infiltration which was associated with greater infarct size and significantly worse neurological scores (Chopp et al., 1994). Systemic neutrophil depletion has also been shown to reduce brain oedema and levels of atrophy post-TBI injury (Kenne et al., 2012). Use of an anti-CD11d antibody in a model of repeated concussion shows reduced neutrophil and macrophage infiltration to the CNS. This is concurrent with reductions in lipid peroxidation, astrocyte activation, neuronal loss and improved neurological outcome (Shultz et al., 2013). Depletion of peripheral $CCR2^{+}$ macrophages in a controlled cortical impact model of TBI showed a reduction in pro-inflammatory mediators and also ameliorated dysfunction on a hippocampal dependent cognitive task (Morganti et al., 2015). CCR2 deficient (-/-) mice subjected to controlled cortical impact showed some

amelioration of behaviour in the open field and learning and memory but not anxiety or motor function. There was also no difference in the volume of tissue loss in CCR2 negative animals however there was increased neuronal density compared to WTs subjected to the same TBI. This indicates that CCR2 may control some of the deleterious actions of infiltrating macrophages (Hsieh et al., 2014). CCL2 deficient (-/-) mice were shown not to have a significantly different acute response to closed head TBI. However 2 and 4 weeks post-injury they were significantly different on a number of markers. CCL2 deficient mice at 2 and 4 weeks post-TBI showed a significantly lower lesion volume, macrophage accumulation and astrogliosis concurrent with improved functional recovery (Semple et al., 2010b).

Neutrophils are thought to exert their neurotoxic functions by production of increased activity of NADPH oxidase and MPO, production of proinflammatory cytokines, chemokines, integrins and cell adhesion molecules and release of proteases such as elastase and MMP-9 (Jin et al., 2010). However little is known about the function of infiltrating macrophages in CNS injury. It is thought that macrophages can be both beneficial and detrimental to the post-injury brain: M2 polarised macrophages function in a phagocytic capacity, while M1 macrophages are pro-inflammatory. TREM2 deficiency prevents macrophage phagocytosis, which proved to exacerbate damage in an ischemic model (Kawabori et al., 2015). White matter injury post-TBI is worse when there is a stronger M1 macrophage polarisation post-injury. Experiments indicate that M1 macrophage polarisation can increase oligodendrocyte death in an *in vitro* model of ischemia. This theory indicates that the activation of primed microglia which may be susceptible to acting in a pro-inflammatory manner in a vulnerable brain, would be detrimental to cognitive outcomes. Individuals experiencing insults superimposed upon existing neurodegenerative disease may suffer more severe leukocyte recruitment and worse functional outcomes and understanding the mechanisms of these exaggerated responses may provide potential targets for therapeutic intervention.

Chapter 4

Central effects of systemic TNFα in neurodegeneration

Elements of this chapter have been published in:
Skelly et al., 2013, Plos One 8(12), DOI: 10.1371/journal.pone.0069123
Reis et al., 2015, Neuropathology and Applied Neurobiology (online pub), DOI:10.1111/nan.12232

4.1 - Summary

Systemic infection has been shown to exacerbate progression of neurodegeneration in AD cohorts, this was found to be significantly correlated with levels of systemic circulating TNFα. Earlier studies have shown that systemic LPS induced inflammation in the ME7 prion disease model can significantly increase working memory deficits and exacerbate sickness behaviour in comparison to NBH controls. It is now of significant interest to examine the effect of endogenous cytokines such as TNFα on working memory, sickness behaviour and pathology. A single acute dose of systemic TNFα (250μg/kg) exacerbated features of sickness behaviour; including core body temperature changes, open field activity and body weight, in ME7 compared to NBH. A lower dose (50μg/kg) can induce a transient cognitive deficit in a hippocampal dependent task in ME7 animals but not in NBH animals. However these changes are independent of any changes in features of pathology examined. We hypothesised that there would be increased apoptosis and evidence of axonal damage following systemic TNFα in ME7 animals. TUNEL labelling of apoptotic cells was not altered by TNFα challenge. High dose TNFα (250μg/kg) does not significantly alter any features of ME7 pathology. APP immunolabelling was used to examine axonal pathology, while there was no TNFα effect we discovered a novel feature of pathology; a robust aggregation of APP varicosities in the PO and VPM nuclei of the thalamus, overlapping with significant neuronal loss in the PO and significant synaptic loss in the VPM. Given systemic TNFα administration did not significantly alter ME7 pathology we utilised systemic administration of XPRO1595 a dominant negative TNFα inhibitor prior to systemic administration of LPS. This showed that the exacerbation of ME7 pathology by LPS was independent of TNFα actions. The timepoint used in the ME7 model is one with severe and widespread pathology, the mild inflammation caused by systemic TNFα in comparison to systemic LPS was not sufficient to alter this severe pathology. It would be of great interest to examine the effects of TNFα on a less severe model of pathology.

4.2 - Introduction

Systemic inflammation has been shown in animal models of neurodegeneration to exacerbate the progression of disease. In 2002 Combrinck et al, showed that ME7 animals displayed an exaggerated response to systemic LPS. They displayed a heightened hypothermic response and profound hypo-activity at 19 weeks post-LPS-inoculation alongside raised levels of IL-1β protein in the brain (Combrinck et al., 2002). In 2009 Cunningham et al assessed animals 12 weeks post inoculation. In that study, multiple evaluations of behaviour were shown to be modified by ME7 at 12 weeks. Burrowing behaviour was still impaired at 24 hours post ME7+LPS where NBH+LPS had recovered. Open field activity was inhibited to 80% in ME7+LPS but only to 50% in NBH+LPS. Core body temperature showed a significant hypothermia in ME7+LPS with no observable alteration in NBH+LPS (Cunningham et al., 2009a). The ME7 model of neurodegeneration displays an exaggerated sickness behaviour response upon LPS stimulation.

A progressive worsening of motor skills and exploratory behaviour was observed following a single systemic LPS dose in ME7 animals. Animals were trained on the horizontal bar and inverted screen task from 12 weeks post-inoculation and allowed to explore the open field from 6 weeks post-inoculation. On challenge with LPS at 15 weeks post-inoculation, ME7 animals showed a decrease in performance compared to NBH animals. Over the following 5 weeks the ME7 animals challenged with a single LPS dose scored progressively lower than all other groups on all three of these neurological tests (Cunningham et al., 2009a). This would indicate that a single episode of systemic LPS in a vulnerable animal can induce both acute and long lasting effects on acceleration and progression of disease.

A novel paddling alternation T maze task was used to assess working memory deficits. Animals are trained for a number of weeks beforehand until they achieve a consistent performance of about 80% correct choices on the alternation T maze. At 16 weeks post-inoculation all animals were challenged with systemic LPS and tested with the T-maze. This showed that the NBH+LPS group had no impairments whereas the ME7+LPS group had a significant impairment on the task. All groups recovered to baseline at 26 hours. This showed that the single dose of LPS produced a transient working memory deficit. NBH animals were also tested with

twice the dose of LPS to ascertain whether inflammation alone could cause a working memory deficit (Murray et al., 2010). LPS challenge in NBH animals was not sufficient to induce a working memory deficit. The interplay of both prior neurodegeneration and systemic inflammation is required to induce working memory deficits in the mice.

Systemic LPS in ME7 animals can exacerbate ongoing pathology. TUNEL staining revealed that apoptosis was 2 times higher in ME7 animals following LPS challenge than in saline challenged or unchallenged ME7 animals and 7 times higher than the same challenge in NBH animals. Staining for activated caspase 3 and neurofilament H showed that these dying cells were neurons. This showed that intraperitoneal LPS can induce acute neurodegeneration in ME7 animals where it does not in NBH animals (Cunningham et al., 2005b).

Systemic inflammation was also found to exacerbate behavioural and cognitive functions in aged animals. Aged mice displayed a greater decline in spatial tasks, social exploration, locomotor activity and food consumption following LPS challenge indicating exacerbation of age-associated memory impairments by systemic inflammation (Godbout et al., 2005; Chen et al., 2008). Peripheral LPS administration was also shown to induce atrophy of pyramidal neurons in the CA1 of aged but not adult mice (Richwine et al., 2008). Chronic infection with Bacillus Calmette-Guérin in aged animals induced a prolonged set of sickness behaviours. Aged mice did not regain weight lost due to sickness, aged mice also showed decreased locomotor activity and rearing compared to adult mice similarly challenged (Kelley et al., 2013). Using both contextual fear conditioning and the Morris water maze, Barrientos et al displayed an E. coli infection-induced impairment of hippocampal dependent memory in aged rats, exacerbating features of aging. The aged rats also displayed significantly elevated levels of IL-1β in the hippocampus 4 days after E. coli infection, indicating activation of primed microglia (Barrientos et al., 2006). The same group later found that multiple types of long term potentiation (LTP) (increased levels of synaptic strength linked to memory formation) were adversely affected in aged animals following an infection (Chapman et al., 2010).

Systemic inflammation has also been examined in transgenic models of Alzheimer's disease and was found to exacerbate many features of disease. LPS induced elevated cortical and hippocampal IL-1β protein in aged Tg2576 mice, but

not in younger Tg2576 animals or in similarly aged non transgenic littermates. In young and old Tg2576 mice $A\beta_{1-40}$ levels were raised following LPS however $A\beta_{1-42}$ levels were raised only in aged Tg2576 following LPS (Sly et al., 2001). Systemic LPS in an APP transgenic mouse has also been shown to produce exacerbated sickness behaviour with decreased locomotor activity, social interaction and food intake in comparison to WT littermates treated similarly. These animals also showed significantly elevated central IL-6 levels and more severe BBB permeability post-systemic LPS than controls (Takeda et al., 2013). Murine Hepatitis Virus or LPS administration in aged 3xTg-AD mice induced an increase in Tau pathology and LPS treatment caused a significant impairment in learning the Morris Water Maze (Sy et al., 2011).

Incidence of infection in the elderly was found to lead to an increased risk of dementia (Dunn et al., 2005). Viral infection was found to increase the rate of cognitive decline in a study of aging (Aiello et al., 2006). While many systemic inflammatory molecules may exacerbate cognitive decline, the role of systemic TNFα has been of particular note. Holmes et al have described a correlation between systemic circulating levels of TNFα and progression of AD. High baseline TNFα in an AD cohort led to a 4 fold increase in the rate of cognitive decline over a 6 month period, where low baseline TNFα led to no cognitive decline. A systemic inflammatory event (SIE) in an AD patient was also associated with increased circulating TNFα and a 2 fold increase in the rate of cognitive decline (Holmes et al., 2009a).This indicates that long term elevation in systemic TNFα levels has a severely detrimental effect on cognitive function and acute SIE related increases in TNFα can also significantly alter the progression of disease. Following on from these observations Holmes et al used etanercept (a TNFα decoy receptor) subcutaneously once a week in AD patients compared to placebo controls over 6 months. In recent conference proceedings Holmes showed that the etanercept treatment induced an attenuation of cognitive decline in AD patients (Holmes et al., 2014). A larger clinical trial is currently underway. Conference proceedings from the American College of Rheumatology in 2010 have reported that anti-TNFα therapies (infliximab, etanercept, and adalimumab) used in the treatment of rheumatoid arthritis significantly reduce the risk of development of AD (Chou et al., 2010), (this study remains unpublished). In AD patients TNFα elevation in both CSF and serum of patients was found to correlate with disease severity and

progression (Paganelli et al., 2002). Mild cognitive impairment (MCI) patients who later went on to develop AD were found to have elevated levels of TNFR1 and TNFR2, this elevation correlated with increased BACE1 activity in comparison to controls. The levels of TNFRs were also correlated with plasma levels of Aβ and with CSF levels of the axonal damage marker tau (Buchhave et al., 2010). Tarkowski found that MCI patients with elevated CSF levels of TNFα were more likely to progress to AD (Tarkowski et al., 2003). Overall these results indicate that elevated systemic TNFα levels make an individual more likely to suffer from progressive cognitive decline.

When we examined the literature for evidence of TNFα exacerbation of disease in animal models of neurodegeneration we find that this has been little examined. Acute i.c.v. injections of Infliximab a monoclonal anti-TNFα antibody for 3 days, in APP/PS1 mice showed decreased amyloid plaques and decreased tau phosphorylation (Shi et al., 2011). Medeiros et al showed that administering an anti-TNF antibody i.c.v. 15 minutes before i.c.v. Aβ prevented the learning and memory impairments seen in the Morris water maze following i.c.v. Aβ. Similar effects were produced in a TNFR1 knock-out (Medeiros et al., 2007). A study using 3xTg-AD mice crossed with a TNFR1/TNFR2 knockout showed exacerbated amyloidogenic and tau pathologies. Microglia derived from these animals display reduced phagocytic abilities indicating TNFα may be necessary in this process (Montgomery et al., 2011). The majority of these studies have utilised a TNFα blocking or deletion method to determine the effect of TNFα in a neurodegenerative model. This was done with no concurrent infection or inflammatory stimulus. It would be of great interest to determine if an acute systemic administration of TNFα could exacerbate cognitive deficits and pathology in a neurodegenerative model.

4.2.1 – Aims and objectives

To interrogate the central and systemic response of a naïve animal we first established a timecourse of the response to systemic TNFα (50μg/kg) in the blood, hypothalamus and hippocampus of normal animals.

We then aimed to determine whether there were exaggerated effects in animals with prior neurodegenerative disease. We examined the effects of systemic TNFα

(250μg/kg) on sickness behaviour measures in the open field, core body temperature and food intake. Cognitive effects of systemic TNFα (50μg/kg) on NBH and ME7 animals were tested utilising the alternation T-maze. Acute changes in transcription in the hippocampus of NBH and ME7 animals following systemic TNFα (50μg/kg) were examined; we focussed particularly on inflammatory and pro-apoptotic genes.

We aimed to examine the neuropathological effects of a single acute dose of systemically administered TNFα (250μg/kg) in NBH and ME7 animals. To do this we examined apoptosis and markers of axonal pathology such as APP and Synaptophysin. LPS can induce a robust apoptotic cascade in ME7 and we wished to determine the role of TNFα in this effect by utilising pretreatment with XPRO1595 (30mg/kg), a TNFα dominant negative inhibitor, prior to administration of systemic LPS (500μg/kg).

4.3 - Results

4.3.1 - TNFα time course

To assess the impact of intraperitoneal (i.p) injection of TNFα on central and systemic production of cytokines and their downstream genes and proteins, animals were sacrificed at 1, 2, 4, 8 and 24 hours post TNFα (50μg/kg) and 2, 4 and 24 hours post saline. Hippocampal and hypothalamic transcript alterations were quantified using Reverse Transcription Quantitative PCR. Systemic cytokine and chemokine alterations were measured using ELISA. A one-way ANOVA was performed to ascertain the impact of TNFα treatment. If the ANOVA was significant it was followed by Bonferroni's Multiple Comparison Test to compare specific time points to their controls.

4.3.1.1 - Systemic cytokine & chemokine levels

TNFα was injected i.p so the TNFα ELISA shows an increase due to both the injected TNFα and possibly the induction of systemic TNFα (figure 4.1b). There was a main effect of TNFα ($P<0.0001$, $F_{(8,45)}=15.53$) and the post hoc test showed increased TNFα at 1 hour ($P<0.001$) and 2 hours ($P<0.05$).

The IL-1β ELISA shows induction of the protein following TNFα administration ($P<0.0001$, $F_{(8,43)}=10.25$), the levels were time dependent with a small increase at 1 hour ($P<0.05$), leading to a larger increase at 2 hours ($P<0.001$) and declining slightly at 4 hours ($P<0.05$) (figure 4.1a).

IL-6 was increased following TNFα challenge ($P<0.0001$, $F_{(8,46)}=9.578$). IL-6 showed a consistent upregulation through the 1 and 2 hour timepoints ($P<0.001$) (figure 4.1c).

The chemokines CXCL-1 and CCL2 were both raised in the plasma following systemic TNFα challenge, ($P<0.0001$, $F_{(8,43)}=9.123$) and ($P<0.0001$, $F_{(8,43)}=14.08$) respectively. CXCL-1 showed a very strong upregulation at 1 hour ($P<0.001$) followed by a rapid return to baseline (figure 4.1d). CCL2 showed a more prolonged response to the TNFα stimulation (figure 4.1e). There was a strong

induction at 1 hour (P<0.001), 2 hours (P<0.001) and a smaller increase remains at 4 hours (P<0.05).

4.3.1.2 - Hypothalamic transcripts

One way ANOVA showed that TNFα had a robust effect on IL-1β levels in the hypothalamus (P<0.0001, $F_{(8,46)}$=13.41). IL-1β showed a large increase at 1 hour post challenge in mRNA transcripts (P<0.001). IL-1β then returned rapidly to baseline (figure 4.2a).

TNFα showed an increase in expression levels in the hypothalamus at 1, 2 and 4 hours (P<0.0001, $F_{(8,46)}$=101.3). TNFα mRNA increased rapidly to high levels at 1 hour (P<0.001), decreasing slightly but remaining high at 2 hours (P<0.001). It remained slightly increased at 4 hours post challenge (P<0.05) returning to baseline by 8 hours (figure 4.2b).

IL-6 displayed a large increase in transcription in the hypothalamus following systemic TNFα (P<0.0001, $F_{(8,46)}$=8.338). IL-6 increased at 1 hour (P<0.001) and maintained these levels at 2 hours (P<0.001) but returned to baseline by 4 hours (figure 4.2c).

Corticotrophin Releasing Factor (CRF) is an inducer of ACTH which induces production of the stress hormone corticosterone. CRF mRNA showed variability over the time course. The ANOVA showed that systemic TNFα did not have a significant effect on hypothalamic CRF (figure 4.2d).

TNFα challenge significantly increased hypothalamic expression of the chemokines CXCL-1 (P<0.0001, $F_{(8,46)}$=28.00) and CCL2 (P<0.0001, $F_{(8,46)}$=24.07). CXCL-1 showed a massive induction at 1 hour post-challenge (P<0.001) returning to baseline rapidly (figure 4.2e). CCL2 showed a more sustained induction, rising to high levels at 1 hour (P<0.001), sustaining these levels at 2 hours (P<0.001) and decreasing to non-significance at 4 hours (figure 4.2f). These results indicate such a rapid transcription of CXCL-1 and CCL2 mRNA that they are both likely induced at brain surfaces directly by injected TNFα.

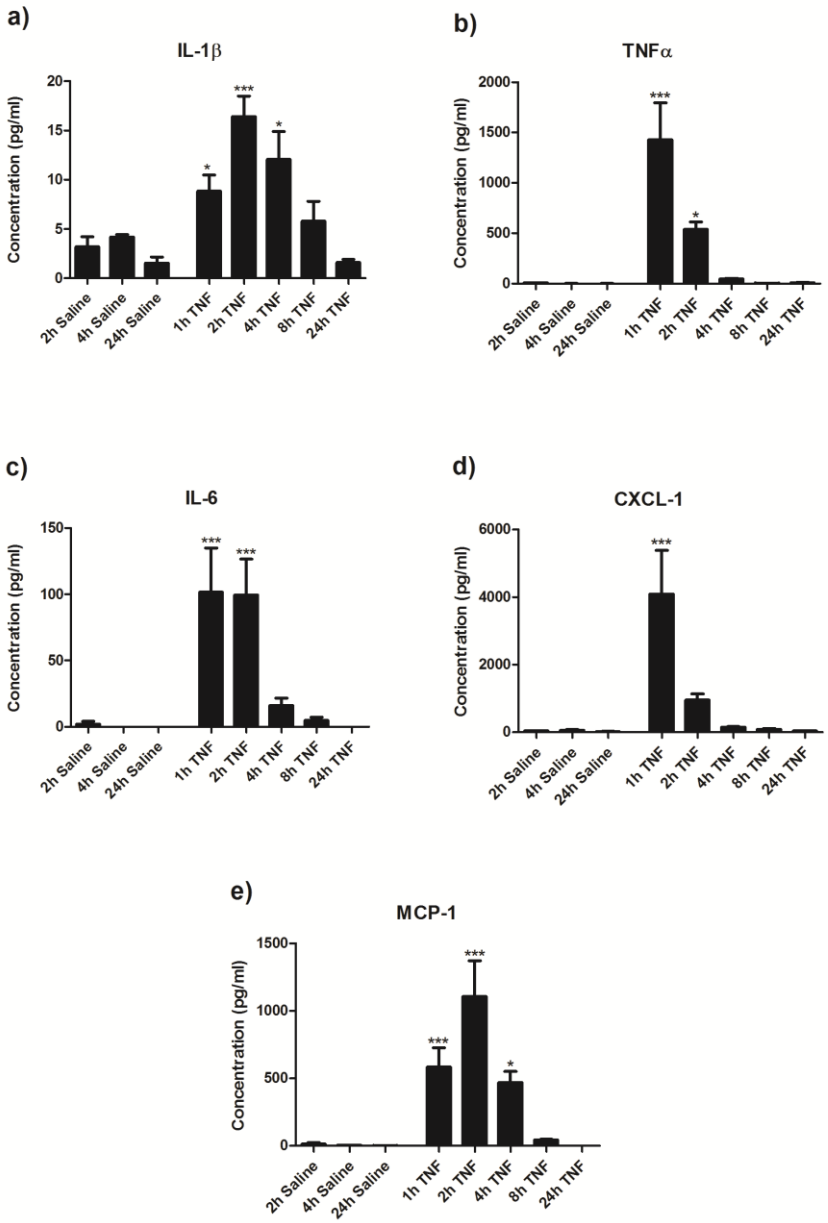

Figure 4.1 Impact of i.p. TNFα on systemic cytokines & chemokines.

Measures of systemic inflammatory markers following i.p TNFα (50µg/kg). Data were analysed using a one-way ANOVA followed by a Bonferroni multiple comparison test comparing each treatment group to its relevant saline group. Statistical significance is denoted by * (P<0.05), **(P<0.01), ***(P<0.001). All data are represented as the mean ±SEM, n=3-5 for all groups.

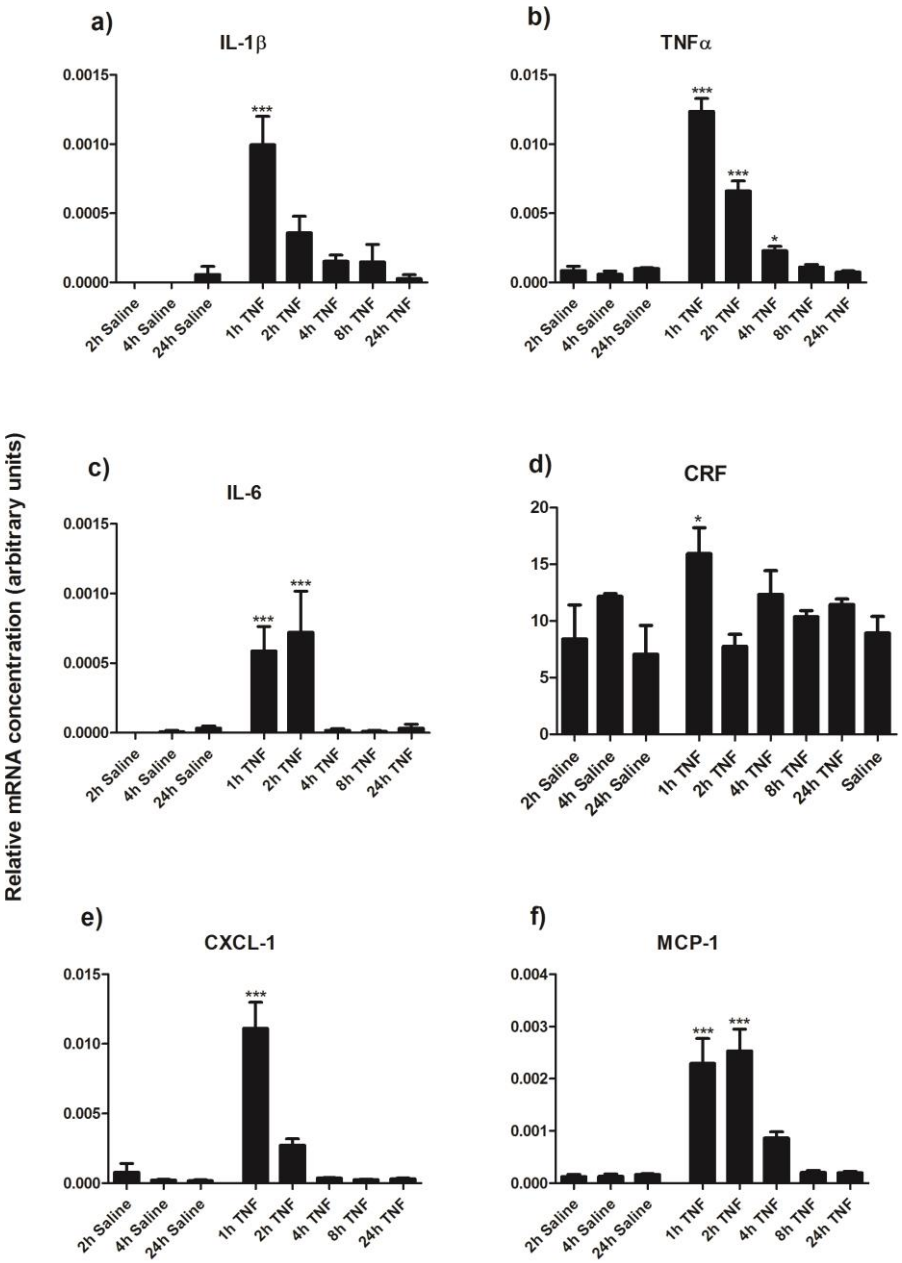

Figure 4.2 Impact of TNFα on Hypothalamic inflammatory transcripts.

Measures of hypothalamic inflammatory transcripts following TNFα (50µg/kg) i.p. Data were analysed using a One Way ANOVA followed by a Bonferroni multiple comparison test comparing each treatment group to its relevant saline group. Statistical significance is denoted by * (P<0.05), **(P<0.01), ***(P<0.001). All data are represented as the mean ±SEM, n=3-5 for all groups.

4.3.1.3 - Hippocampal transcripts

Intraperitoneal challenge with TNFα induced a robust increase in hippocampal TNFα transcripts ($P<0.001$, $F_{(8,47)}=90.93$). TNFα mRNA levels were significantly raised at 1 ($P<0.001$) and 2 hours ($P<0.001$) post challenge returning towards baseline at 4 hours (figure 4.3a). There was not a large IL-1β response to systemic TNFα in the hippocampus ($P<0.001$, $F_{(8,47)}=6.343$). IL-1β displayed a small but significant induction ($P<0.001$) at 1 hour post-systemic TNFα (figure 4.3b).

IL-6 showed a gradual hippocampal elevation to the TNFα challenge ($P<0.01$, $F_{(8,34)}=3.390$). The 1 hour time-point was elevated but did not prove statistically different from Saline while the 2 hour time-point was significantly increased from Saline ($P<0.05$) (figure 4.3c). IFNβ mRNA levels in the hippocampus were not affected by peripheral TNFα treatment ($P>0.05$, $F_{(8,41)}=1.837$) (figure 4.3d).

Hippocampal expression of CCL2 was induced by systemic TNFα administration ($P<0.001$, $F_{(8,47)}=26.56$). CCL2 had a robust increase with large elevations at both 1 ($P<0.001$) and 2 hours ($P<0.001$) (figure 4.3e). Hippocampal CXCL-1 (figure 4.3f) was significantly increased following systemic TNFα challenge($P<0.001$, $F_{(8,47)}=86.54$). CXCL-1 showed a large increase at 1 hour ($P<0.001$) but while it was still increased the fold difference had declined considerably by 2 hours ($P<0.05$).

iNOS (figure 4.4a)appears to be induced further downstream of the peripheral challenge peaking at 2 hours and remaining elevated at 4 hours. There is a main effect of TNFα i.p. ($P<0.001$, $F_{(8,47)}=6.850$) however the effect size is quite small. Pairwise post-hoc comparisons show that levels are significantly elevated at 2 hours ($P<0.001$) and 4 hours ($P<0.05$) compared to their Saline controls. uPAR (figure 4.4b) shows a remarkably large induction post systemic TNFα challenge ($P<0.001$, $F_{(8,45)}=147.6$). This induction occurs early, peaking at 1 hour ($P<0.001$) with a slight decrease at 2 hours, but still significantly elevated with respect to saline challenge ($P<0.001$) and returning to baseline levels by 4 hours.

The macrophage marker CD68 appears to be completely unperturbed at the mRNA level by the peripheral TNFα challenge ($P>0.05$, $F_{(8,45)}=0.4342$) (figure 4.4c). PTX3 is proposed to be altered by astrocyte activation (Zamanian et al., 2012) and to be induced by TNFα and IL-1β (Hennessy et al., 2015). It shows a small change following TNFα ($P<0.001$, $F_{(8,45)}=3.265$). PTX3 is statistically

significantly different from saline at the 1 hour time-point ($P<0.01$) but its induction is less than 1.5 fold (figure 4.4d).

CD11b is another macrophage marker, similarly to CD68 it was unchanged following the peripheral TNFα challenge ($P<0.001$, $F_{(8,45)}=1.911$) (figure 4.4e). Hippocampal transcription of the TNFR1 gene was altered slightly by i.p. TNFα ($P<0.001$, $F_{(8,45)}=3.397$) but it appears to be quite far downstream of TNFα administration. TNFR1 shows a slight but significant increase at 4 hours post treatment ($P<0.05$) (figure 4.4f).

Pro- and anti-apoptotic mRNA transcription

The effects of TNFα on transcription of various elements of the apoptotic cascade was investigated. Fas is a death receptor linked to the TNFα pathway. Hippocampal Fas (figure 4.5a) was highly affected by the peripheral TNFα challenge ($P<0.001$, $F_{(8,45)}=61.13$). Fas shows a significant increase at 1 ($P<0.001$), 2 ($P<0.001$) and 4 hours ($P<0.01$) post challenge. However, Fas Ligand mRNA was not affected by systemic TNFα challenge within the 24 hour period examined ($P>0.05$, $F_{(8,47)}=0.7824$) (figure 4.5b).

p53 is a transcription factor thought to regulate elements of the TNFα apoptotic cascade. Levels of hippocampal P53 mRNA were not altered by systemic TNFα challenge ($P>0.05$, $F_{(8,47)}=1.336$) (figure 4.5c). Noxa and PUMA are p53 dependent apoptosis genes. When produced they interact with mitochondrial anti-apoptotic Bcl-2 family members inducing the apoptosis cascade. Hippocampal NOXA showed a minor but statistically significant induction following systemic TNFα challenge ($P<0.01$, $F_{(8,47)}=3.732$). NOXA was significantly elevated at 2 hours ($P<0.05$) (figure 4.5d).

PUMA (figure 4.5e) showed a main effect of treatment ($P=0.0122$, $F_{(8,47)}=2.904$) however none of the time-points examined by *post hoc* were significantly different. The pro-apoptotic protein Bax (figure 4.5f) was also not transcriptionally altered in the hippocampus following systemic TNFα challenge ($P>0.05$, $F_{(8,47)}=1.372$)

Both RIPK1 and RIPK3 are adapters linked to the TNFR1 cell death pathway. RIPK1 is a purported anti-apoptotic gene whereas RIPK3 attenuates both RIPK1 and NF-KB signalling to induce apoptosis. There was no alteration of RIPK1 mRNA

over the 24 hour time course ($P>0.05$, $F_{(8,47)}=0.7818$) (figure 4.5g). RIPK3 however showed an influence of TNFα treatment ($P<0.001$, $F_{(8,47)}=4.633$). RIPK3 mRNA levels gradually increased over the time course reaching a statistically significant increase 24 hours post systemic TNFα administration ($P<0.01$) (figure 4.5h).

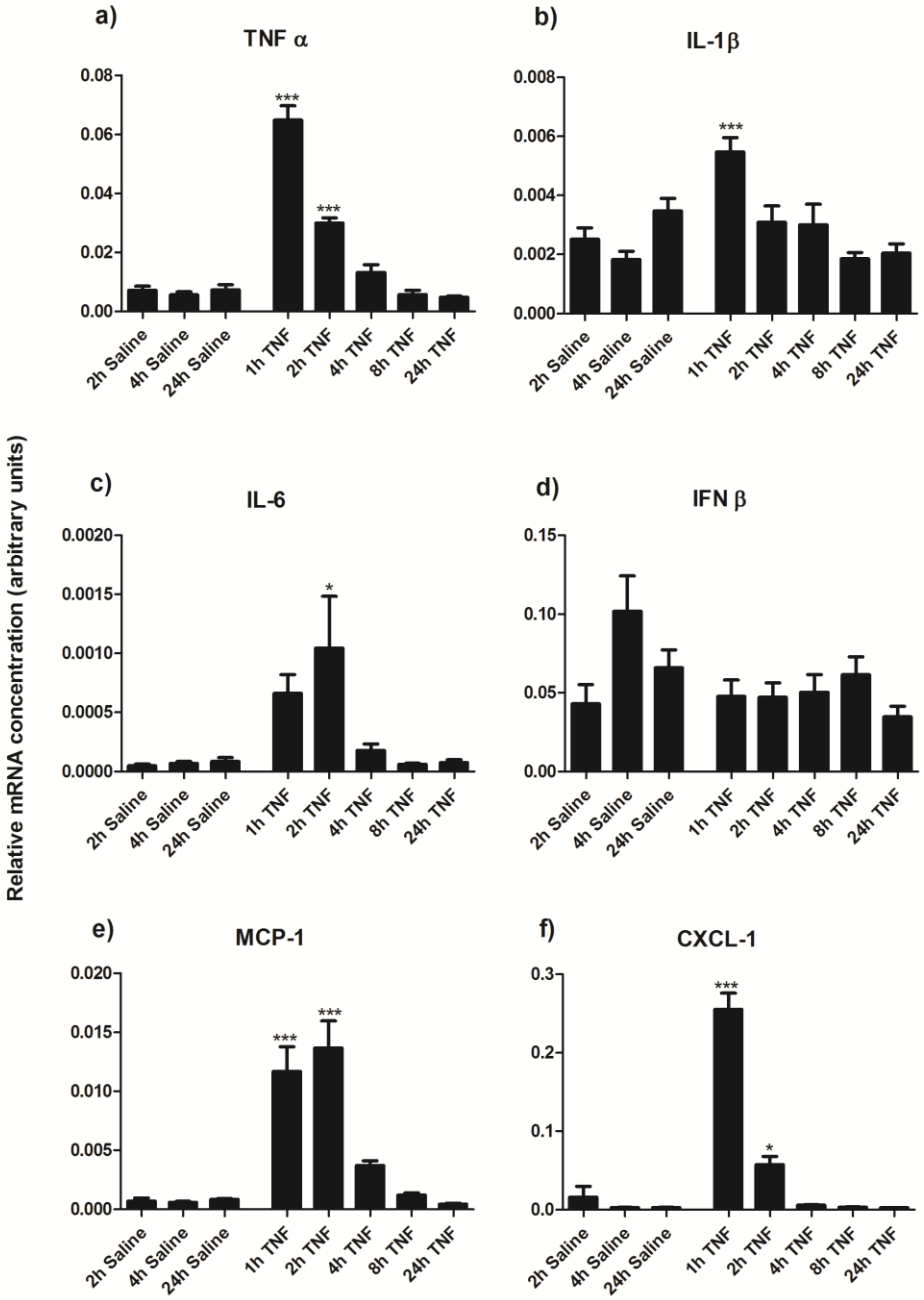

Figure 4.3 Impact of TNFα on Hippocampal inflammatory transcripts.

Measures of hippocampal inflammatory transcripts following TNFα (50µg/kg) i.p. Data were analysed using a one-way ANOVA followed by a Bonferroni multiple comparison test comparing each treatment group to its relevant saline group. Statistical significance is denoted by * (P<0.05), **(P<0.01), ***(P<0.001). All data is represented as the mean ±SEM, n=3-5 for all groups.

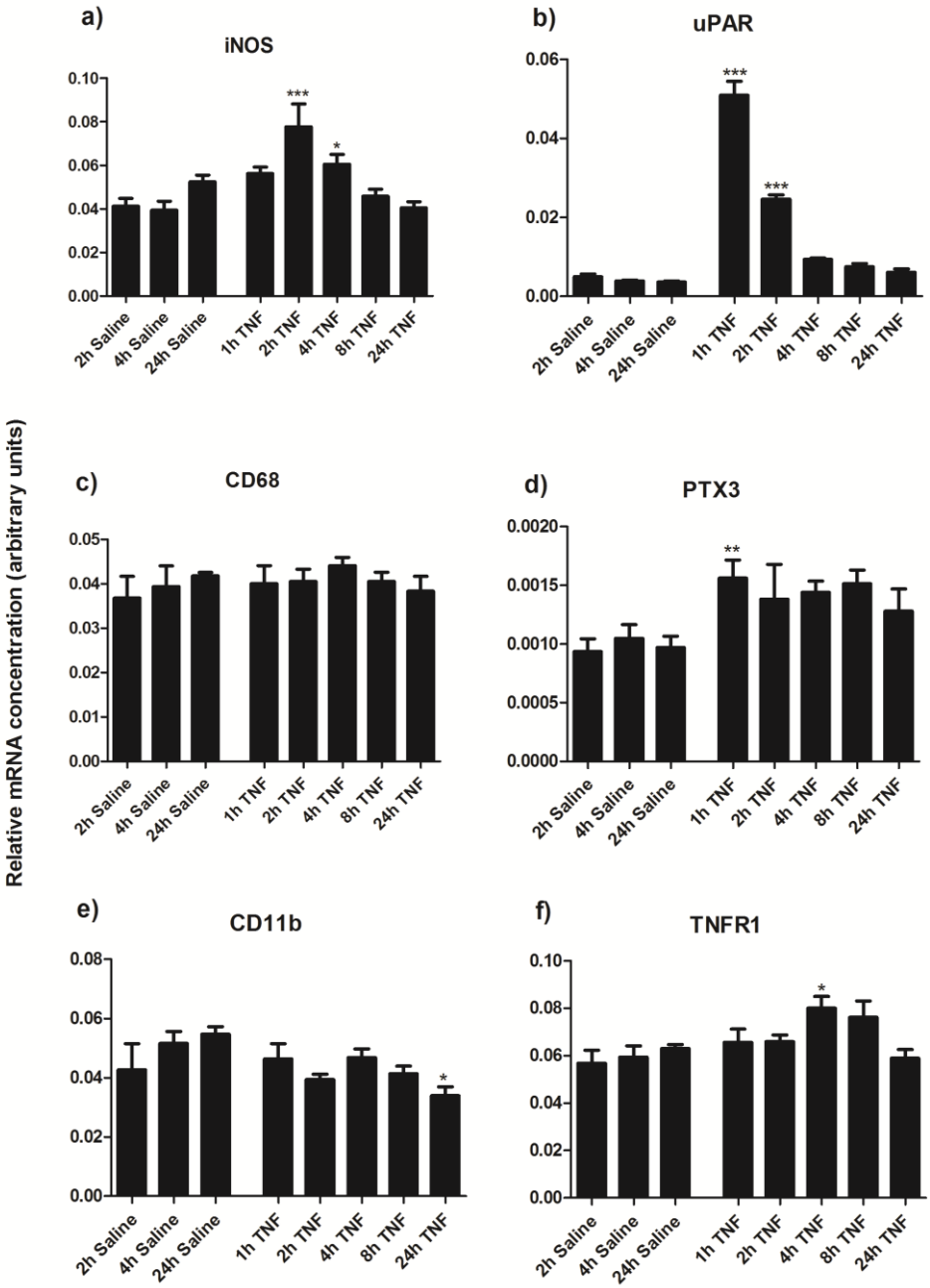

Figure 4.4 Impact of TNFα on Hippocampal inflammatory transcripts.

Measures of hippocampal inflammatory transcripts following TNFα (50µg/kg) i.p. Data were analysed using a one-way ANOVA followed by a Bonferroni multiple comparison test comparing each treatment group to its relevant saline group. Statistical significance is denoted by * (P<0.05), **(P<0.01), ***(P<0.001). All data is represented as the mean ±SEM, =3-5 for all groups.

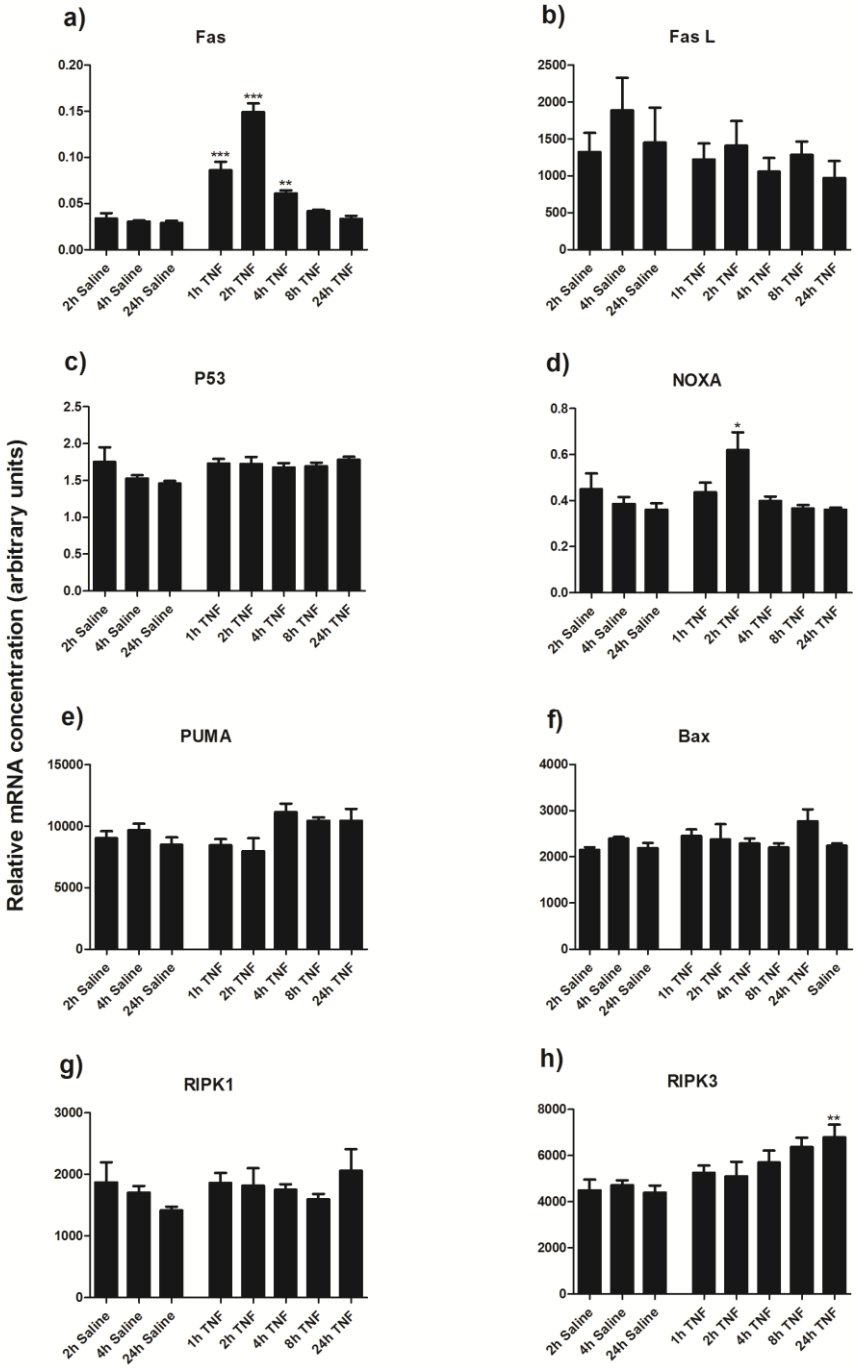

Figure 4.5 Impact of TNFα on Hippocampal pro & anti apoptotic transcripts.

Measures of hippocampal pro & anti apoptotic transcripts following TNFα (50µg/kg) i.p. Data were analysed using a one-way ANOVA followed by a Bonferroni multiple comparison test comparing each treatment group to its relevant saline group. Statistical significance is denoted by * ($P<0.05$), **($P<0.01$), ***($P<0.001$). All data is represented as the mean ±SEM, n=3-5 for all groups.

4.3.2 – TNFα induced sickness behaviour in NBH & ME7 mice

Having characterised systemic TNF-α induced CNS inflammatory changes in normal animals, ME7 and NBH mice were challenged with TNFα (250μg/kg) i.p and monitored on various sickness behaviour parameters over a period of 18 hours in order to assess whether these were different in diseased animals compared to those in normal animals. Sickness behaviour is a conserved set of behaviours involved in the coordination of the body's defence against infection. This involves alterations in core-body temperature, locomotor activity, mood, energy metabolism and motivation. Data were analysed by three way repeated measures ANOVA to analyse the effects of disease,TNFα treatment and time. Bonferroni multiple comparison *post hoc* test was used contingent on main effects of treatment.

TNFα induced acute hypothermia peaking at 2 hours and returning gradually to baseline at 18 hours (figure 4.6a). The reduction in core body temperature is significantly more severe in ME7 animals. There is a main effect of TNFα ($P<0.001$, $F_{(1,174)}=19.91$) and an interaction between disease, treatment and time ($P<0.001$, $F_{(4,174)}=15.94$).

TNFα caused minor weight loss probably by inducing acute hypophagia following treatment ($P<0.0001$, $F_{(1,104)}=34.36$) with an interaction between treatment and time ($P<0.0001$, $F_{(2,104)}=17.63$). Weight loss was exacerbated in ME7 animals treated with TNFα compared to NBH+TNFα animals at the 18 hour timepoint (figure 4.6b).

Rears and open field are measures of sickness behaviour that encompass lethargy and motivation to explore. Following TNFα challenge, there were reduced levels of activity in the open field (figure 4.6d). There was a main effect of TNFα ($P<0.01$, $F_{(1,139)}=8.58$) and an interaction between disease, treatment and time ($P<0.01$, $F_{(3,139)}=4.67$). ME7 animals following TNFα showed a particularly robust decrease in activity at 3 hours ($P<0.001$).

Rearing was examined in the Open Field after systemic TNFα. There was no main effect of treatment however there was a robust interaction between disease, treatment and time ($P<0.001$, $F_{(3,139)}=11.06$). The ME7+TNFα group show a more severe and more prolonged decrease in rearing activity following systemic TNFα treatment (figure 4.6d). Conversely NBH+TNFα animals appeared to have elevated rearing levels in the open field in comparison to NBH+Saline. This may be due to a

lack of habituation due to TNFα administration in this group. However the impact of TNFα n ME7 animals was significantly more severe.

4.3.3 - Cognitive effects of TNFα in ME7 prion mice

ME7 and NBH animals were trained to proficiency on the alternation T maze task over 3 to 4 weeks. Once 80% proficiency had been achieved the animals were challenged with TNFα (50μg/kg) or Saline. They were then tested for working memory deficits on the alternation T maze with 3 blocks of 5 trials between 1 and 7 hours post-challenge and 2 blocks of 5 trials 24 hours post challenge.

Systemically administered TNFα induced a transient deficit in working memory in the T maze task in ME7 animals where there was no deficit in NBH animals. Using a Three way repeated measures ANOVA there was an interaction between disease, treatment and time following systemic TNFα challenge ($P<0.01$, $F_{6,328}=3.09$). An a priori prediction from previous studies in the lab suggested that the effect of TNFα on working memory would be a transient one (figure 4.7). The one hour ($P<0.01$) and three hour ($P<0.05$) timepoints following systemic TNFα in ME7 animals were significantly different from the other treatment groups (Two way ANOVA on individual timepoints).

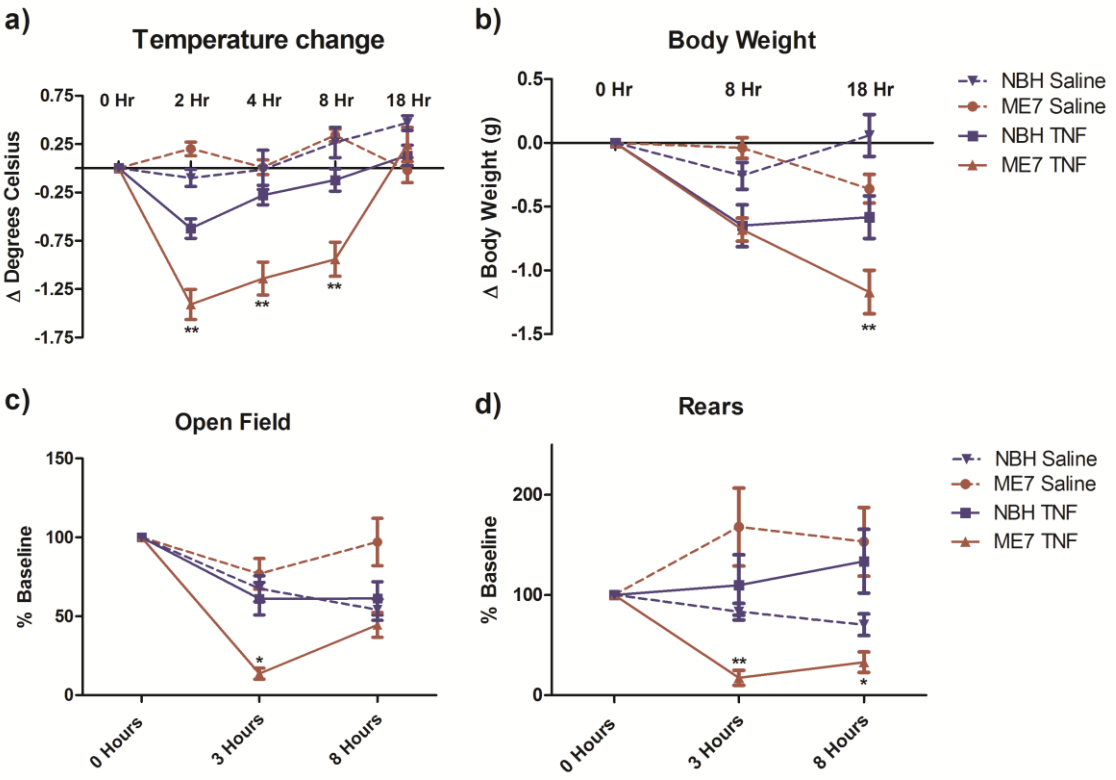

Figure 4.6 Impact of systemic TNFα on sickness behaviour in NBH & ME7.

Measures of sickness behaviour following TNFα (250µg/kg) i.p in ME7 prion disease mice 18 weeks post-inoculation. Temperature change and Body Weight are presented as change from baseline. Rears and Open field are graphed as percentage of baseline. Data were analysed using a three-way ANOVA followed by Bonferronis multiple comparison test comparing each treatment group to its relevant control group. Statistical significance is denoted by * (P<0.05), ** (P<0.01), *** (P<0.001). All data is represented as the mean ±SEM, n=6-15 for all groups.

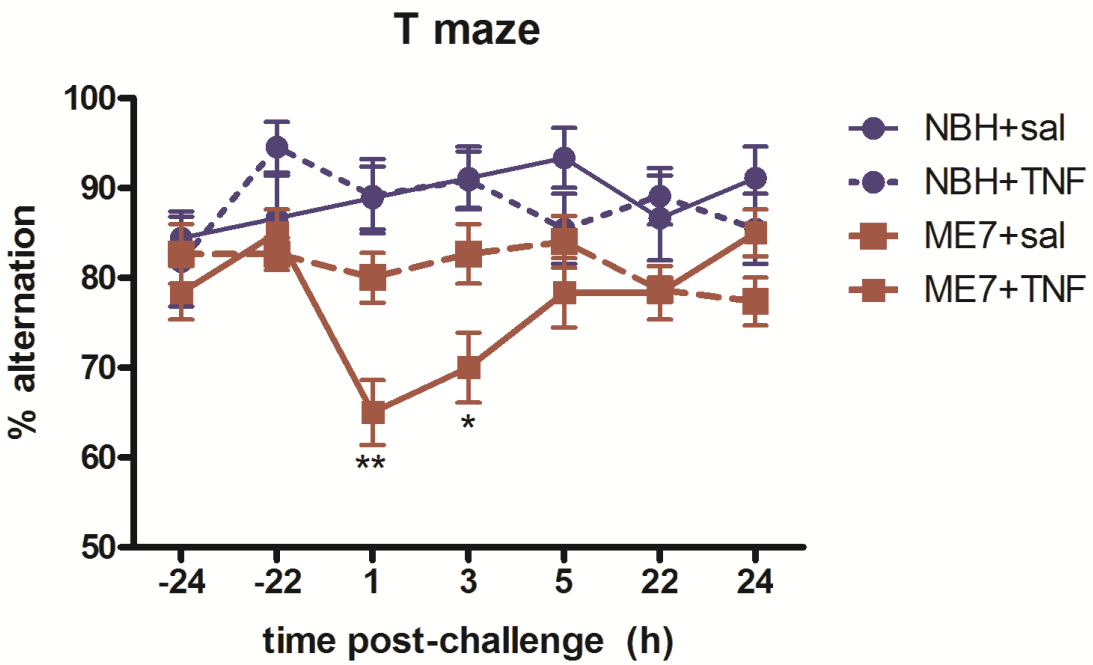

Figure 4.7 Impact of systemic TNFα on working memory in NBH & ME7

Measure of percentage alternation following systemic TNFα (50µg/kg) or Saline in ME7 or NBH animals 16 weeks post-inoculation. Data were analysed using a two-way ANOVA followed by a Bonferroni multiple comparison test comparing individual time-points. Three-way ANOVA was used to test overall significance. Statistical significance is denoted by * (P<0.05), ** (P<0.01), *** (P<0.001). All data is represented as the mean ±SEM, n=9-15 for all groups.

4.3.4 – Impact of systemic TNFα on hippocampal transcripts in NBH & ME7

Balanced groups of NBH and ME7 prion diseased animals were injected i.p with TNFα (50μg/kg). These animals were then sacrificed at 2 hours. Given the alterations in sickness behaviour in ME7 animals these samples were used to ascertain whether there were any exaggerated transcriptional responses to systemic TNFα in the hippocampas. These data were analysed by Two way ANOVA in followed by a Bonferroni *post hoc* comparison.

ME7 prion disease had a large effect on basal levels of hippocampal TNFα (figure 4.8a) mRNA. These levels were not significantly affected by i.p. TNFα administration. Conversely systemic TNFα challenge significanttly increased TNFα mRNA expression in NBH animals. There was a main effect of treatment ($P<0.05$, $F_{(1,15)}=7.261$) and of disease ($P<0.0001$, $F_{(1,15)}=57.53$).

IL-1β was significantly induced in ME7 animals (figure 4.8b). Disease showed a main effect increasing IL-1β mRNA levels ($P<0.0001$, $F_{(1,15)}=23.02$). TNFα did not show a significant effect on IL-1β levels in NBH or ME7 animals but there was a trend towards elevation ($P=0.0864$, $F_{(1,15)}=3.368$).

CCL2 was robustly increased by ME7 (figure 4.8c). It was further elevated by TNFα challenge in NBH animals but not significantly so in ME7 animals. There was a main effect of disease ($P<0.001$, $F_{(1,15)}=22.05$) and a main effect of treatment ($P<0.01$, $F_{(1,15)}=10.85$) but no interaction of these factors.

PTX3 levels were raised in ME7 animals (figure 4.8d). There was a main effect of disease on PTX3 levels ($P<0.0001$, $F_{(1,15)}=119.5$). Systemic TNFα lowered PTX3 levels in ME7 animals. There is a significant impact of TNFα on PTX3 levels in ME7 animals ($P<0.05$).

Transcripts for the death receptor Fas were increased with ME7 prion disease (figure 4.9a). Treatment has a main effect ($P<0.05$, $F_{(1,15)}=4.669$) as did disease ($P<0.001$, $F_{(1,15)}=21.47$). TNFα had no differential effect between diseased and normal animals (i.e. no interaction of disease and treatment).

Fas Ligand (FasL) (figure 4.9b) and p53 (a pro-apoptotic transcription factor) (figure 4.9c) were both increased by disease. Neither gene was significantly affected by TNFα challenge. There were main effects of disease ($P<0.001$, $F_{(1,15)}=30.55$) for FasL and ($P<0.001$, $F_{(1,15)}=25.88$) for p53.

NOXA is a pro apoptotic protein involved in the opening of the mitochondrial permeability transition pore (MPTP). NOXA levels were not robustly altered by disease (figure 4.9d). However, systemic TNFα robustly induced NOXA in ME7 animals but not in NBH animals. There were main effects of disease ($P<0.01$, $F_{(1,15)}=11.98$) and of treatment ($P<0.01$, $F_{(1,15)}=11.12$) and there was also an interaction between treatment and disease ($P<0.05$, $F_{(1,15)}=5.255$). *Post hoc* analysis showed that NOXA mRNA in ME7+TNFα animals was elevated compared to ME7+Saline ($P<0.05$).

Bid and Bim are pro-apoptotic genes involved in the opening of the MPTP. Neither Bid nor Bim levels were affected by either ME7 prion disease or TNFα treatment (figure 4.10a and b). Caspase 6 levels were not affected by treatment (figure 4.10c) but disease elevated caspase 6 mRNA levels (main effect of disease: $P<0.001$, $F_{(1,15)}=44.36$). Anti-apoptotic proteins Bcl-2 and Bcl-Xl mRNA levels also showed no response to either prion disease or TNFα treatment (figure 4.10d and e).

Receptor for advanced glycation end products (RAGE) showed a robust increase of mRNA levels in ME7 prion disease (figure 4.10 f). There was a main effect of disease ($P<0.001$, $F_{(1,15)}=50.93$) but TNFα had no effect on its mRNA levels.

STEAP4 was increased by disease (main effect of disease: ($P<0.001$, $F_{(1, 15)}=19.24$). Its expression was not affected by TNFα (figure 4.11a).

Receptor Activator of Nuclear Factor κ B (RANK) levels are not altered by disease. Though TNFα showed no effect on RANK in NBH animals it induced a significant increase in RANK in the ME7 animals (figure4.11b). There are large levels of induction of RANK following TNFα in the ME7 animal but not in the NBH animal. There is a main effect of treatment ($P<0.05$, $F_{(1,15)}=4.631$). The increase in RANK following TNFα in ME7 was also significantly different to the ME7 Saline treated group ($P<0.05$).

RANK Ligand was increased by disease. The main effect of disease was ($P<0.01$, $F_{(1,15)}=14.18$). RANKL was not significantly affected by TNF treatment (figure 4.11c).

S100b, iNOS and TNFR1 mRNA levels were all increased by disease but were not altered by TNFα challenge (figure 4.11d, e and f). There was a main effect of disease in s100b ($P<0.001$, $F_{(1,15)}=38.28$), iNOS ($P<0.01$, $F_{(1,15)}=13.38$) and TNFR1 ($P<0.001$, $F_{(1,15)}=130.8$).

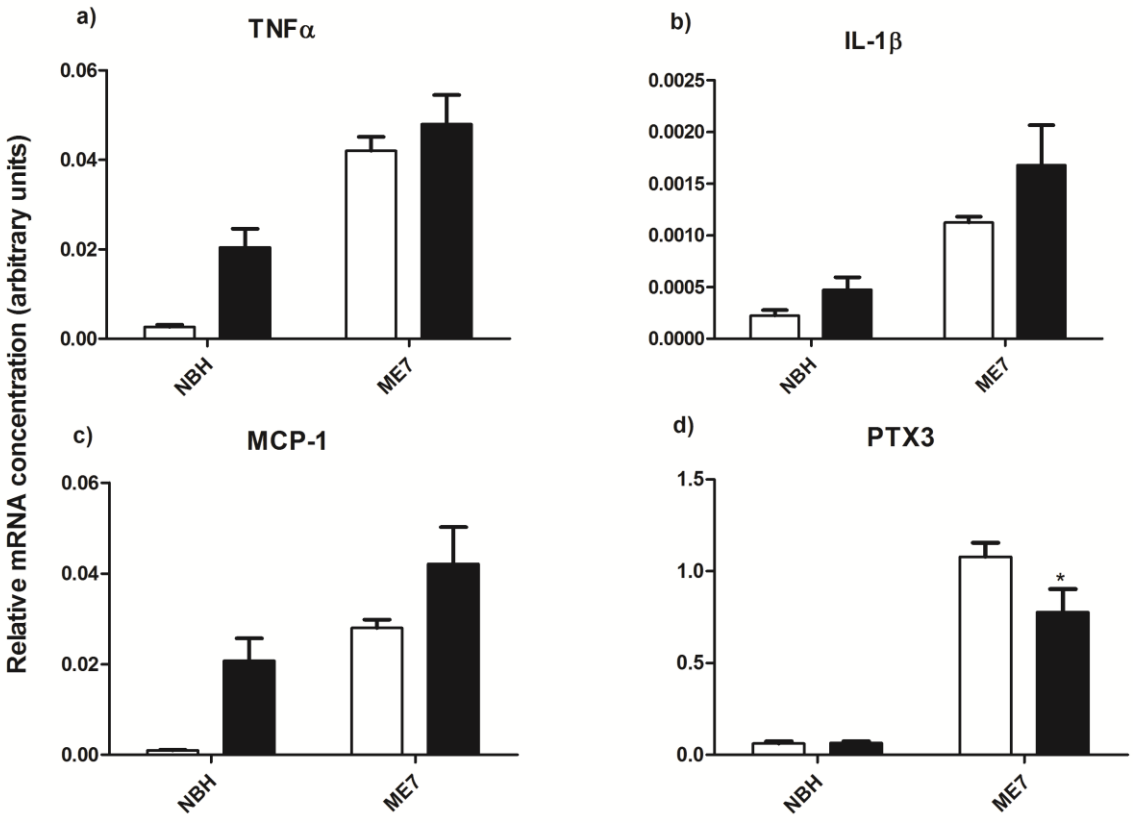

Figure 4.8 Impact of TNFα on hippocampal inflammatory transcripts in ME7 at 2 hours.

Measures of hippocampal inflammatory transcripts following TNFα (50μg/kg) given i.p to 16 week ME7 prion mice, at 2 hours. Data were analysed using a two-way ANOVA followed by a Bonferroni post hoc test comparing treatments within disease. Statistical significance is denoted by * (P<0.05), **(P<0.01), ***(P<0.001). All data are represented as the mean ±SEM, n=3-5 for all groups.

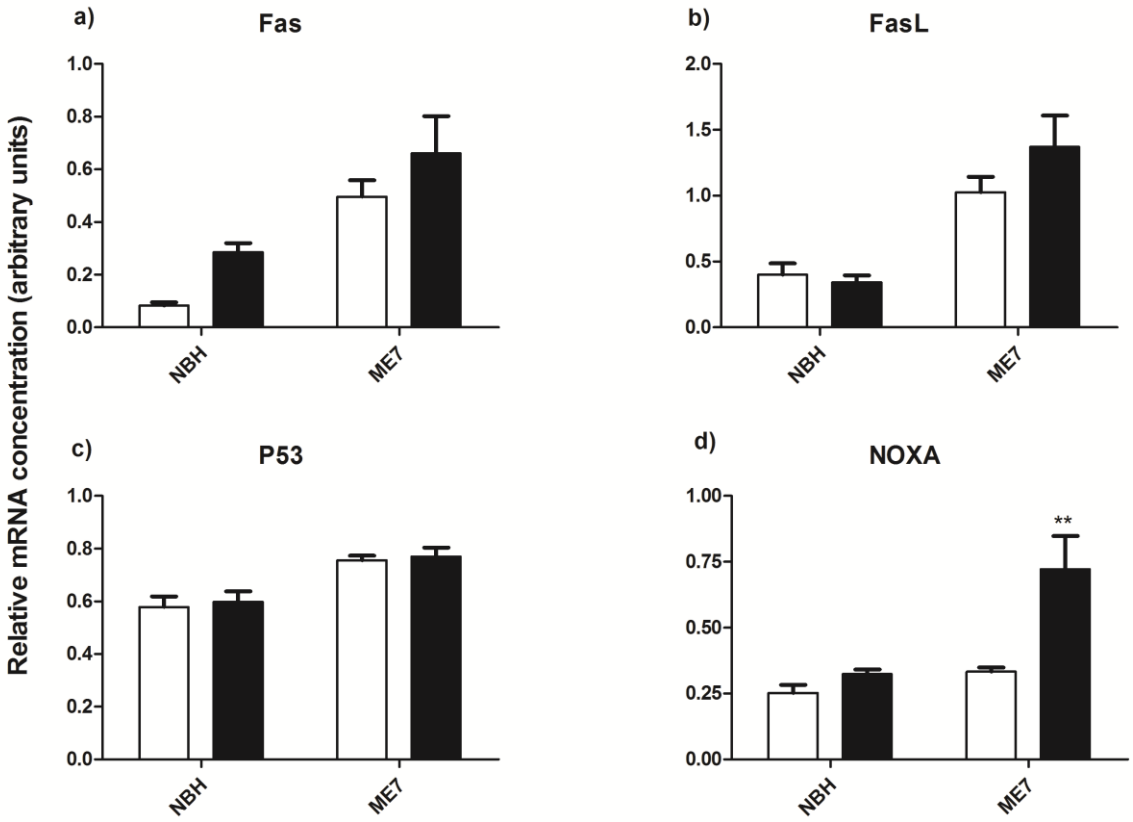

Figure 4.9 Impact of TNFα on hippocampal apoptotic transcripts in ME7 at 2 hours.

Measures of hippocampal apoptotic transcripts following TNFα (50µg/kg) given i.p to 16 week ME7 prion mice, at 2 hours. Data were analysed using a two-way ANOVA followed by a Bonferroni post hoc test comparing treatments within disease. Statistical significance is denoted by * (P<0.05), **(P<0.01), ***(P<0.001). All data are represented as the mean ±SEM, n=3-5 for all groups.

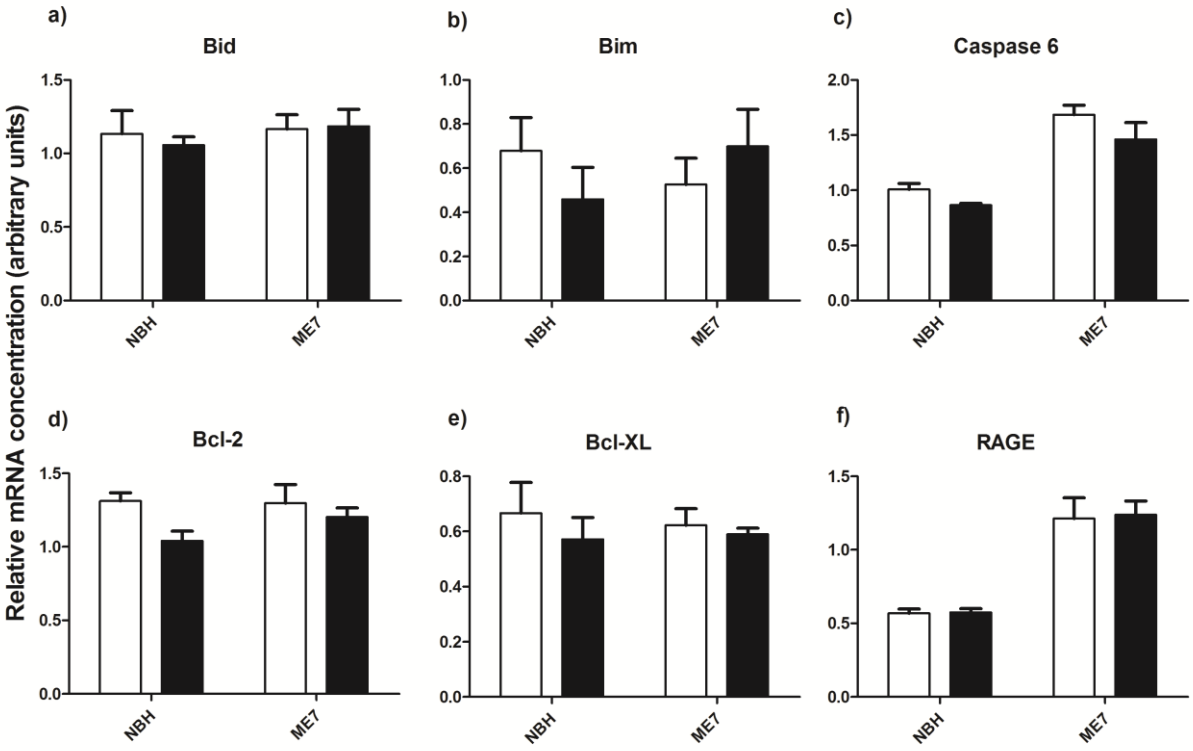

Figure 4.10 Impact of TNFα on hippocampal transcripts in ME7 at 2 hours.

Measures of hippocampal transcripts following TNFα (50µg/kg) given i.p to 16 week ME7 prion mice, at 2 hours. Data were analysed using a two-way ANOVA followed by a Bonferroni post hoc test comparing treatments within disease. Statistical significance is denoted by * ($P<0.05$), **($P<0.01$), ***($P<0.001$). All data are represented as the mean ±SEM, n=3-5 for all groups.

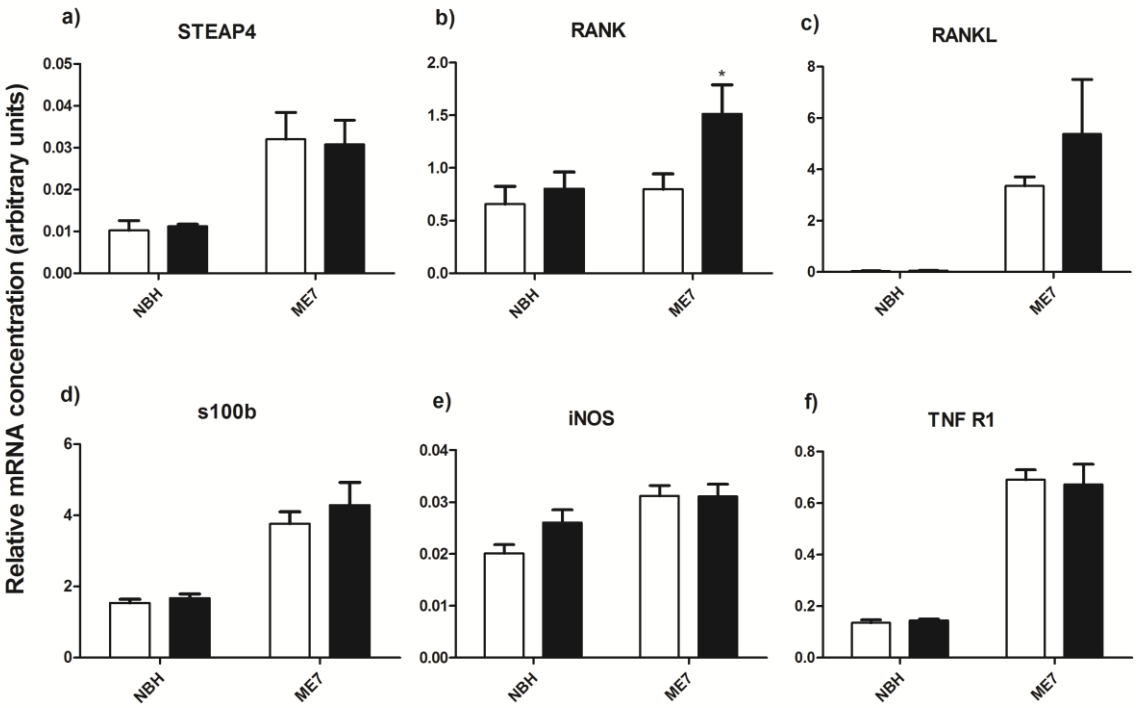

Figure 4.11 Impact of TNFα on hippocampal transcripts in ME7 at 2 hours.

Measures of hippocampal transcripts following TNFα (50µg/kg) given i.p to 16 week ME7 prion mice, at 2 hours. Data were analysed using a two-way ANOVA followed by a Bonferroni post hoc test comparing treatments within disease. Statistical significance is denoted by * (P<0.05), **(P<0.01), ***(P<0.001). All data are represented as the mean ±SEM, n=3-5 for all groups.

4.3.5 – The impact of systemic TNFα administration on ME7 neuropathology.

NBH and ME7 animals were treated with 50μg/kg intraperitoneal TNFα or Saline. They were sacrificed at either 9 or 18 hours. Brains were formalin perfused, embedded in paraffin wax and sectioned at 10μm on a microtome for immunohistochemistry. Markers of apoptosis, and axonal and synaptic pathology were assessed. Any quantifications were analysed using a one-way ANOVA followed by a Dunnets multiple comparison to ME7 Saline.

4.3.5.1 - Apoptosis

Two different labels of apoptosis were used to determine whether there were more apoptotic cells following systemic TNFα in the ME7 model. Caspase 3 is an essential element in the caspase cascade preceding apoptotic cell death. There were many different forms of caspase positive cells, Caspase 3 labelling mainly appeared as a dense stain surrounding a condensed nucleus. There were also variations with a weaker stain or some cells did not contain a condensed nucleus. There were many occurrences of caspase 3 labelling of particles surrounding a labelled cell body; these may be caspase 3 positive varicosities on degenerating axons. Examples are shown in figure 4.12d-f. In all regions counted in ME7 animals there was a significant level of ongoing apoptosis, as shown by large numbers of caspase 3 positive cells in the ME7 groups. TNFα did not alter this parameter at this point in disease. When quantified in a coronal section (figure 4.12a) ME7+Saline proved significantly different to NBH+TNFα ($P<0.001$), but not different to ME7+TNFα.

Terminal deoxynucleotidyl transferase dUTP nick end labelling (TUNEL) can be used to visualise apoptosis as it labels terminal ends of nucleic acids exposed by DNA fragmentation. TUNEL staining appeared throughout the coronal section of ME7 labelled sections. TUNEL labelling mainly appeared as a dense stain surrounding a condensed nucleus. There was a robust level of ongoing apoptosis in ME7 as measured by TUNEL. In the Thalamus the ME7+Saline group had significantly greater levels of apoptosis than the NBH+TNFα group ($P<0.001$)

(figure 4.12c). TUNEL positive labelling of apoptotic cells was not altered by administration of systemic TNFα .

4.3.5.2 – Synaptic pathology

The SY38 antibody labels the synaptic vesicle protein Synaptophysin. In NBH mice synaptophysin labelling (figure 4.13a) displays the laminar structure of the hippocampus. Loss of synaptophysin labelling in ME7 animals (figure 4.13b) shows the destruction of pre-synaptic terminals. In ME7 the hippocampal CA1 area shows a large loss of synaptophysin density in the stratum radiatum. Labelling in the CA1 stratum lacunosum moleculare remains relatively unaffected. This indicates a loss of the Schaeffer collaterals projecting to the stratum radiatum of the CA1. These are responsible for transmission of signals from the CA3 to the CA1. Synaptophysin density was quantified in the hippocampus, shown in figure 4.13e. NBH+TNFα had significantly greater synaptophysin density than ME7+Saline ($P<0.05$). TNFα does not exacerbate the synaptophysin loss in ME7 animals (figure 4.13c and d).

4.3.5.3 - Tau labelling and quantification

Hyperphosphorylated Tau deposits were seen throughout the hippocampus and thalamus of ME7 animals (figure 4.14b). The CA3 region of the hippocampus in particular showed deposits of Tau (figure 4.14b-d). This was quantified by comparing the fraction of the field area labelled by the AT8 antibody across the four treatment groups. The NBH animals showed no Tau deposition. NBH+TNFα was contained significantly less Tau deposition in comparison to ME7+Saline ($P<0.001$). No significant elevation of Tau deposition was seen following TNFα treatment in ME7.

4.3.5.4 - Cathepsin D expression

Cathepsin D is a lysosomal protease. ME7 sections revealed an increase in levels of Cathepsin D (CatD) and a change in localisation of the protease. In NBH CatD is visible most obviously in the neuronal cell soma. In ME7 animals there is a marked increase in levels of cathepsin D (figure 4.15f), but this is most obvious in glial cell populations, in which smaller cell soma are very densely labelled for cathepsin D.

When double-labelled (figure 4.15a-d), CatD labelling was found to be largely discrete with respect to APP but to show some areas of colocalisation with APP deposits (indicated by white arrows). This is only in ME7 animals as the NBH animals do not have APP deposits. TNFα did not appear to have an effect on Cathepsin D levels.

4.3.5.5 - Thalamic pathology

Very marked neuronal loss was evident in ME7 animals compared to the relatively uniform neuronal population present in NBH animals. There is robust thalamic neuronal death, in particular in the posterior nucleus in this model (Reis et al., 2015). Sub-region-specific pathology of the Thalamus was examined in NBH and ME7 animals following systemic TNFα, a comparison of thee markers used is shown inn figure 4.16. A very marked feature of this pathology is a very intense labelling for the amyloid precursor protein APP in the posterior thalamus (PO) and ventral posterior lateral thalamus (VPL) with a much lower intensity present in the ventral posterior medial thalamus (VPM) in ME7 animals (figure 4.16b and d). These APP-positive elements do not resemble axonal end-bulbs or amyloid plaques. A minority of these are large axonal spheroids (approximately 4-8 μm, see also figure 4.17a) but the majority are small (1-3 μm), densely labelled and remarkably numerous puncta. They are also present, but considerably less numerous in the VPM in infected animals and there are no such deposits in the NBH group (Figure 4.16a and c). This APP deposition was not altered significantly by systemic TNFα administration.

Synaptic density was, in general, compromised in ME7 group with significant loss of density in all thalamic areas examined here (figure 4.16 e vs. f). However, this synaptic loss is most severe in the VPL and the VPM while the PO shows relative sparing, demonstrating a clear, but incomplete, dissociation between APP deposits and synaptic loss. Many Synaptophysin-positive spheroids are also evident in the ME7 animals (figure 4.17b), particularly in area of most extreme synaptic loss (VPM/VPL). These spheroids are very similar in form and size to the APP deposits although they are bigger and significantly less numerous than the majority of APP-positive deposits (figure 4.16d vs. h). Synaptic density was not significantly altered following systemic TNFα administration.

Neuronal loss, examined by NeuN labelling, showed that the significant neuronal loss found in the PO nucleus (figure 4.16 i vs. j) of ME7 animals, is therefore strongly associated with the most numerous APP deposits (figure 4b), but not with the strongest synaptic loss (figure 4.16f). That is, the PO is less compromised for synaptophysin immunolabelling than the VPM and VPL (figure 4.16 e and f) but most strongly compromised for NeuN immunolabelling than the VPM and VPL (figure 4.16 i and j). This neuronal loss was not obviously altered by systemic TNFα challenge.

Conversely, immunohistochemistry for PrP^{sc} (figure 4.16 m-p) showed the presence of amyloid throughout all these sub-regions of the thalamus with no clear sub-region or sub cellular selectivity. Likewise, microglial activation was evident across the posterior regions of the thalamus without obviously divergent patterns in the three sub-regions as illustrated using IBA-1 immunolabelling (figure 4.16 q-t). Neither the distribution of PrP^{sc} nor the morphology of IBA-1 microglia was altered by systemic TNFα administration.

Collectively, these markers show that there are clear thalamic sub-region selective neuropathological changes despite relatively uniform labelling with PrP^{Sc} and IBA-1 in these regions. However none of these pathological markers are altered by a single dose of systemic TNFα.

4.3.5.6 - APP deposits

Despite the lack of TNFα induced alterations in ME7 pathology many of these findings were novel, further neuropathological labelling experiments were performed in the thalamus to seek other markers showing a similar pattern of labelling to that observed with APP (aigure 4.17a). Synaptophysin labelling is shown to emphasise the similarity between the larger spheroids labelled with APP and Sy38, however this was most prominent in the VPL (figure 4.17b). Ubiquitin labelling demonstrated a wide distribution of small 'dot-like' structures throughout the thalamus (figure 4.17c) that may correspond to the smaller end of the APP-positive size spectrum, although clearly not as numerous as APP-positive puncta. Relatively frequent and widely distributed labelling of hyper-phosphorylated Tau was observed using AT8 (figure 4.17d) and this appeared to be neuritic and did not resemble the APP labelling. SMI32 labelling of dephosphorylated neurofilament heavy chain showed very clear axonal pathology and this was most clearly visible where axons emerge from the medial lemniscus

into the PO (figure 4.17e), but once again these did not resemble the majority of APP labelling. Finally cathepsin D labelling demonstrated a clear shift from largely neuronal lysosomal labelling in NBH animals (figure 4.17f) to a predominantly glial lysosomal labelling in ME7 animals (figure 4.17g). Larger lysosomes appeared consistent in size with some of the smaller APP puncta.

We performed double labelling immunohistochemistry with confocal microscopy to learn more about the observed APP deposits (figure 4.18). In the area of maximum APP deposition and neuronal death, the PO, there were very few NeuN-positive neurons remaining and there was no co-localisation of APP with NeuN. However, many APP-positive puncta were double labelled with the phosphorylated neurofilament heavy chain marker SMI-31 and in some cases (figure 4.18d) these double-positive puncta had a characteristic 'beads on a string' appearance suggestive of axonal spheroids within an intact axon. Based on the hypothesis that in the absence of numerous neurons in the field with maximum puncta, APP puncta may be largely extracellular and prone to phagocytosis, double labelling with the lysosomal marker cathepsin D identified many elements where APP and cathepsin D colocalised (figure 4.18h). This indicates the presence of APP within the lysosome, and according to the morphology of the associated nuclei, these cells appeared to include both microglia and astrocytes (figure 4.18h). The co-localisation of APP puncta with microglia was confirmed by double labelling with IBA-1 (figure 4.18l). It is important to point out that in each case, the majority of APP-positive puncta were not double-labelled. We were unable to perform co-localisation of APP with Ubiquitin or synaptophysin due to incompatible antigen retrieval protocols.

4.3.5.7 - SMI-31 and SMI-32

Figure 4.19 a-h shows SMI-31 labelled phosphorylated 200kDa neurofilaments. Neurofilaments are structural elements of axons appearing in large bundles in white matter tracts throughout the brain. SMI-31 is largely conserved through the thalamus in ME7, however it does show disruption in its structure. There is a large amount of disorganisation of SMI-31 throughout the thalamus. Swellings were visible on axonal bundles in the upper thalamic region (figure 4.19d, f and h).

Figure 4.19 i-p shows SMI-32 labelled unphosphorylated 200kDa neurofilaments. SMI-32 can be seen distinctly in the white matter tracts, the medullary lamina, which cuts through the thalamus on either side of the brain. SMI-32 staining is

largely diminished in the thalamus of ME7 animals. There are large numbers of abnormal spherical swellings within axons that do not appear in NBH animals (figure 4.19 j vs l). Given the robustness of this pathology in ME7 animals, and its variability, it is difficult to determine whether TNFα had any effect on either SMI-31 or SMI-32.

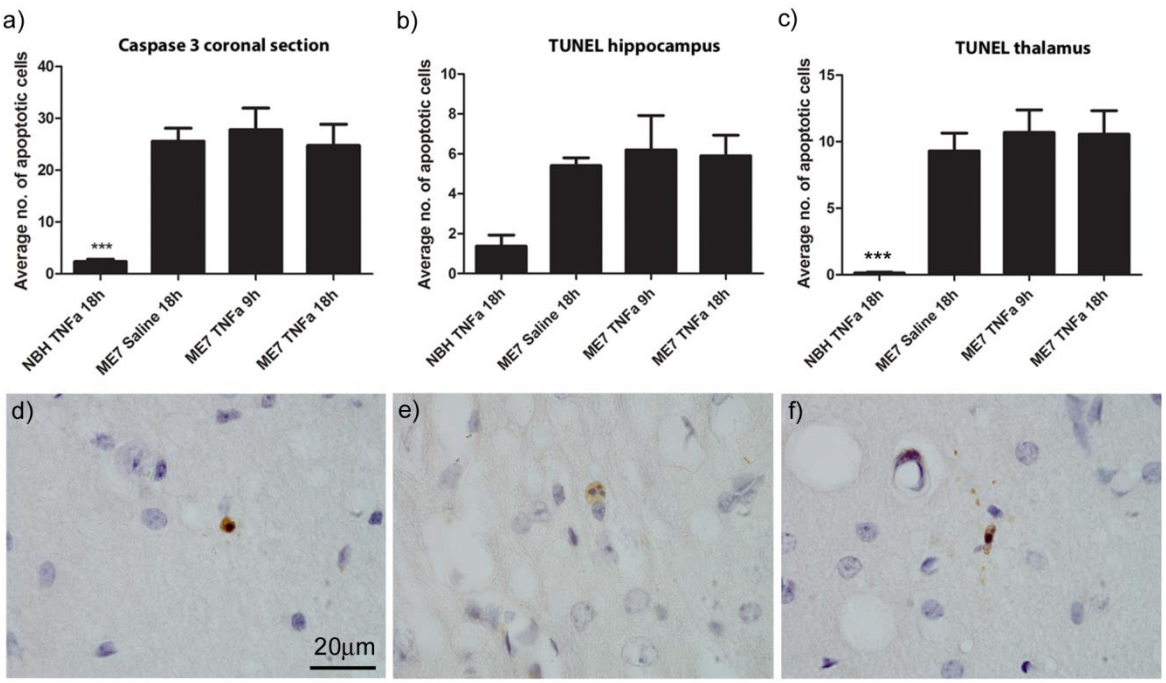

Figure 4.12 Apoptosis quantification post-systemic TNFα

ME7and NBH animals at 18 weeks post inoculation, 9 or 18 hours post i.p. saline or TNFα (250µg/kg). Caspase 3 and TUNEL positive cells were counted in a double blind manner. a) quantification of caspase 3 positive cells in a coronal section, b) quantification of TUNEL positive cells in the hippocampi of a section, c) quantification of TUNEL positive cells in the thalamus of a section. Data were analysed by one-way ANOVA followed by a Bonferroni multiple comparison test comparing each treatment group to the NBH+TNFα group. Statistical significance is denoted by * ($P<0.05$), **($P<0.01$), ***($P<0.001$). All data is represented as the mean ±SEM, n=3-5 for all groups. (d-f) representative micrographs of the various forms in which caspase 3 labelled apoptotic cells are shown (x100, scale = 20µm).

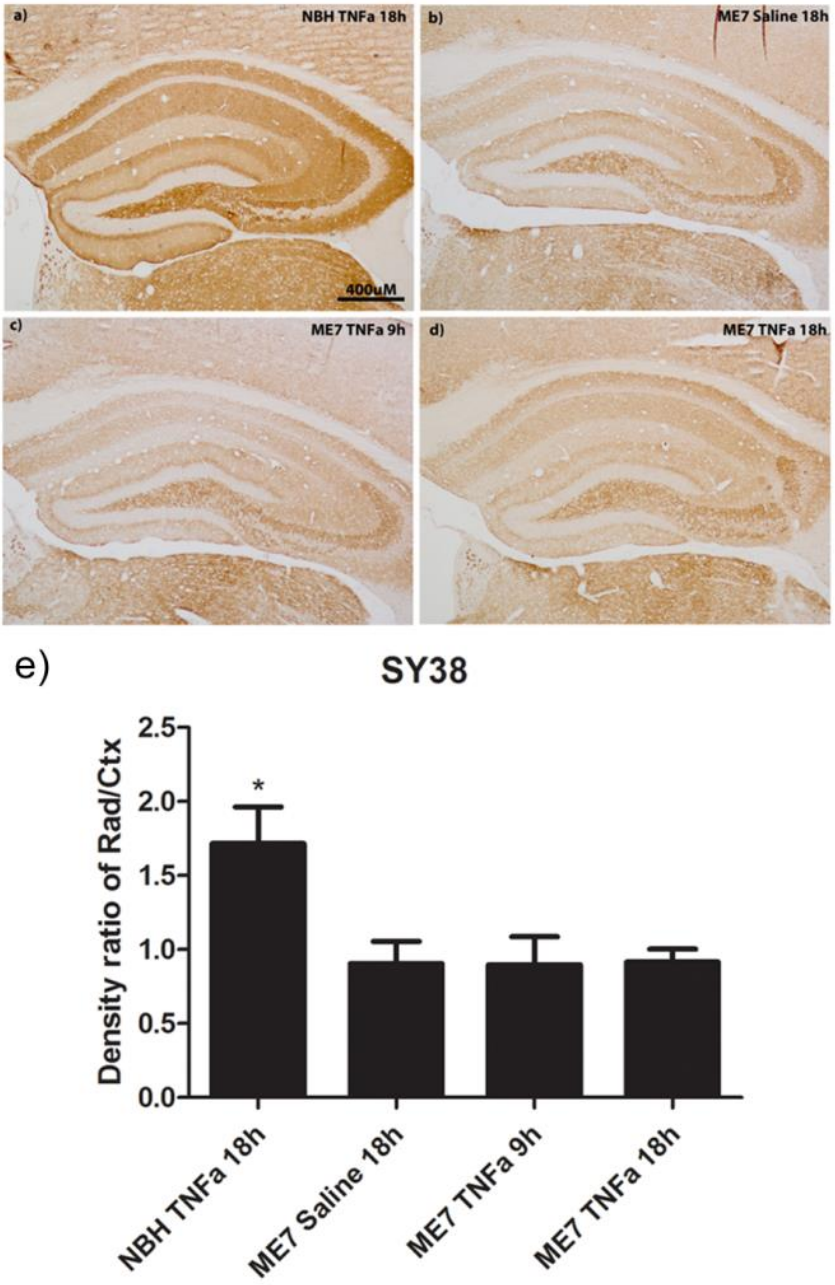

Figure 4.13 Hippocampal synaptophysin labelling and density analysis

ME7and NBH animals at 18 weeks post inoculation, 9 or 18 hours post i.p. saline or TNFα (250µg/kg). Representative images of Synaptophysin density labelled by SY38 are shown (a-d) Data were analysed by one-way ANOVA followed by a Bonferroni multiple comparison test comparing each treatment group to the NBH+TNFα group (e). Statistical significance is denoted by *(P<0.05), **(P<0.01), ***(P<0.001). All data is represented as the mean ±SEM, n=3-5 for all groups. (x5, scale=400µm).

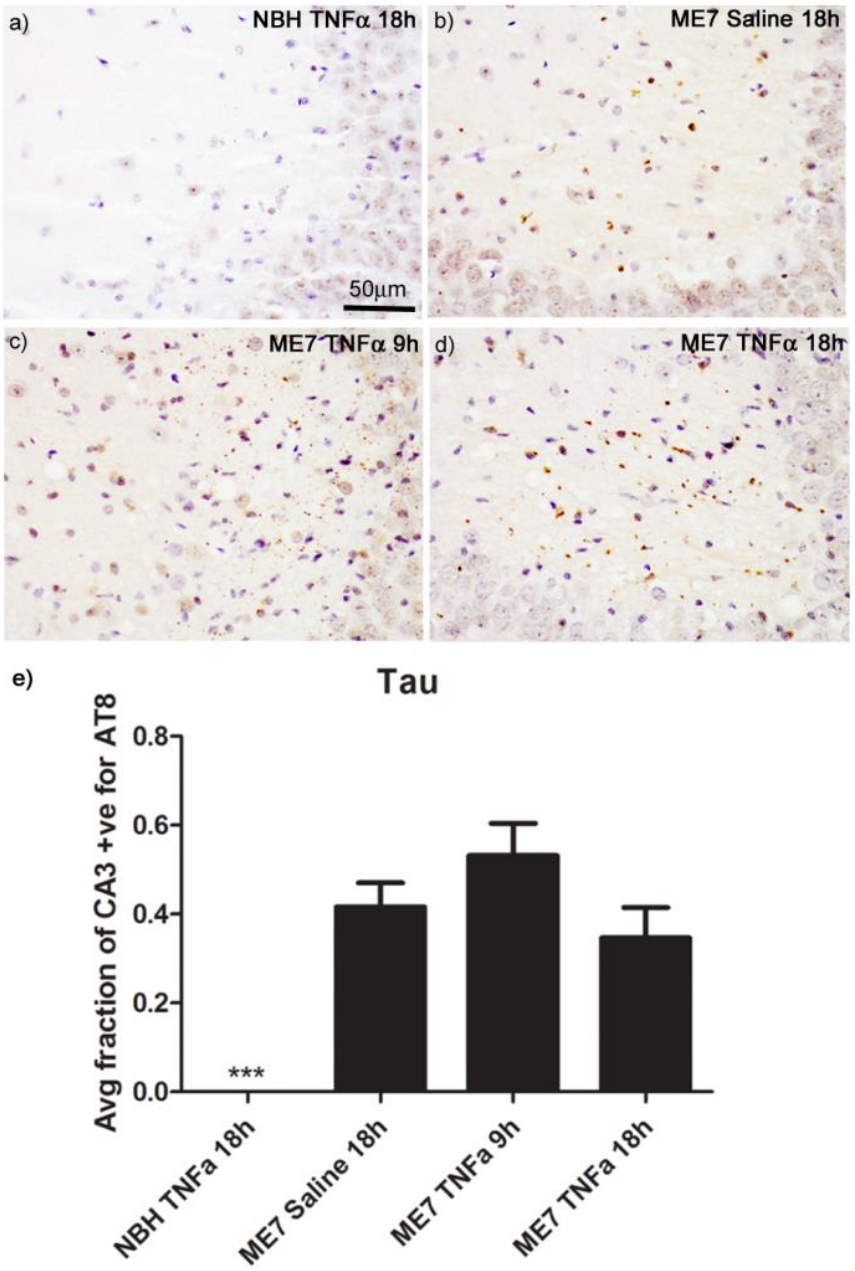

Figure 4.14 Hyperphosphorylated Tau labelling and quantification

ME7and NBH animals at 18 weeks post inoculation 9 or 18 hours post i.p. saline or TNFα (250µg/kg). Hyperphosphorylated Tau was visualised using the AT8 antibody. Shown here is the CA3 region of the hippocampus (a-d) where Tau labelling is most prominent (x40, scale = 50µm). Data were analysed using a one-way ANOVA followed by a Bonferroni multiple comparison test comparing each treatment group to the NBH+TNFα group (e). Statistical significance is denoted by * ($P<0.05$), **($P<0.01$), ***($P<0.001$). All data is represented as the mean ±SEM, n=3-5 for all groups.

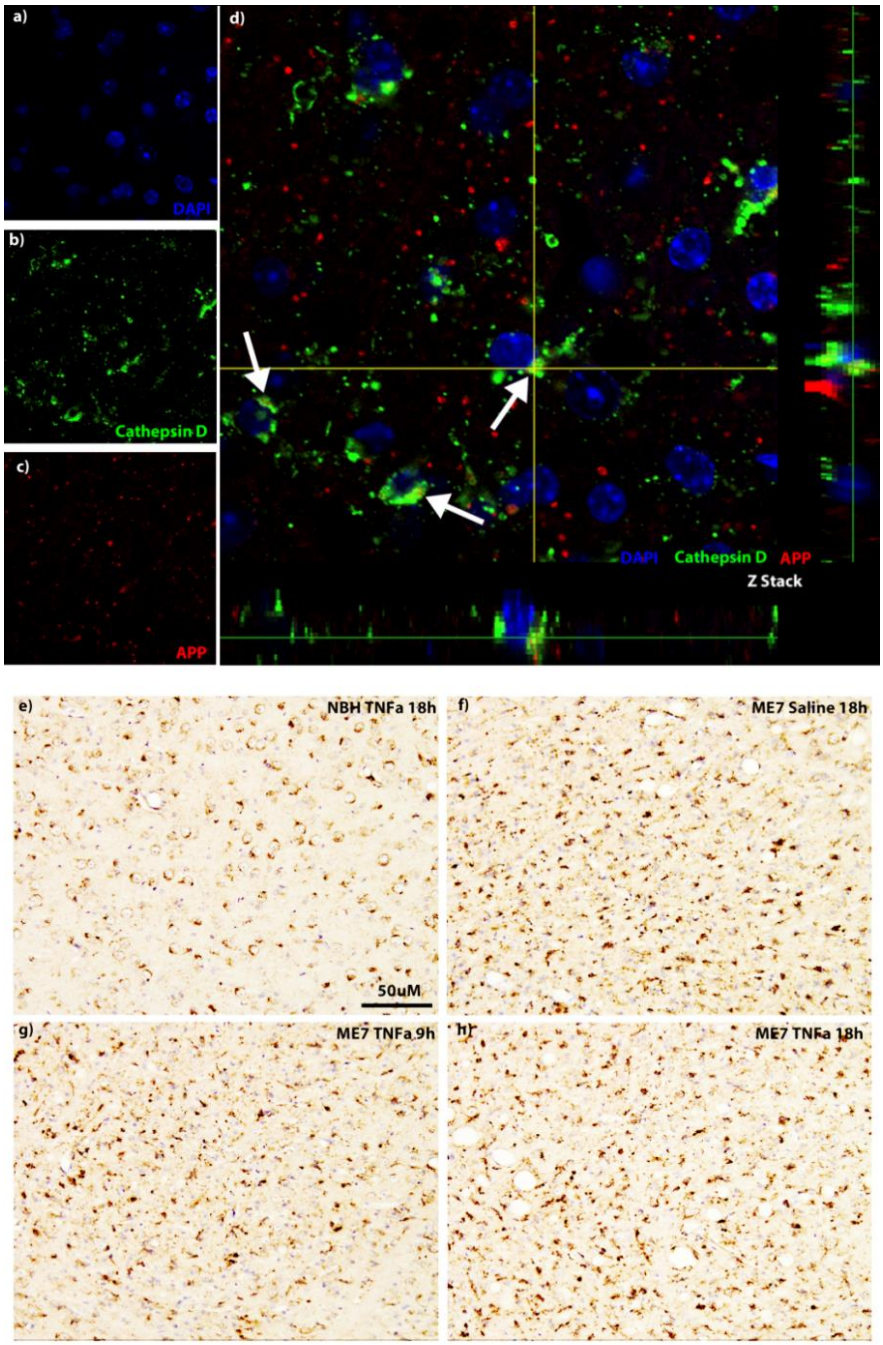

Figure 4.15 Immunolabelling of Cathepsin D and colocalisation with APP

ME7and NBH animals at 18 weeks post inoculation 9 or 18 hours post i.p. saline or TNFα (250µg/kg). Cathepsin D was visualised fluorescently at (488nm - green) with APP at (568nm - red) (a-d). Areas of colocalisation are indicated by white arrows. Bright field immunolabelling is shown (e-h) in the thalamus(x40, scale = 50µm).

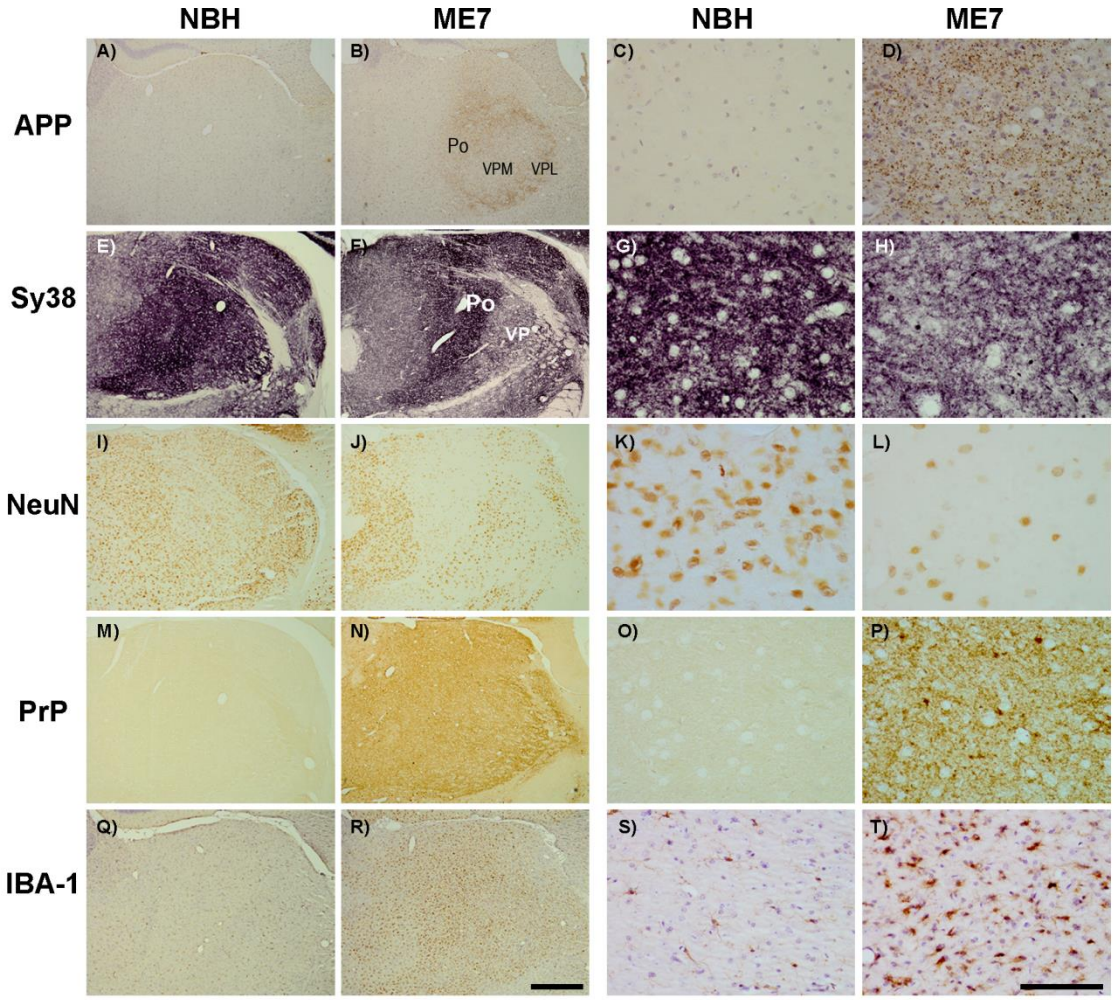

Figure 4.16 Sub-region selective thalamic pathology.

Photomicrographs of thalamic regions (Po, VPM and VPL) immunostained for APP, Sy38, NeuN, PrP and IBA-1 of NBH (A,E,I,M,Q) and ME7 (B,F,J,N,R) animals with respective photomicrographs on high magnification (NBH: C,G,K,O,S); ME7: D,H,L,P,T). Strong labelling was observed for APP (A vs B) in the posterior thalamus (Po) and the VPL, but less so in the VPM. Sy38 showed robust synaptic loss but this was less obvious in the Po than in the VP areas (E vs F). Strong loss of NeuN-positive neurons was observed in PO but less obviously in VP areas (I vs J). Conversely, PrP (N) and IBA-1-positive microglial activation (R) appeared generalised in ME7 in that it didn't show any apparent sub-region specificity. Scale bars of low and high power: 500µm and 100 µm, respectively.

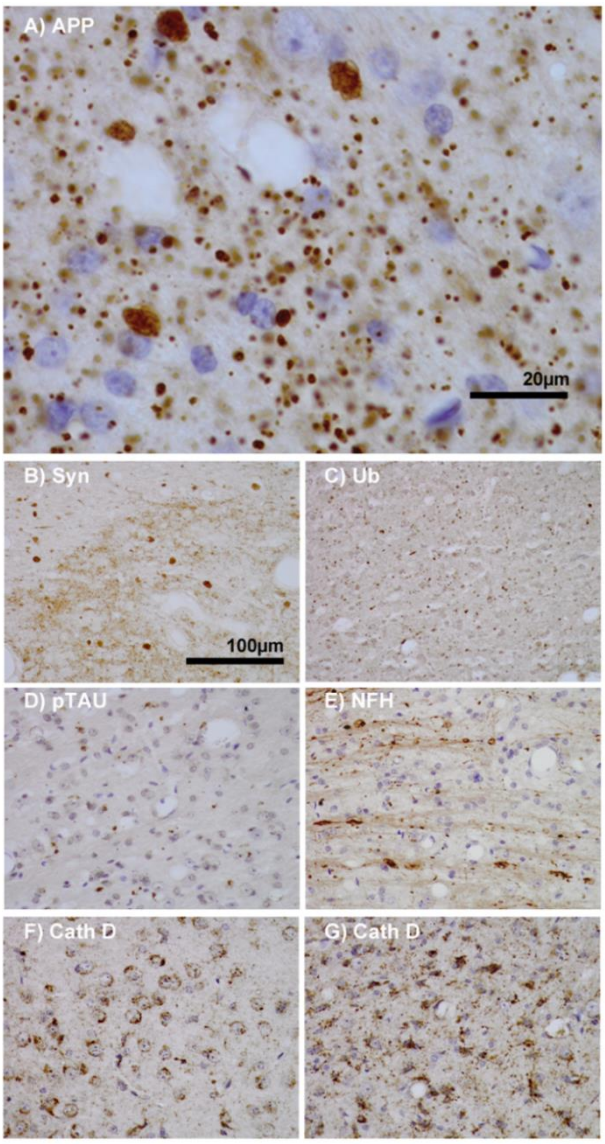

Figure 4.17 Features of thalamic pathology

A) High power (100x Objective) photo-micrographs of thalamic APP pathology shows large numbers of 1-2 µm diameter positive elements as well as smaller numbers of much larger spheroids (>6µm). For comparative purposes a number of other pathological features were examined for similarities and these were photographed at 40x. B) Sy38 shows large spheroids of similar size to APP and significant overall loss, but no small deposits. C) Ubiquitin shows large numbers of small 'dot-like' deposits that are similar in size but very much fewer that those observed with APP. D) Phospho Tau (AT8) labelling shows frequent apparently neuritic labelling. E) SMI-32, neurofilament H labelling showed strong spheroid labelling in axons emerging from the medial lemniscus but much fewer spheroids in the gray matter. F) Cathepsin D showed typical lysosomal labelling of small spherical structures in a perinuclear location, predominantly visible in neurons of the PO in NBH animals. G) Cathepsin D in ME7 animals showed predominantly glial localisation and consisted of larger structures or accumulations in perinuclear but also in some glial processes.

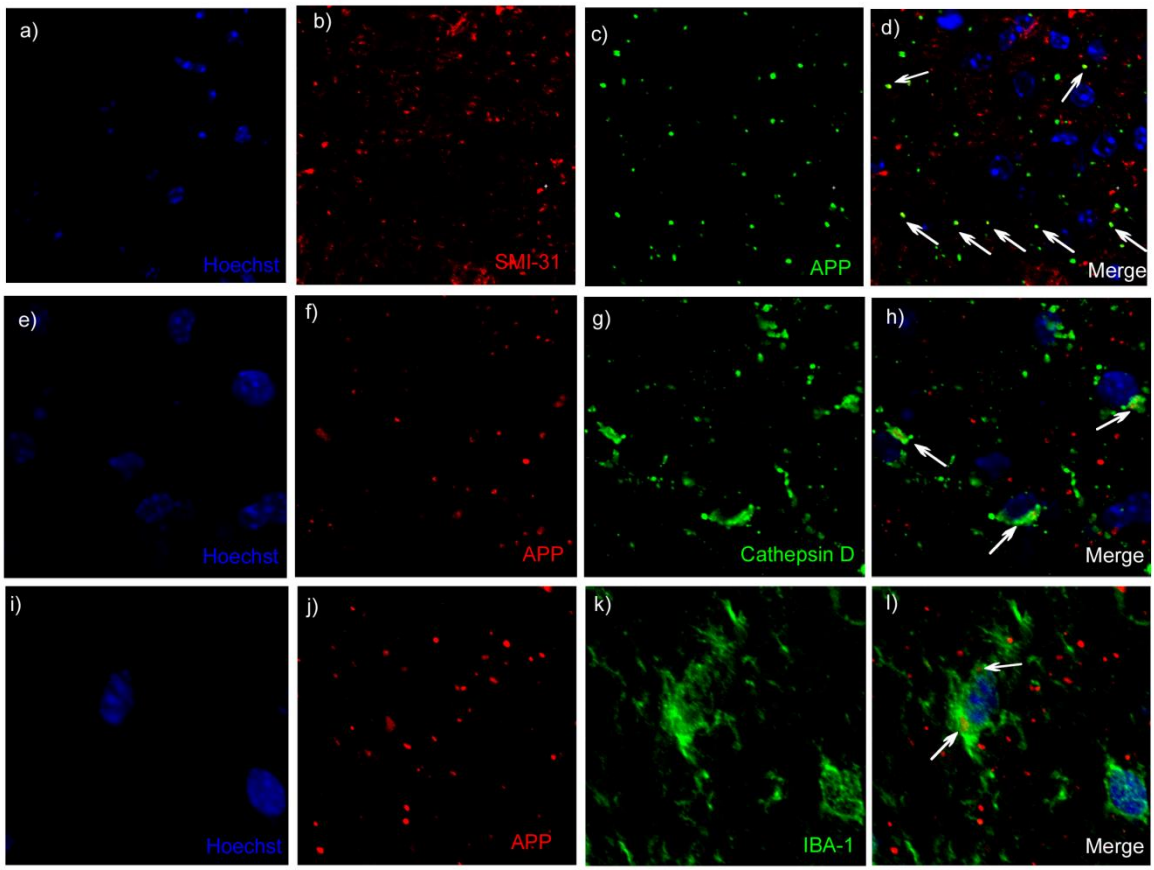

Figure 4.18 Identification of APP-positive elements.

Confocal microscopic images show the nuclear stain Hoechst 33258 (a, e and i) and APP-positive elements as distributed puncta (c, f and j). Neurofilament heavy chain labelling with SMI-31 (b) and APP-positive elements (c) show some co-localisation in (d). The lysosomal protease cathepsin D shows relatively condensed labelling in a perinuclear region of multiple cells (g) and a number of APP-positive elements (f) co-localise with cathepsin D (h). APP-positive puncta (j) are also largely distinct from IBA-1 positive microglia (k) but some co-localisation with these microglia does occur (l). Areas of colocalisation are indicated with white arrows.

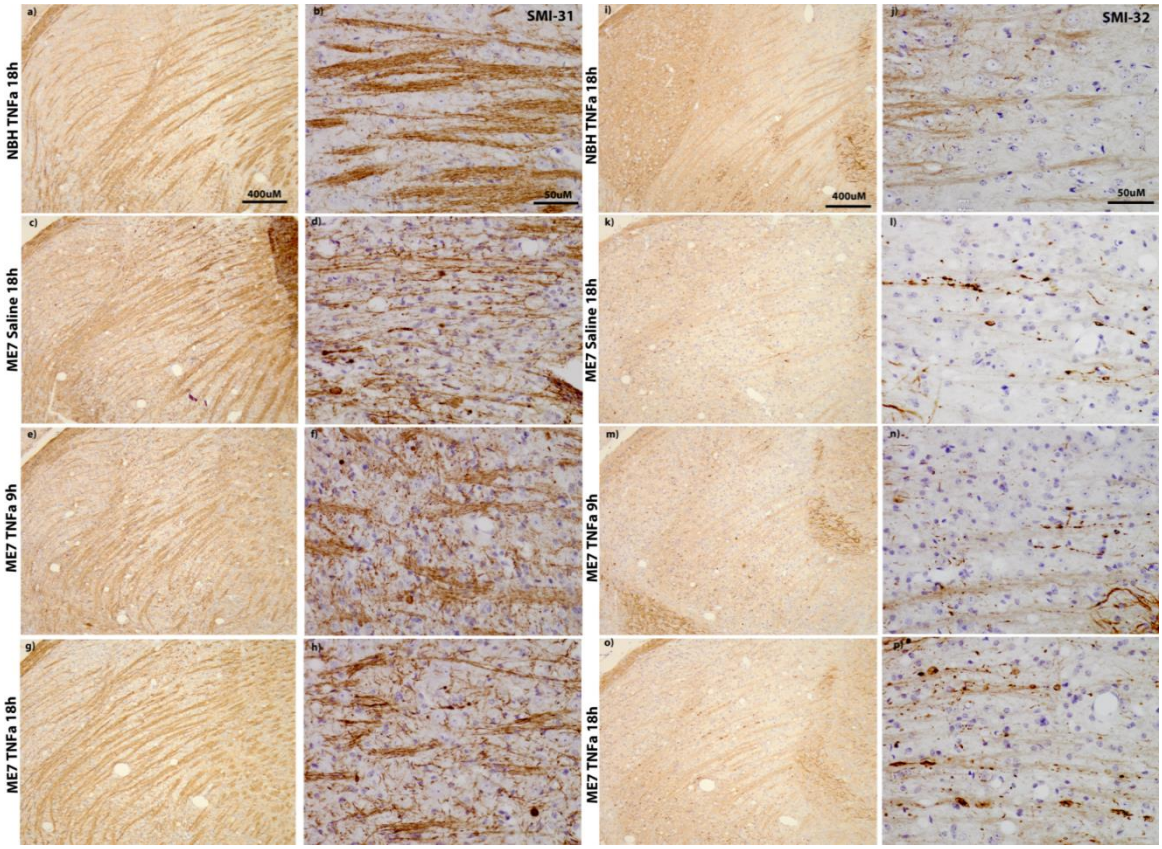

Figure 4.19 SMI-31 and SMI-32 comparison

ME7and NBH animals at 18 weeks post inoculation, 9 or 18 hours post i.p. saline or TNFα (250µg/kg). SMI-31 reacts with a phosphorylated epitope on neurofilament H. SMI-32 reacts with a non-phosphorylated epitope on neurofilament H. Alterations in axonal neurofilaments occur with ME7 (Scale = 400µm at x5 magnification and 50µm at x40 magnification).

4.3.6 – Central effects of systemic LPS are systemic TNF independent

Given that a single dose of systemic TNFα did not significantly alter the pathology of ME7 animals it was important to determine whether systemic TNFα played any role in the pathological effects seen following systemic administration of LPS (Cunningham et al., 2005a). In order to do this systemic administration of the TNFα dominant negative inhibitor XPRO1595 was utilised. XPRO1595 at 30mg/kg or sterile PBS were administered 1 hour prior to administration of 500μg/kg LPS or sterile saline to ME7 animals at 18 weeks. Animals were sacrificed 18 hours post-LPS administration, brains were formalin perfused and embedded in paraffin wax for sectioning on a microtome. All data was analysed by two way ANOVA followed by a Bonferroni multiple comparison *post hoc*.

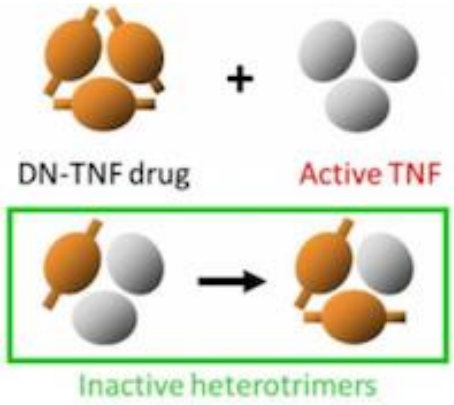

Figure 4.20 Mechanism of XPRO1595

Systemic administration of XPRO1595 induces de-activation of circulating TNFα by disrupting TNFα heterotrimers.

4.3.6.1 – XPRO1595 does not diminish LPS induced apoptosis

Systemic LPS challenge induced a greater level of apoptosis in the hippocampus ($P<0.0001$, $F_{(1,19)}=48.23$) and thalamus ($P<0.001$, $F_{(1,19)}=20.39$) of ME7 animals as shown in figure 4.21. There was no effect of XPRO1595 pretreatment on the level of LPS induced apoptosis in these regions. This indicates that CNS apoptosis induced by systemic LPS is independent of systemic TNFα.

4.3.6.2 – XPRO1595 does not alter cell infiltration post-LPS

Systemic LPS challenge induced a significant infiltration of MBS-1 positive neutrophils in ME7 animals ($P<0.0001$, $F(1,15)=160.0$). This infiltration was not altered by prior blocking of systemic TNFα (figure 4.22a).

There was no significant alteration of the CD3 positive T cell population in the ME7 brain following systemic LPS challenge. There was a trend towards an increase in the Thalamus ($P=0.0535$). There were also no alterations to this population following systemic XPRO1595 administration.

4.3.6.3 – Validation of XPRO1595

To ensure that XPRO1595 was performing as predicted we performed a validation of the drug administering XPRO1595 (30mg/kg) i.p. 1 hour prior to TNFα (50μg/kg) i.p. Sickness behaviour responses induced by systemic TNFα were examined. XPRO1595 abrogated the decrease in core body temperature observed following systemic TNFα ($P<0.01$, $t=6.517$, $df=4$). XPRO1595 also diminished the decline in open field activity seen following TNFα administration ($P<0.01$, $t=3.793$, $df=4$). XPRO1595 pre-treated animals did not perform significantly differently to PBS pre-treated animals when rears were measured.

Circulating proteins following XPRO1595+TNFα administration (figure 4.23) showed significantly elevated TNFα in the plasma compared to the PBS+TNFα group (figure 4.23a). This is accounted for by the XPRO1595 administered as this will increase the number of TNFα positive heterotrimers. However, circulating levels of CCL2 revealed that while the XPRO1595 pretreatment did slightly diminish the TNFα induced CCL2, however the effect size is very small (figure 4.23b).

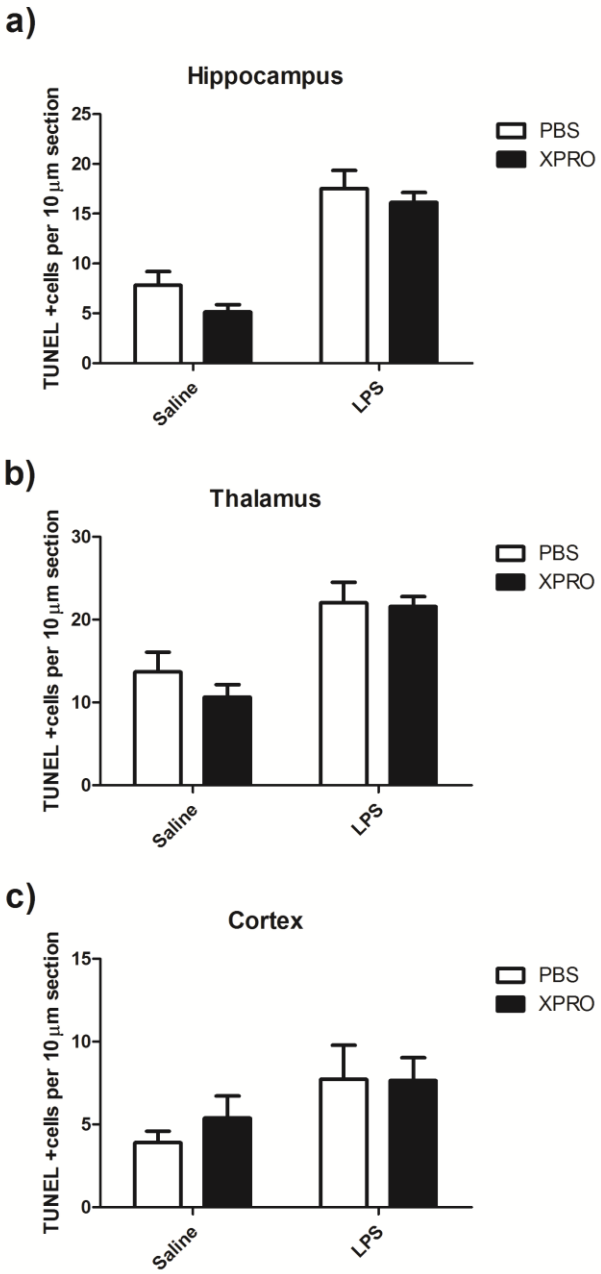

Figure 4.21 Analysis of ME7 apoptosis 18 hours post-systemic LPS

ME7 animals 18 weeks post-inoculation, 18 hours post i.p. saline or LPS (500µg/kg). Animals were pretreated with either PBS or XPRO1595 (30mg/mg). Apoptotic cells were immunolabelled using TUNEL. TUNEL positive cells were quantified in a blinded manner and data were analysed using a two-way ANOVA followed by a Bonferroni multiple comparison test. Main effects are described in the text. All data are represented as the mean ±SEM, n=3-6 for all groups.

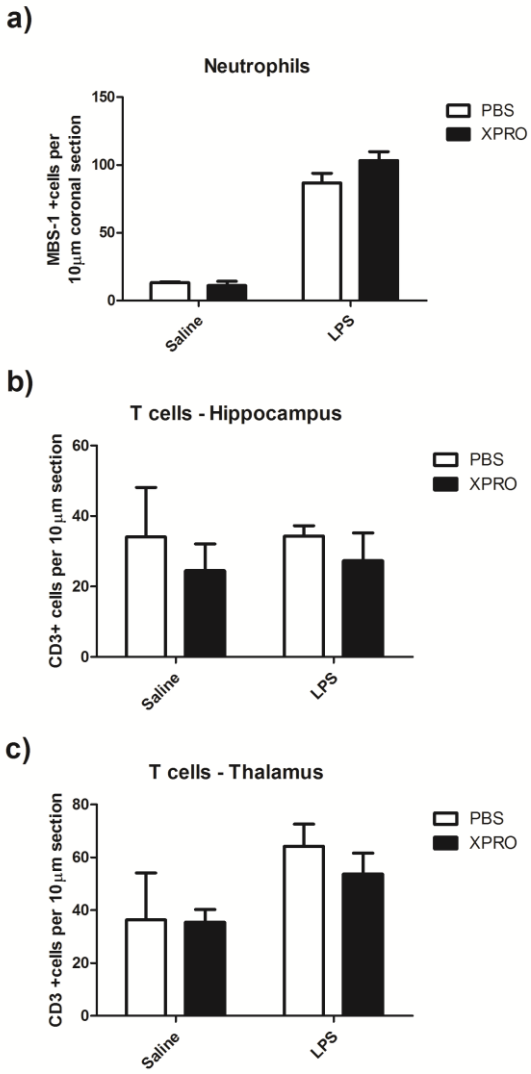

Figure 4.22 Quantification of infiltration in ME7 animals 18 hours post systemic LPS

ME7 animals 18 weeks post-inoculation, 18 hours post i.p. saline or LPS (500µg/kg). Animals were pretreated with either PBS or XPRO1595 (30mg/mg). Infiltrating neutrophils were immunolabelled using the MBS-1 antibody and infiltrating T cells were labelled using the CD3 antibody. Cells were quantified in a blinded manner and data were analysed using a two-way ANOVA followed by a Bonferroni multiple comparison test. Main effects are described in the text. All data are represented as the mean ±SEM, n=3-6 for all groups.

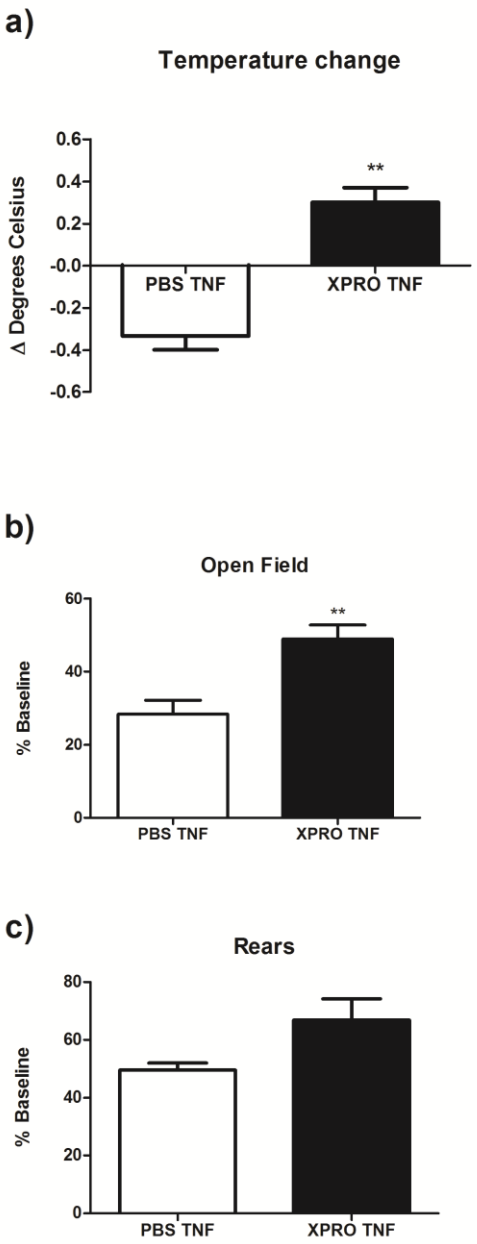

Figure 4.22 Validation of XPRO159, Behavioural measures

C57 mice were treated with PBS or XPRO1595 (30mg/mg) 1 hour prior to TNFα (50μg/kg) challenge. Core body temperature and activity in the open field were baselined prior to XPRO1595 administration and measured 2 hours post-TNFα challenge. Data were analysed using a Student's t test. Statistical significance is denoted by **(P<0.01). All data are represented as the mean ±SEM, n=3-4 for all groups.

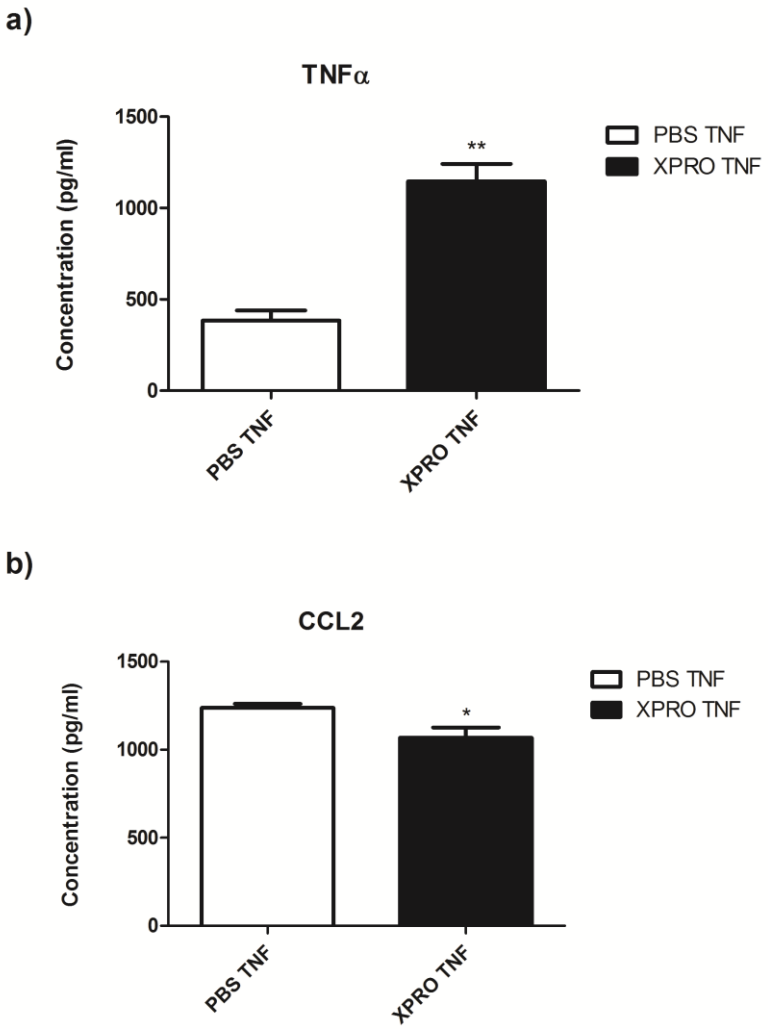

Figure 4.23 Validation of XPRO159, systemic cytokines

C57 mice were treated with PBS or XPRO1595 (30mg/mg) 1 hour prior to TNFα (50µg/kg) challenge. Systemic circulating TNFα and CCL2 were measured 3 hours post-TNFα challenge. Data were analysed by One way ANOVA followed by a Dunnetts multiple comparison post hoc. Statistical significance is denoted by **(P<0.01) and *(P<0.05). All data are represented as the mean ±SEM, n=3-4 for all groups.

4.4 – Discussion

Systemic TNFα was found to profoundly exacerbate sickness behaviour as well as producing a transient cognitive deficit in in the ME7 prion disease model. However a high dose of systemic TNFα did not robustly alter the prior pathology of the ME7 prion disease model. Blocking systemic TNFα prior to systemic LPS administration did not significantly alter the central consequences of systemic LPS administration in ME7 animals.

4.4.1 - Molecular effects of systemic TNFα

A timecourse was performed to identify the normal course of systemic and CNS responses to a single acute systemic TNFα challenge. We then used these molecular signatures and temporal patterns to define the parameters that would be examined when assessing whether TNFα had differential effects in the diseased brain. Due to elevations observed in the time-course focus was placed upon apoptotic pathways in the examination of TNFα effects in the degenerating brain. The expression of both Fas and FasL are increased during disease but neither of these were significantly augmented by TNFα in disease. This may be due to a ceiling effect given the robust increase in Fas by disease alone. Fas is a member of the TNF superfamily and it is also a death receptor. The elevation of Fas in disease could have detrimental consequences for neuronal function (Ethell and Buhler, 2003; Towfighi et al., 2004). While the Fas pathway is not further elevated by TNFα in disease, an integral molecule further down the apoptosis pathway was further elevated in disease by TNFα. NOXA is integral to the formation of the mitochondrial permeability transition pore (MPTP). NOXA is a p53-dependent gene and its induction suggests an activation of this pathway. Opening of the MPTP initiates activation of caspases in apoptosis. The elevation of NOXA by TNFα may allow the elevated levels of Fas-FasL present in disease to effect more apoptosis. However the activation of many apoptotic proteins is dependent on post-translational modifications and sub cellular localisation which may require alternative pathways.

4.4.2 – Behavioural effects of TNFα

TNFα has previously been shown to induce sickness behaviour in normal animals, decreasing activity in the open field and inducing a change in core body temperature (Skelly et al., 2013a). Examination of sickness behaviour following systemic TNFα in NBH and ME7 animals showed that there was a greatly exaggerated effect on movement and exploration in the open field, core body temperature and body weight in the ME7 animals compared to NBH animals. This indicates the development of a exacerbated central response to increased systemic TNFα, this expands upon this exacerbated response which was previously demonstrated using LPS in ME7 animals (Combrinck et al., 2002). Combrinck et al in 2002 hypothesised that exaggerated levels of CNS IL-1β were responsible for the exacerbated sickness behaviour observed following systemic LPS. However, in this study there is no significant exacerbation of hippocampal IL-1β following systemic TNFα, therefore elevated central IL-1β may not account for the exacerbated levels of sickness behaviour observed. However the time-point examined here may be too late to see significant alterations in IL-1β mRNA, also IL-1β protein levels would be important to consider as they could change independently of mRNA levels. It is of interest to note that in normal animals hypothalamic IL-1β had a greater fold increase following systemic TNFα than hippocampal IL-1β, given that many of the sickness behaviour responses are linked to hypothalamic control it would be interesting to examine the hypothalamus in ME7+TNFα for IL-1β changes.

It has previously been described in the literature that aged mice display a concomitant increase in cFos positive neurons and an exacerbated sickness behaviour response to systemic LPS (Gaykema et al., 2007). Unpublished data from the Cunningham lab has also shown exaggerated cFos responses in the amygdala of ME7 animals following systemic IL-1β, TNFα or LPS. We have previously shown that the levels of cFos in the amygdala can be upregulated by systemic IL-1β but not TNFα in normal animals, perhaps the elevation due to prior pathology increases the susceptibility of these cells to activation (Skelly et al., 2013a). This may contribute to the exacerbated sickness behaviour described here following systemic TNFα. A facet of the immune system unexamined in these studies is the contribution of anti-inflammatory cytokines. IL-10 may play a

particularly important role in limiting the sickness behaviour response as it has previously been shown that ablation of IL-10 leads to a more severe sickness behaviour following systemic LPS (Richwine et al., 2009).

Receptor activator of nuclear factor kappa-B (RANK) and RANK Ligand (RANKL) are essential regulators of osteoclast differentiation in bone remodelling. RANK and RANKL have also been shown to regulate sickness behaviour, with i.c.v. RANKL inducing decreased activity and a febrile response. RANK/RANKL mediates the fever response to i.p. LPS and i.p. and i.c.v. TNFα and IL-1β via COX2 induction of PGE_2 (Hanada et al., 2009). In this study we have shown exaggerated elevation of RANK following TNFα administration in ME7 animals and a disease associated elevation in RANKL. The disease associated alteration of this receptor-ligand pair may be responsible for the exacerbated sickness behaviour response observed post-TNFα. RANK has also previously been shown to be cFos dependent, which may explain the exacerbated sickness behaviour described in aged animals with elevated cFos (Arai et al., 2012). Utilising RANK or RANKL antagonists against a peripheral TNFα challenge may elucidate this further.

4.4.3 –Cognitive effects of TNFα

TNFα has been implicated in many cognitive processes in the brain. Stellwagen and Malenka showed that TNFα is necessary for excitatory synaptic scaling (Stellwagen and Malenka, 2006). TNFα can also enhance synaptic efficacy and modulate neuronal response to injury by regulating surface expression of AMPAR (Beattie et al., 2002). Deficits in TNFα signalling show detrimental cognitive effects. Mice lacking TNFα, TNFR1, and TNFR2 show deficits in both novel object recognition tasks and in spatial learning tasks (Baune et al., 2008). However, excessive amounts of TNFα in the CNS also modify cognition. Blocking i.c.v. TNFα post i.c.v. Aβ1-40 prevents the cognitive decline seen in the Morris water maze following Aβ1-40 alone (Medeiros et al., 2010). Dithiothalidomide (DT) following chronic i.c.v. LPS restored spatial memory deficits caused by LPS. DT restores spatial memory by reducing CNS levels of TNFα and TNFR2. It did not alter hippocampal levels of IL-1β (Belarbi et al., 2012). Imipramine reversal of $A\beta_{25-35}$ induced deficits in Y maze and Morris water maze was correlated with decreasing frontal cortex TNFα levels (Chavant et al., 2010). McAfoose et al show that aged

mice with a TNFα deficiency perform better on spatial learning tasks than wild type animals (McAfoose et al., 2009).

Prior data from our laboratory, using IL-1β, predicted that elevated systemic TNFα in a neurodegeneratively diseased animal would induce a cognitive deficit in the alternation T maze task (Griffin et al., 2013). In ME7 animals systemic TNFα showed a significant decline in percentage alternation in the task compared to ME7+Saline and NBH+ Saline or NBH+TNFα. This proved different at the 1 and 3 hour timepoints compared to a more prolonged deficit (up to 7 hours) observed following systemic LPS application, however this was similar to IL-1β induced deficits (Griffin et al., 2013). Terrando et al, using a model of orthopaedic trauma and surgery to induce post-operative cognitive dysfunction in mice, showed the cognitive effects of TNFα. In the post-operative setting systemic TNFα was shown to be upstream of hippocampal IL-1β. Pre-operative blockade of systemic TNFα abrogated hippocampal IL-1β increases and also reduced hippocampal-dependent memory impairment seen in contextual fear conditioning (CFC) (Terrando et al., 2010). The TNFα results in the T maze are distinct from the Terrando studies using CFC, primarily due to the distinct mechanisms of memory used in the tasks. The T maze is a hippocampal dependent working memory task where CFC is a reference memory task. Secondarily systemic inflammation in a young healthy individual was sufficient to produce deficits on memory consolidation in CFC. TNFα induces deficits only on a susceptible population in the T maze alternation task, demonstrating that it likely arises by a fundamentally different mechanism to consolidation deficits in CFC and is also a more appropriate tool to delineate mechanisms relevant to delirium in the elderly and demented population. However it remains possible that the T maze deficits induced by systemic TNFα in the ME7 model may be due to increased hippocampal IL-1β.

Hippocampal IL-1β increases may correlate with the limited time course of the T maze deficit shown following systemic TNFα in ME7 animals. ME7 animals show a deficit from 1 to 3 hours following peripheral TNFα. In the TNFα time course in normal animals there was a very brief elevation in hippocampal IL-1β at the 1 hour timepoint only. However, in the 2 hour transcripts from ME7+TNFα animals there was slightly but not significantly elevated IL-1β transcripts in the hippocampus. It would be of great interest as to whether there is increased secreted IL-1β protein in the hippocampus of these animals from 1 to 3 hours, as

IL-1β action is post-translationally regulated via inflammasome control of IL-1β maturation and secretion. It is important to note that TNFα had no impact on T maze alternation in the normal animal and the interaction between prior disease and systemically applied TNFα was necessary to induce this deficit.

Since the hippocampal cytokine data indicated that TNFα did not produce exaggerated hippocampal inflammatory transcripts in the prion animals, this makes microglial priming or exaggerated hippocampal inflammation an unlikely explanation for the supra-additive effects of disease and systemic TNFα on cognitive dysfunction in the T-maze. It has been demonstrated previously by the Cunningham lab that microglial priming is not necessary in the induction of a cognitive deficit on the T maze task by systemic LPS (Field et al., 2012). In the Field et al study basal forebrain pathology of the cholinergic system was the underlying susceptibility that induced a cognitive deficit post-systemic LPS. Therefore, it seems more likely that the existing axonal, synaptic and neuronal pathology present in the ME7 animals increases its predisposition to cognitive deficits upon the addition of a systemic inflammatory stressor. Consistent with this it is now clear that the degree of underlying neurodegenerative pathology progressively increases risk for acute cognitive dysfunction upon systemic inflammation in mice and that baseline cognitive function (MMSE) shows an inverse linear correlation with delirium risk upon systemic inflammation in humans (Davis et al., 2015).

Systemic TNFα and IL-1β have previously been shown to produce a hypoglycaemic effect in normal animals (Endo, 1991). Hypoglycaemic episodes have been shown to influence cognition in diabetic patients (Rodrigues Vilela et al., 2014). Work from Del Rey et al showed that central catecholamine depletion exacerbated inflammation induced hypoglycaemia (del Rey et al., 1998). Hypoglycaemia has also been linked to delirious episodes in patients (Maclullich et al., 2008). This may indicate a separate mechanism by which the prior neuropathology of a degenerating brain increases vulnerability to working memory deficits subsequent to increased systemic inflammation.

4.4.4 – Pathological effects of TNFα

Systemic LPS administration can induce a significant increase in apoptotic cells in the ME7 brain (Cunningham et al., 2005b). Several studies have shown that systemic LPS can induce central effects by directly activating CNS vascular endothelial cells and microglia independent of systemic cytokines (Chakravarty and Herkenham, 2005; Chen et al., 2012b). In 2011 Murray et al showed that i.p. Dexamethasone administration prior to LPS challenge depressed production of systemic TNFα, IL-1β and IL-6. Dexamethasone pretreatment did not however attenuate either CNS TNFα production or LPS induced apoptosis indicating a possible link between LPS-induced TNFα and LPS-induced apoptosis (Murray et al., 2011). Systemic TNFα may not play an integral role in systemic LPS dependent apoptosis, however given the elevation of TNFα in many co-morbidities it is important to examine the effects of TNFα alone on pathology.

Following i.p. TNFα in naive animals a subset of pro-apoptotic genes were elevated; Fas, Noxa and RIPK3. Following this observation the effect of systemic TNFα on apoptosis in the neurodegenerating brain was examined; via Caspase 3 and TUNEL immunolabelling 18 hours post challenge. This analysis found that ME7 animals showed an increased level of both of these apoptotic markers compared to NBH+TNFα animals. However ME7+TNFα did not show elevated levels compared to ME7+Saline. This would indicate that a single acute challenge with TNFα at a dose of 250μg/kg is not sufficient to exacerbate apoptosis in the neurodegenerating brain. Since there is already robust apoptosis in ME7 animals compared to NBH animals it might be argued that it would be difficult for TNFα to increase apoptosis rates to a higher level, however prior studies with systemic LPS have already shown its ability to acutely increase the rate of apoptosis (Cunningham et al., 2005b; Murray et al., 2012).

To examine the role of TNFα in LPS-dependent apoptosis the TNFα dominant negative inhibitor XPRO1595 was used prior to systemic LPS challenge in ME7 animals. Administration of systemic LPS showed robust apoptosis at 18 weeks in the prion model, however this proved to be TNFα independent as XPRO1595 pretreatment did not alter LPS induced apoptosis levels. Systemic LPS induced increased neutrophil and T cell infiltration into the ME7 brain, these increased cell numbers were also not diminished by prior XPRO1595 pretreatment. We

performed a validation experiment determining the effect of XPRO1595 on systemic TNFα sickness behaviour and systemic effects. This showed a significant diminution of TNFα effects on core body temperature and immobility in the open field however there was little alteration of systemic TNFα induced CCL2. *In vitro* XPRO1595 was shown to disrupt 80% of TNFα heterotrimers in 20 minutes (Steed et al., 2003), however in a dynaminc *in vivo* system this may take much longer. CCL2 mRNA has been shown to be increased 9 fold 30 minutes after TNFα 10ng/ml *in vitro* (Hao and Baltimore, 2009). The time prior to heterotrimer disruption may be sufficient to drive this CCL2 increase.

In ME7 animals' significant loss of pre-synaptic terminals has previously been shown by immunolabelling of Synaptophysin (Cunningham et al., 2003a; Hilton et al., 2013). There is a significant loss of presynaptic terminals in the stratum radiatum of the CA1 which disrupts the laminar pattern of the hippocampus. There appeared to be no effect of a single dose of systemic TNFα on this process. The tri-synaptic loop is the main circuit of innervation through the hippocampus. In this circuit the entorhinal cortex signals to the dentate gyrus and on to the CA3 via the mossy fibres. This signal is then passed from the CA3 to the CA1 via the Schaeffer collaterals. This circuit is an important component in memory and emotion (Kesner et al., 2004). The loss of pre-synaptic terminals in the CA1 would indicate a loss of the Schaeffer collaterals transferring information from the CA3 to the CA1 which would significantly affect memory. Loss of the CA1 synaptophysin begins at 13 weeks into ME7 prion disease. Of particular note in the CA3 were abnormally aggregated Hyperphosphorylated Tau particles. However work from Asuni et al indicates that aggregations of Tau in the CA3 are not the cause of the loss of CA1 synapses as upregulation of Tau phosphorylation was apparent at 20 weeks in ME7 but not at 13 weeks (Asuni et al., 2010). These data showed that hyper-phosphorylation of Tau is present in the CA3 at 18 weeks, however this would not explain CA1 loss at 13 weeks. It has been shown previously that prion infection elevates levels of CDK5, the kinase responsible for Tau hyper-phosphorylation (Wang et al., 2010). LPS has been shown to increase CDK5 activity and Tau phosphorylation (Kitazawa et al., 2005), it would be interesting to examine the effect of early activation of Tau hyper-phosphorylation in the ME7 model. It has been documented that the burden of Tau deposits in prion disease correlates with the severity and duration of disease (Higuma et al., 2013). While

these Tau deposits in the CA3 are not responsible for CA1 synapse loss they may be an indicator of late stage degenerative processes within the Tri-synaptic loop.

In clinical studies, more rapid cognitive decline in AD patients is independently associated with reported systemic inflammatory events (SIE) and with elevated basal TNFα. It was found that elevated baseline TNFα was more detrimental to cognitive function than a SIE and that it might be the prolonged elevation of TNFα by chronic co-morbidities that is the major driver of decline in these patients (Holmes et al., 2009a). Many chronic co-morbidities such as rheumatoid arthritis, atherosclerosis, obesity and diabetes have now been associated with elevated incident risk of dementia. These co-morbidities have all been revealed to have a significant systemic inflammatory component and the impact of a co-morbidity on an individuals likelihood to develop cognitive decline appears to be highly dependent upon that individuals baseline inflammatory status (Yaffe et al., 2004). Obesity, diabetes and atherosclerosis fall under the umbrella of Metabolic syndrome (MetS), which is the name given to the grouping of at least 3 of the following features; abdominal obesity, hypertension, hyperglycaemia, hypertriglyceridemia and low levels of high-density lipoprotein (HDL). Metabolic syndrome is a significant risk factor for development of AD but it is significant that this association was limited to those MetS cases with elevated serum pro-inflammatory markers (Yaffe et al., 2004) indicating that inflammatory processes associated with, or even underpinning MetS, may contribute to dementia progression. Atherosclerosis, obesity and diabetes are all associated with elevated levels of circulating cytokines especially TNFα (Bruunsgaard et al., 2000; Gregor and Hotamisligil, 2011; Swaroop et al., 2012) as well as with functional deficits in learning, memory and executive functions and increased risk of dementia (Biessels et al., 2006; Cechetto et al., 2008; Miller and Spencer, 2014). It is important to now test the impact of prolonged systemic TNFα expression on CNS pathology. The impact of a repeated systemic TNFα regime on a milder CNS pathology (APP/PS1 mice) will be tested in the final chapter of the current studies.

4.4.5 - Thalamic pathology in ME7

The rest of this discussion will focus on novel findings in thalamic pathology in the ME7 prion disease model. None of these markers were significantly altered by

systemic TNFα, however, they are still novel and of significant interest in the pathogenesis of neurodegeneration. There is severe thalamic degeneration with marked neuronal loss in the posterior nucleus, and widespread degeneration of presynaptic terminals is most marked in the VPM. Intense deposition of APP was also observed in the PO and VPL in particular. Despite the differential pattern of neuronal pathology across these discrete thalamic nuclei, PrP^{Sc} deposition and microglial activation appeared relatively uniform across these three structures, emphasising the selective vulnerability of particular neuronal structures despite equivalent levels of PrP^{Sc}.

The pathology observed here may provide insights for basic processes of neurodegeneration. The most striking novel pathology described here is the very dense APP labelling in the thalamus. This was present particularly in the PO, where neuronal loss was most severe, and in the VPL, with relative sparing of the VPM, where synaptic loss was most severe. This APP pattern is almost entirely absent in the hippocampus and we have found limited evidence of this pathology in other regions. The APP deposits observed here do not resemble the classical axonal end-bulbs of axonal transection, suggesting a distinct type of axonal/neuritic stress, and do not resemble PrP^{Sc} labelling in size or distribution. Double labelling experiments showed some co-localisation with the axonal marker SMI-31, suggesting axonal spheroids, and some of those observed do have a 'beads on a string' appearance. Axonal varicosities may become spheroids in the axon and would be likely to lead to axonal transport deficits and dysfunction in thalamocortical networks. Many of the APP-positive puncta appeared to be extracellular and may be consistent with the extrusion of axonally localised aggregated proteins or varicosities as an early consequence of neuronal/axonal stress (Doehner et al., 2012). These extruded varicosities may remain in the extracellular space and may seed further amyloid, while others can be engulfed by local phagocytes, including microglial cells and astrocytes (Krstic and Knuesel, 2013). Consistent with this idea, some APP deposits co-localised with the lysosomal marker cathepsin D and some with IBA-1-positive microglia, suggesting phagocytosis. Although co-localisation with cathepsin D could theoretically occur in any cell type, it is clear that there is a significant shift from predominantly neuronal cathepsin D in the thalamus of NBH animals to largely phagocyte

cathepsin D in ME7 animals and the observed double-labelled structures were generally larger and localised to glia.

There was significant dot like ubiquitin pathology through the thalamus of the current study. However ubiquitin does not show the same sub-region selectivity or morphology as the APP pathology, it does resemble the previously described perisomatic ubiquitin granules of 1-4 μm (Probst et al., 2001; Lowe et al., 2005), first described as non-plaque dystrophic neuritis (Aronica et al., 1998) outside AD and Pick's disease hippocampal neurons. These structures are thought to be dendritic and are also distinct from 'dot-like' ubiqutin deposits found predominantly in the white matter (Migheli et al., 1992).

Although the APP spheroids are suggestive of axonal and dendritic pathology, and the SMI-32 labelling in the lemniscus confirms that axonal pathology is prevalent in ME7, there is evidence that axonal function can survive a significant degree of dystrophy during amyloidosis and may still recover normal function (Adalbert et al., 2009). Likewise, early neuronal dysfunction can be reversed in prion-diseased animals in which neuronal expression of PrP has been turned off after initiation of synaptic loss (Mallucci et al., 2007). Nonetheless, it is striking that the APP pathology is most severe in the PO, which ultimately sustains massive neuronal loss.

The distinction between the areas of APP pathology is intriguing. Why does the PO lose significant numbers of neurons alongside APP aggregation while the VPL retains its neuronal population but suffers a major loss of presynaptic terminals alongside APP aggregation? Further work from Reis et al., examined the brainstem areas projecting to these nuclei to determine whether pathology in the projecting areas could explain the differential pathology in proximal thalamic nuclei. Reis et al., found significant axonal pathology in the major tract projecting to these thalamic nuclei (medial lemniscus) and significant neuronal loss in some (PrTNvl, gracile and cuneate) but not all (SpI5) of the brainstem nuclei from which these axons originate. The interpolaris that projects to the PO showed a generalised loss of presynaptic terminals but no neuronal loss (Reis et al., 2015). While the neuronal population that projects to the PO is not diminished there is severe neuronal loss and APP deposition in the PO. The PrTN is the brainstem region that projects to the VPM, there was significant neuronal and synaptic loss and presence of APP deposits (Reis et al., 2015). This neuronal loss correlated with the

significant loss of presynaptic terminals and severe APP aggregation in the VPM. While this does not explain the origin of pathology in the PO, pathology in the VPM appears to have originated in the PrTN and spread through neuroanatomical pathways to the VPM.

In prion neurodegeneration there appears to be differential spread of neuropathology dependent on the anatomical tract and perhaps on the neuronal cell type. An initial loss of presynaptic terminals on the dendrites of CA1 neurons in the stratum radiatum of the hippocampus is prominent in the ME7 model of prion disease (Jeffrey et al., 2000; Cunningham et al., 2003b; Gray et al., 2009; Siskova et al., 2013) and this also occurs in other prion strains (Hilton et al., 2013). The CA1 neurons go on to die in significant numbers while the source of the majority of the presynaptic terminals, the CA3 pyramidal neurons, do not show obvious neuronal loss. Therefore, though the CA3 axons lose a very large number of presynaptic terminals it is their target cells, the CA1 pyramidal neurons that die. This may be analogous to the maintenance of neuronal numbers in the interpolaris and loss of neurons in the PO.

This is clearly consistent with the idea of spread of prion-associated pathology along neuroanatomical pathways, previously shown in the optic tract (Scott et al., 1992) and the limbic system (Cunningham et al., 2003b). Those studies typically map the spread of prion protein deposition or gliosis but Reis et al., demonstrated spread of neuronal pathology. It is not clear how pathology first spreads to the posterior thalamic nuclei and why these neurons are relatively selectively targeted, but thereafter, there is significant pathology in the brainstem nuclei that form the major projections to the posterior thalamus (Reis et al., 2015).

4.4.6 – Conclusion

We discovered that a single acute dose of systemic TNFα when superimposed on a degenerative background can significantly transiently disturb working memory and exacerbate sickness behaviours such as the febrile response, inactivity and hypophagia. While many novel and intriguing facets of ME7 pathology were shown, a single dose of systemic TNFα does not further disrupt neuropathology in this model. This may be due to the acute nature of the challenge but also the

severe and advanced nature of the ME7 pathology may limit the ability to detect effects of systemic TNFα as any pathological effects it may induce, may have already plateaued. Systemic LPS induced a significant increase in apoptosis in ME7, this proved to be independent of systemic TNFα. There is a clear dissociation between acute cognitive and motivational effects of systemic TNFα and downstream pathological alterations in the ME7 model. It would be of interest in this case to examine some acute alterations in the CNS following systemic TNFα. COX1 has been shown to mediate LPS induced cognitive deficits, it would be interesting to examine if it also mediated TNFα induced deficits (Griffin et al., 2013). It is necessary to determine whether a chronic regime of repeated TNFα would have pathological effects in a less severe model of neuropathology. In the following chapter we examine some of the same pathological markers in the APP/PS1 transgenic model following repeated systemic administration of 250μg/kg of TNFα.

Chapter 5

Impact of repeated systemic TNFα administration in aged & APP/PS1 transgenic mice

5.1 - Summary

Elevated systemic TNFα has been shown to be associated with significantly more rapid cognitive decline across 6 months in an AD patient cohort. It is not clear whether this might constitute a causal relationship. We examined this relationship using repeated systemic TNFα administration in APP/PS1 and WT mice at 15 months. The effect of repeated TNFα administration was examined in aged mice. The TNFα downstream gene CCL2 showed neither tolerance nor upregulation of the systemic inflammatory response to multiple systemic TNFα challenges. A similar repeated systemic TNFα challenge model was used to examine consequential behaviour and pathology in the APP/PS1 model. This showed that repeated TNFα did not significantly alter learning of the hippocampal dependent Y maze. Repeated systemic TNFα induced a deficit in rearing behaviour in the WT but not the APP/PS1 animals and significant progressive weight loss in the WT mice. This was not apparent in the APP/PS1 mice. Following the second TNFα challenge WT animals did not recover to baseline as TG animals did. This differential effect also remained after the third and fourth challenges. There was no significant difference between these groups when behaviour in the open field was measured.

The pathology of these animals 10 days after the fourth TNFα challenge was examined; we aimed to examine possible long term consequences of repeated TNFα challenge on pathology. We observed a significant decrease in the hippocampal Amyloid β burden with a concurrent increase in aggregations of APP in both the hippocampus and thalamus. Microglia were increased in APP/PS1, however there was no alteration following repeated systemic TNFα. There were elevated numbers of T cells in the APP/PS1 animals. Following repeated TNFα there was a further increase in the APP/PS1s this did not occur in the WT+TNFα group. Repeated TNFα in APP/PS1 animals also diminished the levels of ongoing cell proliferation, a similar decrease did not occur in the WT+TNFα group. These results indicate that repeated systemic TNFα administration has differential effects in aged APP/PS1 and aged WT animals, suggesting important implications for cognitive and functional decline with systemic inflammation.

5.2 - Introduction

Holmes et al., have described an association between systemic circulating levels of TNFα and progression of AD. High baseline TNFα in an AD cohort led to a 4 fold increase in the rate of cognitive decline over a 6 month period, where low baseline TNFα led to no cognitive decline. A systemic inflammatory event (SIE) in an AD patient was also associated with increased circulating TNFα and a 2 fold increase in the rate of cognitive decline (Holmes et al., 2009a). This indicates that long term elevation in systemic TNFα levels has a severely detrimental effect on cognitive function and SIE related increases in TNFα can also significantly alter the progression of disease. Holmes et al also found that neuropsychiatric symptoms associated with sickness behaviour were more frequent in AD patients with high circulating TNFα than those with low circulating TNFα (Holmes et al., 2011). In recent conference proceedings, Holmes et al., described use of etanercept (a TNFα decoy receptor) subcutaneously once a week in AD patients compared to placebo controls over 6 months. Holmes showed that etanercept treatment induced an attenuation of cognitive decline in AD patients (Holmes et al., 2014). A larger clinical trial is currently underway.

Systemic TNFα has been shown to be inversely correlated with total brain volume in a normal aged cohort (Jefferson et al., 2007). When systemic TNFα was examined in relation to brain volume in an AD cohort, levels were found to be inversely correlated with both total brain volume and hippocampal volume (Leung et al., 2013). Systemic TNFα has been shown to increase with age in a study of centenarians.This study also showed that high systemic TNFα is associated with moderate to severe dementia (Bruunsgaard et al., 1999). In AD TNFα elevation in both CSF and serum of patients was found to correlate with disease severity and progression (Paganelli et al., 2002). Mild cognitive impairment (MCI) patients who later went on to develop AD were found to have elevated levels of TNFR1 and TNFR2 that correlated with BACE1 activity compared to controls. The levels of TNFRs were correlated with plasma levels of Aβ and with CSF levels of the axonal damage marker tau (Buchhave et al., 2010). Tarkowski found that MCI patients with elevated CSF levels of TNFα were more likely to progress to AD (Tarkowski et al., 2003). Overall these results indicate that elevated circulating TNFα levels make an individual more likely to progress on to MCI and AD.

Systemic inflammation has also been examined in transgenic models of Alzheimer's disease and was found to exacerbate many features of disease. LPS (2.5mg/kg) induced elevated cortical and hippocampal IL-1β protein in aged Tg2576 mice but not in younger Tg2576 animals or in similarly aged non transgenic littermates. In young and old Tg2576 mice Aβ1-40 levels were raised following LPS however Aβ1-42 levels were raised only in aged Tg2576 following LPS (Sly et al., 2001). Sheng et al,. showed that LPS (500μg/kg) in aged APP_{swe} mice LPS increased brain levels of APP, APP C-terminal fragments, and $A\beta_{1–40}/A\beta_{1–42}$ (Sheng et al., 2003). A single systemic LPS (250μg/kg) challenge in normal (CD-1) mice showed increased levels of $A\beta_{1-42}$ (but decreased levels of $A\beta_{1-40}$) alongside memory impairment in passive avoidance and Morris Water Maze tasks. The elevations in Aβ were likely due to decreased α-secretase and increased β/γ-secretase and APP expression. In the same study repeated daily LPS progressively increased Aβ1-42 levels and induced neuronal death (Lee et al., 2008). Systemic LPS (10mg/kg) in an APP transgenic mouse has also been shown to produce exacerbated sickness behaviour with decreased locomotor activity, social interaction and food intake in comparison to WT littermates treated similarly. These animals also showed significantly elevated central IL-6 levels and more severe BBB permeability post-systemic LPS than controls (Takeda et al., 2013). Murine Hepatitis Virus or LPS (500μg/kg, twice a week, for 6 weeks) administration in aged 3xTg-AD mice induced an increase in Tau pathology via CDK5 activity and LPS treatment caused a significant impairment in learning the Morris Water Maze (Kitazawa et al., 2005; Sy et al., 2011).

A single acute dose of systemic TNFα in the late stages of the ME7 prion disease model was examined; we found significant alterations in behavioural and cognitive measures with no significant alterations of pathology. ME7 pathology is significantly advanced at the time-point used indicating that there may be few effects that a single acute dose could have in such a severe model of pathology. A more prolonged or repeated elevation of systemic TNFα was needed in a less severe pathological model in order to address some of the above issues.

The APP/PS1 double transgenic mouse expressing a chimeric mouse/human amyloid precursor protein (Mo/HuAPP695swe) and a mutant human presenilin 1 (PS1-dE9) both directed to CNS neurons was utilised. This model develops amyloid beta (Aβ) deposits in the brain by six to seven months of age mimicking

familial Alzheimer's disease. This is a much less severe pathological model than the ME7 prion disease model, with less neuronal and synaptic loss despite the robust amyloidosis. We examined these mice at 15 months of age.

It was initially intended to establish a chronic model of systemic TNFα expression by utilising an Adenoviral vector (AdV) expressing rmTNFα. When administered this vector reportedly moves to the liver (Johnson et al., 2006) and produces systemic TNFα for up to 14 days post-administration (Ferrari et al., 2004; De Lella Ezcurra et al., 2010). This AdV was obtained from a collaborator in Argentina. Viability was demonstrated in in cell culture using a cytopathic effect assay. However the vector failed to produce detectable levels of TNFα *in vivo* when a dose response was performed in naïve animals. Peritoneal fluid and serum was examined, TNFα was undetectable in both. In order to mimic chronically elevated systemic TNFα a model of repeated TNFα administration was used in place of the AdV.

The aim of this study was to examine repeated TNFα administration to determine whether there was an upregulation of the systemic response with multiple systemic TNFα challenges in naïve animals. This model was then utilised in WT and APP/PS1 cohorts. Behaviour, cognition and pathology were examined in APP/PS1 animals.

5.3 - Results

5.3.1 – Repeated TNFα in aged C57 mice

Repeated TNFα administration was initially examined by comparing TNFα administered once, twice or three times, seven days apart, to 14 month old C57 mice. Systemic cytokines were examined in this cohort to determine whether tolerance or amplification developed with repeated administration. Treatment administration is described in figure 5.1. Animals were sacrificed at 2 hours and plasma was taken. Liver, hypothalamus, hippocampi and frontal cortex were also taken, however, there was insufficient time available to analyse these samples.

Repeated TNFα administration in aged C57 mice showed no differential effects between one, two or three challenges on either systemic TNFα or CCL2 levels. There was a main effect of TNFα on systemic TNFα levels ($P<0.0001$, $F_{(3,18)}=27.30$) however this effect was not altered by repeated administration (figure 5.2a).

There was a main effect of TNFα treatment on systemic CCL2 levels ($P<0.0001$, $F_{(3,18)}=509.1$). However, this effect was not altered by repeated administration (figure 5.2b).

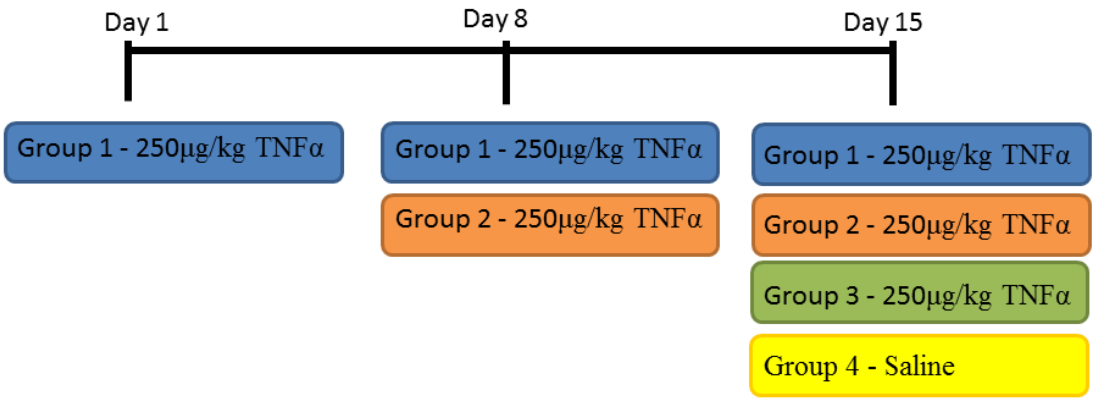

Figure 5.1 Treatment scheme, repeated TNFα administration

Animals were administered 250µg/kg TNFα once, twice or three times, according to the schedule shown. Saline was used as control. Animals were sacrificed 2 hours after the final administration. Plasma was taken to assess cytokine induction.

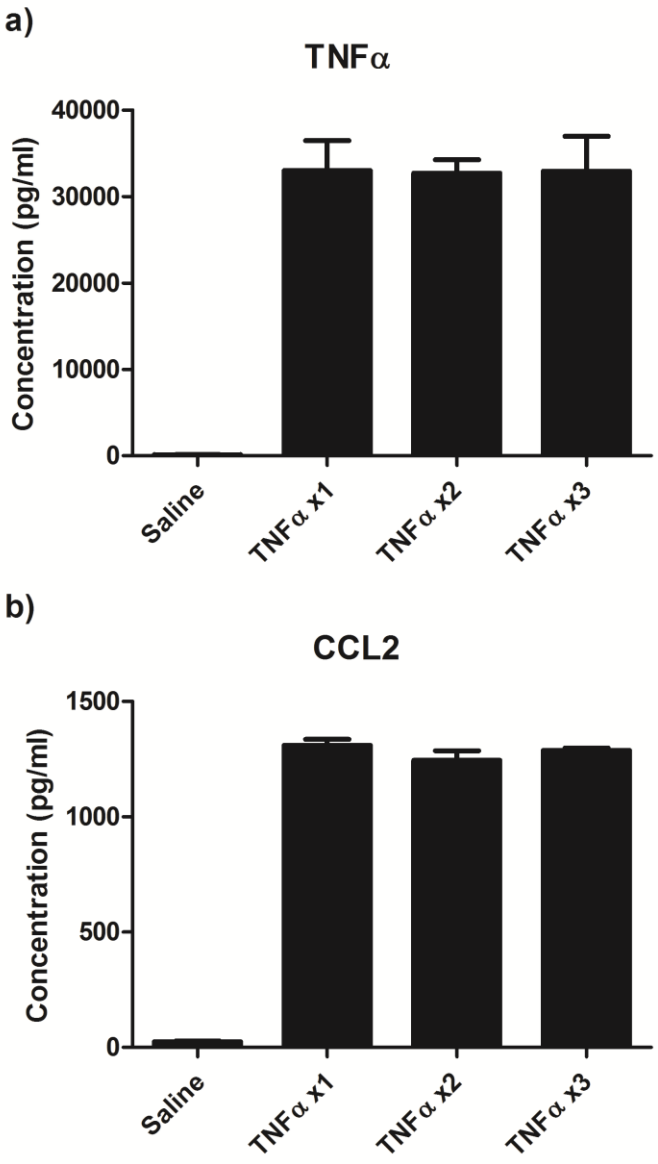

Figure 5.2 Systemic inflammatory cytokines following repeated TNFα challenge

Measures of systemic inflammatory markers following repeated i.p TNFα (250µg/kg) in 14 month old C57 mice. Data were analysed using a one-way ANOVA followed by a Dunnett multiple comparison test comparing each treatment group to the TNFα x1 group. All data are represented as the mean ±SEM, n=4-5 for all groups.

5.3.2 – Cognitive, behavioural and pathological measures following repeated TNFα in aged APP/PS1 mice

The long term cognitive and pathological consequences of repeated TNFα administration were examined in 15 month old APP/PS1 transgenic mice. It was initially intended that cognition would be examined using spontaneous alternation activity in the T maze. Animals were exposed to the T maze prior to TNFα administration, however, exploratory behaviour in the maze proved insufficient to establish spontaneous alternation activity. This limited activity in the maze was likely due to age of the animals as it was equivalent in APP/PS1 and WT. TNFα (250µg/kg) or sterile saline were administered to each animal 4 times, 5 days apart (figure 5.3). Lines crossed and rears in the open field were examined two hours post-challenge. Weight was examined every morning. Cognition was then examined on the hippocampal dependent Y maze task 7 days after the last challenge. Animals were terminally anaesthetised and transcardially perfused for formalin fixation and paraffin embedding 28 days after the first challenge. This tissue was then examined utilising immunolabelling for markers of synaptic and axonal disruption.

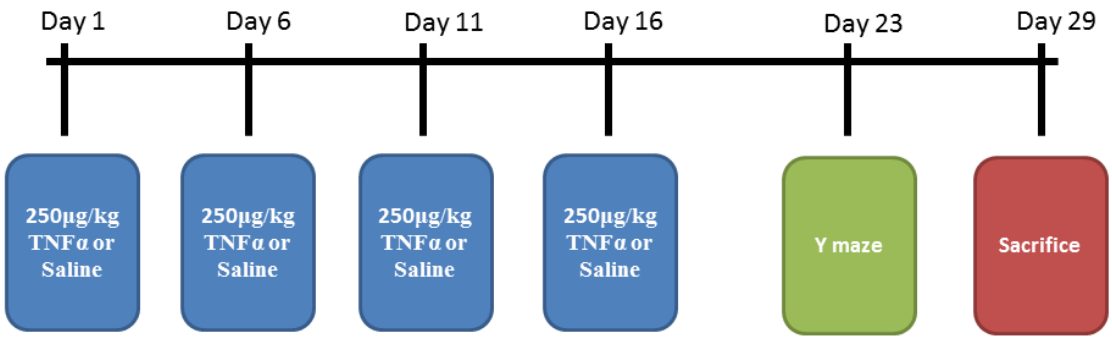

Figure 5.3 Treatment scheme, repeated TNFα administration APP/PS1s

Animals were administered 250µg/kg TNFα or sterile saline on 4 separate occasions each 5 days apart. Cognition was examined in the Y maze task on day 23. Animals were sacrificed on day 29.

5.3.2.1 – Sickness behaviour measures following repeated TNFα

Aged WT+TNFα animals showed a progressive weight loss in response to repeated systemic TNFα, this was consistent with responses to systemic TNFα in the literature (figure 5.4). However, APP/PS1+TNFα showed a diminished responsiveness to TNFα-induced cachexia. There was a main effect of treatment ($P<0.0001$, $F_{(3,374)}=12.6$) and time ($P<0.0001$, $F_{(17,374)}=6.722$) and an interaction between treatment and time ($P<0.001$, $F_{(51,374)}=3.751$). Following the second TNFα challenge the aged WT cohort treated with TNFα did not recover from the weight loss as rapidly as the APP/PS1+TNFα group. This is exacerbated by further challenge and these animals remain significantly different to the APP/PS1+TNFα group at all time-points after day 9 ($P<0.001$).

A main effect of time ($P<0.0001$, $F_{(3,66)}=68.76$) was found when activity in the open field was examined (figure 5.5a). This appeared to indicate habituation to the arena by the animals rather than any differential effect of repeated treatment. There was no difference in activity in the open field, due to strain or treatment, when activity was examined following the final TNFα challenge (figure 5.6a).

Rears in the open field showed a main effect of time ($P<0.001$,$F(3,66)=16.33$) over the 4 test periods (figure 5.5b). However, when rearing activity was examined following the final challenge alone (figure 5.6b), TNFα significantly diminishes the number of rears observed in WT animals ($p<0.01$). Rears in APP/PS1 animals were not altered at this time-point by TNFα.

5.3.2.2 – Cognition in the Y maze

The Y maze is a hippocampal-dependent spatial task examining reference memory and learning. Animals were examined on the Y maze 22 days after the first TNFα challenge and 6 days after the fourth TNFα challenge. This task showed that learning in APP/PS1 animals was significantly impaired in comparison to WT animals ($P<0.0159$, $F_{(1,77)}= 6.82$) (figure 5.7a). Levels of alternation in the Y maze in APP/PS1 animals were close to chance, indicating minimal learning of the task. There was little scope for TNFα to further impair learning in the APP/PS1 strain. WT animals showed learning of this task however there was no significant effect of TNFα on cognition in WT animals ($P=0.44$).

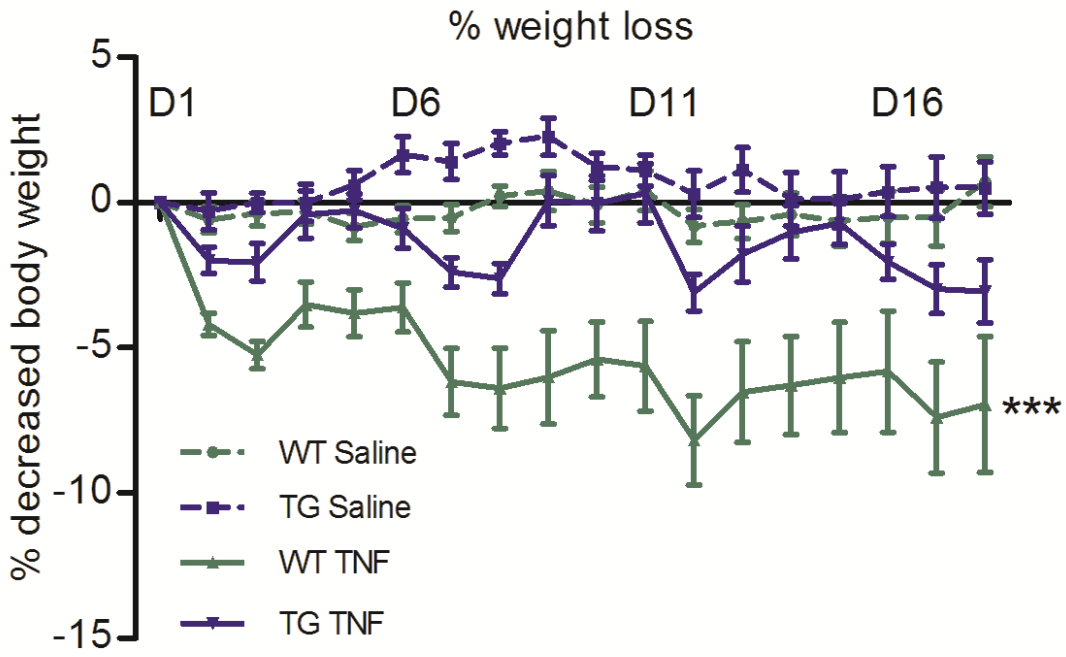

Figure 5.4 The impact of repeated TNFα on percentage weight lost

15 month old WT and APP/PS1 (TG) animals were weighed daily following repeated administration of 250μg/kg TNFα or sterile saline. Data were expressed as percentage lost from baseline weight. Data were analysed using a two-way ANOVA followed by a Bonferroni multiple comparison post hoc. Results are described in the text. Statistical significance is denoted by ***($P<0.001$). All data are represented as the mean ±SEM, n=6-7 for all groups.

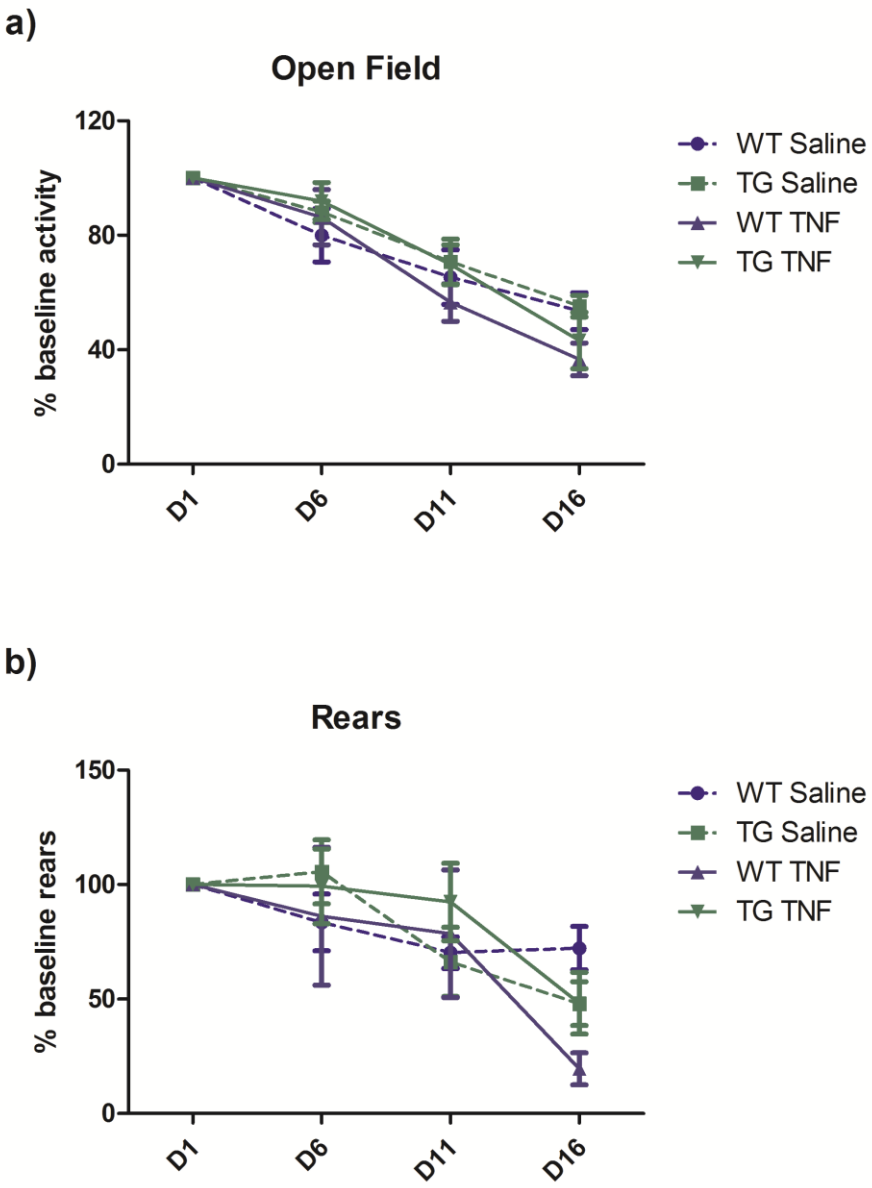

Figure 5.5 The impact of repeated TNFα on rears and Open Field activity

15 month old WT and APP/PS1 (TG) animals were examined on lines crossed and rears in the open field, measures of activity and exploration, following repeated administration of 250μg/kg TNFα or sterile saline. Data were analysed using a two-way ANOVA followed by a Bonferroni multiple comparison post hoc. All data are represented as the mean ±SEM, n=6-7 for all groups.

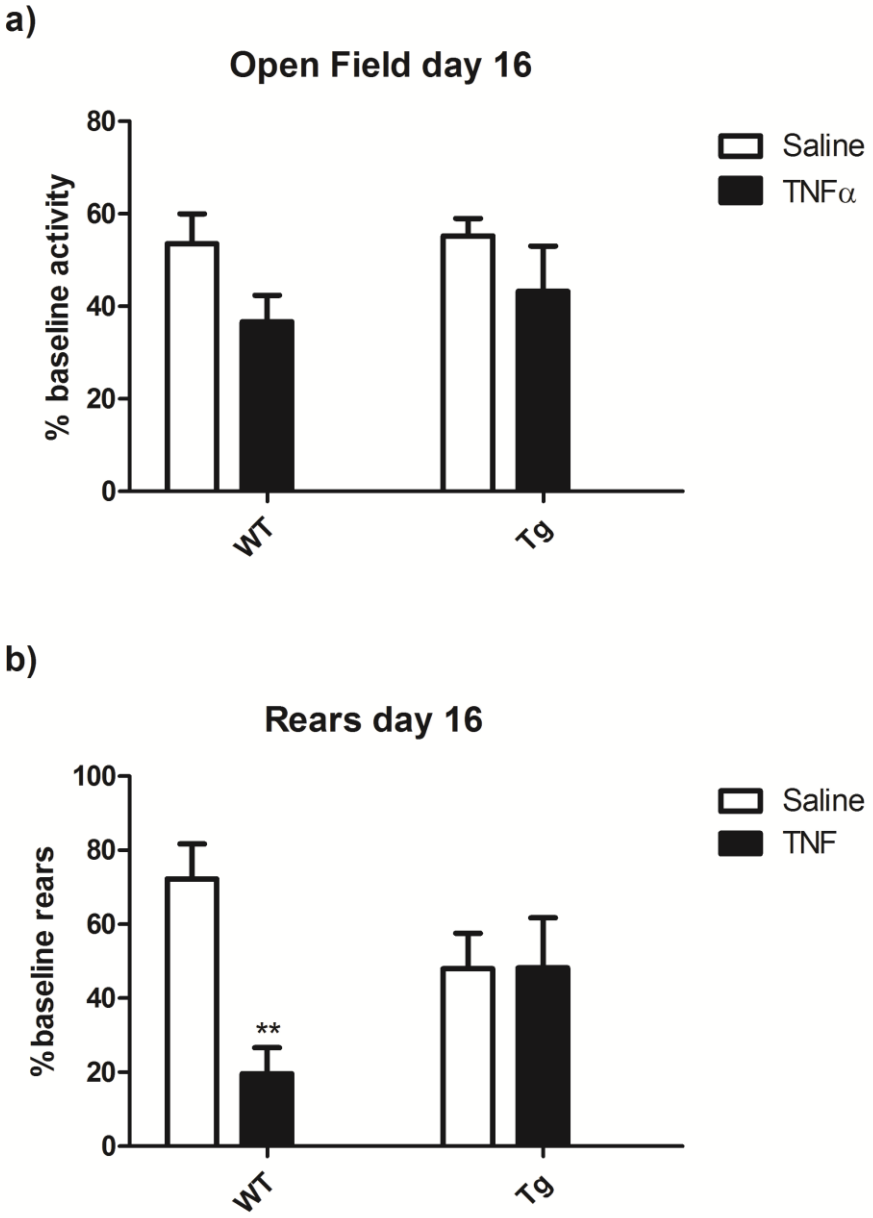

Figure 5.6 The impact of repeated TNFα on rears and open field activity following repeated TNFα challenges

15 month old WT and APP/PS1 (TG) animals were examined on lines crossed and rears in the open field, measures of activity and exploration, following repeated administration of 250μg/kg TNFα or sterile saline. Shown are the results of the tasks following the fourth TNFα challenge. Data were analysed using a two way ANOVA followed by a Bonferroni multiple comparison post hoc. Statistical significance is denoted by **($P<0.01$). All data are represented as the mean ±SEM, n=6-7 for all groups.

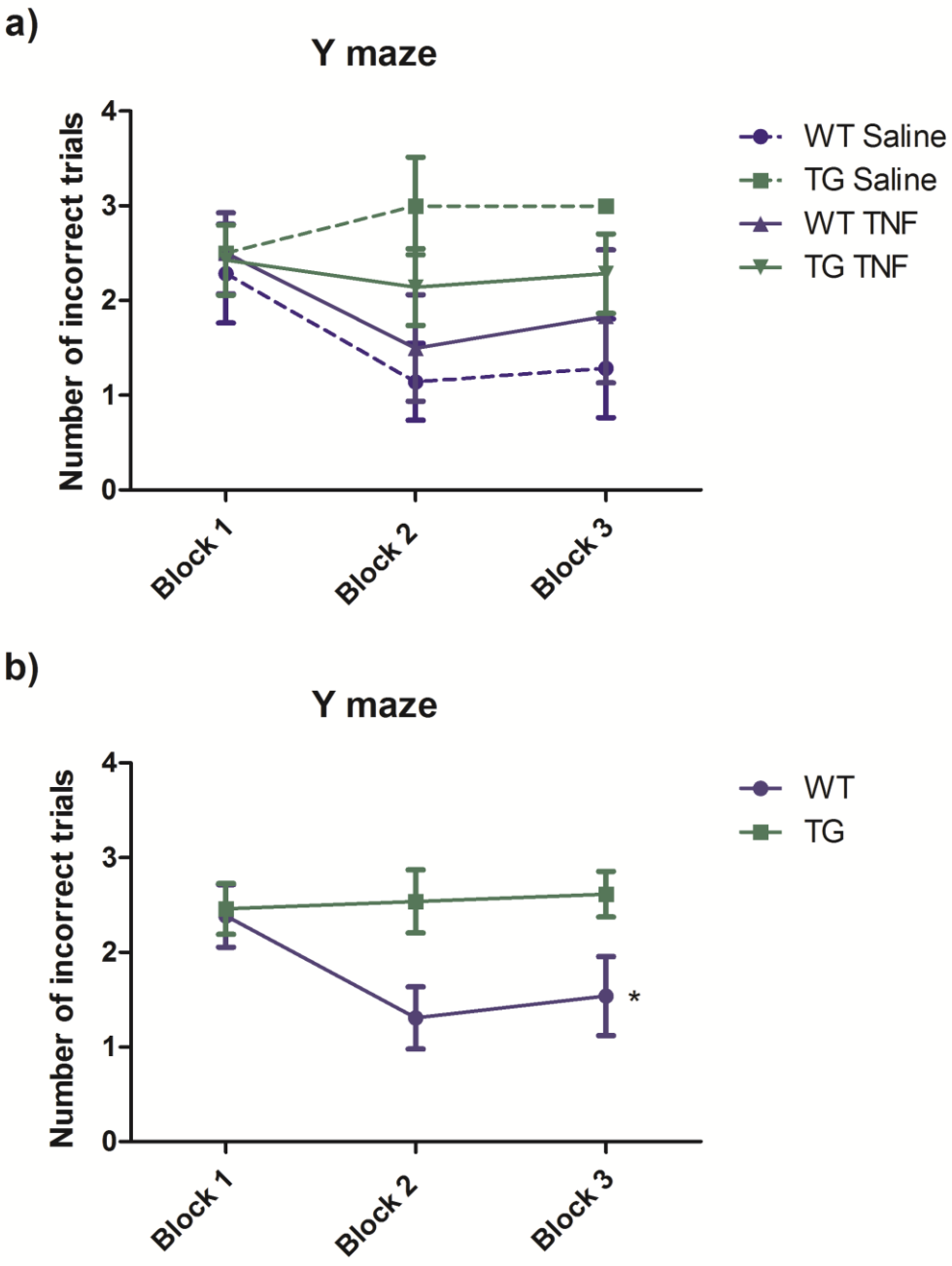

Figure 5.7 The impact of repeated TNFα on cognition in the Y maze

15 month old WT and APP/PS1 (TG) animals were examined on the Y maze, a hippocampal dependent spatial task, following repeated administration of 250μg/kg TNFα or sterile saline. Animals were tested in blocks of 6 trials per day. Data were analysed a) using a three way ANOVA followed by a Bonferroni multiple comparison post hoc b) using a two way ANOVA followed by a Bonferroni multiple comparison post hoc. Statistical significance is denoted by * ($P<0.05$). All data are represented as the mean ±SEM, n=6-7 for all groups.

5.3.3 – Pathological markers following repeated TNFα in aged APP/PS1 mice

The long term cognitive and pathological consequences of repeated TNFα administration were examined in 15 month old APP/PS1 transgenic mice. 250μg/kg TNFα or sterile saline were administered to each animal 4 times, 5 days apart (figure 5.3). Animals were terminally anaesthetised and transcardially perfused for formalin fixation and paraffin embedding 28 days after the first challenge. 10μm sections were cut using a microtome. Sections were examined utilising immunolabelling for markers of synaptic and axonal disruption. All quantifications were performed in duplicate or triplicate per animal and for six to seven animals per treatment group. Images were analysed using Image j. Data were analysed using a Students t test or a two way ANOVA followed by a Bonfferoni multiple comparison *post hoc*.

5.3.3.1 – Amyloid β and APP deposition

Amyloid β (Aβ) deposition was examined using the 6e10 antibody directed against Aβ and APP. There was no Aβ-positive labelling found in WT animals. In APP/PS1 animals there was a significant plaque load (figure 5.8a and c). Analysis of the percentage area occupied by Aβ-positive immunolabelling in the hippocampus of APP/PS1 animals following repeated saline and TNFα treatments (figure 5.8e) showed a reduction in the levels of Aβ deposition in animals treated with TNFα compared to those treated with saline ($P<0.0279$, $t=2.289$, $df=7$). There was no reduction in Aβ deposition in the area of the thalamus quantified (figure 5.8f).
APP immunolabelling, using an antibody directed towards the amino terminus of Amyloid Precursor Protein, shows a similar distribution to Aβ but with a different morphology (figure 5.8b and d). APP was similarly distributed to the Aβ plaques but occupied a smaller area, was less dense and had a different morphology, similar to that seen in the ME7 thalamic pathology in chapter 4. We quantified the hippocampus and thalamus in the same manner used to quantify Aβ deposition. Conversely to that observed with Aβ a significant increase in hippocampal levels of APP deposition (figure 5.8g) was observed following TNFα in TG animals in comparison to saline in TG animals ($P<0.0196$, $t=2.372$, $df=10$). When the

thalamus was examined for percentage area covered by APP positive immunolabelling (figure 5.8h), a significant increase in APP immunolabelling in APP/PS1+TNFα animals in comparison to TG+Saline also ($P<0.0232$, $t=2.273$, $df=10$) was observed.

Further examination of the distribution of APP immunolabelling revealed a significant quantity of punctate APP labelling in the internal capsule of both WT and TG animals (figure 5.9). The internal capsule carries major white matter tracts from the brainstem to the cortex. APP aggregation in this region may indicate axonal damage occurring with age. This would appear to be a feature of aging in these animals as similar labelling has not been found in young animals following APP labelling in ME7. There is significantly more deposition of the punctate APP in the internal capsule of the APP/PS1 animals (figure 5.9c and d). As well as the smaller aggregations, plaque-like aggregations of APP appear in the internal capsule of the APP/PS1 animals.

5.3.3.2 – Neuronal density

We utilised the NeuN label to examine neuronal density in the WT and APP/PS1 animals following repeated systemic TNFα (figure 5.10). On gross examination it appears that there may be a lower neuronal density in the hippocampal and dorsal thalamic region in APP/PS1 animals compared to WT animals (figure 5.10 c and d vs. a and b). However, the APP/PS1 model has widely been described as a model with limited neurodegeneration, and so to comment on neuronal density in this study would require quantification. We could not see a gross effect of TNFα and it would require an in depth quantification strategy to elucidate whether there is an effect of TNFα on the hippocampal or thalamic neuronal populations.

5.3.3.3 – Axonal and synaptic pathology

Axonal and synaptic pathology in the APP/PS1 model was assessed using the phosphorylated neurofilaments marker SMI-32, the Hyperphosphorylated Tau

label AT8 and the pre-synaptic marker SY38 (figure 5.11). Aggregations of this abnormal neurofilament marker SMI-32 in plaque-like deposits were observed in the APP/PS1 model (figure 5.11g and j). This does not occur in WT animals. Such aggregations would imply that there is disruption in neuronal cytoskeletal stability in the APP/PS1 animals.

Hyperphosphorylated Tau labelling revealed punctate aggregations of Tau, likely to be dystrophic neurites, which appeared to localise in the periphery of plaque-like structures in the tissue of the APP/PS1 transgenic animals (figure 5.11h and k). There were tiny amounts of Hyperphosphorylated Tau puncta present in the WT animal. These aggregations were not similar to neurofibrillary tangles in nature. This was greatly elevated in the APP/PS1 brains. However due to the discrete nature of the aggregations it was difficult to discern whether there was any alteration due to repeated systemic TNFα.

Synaptic density was observed utilising SY38 labelling of synaptophysin, we found no gross alterations of synaptic density in the CA1, stratum radiatum and lacunosum moleculare layers of the hippocampus in WT vs. APP/PS1 animals (figure 5.11c and f vs. i and l). However, intense aggregations of SY38 labelling consistent with the distribution and density of the amyloid plaques were found throughout the hippocampus. These aggregations may be indicative of disrupted axonal transport of synaptic proteins or dystrophic neurites at the periphery of amyloid plaque structures. Again, due to the disparate nature of the labelling it was difficult to determine whether repeated systemic TNFα had an impact on Synaptophysin.

5.3.3.4 – Cell populations

Infiltration and proliferation of immune cells into the CNS of the WT or APP/PS1 animals was assessed following repeated systemic TNFα administration. Neutrophils were assessed using the MBS-1 immunolabel. There was no infiltration of neutrophils in WT or APP/PS1 animals prior to, or following, repeated systemic TNFα administration (data not shown). Both the Pu.1 and IBA-1 labels were used to examine myeloid lineage cells in the hippocampus and thalamus. Pu.1 labelling was used to easily quantify the number of myeloid lineage

cells in the hippocampus and dorsal thalamus (figure 5.12m). There was increased numbers of Pu.1 positive cells in the APP/PS1 model. This showed a main effect of strain ($P<0.0001$, $F(1,21)=132.6$) with no effect of systemic TNFα administration. This indicates increased microgliosis or elevated levels of macrophage infiltration in the APP/PS1 animals compared to WT (figure 5.12 a and d vs. g and j) but no further impact of TNFα on this population. Microglial morphology was observed utilising IBA-1 labelling. As well as there being elevated microglial numbers in the APP/PS1 animals, these cells show a robustly condensed morphology in APP/PS1 animals compared to WT (figure 5.12 b and e vs. h and k).

Next CD3 labelling was used to quantify T cells in the CNS. There were very low numbers of T cells in the CNS overall. We found an increase in T cells in the cortex of APP/PS1 animals in comparison to WT animals ($P<0.0001$, $F(1,19)=78.37$). There was no alteration due to systemic TNFα in T cell numbers in the cortex (figure 5.12n). In the hippocampus a similar result was observed with an APP/PS1-induced increase in T cells ($P=0.0004$, $F(1,19)=18.80$) but no increase in T cells due to systemic TNFα (figure 5.12o). The thalamus proved different, showing increased T cells in the APP/PS1 compared to WT ($P=0.0004$, $(F1,19)=18.36$), T cells were further increased due to TNFα in APP/PS1 animals ($P<0.05$) but not in WT animals. APP/PS1 animals show an elevated number of T cells in the thalamus following repeated systemic TNFα, whereas WT animals do not, following the same treatment (figure 5.12p).

When examining the sections we could see evidence of migration of T cells from the choroid plexus in the lateral ventricles through the interventricular foramena (foramen monro, connects lateral and third ventricles) into the white matter tracts of the stria terminalis, the fimbriae and the internal capsule in the thalamus (figure 5.12c, f, i and l).

5.3.3.5 – Proliferation

Ki67 is a marker of proliferation that labels cells entering the active phases of the cell cycle. Proliferation was robustly increased in the hippocampus of APP/PS1 animals. Repeated systemic TNFα administration decreased the strain associated proliferation (figure 5.13a). There was a main effect of strain ($P<0.0001$,

$F_{(1,22)}$=3.53), and main effect of treatment (P=0.0007, $F_{(1,22)}$=15.36) and an interaction between treatment and strain (P<0.01, $F_{(1,22)}$=6.438). There was no significant alteration of proliferation by systemic TNFα in WT animals, TNFα only disrupts the disease-associated proliferation (P<0.001). There were many varieties of positive Ki67 labelling of the nucleus, dependent on the stage of the cell cycle, representative images are shown (figure 5.13 b-d). Figure 5.13b shows 2 nuclei immediately after dividing, 5.13c shows plaque associated proliferating cells and 5.13d shows proliferating cells in the sub granular zone of the dentate gyrus.

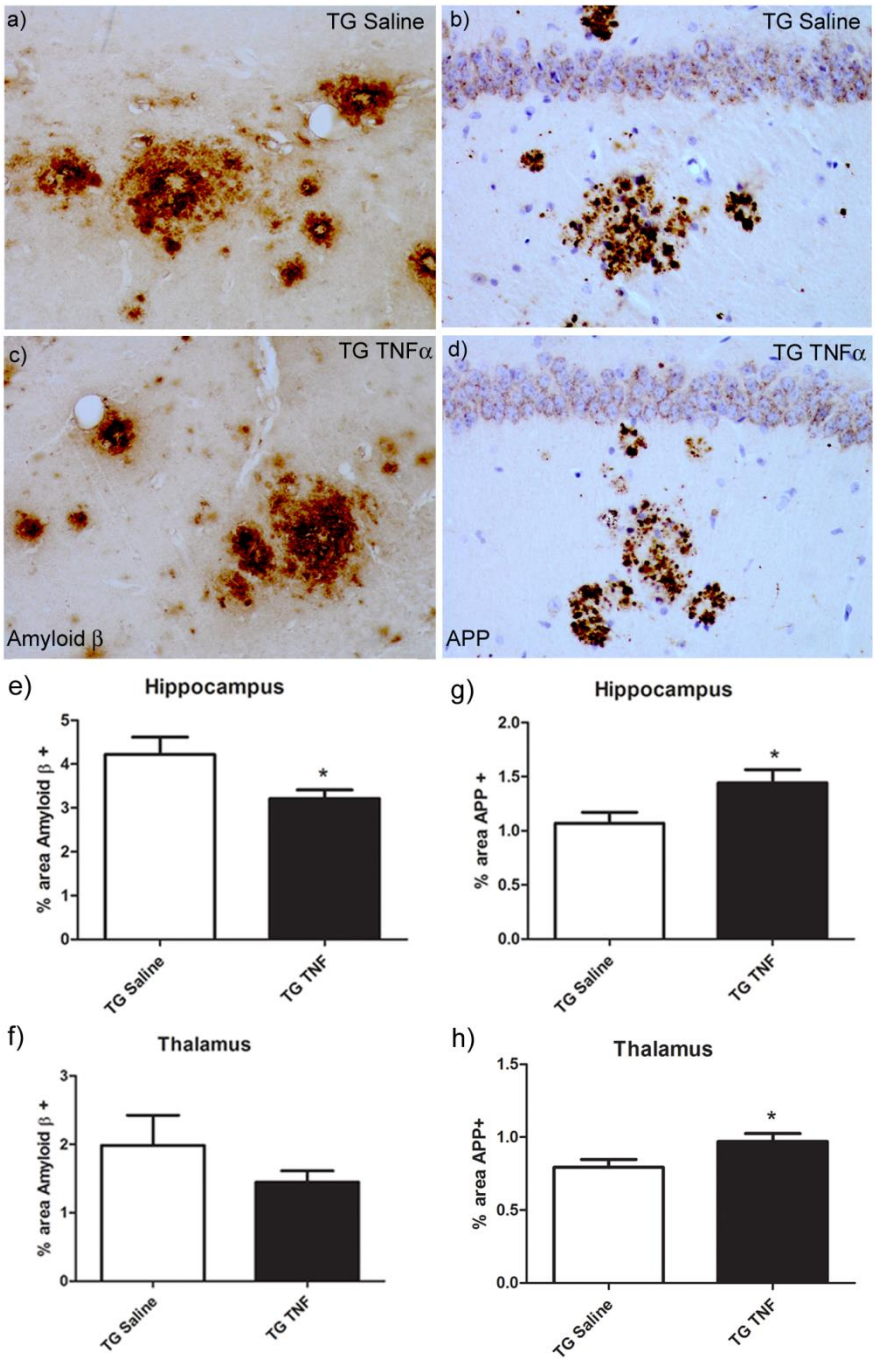

Figure 5.8 The impact of repeated TNFα on amyloid β and APP deposition

15 month old WT and APP/PS1 (TG) animals were immunolabelled for amyloid β and APP following repeated administration of 250μg/kg TNFα or sterile saline. Percentage area covered by Aβ and APP was quantified in the hippocampus and thalamus using Image J. Data were analysed using a Student's t test. Statistical significance is denoted by * ($P<0.05$). All data are represented as the mean ±SEM, n=6-7 for all groups. Representative images of plaques in the CA1 region shown at x40.

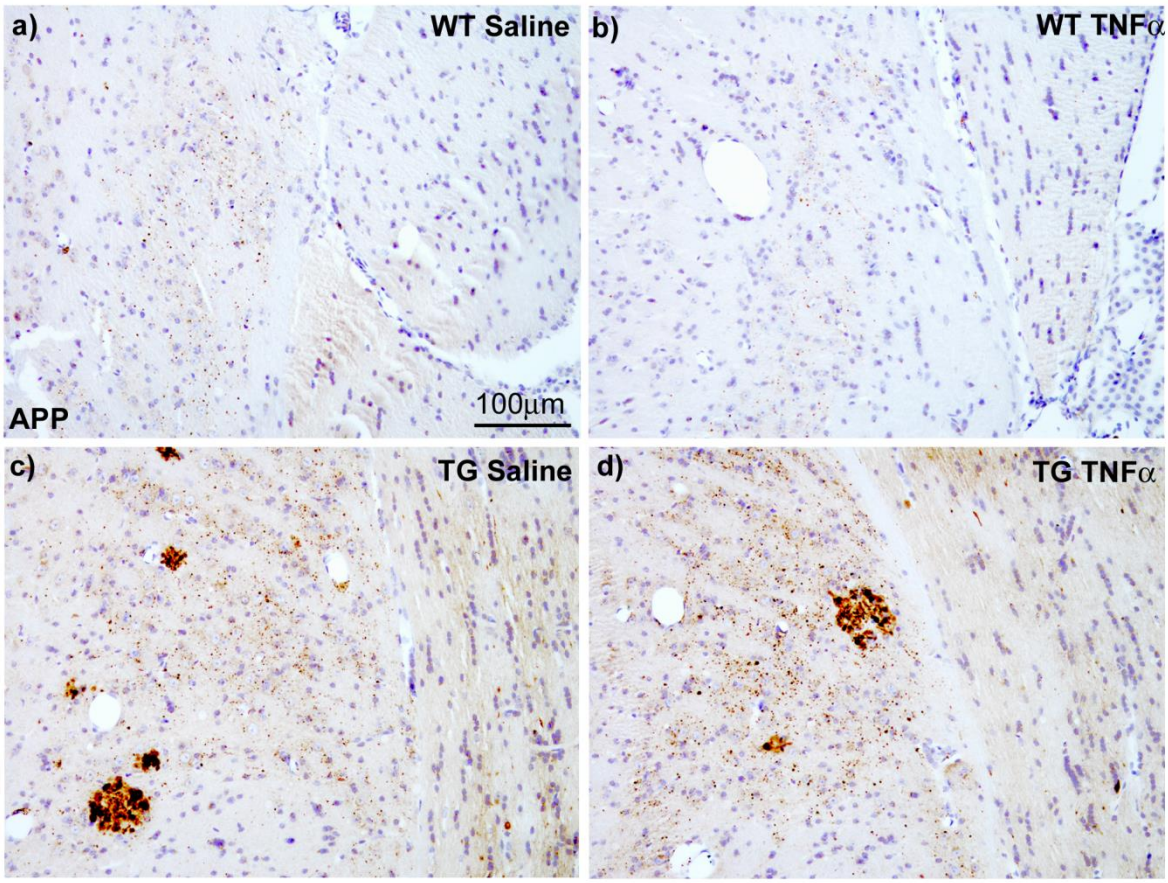

Figure 5.9The impact of repeated TNFα on internal capsule APP deposition

15 month old WT and APP/PS1 (TG) animals were immunolabelled for APP following repeated administration of 250µg/kg TNFα or sterile saline. The internal capasule and fimbriae are shown. Representative images are shown at x20, scale bar = 100µm.

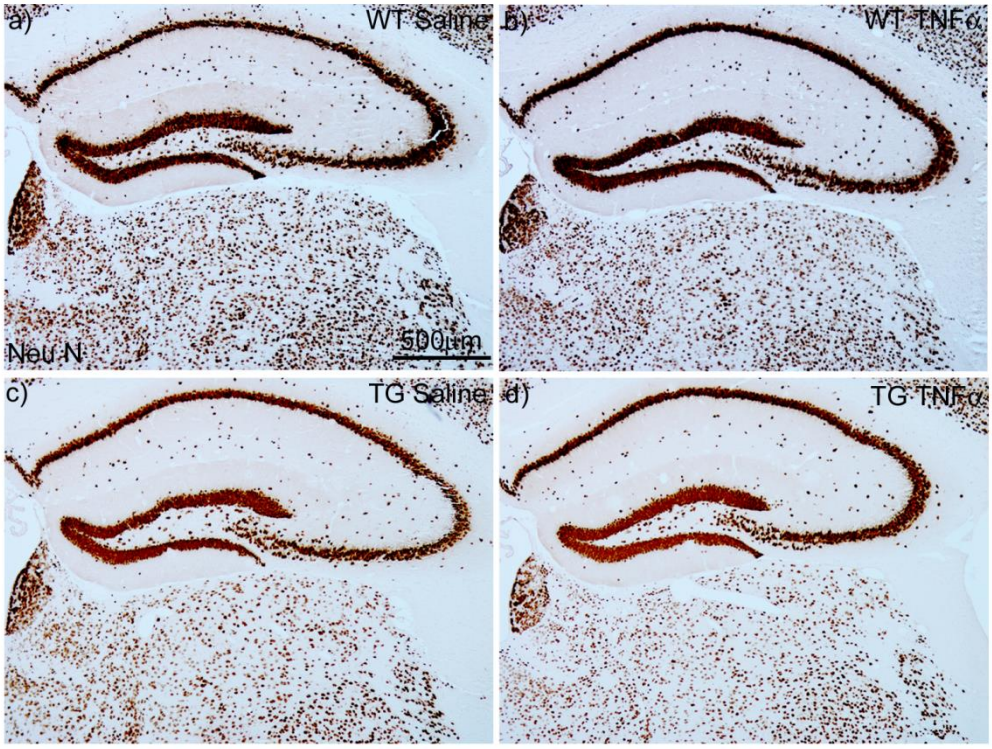

Figure 5.10 Examination of Neuronal immunolabelling post-repeated TNFα

15 month old WT and APP/PS1 (TG) animals Neurons were immunolabelled using NeuN following repeated administration of 250µg/kg TNFα or sterile saline. The hippocampus and dorsal thalamus are shown. Representative images are shown at x5, scale bar = 500µm.

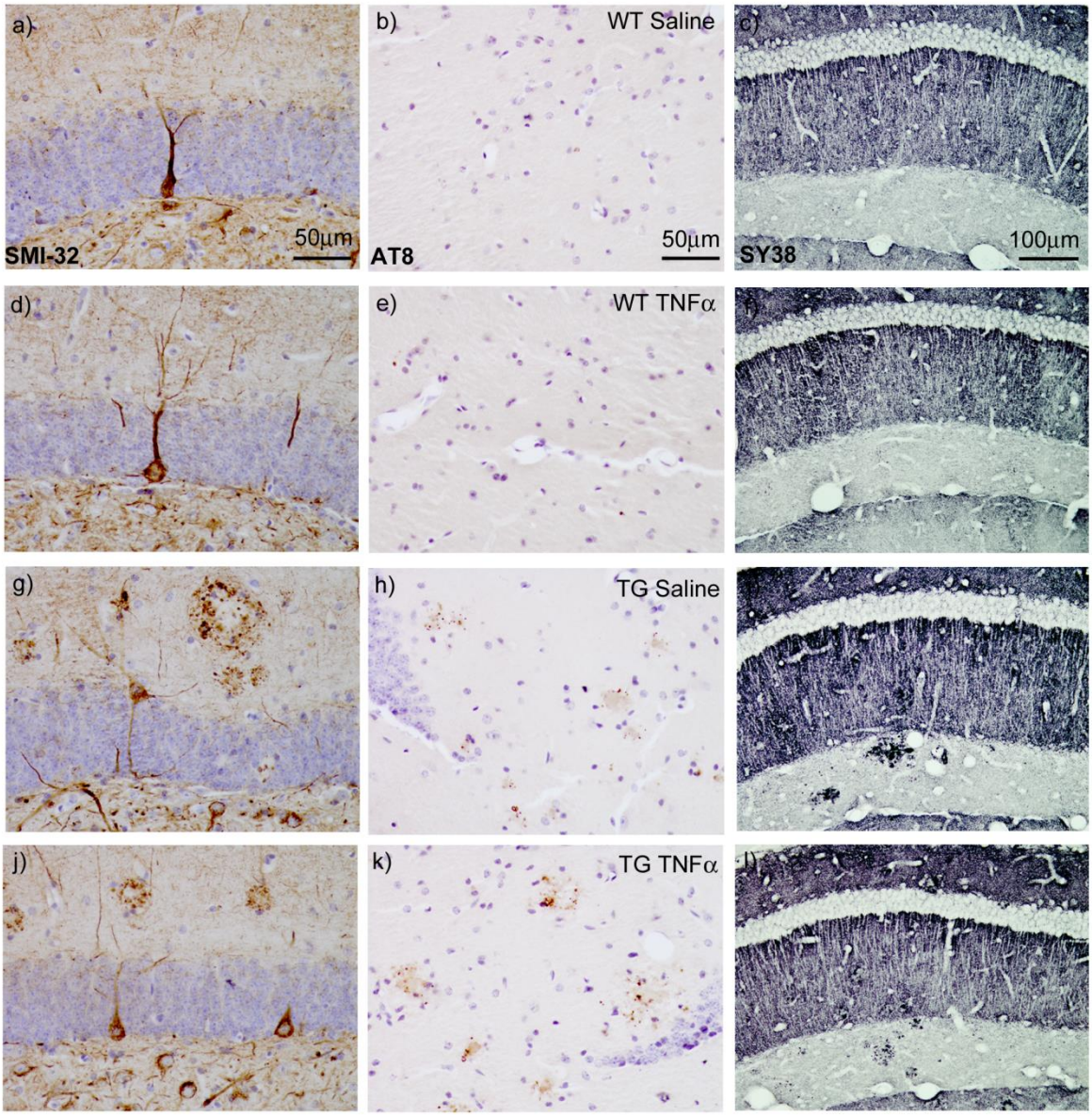

Figure 5.11 Examination of axonal & synaptic pathology post-repeated TNFα

15 month old WT and APP/PS1 (TG) animals were immunolabelled following repeated administration of 250µg/kg TNFα or sterile saline. (a, d, g and j) are labelled for SMI-32 which labels phosphorylated neurofilaments, the dentate gyrus is shown (Magnification x40, scale bar = 50µm). (b, e, h and k) are labelled for hyperphosphoylated Tau using AT8, the hippocampus is shown (Magnification x40, scale bar = 50µm). (c, f, I and l) are labelled for Synaptophysin a pre-synaptic protein using SY38, the CA1, stratum radiatum and lacunosum moleculare are shown (Magnification x20, scale bar = 100µm).

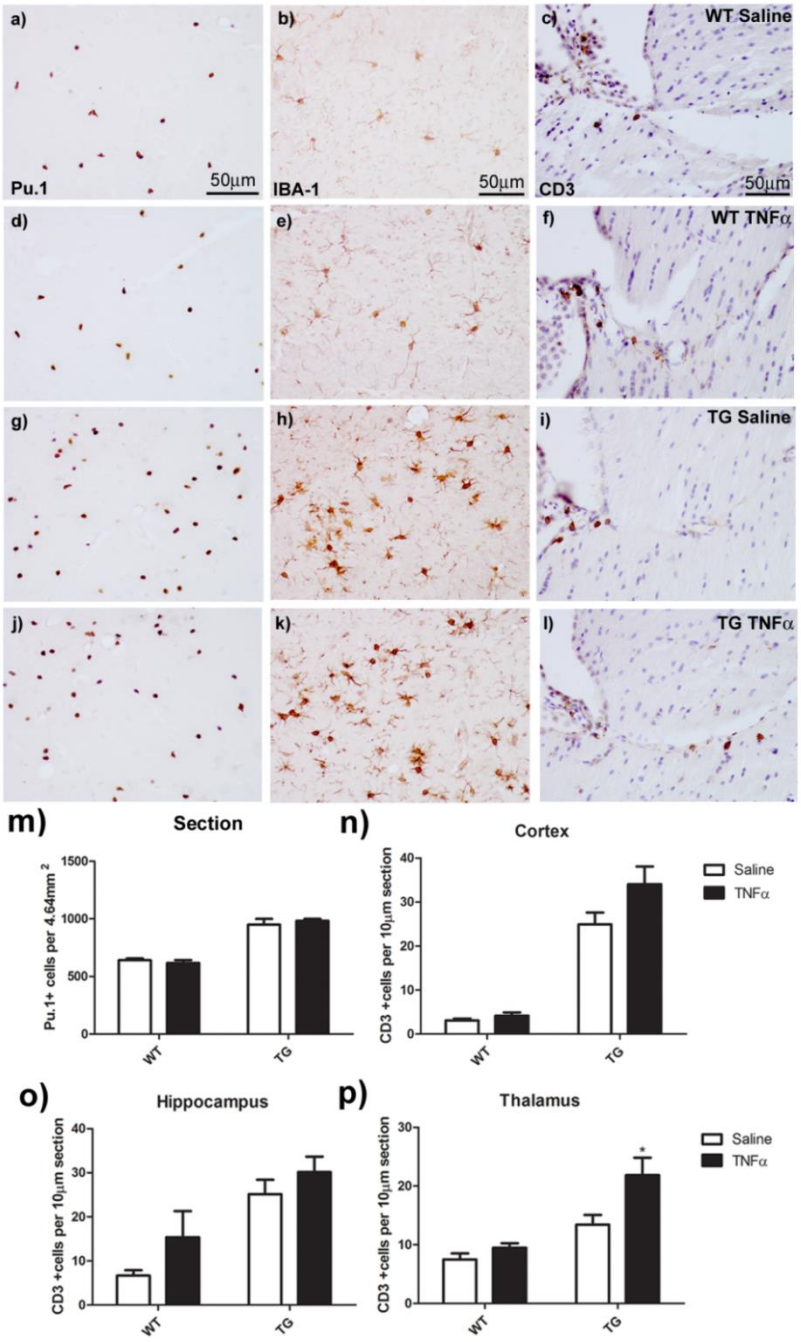

Figure 5.12 Examination of microglia and T cells post-repeated TNFα

15 month old WT and APP/PS1 (TG) animals were immunolabelled following repeated administration of 250µg/kg TNFα or sterile saline. (a, d, g and j) are labelled for microglia using Pu.1 (Magnification x40, scale bar = 50µm). (b, e, h and k) show microglial morphology using IBA-1 (Magnification x40, scale bar = 50µm). (c, f, I and l) are labelled for T cells using CD3 (Magnification x20, scale bar = 100µm). m) Pu.1+ cells were quantified using Image J. n-p) CD3+ cells were quantified manually. Data were analysed using a two way ANOVA followed by a Bonferroni multiple comparison post hoc. Statistical significance is denoted by * ($P<0.05$). All data are represented as the mean ±SEM, n=6-7 for all groups.

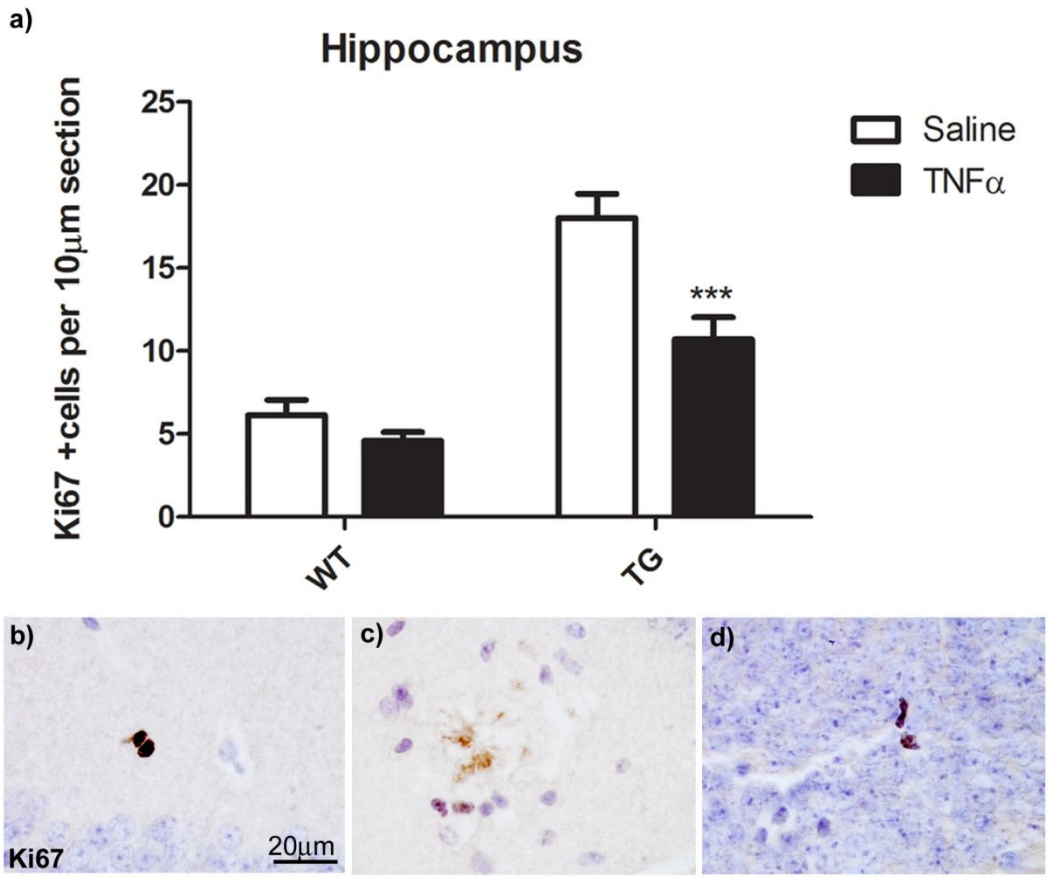

Figure 5.13 Examination of proliferation post-repeated TNFα

15 month old WT and APP/PS1 (TG) animals were immunolabelled following repeated administration of 250μg/kg TNFα or sterile saline. a) Ki67+ cells were counted manually. Data were analysed using a two way ANOVA followed by a Bonferroni multiple comparison post hoc. Statistical significance is denoted by ***(P<0.001). All data are represented as the mean ±SEM, n=6-7 for all groups. Representative images of Ki67 positive cells are shown (b-d) x100, scale bar = 20μm.

5.4 –Discussion

Repeated administration of systemic TNFα (250μg/kg) in aged C57s was not found to alter the systemic response to TNFα when TNFα and CCL2 were examined. Repeated administration of TNFα (250μg/kg) in APP/PS1 versus WT animals found that there was a significantly greater loss of body weight in WT animals compared to APP/PS1 animals. However there was no significant effect of prior administration of repeated TNFα on performance in the Y maze. Neuropathology in 15 month old APP/PS1 animals was fundamentally altered by repeated systemic TNFα administration. CNS Aβ deposition was reduced while APP deposition was increased. There were increased numbers of T cells in the thalamus of APP/PS1 animals treated with TNFα compared to those treated with saline, this did not occur in WT animals. Repeated TNFα administration also reduced the level of proliferation in the hippocampus of APP/PS1 animals compared to saline. Markers of synaptic and axonal pathology were not grossly altered by repeated TNFα administration, although quantitative analysis is required to reveal any subtle differences that may exist.

5.4.1 – Systemic effects of repeated systemic TNFα administration

Systemic responses to repeated systemic TNFα administration in aged naïve animals revealed no alteration in blood TNFα or CCL2 in animals when challenged once, twice or three times with systemic TNFα. Systemic LPS has been shown to display altered central and systemic responses dependent on the number of administrations and on their timing. 3 repeated LPS (3mg/kg) administrations within 28 hours showed a significant upregulation in systemic TNFα and also in central CCL2 and TNFα in comparison to a single LPS administration (Erickson and Banks, 2011). With a more spaced out dose regimen, LPS once a day for three days, the opposite was shown; systemic IFNγ, TNFα and IL-12 all show diminishing responses following the second challenge indicating development of tolerance rather than upregulation (Puntener et al., 2012). This study only examined TNFα and CCL2 response, these limited data indicate that there may be no alterations in the systemic response to multiple TNFα administration in the periphery. It will be necessary to examine the effects of this paradigm in the CNS

also. The timing of these challenges may perhaps be too spread out to observe an upregulation or tolerance as the majority of repeated inflammatory stimuli experiments utilise a daily or more frequent administration where this experiment used a once a week regimen to mimic repeated inflammatory events.

5.4.2– Behavioural and cognitive effects of repeated systemic TNFα administration in APP/PS1s

Sickness behaviour was examined in aged APP/PS1 and WT animals treated with repeated systemic administration of TNFα, no significant alterations in activity in the open field was found. However, APP/PS1 showed what appeared to be a less sensitive response to systemic TNFα in comparison to WT+TNFα when we looked at weight loss and exploration in the open field. WT+TNFα animals showed a progressive weight loss with repeated TNFα administration, however APP/PS1+TNFα animals showed complete recovery following each administration. There is conflicting evidence in the literature with regards to TNFα cachectic and anorectic effects. Firstly the majority of the literature is in rats, secondly, the timing of the TNFα dose regimen may be extremely important in determining whether tolerance develops. When the TNFα administrations are spread out over time there is no tolerance to the loss of body weight. Ten Hagen et al showed a progressive weight loss in rats when they received TNFα (200μg/kg) every 4 days, 5 times. This regimen caused severe diarrhea after every administration and weight loss of ~36% by the end-point (ten Hagen et al., 2002). In comparison, when the TNFα challenges are closer in time to each other, tolerance develops and the anorectic effect is diminished. TNFα (4mg/kg s.c.) daily for 5 days in rats showed a tolerance to the febrile response and slight early decrease in food intake but no weight loss at the end-point (Kettelhut and Goldberg, 1988). Daily treatment with TNFα (250μg/kg) for 5 days showed decreased nutrient intake on day one, followed by a rebound on day two with increased nutrient intake and regaining of any lost weight. This regimen did however induce a significant and persistent hyperlipidemia indicating alterations of adipose functions post-repeated TNFα (Grunfeld et al., 1989). Similarly Fraker et al., showed that 100μg/kg twice daily in rats showed an initial decrease in food intake and loss in body weight however by day three the food intake had doubled

and body weight was returned to normal. This group also showed that weight loss and the timing of initiation of tolerance to the anorectic effect was dose dependent, i.e. a lower dose showed a more rapid recovery to normal nutrient consumption (Fraker et al., 1988). There has been very little work performed on repeated TNFα administration in mice. Administration of 250μg/kg of TNFα every second day for 3 weeks in mice showed no tolerance of the cachectic effect. There was consistent and progressive weight loss observed in mice with this repeated TNFα regimen (Cope et al., 1997). Though the treatment regimen is different to the regimen used here (same dose, every second day for three weeks versus once every 5 days for 16days) these results, and the Ten Hagen results discussed above, would imply that the progressive weight loss observed in the WT+TNFα group is normal while the recovery of the APP/PS1+TNFα group is abnormal. The APP/PS1+TNFα group have not developed tolerance as they do lose weight after each administration; however after each challenge they recover to baseline more rapidly than the WT+TNFα group. Tg2576 AD mice were found to have abnormally low circulating leptin levels and an aberrant hypothalamic response to leptin. Tg2576 mice showed decreased adiposity due to an increased metabolic rate and normal feeding behaviours, conversely low levels of leptin should increase food intake and decrease energy expenditure (Ishii et al., 2014). The abnormal weight loss in the APP/PS1+TNFα group may be due to aberrant hypothalamic responses to TNFα-induced leptin. TNFα action on the hypothalamus has been shown to increase leptin release (Kim et al., 2015) which should result in decreased food intake. Action of TNFα on the hypothalamus has also been shown to induce lipolysis of adipose tissue (Kim et al., 2015). The initial weight loss observed in both strains may be evidence of lipolysis due to TNFα action on the hypothalamus. Examination of Free Fatty Acids in the serum would verify this theory. The progressive weight loss observed in the WT+TNFα group may be TNFα-induced cachexia; aberrant hypothalamic responses in the APP/PS1 model may limit their cachectic response. The question of whether limiting inflammation-induced cachexia results in a better outcome in APP/PS1 animals requires further examination.

This diminished responsiveness to TNFα in the APP/PS1 group could not be shown to be detrimental or protective on the cognitive tasks examined. This entire cohort, WT and APP/PS1, displayed limited exploratory activity in the T maze and

were unresponsive to food reward stimuli perhaps due to advanced age. This meant spontaneous alternation in the T maze was not an option for examining working memory. When examined in the Y maze the APP/PS1 strain showed little to no learning of the task and the WT animals, even though they were aged, could learn the task. There was no significant effect of TNFα treatment in either strain. However TNFα in APP/PS1 showed no effect on rears in the open field following the fourth TNFα administration, in comparison the WT+TNFα group was significantly impaired on rears in comparison to WT+saline at the same time-point. This, similarly to the aberrant weight loss response observed in the APP/PS1+TNFα group is likely due to altered hypothalamic function. Ablation of catecholamine neurons in the paraventricular nucleus of the hypothalamus was previously shown to ablate LPS-induced deficits in exploratory activity (Gaykema and Goehler, 2011). Even though APP/PS1 deficits in the Y maze were not exacerbated by this repeated TNFα paradigm, the deficits present in APP/PS1 are possibly due to ongoing inflammatory processes in this strain. Knock-out of TNFR1 in the APP23 model showed a significant reduction in learning and memory deficits in this model (He et al., 2007). Medeiros et al showed that administering an anti-TNF antibody i.c.v. 15 minutes before i.c.v Aβ prevented the learning and memory impairments seen in the Morris water maze following i.c.v. Aβ. Similar effects were produced in a TNFR1 knock-out (Medeiros et al., 2007). These results indicate a role for TNFα in the development of the cognitive deficits shown with APP accumulation and Aβ deposition.

5.4.3 – Amyloid beta and APP roles in pathology

Robust amyloidosis was observed throughout the hippocampus, cortex and to a lesser extent, the thalamus. Though the 6e10 antibody is marketed as primarily labelling Amyloid β it also appears to label the precursor APP (McAlpine et al., 2009; Youmans et al., 2012). When the labelling of the APP-specific antibody used was quantified we observed an increased deposition in APP deposition and aggregation in the hippocampus and thalamus of APP/PS1 animals following repeated systemic TNFα. When we examined 6e10 labelling we saw a significant decrease in 6e10 labelling in the hippocampus. Given the increase of APP positive labelling in the same region it is reasonable to assume that the decrease in 6e10

labelling is due to a significant decrease in Aβ deposition. It is also of interest to note the APP pathological formations in the white matter tract of the internal capsule in all animals; this is likely due to the age of the animals. APP has long been used as a marker of white matter tract damage (Gentleman et al., 1993) and APP pathology in the internal capsule implies that aging significantly damages the main tract between the thalamus and the cortex responsible for sensory function. APP deposition in the internal capsule has previously been found following traumatic brain injury (Hortobagyi et al., 2007).

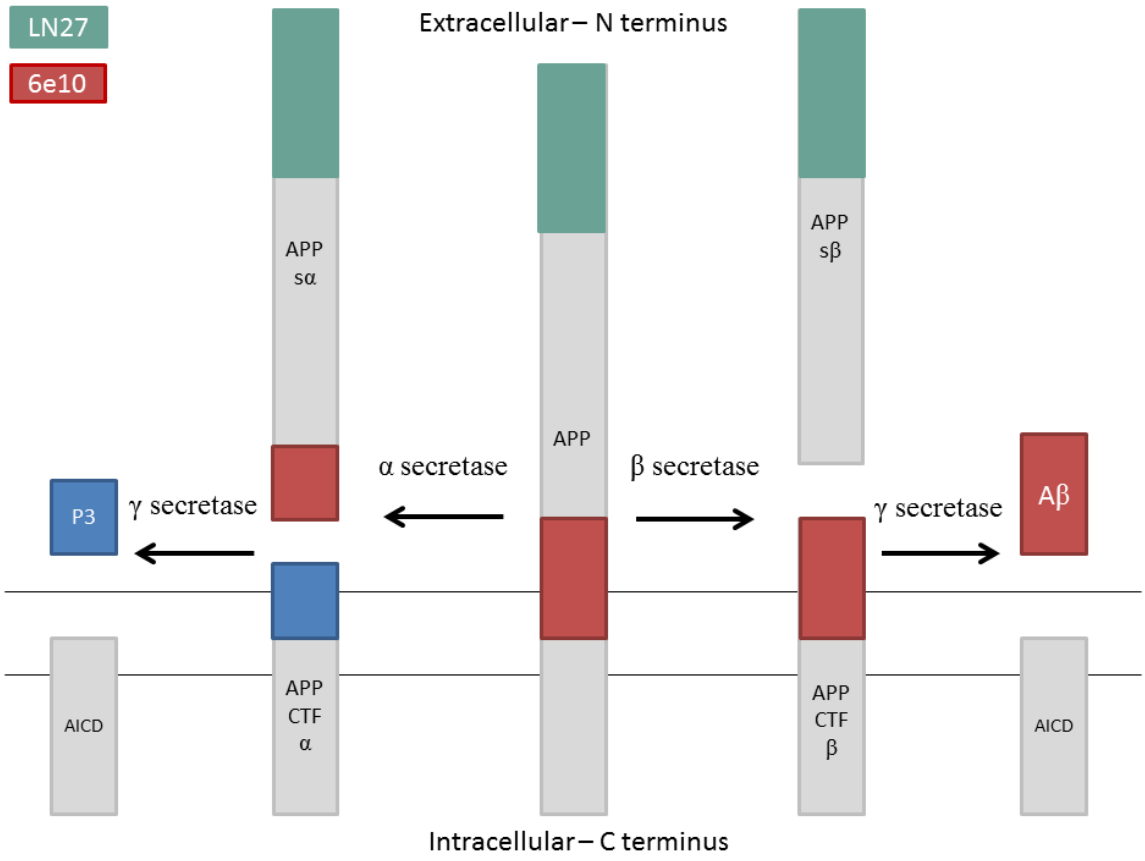

Figure 5.14 Immunolabelling of different APP cleavage products

6e10 can label Aβ, APP, APPsα and APP CTF-β. LN27, the APP specific antibody can label APP, APPsα and APPsβ but cannot label any of the various Aβ cleavage forms.

Acute central LPS in AD transgenics has been shown to decrease Aβ/APP load via increases in microglial phagocytosis (DiCarlo et al., 2001; Herber et al., 2004; Herber et al., 2007), however chronic systemic LPS or bacterial infection has been

shown to increase both Aβ and APP load (Sheng et al., 2003). The role of central TNFα has been examined in the effects of chronic systemic LPS on Aβ and APP processing. McAlpine et al., found that chronic peripheral LPS administration in 3xTg-AD mice induced significant increases in 6e10 intraneuronal immunoreactivity, this was then shown to be neither Aβ nor full length APP but β C-Terminal Fragments (β-CTF) and α-C-Terminal Fragments (α-CTF). Chronic inhibition of central TNFα, using XENP345, a dominant negative TNFα inhibitor, was found to inhibit the increases in 6e10 immunoreactivity post-chronic systemic LPS (McAlpine et al., 2009). TNFα has been implicated in the processing of Aβ and APP previously. APP23 transgenics crossed with TNFR1$^{-/-}$ showed decreased 6e10 positive labelling, and $A\beta_{1-40}$/$A\beta_{1-42}$ protein alongside decreased BACE1 levels and activity (He et al., 2007). This alteration in Aβ processing attenuated deficits seen in learning and memory and age-associated neuronal loss in this model. Use of i.c.v. infliximab, an anti-TNFα antibody, for 3 days in 12 month APP/PS1 mice also showed decreases in amyloid staining (Shi et al., 2011). TNFα has been shown to increase APP expression in cultured human astrocytic cells (Lahiri et al., 2003) while it has also been shown to increase BACE1 activity via NF-κB activation (Chen et al., 2012a). However the effects of repeated systemic TNFα on Aβ may differ from LPS administration or TNFα inhibition. Repeated systemic TNFα administration may alter microglial phagocytic activities with regards to Aβ. CCR2-/- APP/PS1 animals were shown to have significantly increased soluble Aβ and plaques (Naert and Rivest, 2011). Heneka et al showed that a key mutation in human APP compared to mouse APP allows nitrosylation of Aβ. This is a key step in the seeding of an Aβ plaque (Kummer et al., 2011). However systemic poly I:C challenge in a non-APP overexpressing mouse was shown to induce aggregation and deposition of APP. Systemic Poly I:C in the 3xTg-AD model showed an altered plaque composition with the core being composed primarily of non-fibrillar APP deposits which were then surrounded by Aβ (Krstic et al., 2012). These data appear to indicate that a systemic inflammatory event can alter APP processing and subsequent aggregation and deposition. The increased APP labelling found in this study is consistent with the work described by Krstic et al,.

Whether these alterations in the Aβ/APP ration are related to cognition may be debatable. High levels of Aβ pathology has long been found in Non Demented -

High Pathology Controls (ND-HPC), these post mortem brains show levels of Aβ and NFTs equivalent to AD patients however they do not display the synapse loss associated with AD (Lue et al., 1996). When we examined synaptic density in this study there were no gross alterations in synaptic density according to strain, density was not obviously affected by TNFα treatment either. Another study examining AD and ND-HPCs showed that there was little difference between these cohorts when Amyloid processing products were examined. The main differences occurred in inflammatory molecules such as VEGF and s100B (Maarouf et al., 2011). Morimoto et al., have shown that the post mortem CNS inflammatory profile of Low Pathology Controls (LPC) and High Pathology Controls (HPC) is the same. When they compared HPCs with AD there was a significant elevation in inflammation in the AD brain in comparison to the HPC brains. The AD cohort showed elevated cerebellum TNFα and elevated temporal lobe IL-1β, IL-10, IL-33, IL-13, IL-18 and increased TACE activity in comparison to the HPC cohort (Morimoto et al., 2011). This indicates that a pro-inflammatory CNS profile is required alongside CNS amyloid pathology to drive dementia. It has also been shown in the literature that dementia is less associated with typical AD markers following an inflammatory delirious event (Davis et al., 2012). In the current study elevation of systemic TNFα did not alter amyloid beta or APP deposition in aged wild types, or induce a reference memory and learning deficit in WT animals. However this study is neither a severe inflammatory challenge in comparison to much of the literature nor an entirely chronic inflammatory paradigm. To truly establish the etiology of sporadic late onset dementia a study of life long elevated systemic inflammation appears necessary, many groups are working on establishing this paradigm using dietary influences such as high fat diet or atherogenic diets to establish a pro-inflammatory baseline.

5.4.4– Alterations of cell populations in APP/PS1s post-repeated systemic TNFα

The cellular populations of the CNS following repeated systemic TNFα administration in aged WT and APP/PS1 animals were examined, no significant alteration in the morphology or numbers of microglial cells was found following treatment. The APP/PS1 strain had a significantly greater number of microglial

cells in the hippocampus and dorsal thalamus in comparison to WT animals. The morphology of the microglia in the APP/PS1 model also appeared significantly more activated than the morphology of WT microglia; cell bodies are condensed and processes are retracted and many appear to be aggregated around plaques. When we examined CD3 positive T cells in this study we found a significant elevation in the APP/PS1 model in comparison to WT. The number of T cells present in the thalamus was further elevated in the APP/PS1 animals post-TNFα, this contrasts with no alteration in T cell numbers in response to repeated TNFα in the WT cohort. While there is a larger number of T cells in APP/PS1 post-TNFα the number is rather small and possibly inconsequential. Aβ-stimulated T cells can effectively enter the CNS and clear Aβ plaques in APP/PS1 mice and also upregulate microglial markers (Fisher et al., 2010). However whether this clearance is beneficial to cognitive and functional outcomes remains unexamined in the literature.

Studies have shown that the choroid plexus is a reservoir for T cells, and T cells can cross the Blood-CSF-Barrier from the choroid plexus into the parenchyma only when the choroid plexus has been primed by inflammation (Engelhardt and Ransohoff, 2005). We have shown representative images of T cells in the choroid plexus of the TNFα treated cohort. This appeared to be the route of entry into the parenchyma for many of the new thalamic T cells. Jimenez et al show that as APP/PS1 mice age the microglial phenotype changes from a primarily anti-inflammatory phagocytic type at 6 months to a pro-inflammatory cytotoxic phenotype at 18 months. This timing correlates with increases in oligomeric Aβ expression in the APP/PS1 CNS, which was shown to induce increased microglial TNFα expression, and a significant elevation in T cell infiltration into the CNS (Jimenez et al., 2008). Infection with *Bordetella pertussis* in aged APP/PS1 mice was shown to significantly elevate microglial TNFα, IL-1β and IL-6 mRNA. This infection paradigm also further increased age-associated increases in the T cell chemoattractant CCL3 and increased the numbers of T cells present in the CNS 2 months post-infection (McManus et al., 2014). Blocking systemic TNFα in a focal cerebral ischaemia model was shown to significantly decrease microglial activity, CNS TNFα protein and the splenic T cell response alongside improved cognitive consequences of ischaemia (Clausen et al., 2014b). This could indicate a role for central TNFα in the infiltration of T cells in the APP/PS1 model.

Recently, systemic TNFα acting on hypothalamic TNFR1 has been shown to have an important role in mediating the initiation of adaptive immunity and mobilising adipose and splenic T cell activation. Hypothalamic TNFα has been shown to increase adipose lipolysis via mRNA alterations and induce the release of adipose leptin. Leptin release and lipolysis together mediate increased circulating adipose tissue and splenic T cells (Kim et al., 2015). While there is no increase in T cells in the CNS following repeated systemic TNFα in WT it is likely that this is due to a less permeable BBB in comparison to the APP/PS1 (Takeda et al., 2013). Both the altered weight loss response observed in APP/PS1 animals and their increased CNS T cell response to systemic repeated TNFα may indicate altered hypothalamic actions of TNFα in this strain.

When we examined the neuronal populations of these cohorts, it appears on gross observation that there may be a decrease in neuronal numbers associated with the APP/PS1 strain. Studies have reported a 35% neuronal loss in the pyramidal layer of the hippocampus in 22 month old and 17 month old APP/PS1 mice respectively (Sadowski et al., 2004; Schmitz et al., 2004). However, the overarching opinion of the field is that APP overexpressing models show extremely limited neurodegeneration (Stein and Johnson, 2002; Wirths and Bayer, 2010). Increased gliosis and neurogenesis was observed in APP/PS1 animal at 9 months (Yu et al., 2009). However, the long term survival of new born neurons was significantly diminished by the existing APP/PS1 pathology (Verret et al., 2007). It is necessary to quantify the neuronal numbers in this study, this could be achieved by stereological matching of areas and examination of NeuN density in the cortex or thalamus or haematoxylin labelling in the CA1. There was no time remaining in this project to complete this task. Determining whether the decline in Ki67 positive proliferation is a decline in global proliferation or specifically in neurogenesis would also merit inverstigation in further studies.

5.4.5 - Conclusion

Differential responses were found in the APP/PS1 strain in comparison to the WT strain following repeated systemic TNFα administration. WT+TNFα showed a progressive weight loss on the repeated dose regime while APP/PS1+TNFα showed full recovery to baseline following each challenge. The APP/PS1 strain

also showed elevated numbers of infiltrating T cells in response to TNFα. Both of these results may indicate a differential hypothalamic response in the APP/PS1 strain to systemic inflammation. Behaviours associated with early AD are often ascribed to hypothalamic dysfunction (Touitou et al., 1986; Satlin et al., 1995).

Examination of APP/PS1-specific pathology found that both Aβ and APP deposition were altered by repeated systemic TNFα administration. There was decreased Aβ deposition in the hippocampus post-TNFα but increased APP deposition; this indicates a differential effect of the pro-inflammatory cytokine TNFα on these pathologies. Increased TNFα is shown here to decrease Aβ deposition, however, reducing Aβ deposition in AD cohorts has been found to be ineffective at ameliorating the disease process (Holmes et al., 2008). Ongoing studies indicate that inhibiting TNFα can ameliorate cognition (Holmes et al., 2014). Could this be an indicator that TNFα driven APP aggregation and deposition is detrimental to cognition and progression of disease?

The validity of APP overexpressing models is limited, as the mutations used to create this model do not exist together in humans and do not exist in the late onset sporadic AD that affects the majority of dementia patients. The examination of systemic inflammation as a driver of dementia in naïve models requires further work. The work of the Knuesel group showing APP aggregation following prenatal Poly I:C challenge presents an alternative hypothesis of purely immune driven disruption of neuronal function and APP aggregation. Further studies of primarily immune driven cognitive dysfunction are required.

Chapter 6

Discussion

6.1 - Discussion

It was known prior to the outset of this thesis that secondary inflammatory events could activate microglia primed by prior neurodegeneration and have negative consequences (Murray et al., 2012). The work laid out here has significantly expanded this knowledge showing that the astrocyte population of the diseased brain can also react in an exaggerated manner to inflammation and that TNFα and IL-1β can activate primed astrocytes to produce exaggerated chemokine synthesis and inflammatory cell infiltration. There was an exaggerated sickness behaviour response and working memory deficits in response to systemic TNFα in ME7, without an exaggerated CNS inflammatory response. An altered pathology was shown in response to repeated systemic TNFα in the APP/PS1 model. These results describe a range of CNS vulnerabilities arising from ongoing neurodegeneration or amyloidosis.

6.2 - Glial priming and its implications

One of the primary findings of this work is that the astrocytic population of the neurodegenerating brain exists in a primed state similarly to the previously established microglial priming. Microglial priming was first described in the ME7 prion model 10 years ago (Cunningham et al., 2005b); it was defined as an exaggerated production of IL-1β and iNOS in response to a secondary inflammatory stimulus. Since the original description it has been found to be a generic biological phenomenon across multiple models of neuronal degeneration, aging (Godbout et al., 2005), PD (Pott Godoy et al., 2008), AD (Sly et al., 2001) and Wallerian Degeneration (Palin et al., 2008). Sly et al., showed an increased CNS IL-1β mRNA and protein response to LPS (25μg/mouse i.p.) in aged Tg2576 in comparison to WT controls and in comparison to young Tg2576. The work described in this thesis expands upon this by showing, through morphology, that elevated central IL-1β protein seen in response to systemic LPS in an APP overexpression model of AD is microglial in origin. Many are now interested in the role of the NLRP3 inflammasome and while it seems clear that the IL-1β processing enzyme Caspase 1 is activated in APP/PS1 animals it is clear that the

expression of pro-IL-1β is low in these animals (Heneka et al., 2013). The secondary challenge described here; central IL-1β and central or peripheral LPS produces very robust new IL-1β which can be readily processed by the disease induced inflammasome. This has significant implications for inflammatory events in AD.

The response of astrocytic cells to a secondary inflammatory stimulus in ME7 and APP/PS1 models was examined. The phenomenon of primed astrocytic cells appeared in ME7 and APP/PS1 with astrocytes in both models showing exaggerated astrocytic CCL2 and CXCL1 responses to central IL-1β and TNFα in ME7, and central IL-1β, central and peripheral LPS in APP/PS1. There is a less robust response to peripheral LPS in comparison to central LPS in APP/PS1 this is likely due to the route of administration, while LPS can act directly on the brain this route likely diminishes the downstream impact on parenchymal cells in comparison to direct central administration. When downstream cell infiltration was examined in the ME7 model the exaggerated early chemokine response resulted in an exaggerated cellular infiltration at later time points. Though we did not explicitly examine the later timepoints in the APP/PS1 model, I would predict that similar exaggerated cellular infiltration would also occur in the APP/PS1 following these challenges. The description of astrocyte priming in two very different models is especially important. ME7 prion disease shows a widespread amyloidosis with PrP^{sc} throughout the CNS and severe neuronal and synaptic loss in the hippocampus and brainstem. The APP/PS1 transgenic model shows florid aggregation of APP and Aβ positive plaques throughout the cortex, hippocampus and dorsal thalamus with limited neuronal loss in the hippocampus and thalamus (Stein and Johnson, 2002; Wirths and Bayer, 2010). Multiple models of neurodegenerative pathology show increased propensity of the astrocyte population to produce exaggerated levels of chemokines in response to multiple secondary stimuli, which suggests that the existence of primed astrocytes is, similarly to the existence of primed microglia, a biologically generic phenomenon.

It is well established that cell infiltration is a standard response to CNS injury, however if CNS injury was superimposed on a degenerative background inducing activation of primed microglial and astrocyte responses this would induce an exaggerated cellular infiltration in response to the injury. Exaggerated neutrophil, t-cell and macrophage infiltrations were observed following central TNFα and IL-

1β administration in the ME7 neurodegenerative model. APP/PS1 reacted acutely in a similar manner with an exaggerated parenchymal astrocyte CCL2 and CXCL1 production following central IL-1β and LPS. This would suggest if APP/PS1 animals were examined at the appropriate time-points following these insults, there would be an exaggerated cellular infiltration similar to ME7. It has previously been shown that exaggerated cell infiltration post-central injury is detrimental to functional recovery. Exacerbating the LPS induced PMN recruitment with co-application of IGF-1 resulted in intracerebral haemorrhage and a high mortality rate (Pang et al., 2010). Neutrophils that have transmigrated over the BB into the CNS have been shown to have a neurotoxic profile (Allen et al., 2012). Increasing the infiltration of neurotoxic neutrophils post ischaemia via administration of systemic IL-1β has been shown to exacerbate the infarct size and consequent neurological deficit (McColl et al., 2007). Infiltrating macrophages are responsible for seizures that occur post-Theiler's murine encephalomyelitis infection (Cusick et al., 2013). Depletion of peripheral $CCR2^{+}$ macrophages in a controlled cortical impact model of TBI showed a reduction in pro-inflammatory mediators and also ameliorated dysfunction on a hippocampal dependent cognitive task (Morganti et al., 2015). These results all indicate that exacerbation of the cellular infiltration post-CNS injury is likely detrimental to future cognition and function.

Neurodegeneration and aging, both of which prime microglia and astrocytes in experimental animal models have been found to exacerbate central injury. Aging has been found to exacerbate the effects of TBI and stroke; a prolonged morphological alteration of microglia and astrocytes has been observed in aged animals compared to adult animals following TBI (Sandhir et al., 2008). Prolonged oedema, increased permeability of the BBB and increased neuronal death was found in aged compared to adult animals post-TBI (Onyszchuk et al., 2008). Age was also found to be a significant determinant of clinical outcomes when examined with regard to stroke (Arsava et al., 2014). Age was shown to exacerbate BBB permeability, infarct volume, oedema formation, mortality and functional outcomes following MCAO in mice (Kelly et al., 2009). Prior neurodegenerative disease has also been shown to exacerbate the outcome of stroke and TBI. Animals with Cerebral Amyloid Angiopathy were found to display

larger infarct volumes following focal cerebral ischaemia (Milner et al., 2014). TBI in APP/PS1 mice leads to a prolonged inflammatory response and persistent cognitive deficits in comparison to WT(Webster et al., 2015). The exacerbation of acute injury by pre-existing chronic disease is likely due to the primed state of microglia and astrocytes facilitating the increased production of cytokines and chemokines, the molecules determining the intensity of the resulting inflammatory response. Increased infarct and oedema occur in many of the above studies due to aging or prior neurodegeneration, this would be indicate that the primed astrocytes due to aging/neurodegeneration may be influencing the functional outcomes through exacerbated infiltration of peripheral immune cells. This could provide a novel treatment target for stroke and TBI superimposed upon aged or degenerative pathologies.

We have been discussing how priming arising during chronic disease makes response to new acute stimuli more severe. However similar acute inflammatory stimuli occurring in advance of or following acute brains insults such as stroke or TBI may provide some benefits. Chen et al showed that LPS (1mg/kg for 4 days) prior to a cryogenic injury to the parietal cortex was neuro-protective showing a smaller lesion volume and decreased apoptosis, this was mediated by TLR4 on microglial cells (Chen et al., 2012b). A more recent study showed that both TLR2 (Pam3CSK4 – 5mg/kg) and TLR4 (LPS - 1mg/kg) stimulation were neuro-protective showing less neuronal death, via a MyD88 dependent pathway, prior to Kainic Acid administration to the striatum (Larochelle et al., 2015). However TLR3 stimulation with Poly I:C was not protective in this study. Systemic LPS was found to protective when administered prior to or following a central IL-1β (1μg/μl) challenge indicating that the timing of protection is flexible (Davis et al., 2005). Systemic IL-1β was not protective against central IL-1β injury; this would be consistent with the TLR dependency described in the above studies. Administration of a virus (AdLuc $5x10^9$ pfu) prior to a central IL-1β (1μg/μl) challenge showed an exacerbation of injury with an increased infiltration of neutrophils and macrophages to the CNS (Couch et al., 2014). LPS (1μg/μl i.c.) prior to i.c. Kainic acid (0.25nM) showed protection dependent on the anti-inflammatory mediator TGF-β (Boche et al., 2003). Pre and post-conditioning may be mediated by increasing the propensity of microglial cells to react in a more anti-

inflammatory mechanism with a second acute stimulus. However chronic disease primes the microglial population to react in a more pro-inflammatory manner, via increased IL-1β, on acute stimulation.

It has been suggested that the activation of microglial phagocytosis of Aβ would be beneficial to the AD brain. The Morgan group have shown that intracerebral LPS can increase microglial phagocytosis and clearance of diffuse amyloid in the tg2576 APP overexpressing strain (Herber et al., 2004; Herber et al., 2007); however when a similar LPS challenge is administered to rTG4510 Tau overexpressing mice it significantly exacerbated Tau pathology (Lee et al., 2010). The O'Banion group showed that activation of an IL-1β transgene for four weeks in an APP/PS1 mouse activates glial cells and significantly reduces Aβ plaque load (Shaftel et al., 2007). When the effects of this transgene were examined in normal animals it was found to impair contextual and spatial memory as well as increasing neuronal death in the hippocampus (Moore et al., 2009; Hein et al., 2010). Central overexpression of TNFα, IL-6 and IFN-γ via a recombinant Adeno-Associated Virus (rAAV) has been shown to induce a massive gliosis, activation of microglia and astrocytes in an APP tgCRND8 model and a subsequent increase in phagocytosis of Aβ (Chakrabarty et al., 2010a; Chakrabarty et al., 2010b; Chakrabarty et al., 2011). However I would question whether the removal of Aβ sufficiently ameliorates cognition and function enough to justify the massive upregulation of glial activity which may not prove beneficial? It has been established in clinical cohorts that removal of Aβ in AD patients did not ameliorate cognition or function (Salloway et al., 2014). The same group have shown that the rAAV induced central overexpression of IFNγ can result in demyelination of the corpus callosum and cerebellum, calcification of the basal ganglia, neuronal loss in the nigral striatum and severe motor deficits. These may be the downstream effects of massive upregulation of microglial and astrocyte activity that are overlooked when we focus on Aβ clearance. Indicating that activation of microglia merely to phagocytose Aβ may not prove an effective strategy in disease.

6.3 – Systemic inflammation exacerbating central deficits

So far this discussion has focused mainly on the activation of primed microglia and astrocytes by elevation of central inflammation. However the activation of primed glia by systemic inflammation was also shown. It was previously demonstrated by the Cunningham lab that systemic LPS could activate primed microglia in the ME7 brain to produce exaggerated IL-1β levels (Murray et al., 2011). Central IL-1β and LPS showed robust activation of primed microglia and astrocytes in APP/PS1 however systemic LPS showed a similar but more limited activation of primed microglia and astrocytes in the APP/PS1 model. This compounds the validity of the statement that activation of primed cells in the CNS of degenerating models is a generic phenomenon and of great importance. The activation of primed glia by systemic inflammatory stimuli was further examined, using systemic TNFα. Central transcripts following a systemic TNFα challenge were not elevated with respect to NBH+TNFα, indicating no activation of primed microglial or astrocyte responses. The differential activation of primed central glia may be due to the differential pathways used by LPS and TNFα to communicate with the CNS. It was previously shown that the microglial IL-1β induced by systemic LPS is independent of systemic cytokine activation (Murray et al., 2011). However when we examined sickness behaviour following systemic TNFα in the ME7 model we found an exacerbated sickness behaviour response across, core body temperature, body weight, movement and rears in the open field. Cognition in ME7 was also transiently affected by systemic TNFα challenge, inducing a decline in working memory function in ME7 not seen in NBH controls. The fact that there was no detectable activation of primed glial cells by systemic TNFα would imply that while there is an ongoing inflammatory vulnerability in the ME7 brains, there may also be a concurrent neuronal vulnerability. To expand upon this: we can see that degenerating brains react in an exaggerated pro-inflammatory manner to endogenous and exogenous central inflammatory stimuli and exogenous systemic stimuli. However while normal and ME7 animals show robust, relatively similar inflammatory responses to systemic TNFα, ME7 animals did show a significantly heightened neuronal response. Therefore perhaps while there was no exaggerated inflammatory central response to systemic TNFα the neurons remaining in the ME7 brain displayed a heightened response to equivalent inflammation. Nonetheless, the existing inflammatory state may contribute to vulnerability such that acutely produced mediators, such as TNFα, despite being produced at similar

levels may have quite different effects in the susceptible animal. With respect to working memory deficits in the ME7 model, COX1 induced prostaglandins have been shown to mediate LPS induced cognitive deficits independently of central inflammation (Griffin et al., 2013). While TNFα did not increase central inflammation perhaps it altered COX1 activity and thus neuronal activity. The caveat to this hypothesis is that many inflammatory mediators are elevated by prion disease and there may be a synergy between the normal inflammation induced by systemic TNFα and the pre-existing disease induced pro-inflammatory mediators. For example central IL-1β has been implicated in cognitive alterations induced by systemic TNFα (Terrando et al., 2010), there was a minimal increase in IL-1β mRNA post-systemic TNFα in ME7, but it is well known that IL-1β protein is controlled by post-translational modifications via the inflammasome (Heneka et al., 2013). Elevation in inflammasome elements in prion disease (Hafner-Bratkovic et al., 2012) may result in larger IL-1β protein despite limited detectable increases in mRNA. It remains a limitation of this study that we did not examine protein at this timepoint post-systemic TNFα.

While systemic TNFα was sufficient to induce an exacerbated sickness behaviour response and working memory deficits in the ME7 model it did not significantly alter the severe pathology present in the ME7 pathology at 18 week the time-point examined. It would be of significant interest to examine whether systemic TNFα at an earlier time-point in disease would alter ME7 prion pathology. A single systemic LPS challenge is sufficient to exacerbate ME7 pathology at the 18 week time-point used but perhaps a single TNFα challenge just will not be sufficient, as systemic LPS can induce alterations in CNS activity independently of systemic cytokines (Murray et al., 2011). In fact CNS effects of LPS have been shown to be dependent on central TLR4 expression and independent of systemic TLR4 expression (Stein and Johnson, 2002; Chen et al., 2012b). Singh & Jiang showed that while LPS altered hypothalamic function it does not enter the CNS (Singh and Jiang, 2004). LPS binds endothelial cells via TLR4 and can increase BBB permeability and CNS TNFα and IL-1βvia endothelial cell action (Singh et al., 2007). As LPS directly communicates with the CNS, its pathological consequences may be due to pathways that are not related to those activated by systemic TNFα administration. Blocking systemic TNFα prior to systemic LPS administration did

not alter the new central pathology induced by systemic LPS, indicating that the effect is independent of systemic TNFα. Given that LPS induced apoptosis independent of systemic TNFα it is intriguing as to how it may affect its changes in the CNS. LPS can induce central cytokines in an exaggerated manner in the ME7 model. Examination of mRNA transcripts post-systemic LPS for central IL-1β and TNFα were robustly exacerbated, as was the level of apoptosis (Cunningham et al., 2005b). The same transcripts post-systemic TNFα revealed no robust alteration. This could indicate that central cytokine induction is responsible for systemic LPS induced neuronal death. The Pitossi group have shown that central IL-1β can induce neuronal death (without producing TNFα) and central TNFα can also induce neuronal death (without producing IL-1β) (Ferrari et al., 2006; De Lella Ezcurra et al., 2010). Repeated systemic LPS has been shown to induce neuronal death in the otherwise naïve brain via a complement cascade-induced phagocytosis (Bodea et al., 2014). A single acute dose of systemic TNFα could not significantly alter ME7 pathology and systemic TNFα did not play a role in LPS induced pathology, however the chronic elevation of systemic TNFα may tell us a different story.

6.4 - Chronic co-morbidities and dementia

On examination of a repeated systemic TNFα regimen in APP/PS1 a relatively mild but significant exacerbation of pathology was found. This indicates that despite acute systemic TNFα not altering ME7 pathology, a more chronic administration of TNFα can exacerbate a mild neuropathology. Holmes et al., have described an association between systemic circulating levels of TNFα and progression of cognitive decline in AD. High baseline TNFα in an AD cohort led to a 4 fold increase in the rate of cognitive decline over a 6 month period, where low baseline TNFα led to no cognitive decline (Holmes et al., 2009a). TNFα has been shown to be inversely correlated with total brain volume in a normal aged cohort (Jefferson et al., 2007) and levels were found to be inversely correlated with both total brain volume and hippocampal volume in an AD cohort (Leung et al., 2013). Systemic TNFα has been shown to increase with age in a study of centenarians, this study also showed that high systemic TNFα is associated with moderate to severe

dementia (Bruunsgaard et al., 1999). In AD TNFα elevation in both CSF and serum of patients was found to correlate with disease severity and progression (Paganelli et al., 2002).

Repeated systemic TNFα also significantly altered the profile of pathology in the hippocampus and thalamus of APP/PS1 animals. Following repeated systemic TNFα sequelae there is a move from primarily Aβ mediated pathology to an increase in APP aggregate pathology. Heneka et al., showed that a key mutation in human APP compared to mouse APP allows nitrosylation of Aβ which is a key step in the seeding of an Aβ plaque (Kummer et al., 2011). However systemic poly I:C challenge in a non-APP overexpressing mouse was shown to induce aggregation and deposition of APP. Systemic Poly I:C, prior to development of plaque pathology at 4 months, in the 3xTg-AD model showed an altered plaque composition at 15 months, with the core of plaques abnormally being composed primarily of non fibrillar APP deposits which were then surrounded by Aβ (Krstic et al., 2012). These data appear to indicate that a systemic inflammatory event can alter APP processing and subsequent aggregation and deposition. The increased APP labelling found in this study is consistent with the work described by Krstic et al., Inflammatory delirious episodes have previously been described as a significant risk factor for dementia, exacerbating pre-existing dementia and decreasing the link between dementia and typical pathological markers of AD. Following a delirious episode a post-mortem dementia brain was less likely to have the neuritic amyloid plaques or Braak staging associated with dementia without delirium. If repeated systemic TNFα is moving the APP/PS1 pathology in a similar direction this could intimate that it would exacerbate dementia similarly to a delirious episode. This is in agreement with the Holmes data which showed that high baseline TNFα in an AD cohort resulted in a fourfold faster cognitive decline compared to those with low baseline TNFα, a systemic inflammatory event that elevated systemic TNFα caused a twofold increased rate of cognitive decline, and when an individual suffered from high baseline TNFα and a systemic inflammatory event their rate of cognitive decline was tenfold that of an individual without either (Holmes et al., 2009a).

A semi-chronic model of repeated systemic TNFα administration in an APP/PS1 model showed significantly altered behaviours in the APP/PS1 model in comparison to WT post-TNFα. APP/PS1 animals showed an limited weight loss, an unaffected rears response and increased infiltrating T cells. These measures are thought to be controlled via the hypothalamus. Weight loss in AD has been shown to significantly correlate with stage of disease, and acceleration of weight loss was shown to be a significant predictor of mortality (White et al., 1998). It was recently shown that i.c.v. administered Aβ oligomers can control hypothalamic regulation of glucose tolerance and food intake via TNFα (Clarke et al., 2015). Tg2576 AD mice were found to have abnormally low leptin and an aberrant hypothalamic response to leptin. Tg2576 mice showed decreased adiposity due to an increased metabolic rate and normal feeding behaviours. Conversely, low levels of leptin should increase food intake and decrease energy expenditure (Ishii et al., 2014). TNFα action on the hypothalamus has been shown to increase leptin release (Kim et al., 2015), this should result in decreased food intake and consequently progressive weight loss (Cope et al., 1997). However, the data presented in this thesis indicate that the APP/PS1 model had an inappropriate modification of body weight in comparison to WT post-TNFα. This may indicate hypothalamic modifications due to disease, there may also be a delineation between TNFα induced anorexia (decreased food intake) and TNFα induced cachexia (loss of muscle mass) between the WT and APP/PS1 strains. Many hypothalamic behaviours are reportedly disrupted in early AD, especially circadian rhythms and core body temperature (Touitou et al., 1986; Satlin et al., 1995). Bone density has also been shown to be under hypothalamic control and to correlate with hypothalamic volume in early AD (Loskutova et al., 2010). Interestingly RANK/RANKL key regulators of bone density and sickness behaviours were found to be altered by ME7 and further altered at the mRNA level following a single acute dose of TNFα. The hypothalamus is important to examine when determining the effects of systemic co-morbidities on central disease.

This leads to the question, can a chronic mild upregulation of systemic inflammation lead to development of dementia? The prime risk factors for dementia are inflammatory in nature, aging, obesity, diabetes, atherosclerosis and hypertension (Hofman et al., 1997; Ott et al., 1999; Whitmer et al., 2005; Fitzpatrick et al., 2009). The impact of low-grade inflammation on brain aging was

shown using parabiosis, aged and young animals are sutured together at the flanks and ultimately share the same circulation (Villeda et al., 2011). This demonstrated that exposure to the bloodstream of the aged mouse brought about impaired neurogenesis, electrophysiological evidence of impaired memory function and cognitive impairments in the young animals. However, old mice exposed to the young bloodstream showed recovery is possible when exposed to the young bloodstream. A number of inflammatory factors present in the blood of aged rodents and people were examined, and the chemokine eotaxin (CCL11), was capable of producing the same deficits as exposure to blood from aged rodents (Villeda et al., 2011). These animals had no specific disease state and simply the elevated inflammatory state of aging was sufficient to bring about some cognitive decline. The superimposition of this age associated inflammation on an already vulnerable brain will likely have more significant consequences. Deletion of NLRP3 a regulator of IL-1β maturation, showed that animals developed without age related aspects of functional decline, and showed decreased CNS inflammation and extended life span (Youm et al., 2013). Interestingly, decreasing sterile inflammation associated with aging by this method also ameliorated age-associated hypothalamic alterations in glucose metabolism. 25 years later the observation that founded this field, the protective effect of NSAIDs in AD, is still a relevant point, reminding us that while inflammation exacerbates ongoing neurodegenerative processes it seems likely that inflammation preceding AD symptomology is an integral part of the disease process and we must now be aware of life long inflammatory status as an indicator of vulnerability to neurodegenerative disease.

6.5 - Conclusion

There is much yet to be done in the examination of neurodegeneration and the impact inflammation plays in its development. I believe that the data described in this thesis greatly expands the knowledge in the field. The concept of astrocyte priming may prove integral to the study of stroke and TBI in aged or neurodegenerating individuals. It remains to be determined whether sterile

inflammatory co-morbidities can drive dementia through activation of primed glia. However, the effect of repeated systemic TNFα on an amyloidosis model was significant and merits more attention.

Significant research time and investment has been expended upon theories surrounding the amyloid β hypothesis of AD. While this was incredibly important, clinical trials have shown us that removal of Aβ from AD patients using vaccinations was effective but did not modify the course of disease. The importance of the inflammatory components of dementia must be recognised and utilised if we want to advance therapies in this disease. A comprehensive meta-analysis of relative risk for dementia versus physical inactivity, smoking, midlife hypertension, midlife obesity, and diabetes showed that a third of global Alzheimer's cases were likely attributable to these preventable risk factors (Norton et al., 2014). Perhaps as well as investing in research for the non-modifiable cases of AD we should also focus more on mid-life cardiovascular health, diet and exercise as simple yet effective anti-inflammatory interventions?

References

(1994) The Canadian Study of Health and Aging: risk factors for Alzheimer's disease in Canada. Neurology 44:2073-2080.

Aaltonen KJ, Virkki LM, Malmivaara A, Konttinen YT, Nordstrom DC, Blom M (2012) Systematic review and meta-analysis of the efficacy and safety of existing TNF blocking agents in treatment of rheumatoid arthritis. PloS one 7:e30275.

Abraham J, Johnson RW (2009) Central inhibition of interleukin-1beta ameliorates sickness behavior in aged mice. Brain, behavior, and immunity 23:396-401.

Adalbert R, Nogradi A, Babetto E, Janeckova L, Walker SA, Kerschensteiner M, Misgeld T, Coleman MP (2009) Severely dystrophic axons at amyloid plaques remain continuous and connected to viable cell bodies. Brain 132:402-416.

Aiello AE, Haan M, Blythe L, Moore K, Gonzalez JM, Jagust W (2006) The influence of latent viral infection on rate of cognitive decline over 4 years. Journal of the American Geriatrics Society 54:1046-1054.

Aisen PS (2002) The potential of anti-inflammatory drugs for the treatment of Alzheimer's disease. Lancet neurology 1:279-284.

Allan SM, Tyrrell PJ, Rothwell NJ (2005) Interleukin-1 and neuronal injury. Nat Rev Immunol 5:629-640.

Allen C, Thornton P, Denes A, McColl BW, Pierozynski A, Monestier M, Pinteaux E, Rothwell NJ, Allan SM (2012) Neutrophil cerebrovascular transmigration triggers rapid neurotoxicity through release of proteases associated with decondensed DNA. Journal of immunology 189:381-392.

Altavilla D, Squadrito F, Ammendolia L, Squadrito G, Campo GM, Canale P, Ioculano M, Musolino C, Alonci A, Sardella A, Urna G, Saitta A, Caputi AP (1996) Monocytes and lymphocytes as active participants in the pathogenesis of experimental shock. Inflammation research : official journal of the European Histamine Research Society [et al] 45:398-404.

Alvarez A, Cacabelos R, Sanpedro C, Garcia-Fantini M, Aleixandre M (2007) Serum TNF-alpha levels are increased and correlate negatively with free IGF-I in Alzheimer disease. Neurobiology of aging 28:533-536.

An Y, Chen Q, Quan N (2011) Interleukin-1 exerts distinct actions on different cell types of the brain in vitro. Journal of inflammation research 2011:11-20.

Andersen K, Launer LJ, Ott A, Hoes AW, Breteler MM, Hofman A (1995) Do nonsteroidal anti-inflammatory drugs decrease the risk for Alzheimer's disease? The Rotterdam Study. Neurology 45:1441-1445.

Andersson PB, Perry VH, Gordon S (1992a) The acute inflammatory response to lipopolysaccharide in CNS parenchyma differs from that in other body tissues. Neuroscience 48:169-186.

Andersson PB, Perry VH, Gordon S (1992b) Intracerebral injection of proinflammatory cytokines or leukocyte chemotaxins induces minimal myelomonocytic cell recruitment to the parenchyma of the central nervous system. The Journal of experimental medicine 176:255-259.

Andre C, Dinel AL, Ferreira G, Laye S, Castanon N (2014) Diet-induced obesity progressively alters cognition, anxiety-like behavior and lipopolysaccharide-induced depressive-like behavior: Focus on brain indoleamine 2,3-dioxygenase activation. Brain, behavior, and immunity.

Anstey KJ, Lipnicki DM, Low LF (2008) Cholesterol as a risk factor for dementia and cognitive decline: a systematic review of prospective studies with

meta-analysis. The American journal of geriatric psychiatry : official journal of the American Association for Geriatric Psychiatry 16:343-354.
Arai A, Mizoguchi T, Harada S, Kobayashi Y, Nakamichi Y, Yasuda H, Penninger JM, Yamada K, Udagawa N, Takahashi N (2012) Fos plays an essential role in the upregulation of RANK expression in osteoclast precursors within the bone microenvironment. Journal of cell science 125:2910-2917.
Araujo DM, Lapchak PA (1994) Induction of immune system mediators in the hippocampal formation in Alzheimer's and Parkinson's diseases: selective effects on specific interleukins and interleukin receptors. Neuroscience 61:745-754.
Aronica E, Dickson DW, Kress Y, Morrison JH, Zukin RS (1998) Non-plaque dystrophic dendrites in Alzheimer hippocampus: a new pathological structure revealed by glutamate receptor immunocytochemistry. Neuroscience 82:979-991.
Arsava EM, Vural A, Akpinar E, Gocmen R, Akcalar S, Oguz KK, Topcuoglu MA (2014) The detrimental effect of aging on leptomeningeal collaterals in ischemic stroke. Journal of stroke and cerebrovascular diseases : the official journal of National Stroke Association 23:421-426.
Aslam M, Ahmad N, Srivastava R, Hemmer B (2012) TNF-alpha induced NFkappaB signaling and p65 (RelA) overexpression repress Cldn5 promoter in mouse brain endothelial cells. Cytokine 57:269-275.
Asuni AA, Perry VH, O'Connor V (2010) Change in tau phosphorylation associated with neurodegeneration in the ME7 model of prion disease. Biochemical Society transactions 38:545-551.
Badan I, Buchhold B, Hamm A, Gratz M, Walker LC, Platt D, Kessler C, Popa-Wagner A (2003) Accelerated glial reactivity to stroke in aged rats correlates with reduced functional recovery. Journal of cerebral blood flow and metabolism : official journal of the International Society of Cerebral Blood Flow and Metabolism 23:845-854.
Ballatore C, Brunden KR, Trojanowski JQ, Lee VM, Smith AB, 3rd, Huryn DM (2011) Modulation of protein-protein interactions as a therapeutic strategy for the treatment of neurodegenerative tauopathies. Current topics in medicinal chemistry 11:317-330.
Ballestas ME, Benveniste EN (1995) Interleukin 1-beta- and tumor necrosis factor-alpha-mediated regulation of ICAM-1 gene expression in astrocytes requires protein kinase C activity. Glia 14:267-278.
Banks WA, Ortiz L, Plotkin SR, Kastin AJ (1991) Human interleukin (IL) 1 alpha, murine IL-1 alpha and murine IL-1 beta are transported from blood to brain in the mouse by a shared saturable mechanism. The Journal of pharmacology and experimental therapeutics 259:988-996.
Bao Dang Q, Lapergue B, Tran-Dinh A, Diallo D, Moreno JA, Mazighi M, Romero IA, Weksler B, Michel JB, Amarenco P, Meilhac O (2013) High-density lipoproteins limit neutrophil-induced damage to the blood-brain barrier in vitro. Journal of cerebral blood flow and metabolism : official journal of the International Society of Cerebral Blood Flow and Metabolism 33:575-582.
Barone FC, Arvin B, White RF, Miller A, Webb CL, Willette RN, Lysko PG, Feuerstein GZ (1997) Tumor necrosis factor-alpha. A mediator of focal ischemic brain injury. Stroke; a journal of cerebral circulation 28:1233-1244.
Barrientos RM, Sprunger DB, Campeau S, Watkins LR, Rudy JW, Maier SF (2004) BDNF mRNA expression in rat hippocampus following contextual learning

is blocked by intrahippocampal IL-1beta administration. Journal of neuroimmunology 155:119-126.

Barrientos RM, Higgins EA, Biedenkapp JC, Sprunger DB, Wright-Hardesty KJ, Watkins LR, Rudy JW, Maier SF (2006) Peripheral infection and aging interact to impair hippocampal memory consolidation. Neurobiology of aging 27:723-732.

Barron AM, Rosario ER, Elteriefi R, Pike CJ (2013) Sex-specific effects of high fat diet on indices of metabolic syndrome in 3xTg-AD mice: implications for Alzheimer's disease. PloS one 8:e78554.

Baune BT, Wiede F, Braun A, Golledge J, Arolt V, Koerner H (2008) Cognitive dysfunction in mice deficient for TNF- and its receptors. American journal of medical genetics Part B, Neuropsychiatric genetics : the official publication of the International Society of Psychiatric Genetics 147B:1056-1064.

Beattie EC, Stellwagen D, Morishita W, Bresnahan JC, Ha BK, Von Zastrow M, Beattie MS, Malenka RC (2002) Control of synaptic strength by glial TNFalpha. Science 295:2282-2285.

Belarbi K, Jopson T, Tweedie D, Arellano C, Luo W, Greig NH, Rosi S (2012) TNF-alpha protein synthesis inhibitor restores neuronal function and reverses cognitive deficits induced by chronic neuroinflammation. Journal of neuroinflammation 9:23.

Biessels GJ, Staekenborg S, Brunner E, Brayne C, Scheltens P (2006) Risk of dementia in diabetes mellitus: a systematic review. Lancet neurology 5:64-74.

Binder LI, Guillozet-Bongaarts AL, Garcia-Sierra F, Berry RW (2005) Tau, tangles, and Alzheimer's disease. Biochimica et biophysica acta 1739:216-223.

Blond D, Campbell SJ, Butchart AG, Perry VH, Anthony DC (2002) Differential induction of interleukin-1beta and tumour necrosis factor-alpha may account for specific patterns of leukocyte recruitment in the brain. Brain research 958:89-99.

Bluthe RM, Laye S, Michaud B, Combe C, Dantzer R, Parnet P (2000) Role of interleukin-1beta and tumour necrosis factor-alpha in lipopolysaccharide-induced sickness behaviour: a study with interleukin-1 type I receptor-deficient mice. The European journal of neuroscience 12:4447-4456.

Bluthe RM, Pawlowski M, Suarez S, Parnet P, Pittman Q, Kelley KW, Dantzer R (1994) Synergy between tumor necrosis factor alpha and interleukin-1 in the induction of sickness behavior in mice. Psychoneuroendocrinology 19:197-207.

Boche D, Cunningham C, Gauldie J, Perry VH (2003) Transforming growth factor-beta 1-mediated neuroprotection against excitotoxic injury in vivo. Journal of cerebral blood flow and metabolism : official journal of the International Society of Cerebral Blood Flow and Metabolism 23:1174-1182.

Bodea LG, Wang Y, Linnartz-Gerlach B, Kopatz J, Sinkkonen L, Musgrove R, Kaoma T, Muller A, Vallar L, Di Monte DA, Balling R, Neumann H (2014) Neurodegeneration by activation of the microglial complement-phagosome pathway. The Journal of neuroscience : the official journal of the Society for Neuroscience 34:8546-8556.

Bolton SJ, Anthony DC, Perry VH (1998) Loss of the tight junction proteins occludin and zonula occludens-1 from cerebral vascular endothelium during neutrophil-induced blood-brain barrier breakdown in vivo. Neuroscience 86:1245-1257.

Bour A, Grootendorst J, Vogel E, Kelche C, Dodart JC, Bales K, Moreau PH, Sullivan PM, Mathis C (2008) Middle-aged human apoE4 targeted-replacement mice show retention deficits on a wide range of spatial memory tasks. Behavioural brain research 193:174-182.

Boyd TD, Bennett SP, Mori T, Governatori N, Runfeldt M, Norden M, Padmanabhan J, Neame P, Wefes I, Sanchez-Ramos J, Arendash GW, Potter H (2010) GM-CSF upregulated in rheumatoid arthritis reverses cognitive impairment and amyloidosis in Alzheimer mice. Journal of Alzheimer's disease : JAD 21:507-518.

Brambilla R, Morton PD, Ashbaugh JJ, Karmally S, Lambertsen KL, Bethea JR (2014) Astrocytes play a key role in EAE pathophysiology by orchestrating in the CNS the inflammatory response of resident and peripheral immune cells and by suppressing remyelination. Glia 62:452-467.

Brambilla R, Hurtado A, Persaud T, Esham K, Pearse DD, Oudega M, Bethea JR (2009) Transgenic inhibition of astroglial NF-kappa B leads to increased axonal sparing and sprouting following spinal cord injury. Journal of neurochemistry 110:765-778.

Brambilla R, Bracchi-Ricard V, Hu WH, Frydel B, Bramwell A, Karmally S, Green EJ, Bethea JR (2005) Inhibition of astroglial nuclear factor kappaB reduces inflammation and improves functional recovery after spinal cord injury. The Journal of experimental medicine 202:145-156.

Breitner JC, Gau BA, Welsh KA, Plassman BL, McDonald WM, Helms MJ, Anthony JC (1994) Inverse association of anti-inflammatory treatments and Alzheimer's disease: initial results of a co-twin control study. Neurology 44:227-232.

Bromander S, Anckarsater R, Kristiansson M, Blennow K, Zetterberg H, Anckarsater H, Wass CE (2012) Changes in serum and cerebrospinal fluid cytokines in response to non-neurological surgery: an observational study. Journal of neuroinflammation 9:242.

Bronner MB, Knoester H, Sol JJ, Bos AP, Heymans HS, Grootenhuis MA (2009) An explorative study on quality of life and psychological and cognitive function in pediatric survivors of septic shock. Pediatric critical care medicine : a journal of the Society of Critical Care Medicine and the World Federation of Pediatric Intensive and Critical Care Societies 10:636-642.

Bruhl H, Cihak J, Plachy J, Kunz-Schughart L, Niedermeier M, Denzel A, Rodriguez Gomez M, Talke Y, Luckow B, Stangassinger M, Mack M (2007) Targeting of Gr-1+,CCR2+ monocytes in collagen-induced arthritis. Arthritis and rheumatism 56:2975-2985.

Bruunsgaard H, Skinhoj P, Pedersen AN, Schroll M, Pedersen BK (2000) Ageing, tumour necrosis factor-alpha (TNF-alpha) and atherosclerosis. Clinical and experimental immunology 121:255-260.

Bruunsgaard H, Andersen-Ranberg K, Jeune B, Pedersen AN, Skinhoj P, Pedersen BK (1999) A high plasma concentration of TNF-alpha is associated with dementia in centenarians. The journals of gerontology Series A, Biological sciences and medical sciences 54:M357-364.

Buchhave P, Zetterberg H, Blennow K, Minthon L, Janciauskiene S, Hansson O (2010) Soluble TNF receptors are associated with Abeta metabolism and conversion to dementia in subjects with mild cognitive impairment. Neurobiology of aging 31:1877-1884.

C. Holmes CC, E. Zotova, J. Woolford, C. Dean, S. Kerr, D. Culliford, V.H. Perry. (2009) Systemic inflammation and disease progression in Alzheimer disease. Neurology 73:768-774.

Cacabelos R, Alvarez XA, Fernandez-Novoa L, Franco A, Mangues R, Pellicer A, Nishimura T (1994) Brain interleukin-1 beta in Alzheimer's disease and vascular dementia. Methods and findings in experimental and clinical pharmacology 16:141-151.

Cameron B, Landreth GE (2010) Inflammation, microglia, and Alzheimer's disease. Neurobiology of disease 37:503-509.

Campbell SJ, Carare-Nnadi RO, Losey PH, Anthony DC (2007) Loss of the atypical inflammatory response in juvenile and aged rats. Neuropathology and applied neurobiology 33:108-120.

Campbell SJ, Wilcockson DC, Butchart AG, Perry VH, Anthony DC (2002) Altered chemokine expression in the spinal cord and brain contributes to differential interleukin-1beta-induced neutrophil recruitment. Journal of neurochemistry 83:432-441.

Campbell SJ, Perry VH, Pitossi FJ, Butchart AG, Chertoff M, Waters S, Dempster R, Anthony DC (2005) Central nervous system injury triggers hepatic CC and CXC chemokine expression that is associated with leukocyte mobilization and recruitment to both the central nervous system and the liver. The American journal of pathology 166:1487-1497.

Campbell SJ, Meier U, Mardiguian S, Jiang Y, Littleton ET, Bristow A, Relton J, Connor TJ, Anthony DC (2010) Sickness behaviour is induced by a peripheral CXC-chemokine also expressed in multiple sclerosis and EAE. Brain, behavior, and immunity 24:738-746.

Cao C, Matsumura K, Yamagata K, Watanabe Y (1998) Cyclooxygenase-2 is induced in brain blood vessels during fever evoked by peripheral or central administration of tumor necrosis factor. Brain research Molecular brain research 56:45-56.

Castanos-Velez E, Maerlan S, Osorio LM, Aberg F, Biberfeld P, Orn A, Rottenberg ME (1998) Trypanosoma cruzi infection in tumor necrosis factor receptor p55-deficient mice. Infection and immunity 66:2960-2968.

Cechetto DF, Hachinski V, Whitehead SN (2008) Vascular risk factors and Alzheimer's disease. Expert review of neurotherapeutics 8:743-750.

Chakrabarty P, Herring A, Ceballos-Diaz C, Das P, Golde TE (2011) Hippocampal expression of murine TNFalpha results in attenuation of amyloid deposition in vivo. Molecular neurodegeneration 6:16.

Chakrabarty P, Ceballos-Diaz C, Beccard A, Janus C, Dickson D, Golde TE, Das P (2010a) IFN-gamma promotes complement expression and attenuates amyloid plaque deposition in amyloid beta precursor protein transgenic mice. J Immunol 184:5333-5343.

Chakrabarty P, Jansen-West K, Beccard A, Ceballos-Diaz C, Levites Y, Verbeeck C, Zubair AC, Dickson D, Golde TE, Das P (2010b) Massive gliosis induced by interleukin-6 suppresses Abeta deposition in vivo: evidence against inflammation as a driving force for amyloid deposition. FASEB journal : official publication of the Federation of American Societies for Experimental Biology 24:548-559.

Chakravarty S, Herkenham M (2005) Toll-like receptor 4 on nonhematopoietic cells sustains CNS inflammation during endotoxemia, independent of systemic cytokines. The Journal of neuroscience : the official journal of the Society for Neuroscience 25:1788-1796.

Chapman TR, Barrientos RM, Ahrendsen JT, Maier SF, Patterson SL (2010) Synaptic correlates of increased cognitive vulnerability with aging: peripheral immune challenge and aging interact to disrupt theta-burst late-phase long-term potentiation in hippocampal area CA1. The Journal of neuroscience : the official journal of the Society for Neuroscience 30:7598-7603.

Chavant F, Deguil J, Pain S, Ingrand I, Milin S, Fauconneau B, Perault-Pochat MC, Lafay-Chebassier C (2010) Imipramine, in part through tumor necrosis factor alpha inhibition, prevents cognitive decline and beta-amyloid accumulation in a mouse model of Alzheimer's disease. The Journal of pharmacology and experimental therapeutics 332:505-514.

Chen CH, Zhou W, Liu S, Deng Y, Cai F, Tone M, Tone Y, Tong Y, Song W (2012a) Increased NF-kappaB signalling up-regulates BACE1 expression and its therapeutic potential in Alzheimer's disease. Int J Neuropsychopharmacol 15:77-90.

Chen CJ, Kono H, Golenbock D, Reed G, Akira S, Rock KL (2007a) Identification of a key pathway required for the sterile inflammatory response triggered by dying cells. Nature medicine 13:851-856.

Chen H, Chopp M, Zhang RL, Bodzin G, Chen Q, Rusche JR, Todd RF, 3rd (1994) Anti-CD11b monoclonal antibody reduces ischemic cell damage after transient focal cerebral ischemia in rat. Annals of neurology 35:458-463.

Chen J, Buchanan JB, Sparkman NL, Godbout JP, Freund GG, Johnson RW (2008) Neuroinflammation and disruption in working memory in aged mice after acute stimulation of the peripheral innate immune system. Brain, behavior, and immunity 22:301-311.

Chen X, Ding WX, Ni HM, Gao W, Shi YH, Gambotto AA, Fan J, Beg AA, Yin XM (2007b) Bid-independent mitochondrial activation in tumor necrosis factor alpha-induced apoptosis and liver injury. Molecular and cellular biology 27:541-553.

Chen YM, Chiang WC, Lin SL, Wu KD, Tsai TJ, Hsieh BS (2004) Dual regulation of tumor necrosis factor-alpha-induced CCL2/monocyte chemoattractant protein-1 expression in vascular smooth muscle cells by nuclear factor-kappaB and activator protein-1: modulation by type III phosphodiesterase inhibition. The Journal of pharmacology and experimental therapeutics 309:978-986.

Chen Z, Jalabi W, Shpargel KB, Farabaugh KT, Dutta R, Yin X, Kidd GJ, Bergmann CC, Stohlman SA, Trapp BD (2012b) Lipopolysaccharide-induced microglial activation and neuroprotection against experimental brain injury is independent of hematogenous TLR4. The Journal of neuroscience : the official journal of the Society for Neuroscience 32:11706-11715.

Cheng R, Qiu J, Zhou XY, Chen XH, Zhu C, Qin DN, Wang JW, Ni YH, Ji CB, Guo XR (2011) Knockdown of STEAP4 inhibits insulin-stimulated glucose transport and GLUT4 translocation via attenuated phosphorylation of Akt, independent of the effects of EEA1. Molecular medicine reports 4:519-523.

Chio CC, Chang CH, Wang CC, Cheong CU, Chao CM, Cheng BC, Yang CZ, Chang CP (2013) Etanercept attenuates traumatic brain injury in rats by reducing early microglial expression of tumor necrosis factor-alpha. BMC neuroscience 14:33.

Choi K, Ni L, Jonakait GM (2011) Fas ligation and tumor necrosis factor alpha activation of murine astrocytes promote heat shock factor-1 activation and

heat shock protein expression leading to chemokine induction and cell survival. Journal of neurochemistry 116:438-448.
Chopp M, Zhang RL, Chen H, Li Y, Jiang N, Rusche JR (1994) Postischemic administration of an anti-Mac-1 antibody reduces ischemic cell damage after transient middle cerebral artery occlusion in rats. Stroke; a journal of cerebral circulation 25:869-875; discussion 875-866.
Chou RC, Kane MA, Ghimire S, Gautam S (2010) TUMOR NECROSIS FACTOR INHIBITION REDUCES THE INCIDENCE OF ALZHEIMER'S DISEASE IN RHEUMATOID ARTHRITIS PATIENTS. In: American College of Rheumatology Annual Scientific Meeting - Proceedings: Dartmouth.
Chung IY, Benveniste EN (1990) Tumor necrosis factor-alpha production by astrocytes. Induction by lipopolysaccharide, IFN-gamma, and IL-1 beta. J Immunol 144:2999-3007.
Clarke JR et al. (2015) Alzheimer-associated Abeta oligomers impact the central nervous system to induce peripheral metabolic deregulation. EMBO molecular medicine 7:190-210.
Clausen B, Degn M, Martin N, Couch Y, Karimi L, Ormhoj M, Mortensen ML, Gredal H, Gardiner C, Sargent, II, Szymkowski DE, Petit GH, Deierborg T, Finsen B, Anthony D, Lambertsen K (2014a) Systemically administered anti-TNF therapy ameliorates functional outcomes after focal cerebral ischemia. Journal of neuroinflammation 11:203.
Clausen BH, Degn M, Martin NA, Couch Y, Karimi L, Ormhoj M, Mortensen ML, Gredal HB, Gardiner C, Sargent, II, Szymkowski DE, Petit GH, Deierborg T, Finsen B, Anthony DC, Lambertsen KL (2014b) Systemically administered anti-TNF therapy ameliorates functional outcomes after focal cerebral ischemia. Journal of neuroinflammation 11:203.
Collins JS, Perry RT, Watson B, Jr., Harrell LE, Acton RT, Blacker D, Albert MS, Tanzi RE, Bassett SS, McInnis MG, Campbell RD, Go RC (2000) Association of a haplotype for tumor necrosis factor in siblings with late-onset Alzheimer disease: the NIMH Alzheimer Disease Genetics Initiative. American journal of medical genetics 96:823-830.
Collins LM, Toulouse A, Connor TJ, Nolan YM (2012) Contributions of central and systemic inflammation to the pathophysiology of Parkinson's disease. Neuropharmacology 62:2154-2168.
Colton CA, Mott RT, Sharpe H, Xu Q, Van Nostrand WE, Vitek MP (2006) Expression profiles for macrophage alternative activation genes in AD and in mouse models of AD. Journal of neuroinflammation 3:27.
Combrinck MI, Perry VH, Cunningham C (2002) Peripheral infection evokes exaggerated sickness behaviour in pre-clinical murine prion disease. Neuroscience 112:7-11.
Cope AP, Liblau RS, Yang XD, Congia M, Laudanna C, Schreiber RD, Probert L, Kollias G, McDevitt HO (1997) Chronic tumor necrosis factor alters T cell responses by attenuating T cell receptor signaling. The Journal of experimental medicine 185:1573-1584.
Couch Y, Davis AE, Sa-Pereira I, Campbell SJ, Anthony DC (2014) Viral pre-challenge increases central nervous system inflammation after intracranial interleukin-1beta injection. Journal of neuroinflammation 11:178.
Crompton M (2000) Bax, Bid and the permeabilization of the mitochondrial outer membrane in apoptosis. Current opinion in cell biology 12:414-419.

Cui M, Huang Y, Tian C, Zhao Y, Zheng J (2011) FOXO3a inhibits TNF-alpha- and IL-1beta-induced astrocyte proliferation:Implication for reactive astrogliosis. Glia 59:641-654.

Culmsee C, Mattson MP (2005) p53 in neuronal apoptosis. Biochemical and biophysical research communications 331:761-777.

Cunningham C, Maclullich AM (2012) At the extreme end of the psychoneuroimmunological spectrum: Delirium as a maladaptive sickness behaviour response. Brain, behavior, and immunity.

Cunningham C, Hennessy E (2015) Co-morbidity and systemic inflammation as drivers of cognitive decline: new experimental models adopting a broader paradigm in dementia research. Alzheimer's research & therapy 7:33.

Cunningham C, Wilcockson DC, Boche D, Perry VH (2005a) Comparison of inflammatory and acute-phase responses in the brain and peripheral organs of the ME7 model of prion disease. Journal of virology 79:5174-5184.

Cunningham C, Wilcockson DC, Campion S, Lunnon K, Perry VH (2005b) Central and systemic endotoxin challenges exacerbate the local inflammatory response and increase neuronal death during chronic neurodegeneration. The Journal of neuroscience : the official journal of the Society for Neuroscience 25:9275-9284.

Cunningham C, Campion S, Lunnon K, Murray CL, Woods JF, Deacon RM, Rawlins JN, Perry VH (2009a) Systemic inflammation induces acute behavioral and cognitive changes and accelerates neurodegenerative disease. Biological psychiatry 65:304-312.

Cunningham C, Deacon R, Wells H, Boche D, Waters S, Diniz CP, Scott H, Rawlins JNP, Perry VH (2003a) Synaptic changes characterize early behavioural signs in the ME7 model of murine prion disease. European Journal of Neuroscience 17:2147-2155.

Cunningham C, Deacon R, Wells H, Boche D, Waters S, Diniz CP, Scott H, Rawlins JN, Perry VH (2003b) Synaptic changes characterize early behavioural changes in the ME7 model of murine prion disease. Eur J Neurosci 17:2147-2155.

Cunningham O, Campion S, Perry VH, Murray C, Sidenius N, Docagne F, Cunningham C (2009b) Microglia and the urokinase plasminogen activator receptor/uPA system in innate brain inflammation. Glia 57:1802-1814.

Cusick MF, Libbey JE, Patel DC, Doty DJ, Fujinami RS (2013) Infiltrating macrophages are key to the development of seizures following virus infection. Journal of virology 87:1849-1860.

Czabotar PE, Colman PM, Huang DC (2009) Bax activation by Bim? Cell death and differentiation 16:1187-1191.

Czirr E, Wyss-Coray T (2012) The immunology of neurodegeneration. The Journal of clinical investigation 122:1156-1163.

Dantzer R (2001) Cytokine-induced sickness behavior: mechanisms and implications. Annals of the New York Academy of Sciences 933:222-234.

Dantzer R, Kelley KW (2007) Twenty years of research on cytokine-induced sickness behavior. Brain, behavior, and immunity 21:153-160.

Dantzer R, Bluthe RM, Gheusi G, Cremona S, Laye S, Parnet P, Kelley KW (1998) Molecular basis of sickness behavior. Annals of the New York Academy of Sciences 856:132-138.

Davalos D, Grutzendler J, Yang G, Kim JV, Zuo Y, Jung S, Littman DR, Dustin ML, Gan WB (2005) ATP mediates rapid microglial response to local brain injury in vivo. Nature neuroscience 8:752-758.

Davis AE, Campbell SJ, Wilainam P, Anthony DC (2005) Post-conditioning with lipopolysaccharide reduces the inflammatory infiltrate to the injured brain and spinal cord: a potential neuroprotective treatment. The European journal of neuroscience 22:2441-2450.

Davis DH, Muniz Terrera G, Keage H, Rahkonen T, Oinas M, Matthews FE, Cunningham C, Polvikoski T, Sulkava R, MacLullich AM, Brayne C (2012) Delirium is a strong risk factor for dementia in the oldest-old: a population-based cohort study. Brain : a journal of neurology 135:2809-2816.

Davis DH, Skelly DT, Murray C, Hennessy E, Bowen J, Norton S, Brayne C, Rahkonen T, Sulkava R, Sanderson DJ, Rawlins JN, Bannerman DM, MacLullich AM, Cunningham C (2014) Worsening Cognitive Impairment and Neurodegenerative Pathology Progressively Increase Risk for Delirium. The American journal of geriatric psychiatry : official journal of the American Association for Geriatric Psychiatry.

Davis DH, Skelly DT, Murray C, Hennessy E, Bowen J, Norton S, Brayne C, Rahkonen T, Sulkava R, Sanderson DJ, Rawlins JN, Bannerman DM, MacLullich AM, Cunningham C (2015) Worsening cognitive impairment and neurodegenerative pathology progressively increase risk for delirium. The American journal of geriatric psychiatry : official journal of the American Association for Geriatric Psychiatry 23:403-415.

De Lella Ezcurra AL, Chertoff M, Ferrari C, Graciarena M, Pitossi F (2010) Chronic expression of low levels of tumor necrosis factor-alpha in the substantia nigra elicits progressive neurodegeneration, delayed motor symptoms and microglia/macrophage activation. Neurobiology of disease 37:630-640.

De Souza CT, Araujo EP, Bordin S, Ashimine R, Zollner RL, Boschero AC, Saad MJ, Velloso LA (2005) Consumption of a fat-rich diet activates a proinflammatory response and induces insulin resistance in the hypothalamus. Endocrinology 146:4192-4199.

del Rey A, Monge-Arditi G, Besedovsky HO (1998) Central and peripheral mechanisms contribute to the hypoglycemia induced by interleukin-1. Annals of the New York Academy of Sciences 840:153-161.

Deli MA, Descamps L, Dehouck MP, Cecchelli R, Joo F, Abraham CS, Torpier G (1995) Exposure of tumor necrosis factor-alpha to luminal membrane of bovine brain capillary endothelial cells cocultured with astrocytes induces a delayed increase of permeability and cytoplasmic stress fiber formation of actin. Journal of neuroscience research 41:717-726.

Dey A, Hao S, Erion JR, Wosiski-Kuhn M, Stranahan AM (2014) Glucocorticoid sensitization of microglia in a genetic mouse model of obesity and diabetes. Journal of neuroimmunology 269:20-27.

DiCarlo G, Wilcock D, Henderson D, Gordon M, Morgan D (2001) Intrahippocampal LPS injections reduce Abeta load in APP+PS1 transgenic mice. Neurobiology of aging 22:1007-1012.

Dickstein JB, Moldofsky H, Lue FA, Hay JB (1999) Intracerebroventricular injection of TNF-alpha promotes sleep and is recovered in cervical lymph. The American journal of physiology 276:R1018-1022.

Didier N, Romero IA, Creminon C, Wijkhuisen A, Grassi J, Mabondzo A (2003) Secretion of interleukin-1beta by astrocytes mediates endothelin-1 and

tumour necrosis factor-alpha effects on human brain microvascular endothelial cell permeability. Journal of neurochemistry 86:246-254.
Dinarello CA (1984) Interleukin-1. Reviews of infectious diseases 6:51-95.
Doehner J, Genoud C, Imhof C, Krstic D, Knuesel I (2012) Extrusion of misfolded and aggregated proteins--a protective strategy of aging neurons? Eur J Neurosci 35:1938-1950.
Drake C et al. (2011) Brain inflammation is induced by co-morbidities and risk factors for stroke. Brain, behavior, and immunity 25:1113-1122.
Dunn AJ (2006) Effects of cytokines and infections on brain neurochemistry. Clin Neurosci Res 6:52-68.
Dunn N, Mullee M, Perry VH, Holmes C (2005) Association between dementia and infectious disease: evidence from a case-control study. Alzheimer disease and associated disorders 19:91-94.
Dvoriantchikova G, Barakat D, Brambilla R, Agudelo C, Hernandez E, Bethea JR, Shestopalov VI, Ivanov D (2009) Inactivation of astroglial NF-kappa B promotes survival of retinal neurons following ischemic injury. The European journal of neuroscience 30:175-185.
Ehlers S, Holscher C, Scheu S, Tertilt C, Hehlgans T, Suwinski J, Endres R, Pfeffer K (2003) The lymphotoxin beta receptor is critically involved in controlling infections with the intracellular pathogens Mycobacterium tuberculosis and Listeria monocytogenes. J Immunol 170:5210-5218.
Emsley HC, Smith CJ, Georgiou RF, Vail A, Hopkins SJ, Rothwell NJ, Tyrrell PJ (2005) A randomised phase II study of interleukin-1 receptor antagonist in acute stroke patients. Journal of neurology, neurosurgery, and psychiatry 76:1366-1372.
Endo Y (1991) Parallel relationship between the increase in serotonin in the liver and the hypoglycaemia induced in mice by interleukin-1 and tumour necrosis factor. Immunology letters 27:75-79.
Endres R, Luz A, Schulze H, Neubauer H, Futterer A, Holland SM, Wagner H, Pfeffer K (1997) Listeriosis in p47(phox-/-) and TRp55-/- mice: protection despite absence of ROI and susceptibility despite presence of RNI. Immunity 7:419-432.
Engelhardt B, Ransohoff RM (2005) The ins and outs of T-lymphocyte trafficking to the CNS: anatomical sites and molecular mechanisms. Trends in immunology 26:485-495.
Erickson MA, Banks WA (2011) Cytokine and chemokine responses in serum and brain after single and repeated injections of lipopolysaccharide: multiplex quantification with path analysis. Brain, behavior, and immunity 25:1637-1648.
Erion JR, Wosiski-Kuhn M, Dey A, Hao S, Davis CL, Pollock NK, Stranahan AM (2014) Obesity elicits interleukin 1-mediated deficits in hippocampal synaptic plasticity. The Journal of neuroscience : the official journal of the Society for Neuroscience 34:2618-2631.
Ethell DW, Buhler LA (2003) Fas ligand-mediated apoptosis in degenerative disorders of the brain. J Clin Immunol 23:439-446.
Fenn AM, Gensel JC, Huang Y, Popovich PG, Lifshitz J, Godbout JP (2014) Immune activation promotes depression 1 month after diffuse brain injury: a role for primed microglia. Biological psychiatry 76:575-584.
Ferrari CC, Pott Godoy MC, Tarelli R, Chertoff M, Depino AM, Pitossi FJ (2006) Progressive neurodegeneration and motor disabilities induced by chronic

expression of IL-1beta in the substantia nigra. Neurobiology of disease 24:183-193.

Ferrari CC, Depino AM, Prada F, Muraro N, Campbell S, Podhajcer O, Perry VH, Anthony DC, Pitossi FJ (2004) Reversible demyelination, blood-brain barrier breakdown, and pronounced neutrophil recruitment induced by chronic IL-1 expression in the brain. The American journal of pathology 165:1827-1837.

Field R, Campion S, Warren C, Murray C, Cunningham C (2010) Systemic challenge with the TLR3 agonist poly I:C induces amplified IFNalpha/beta and IL-1beta responses in the diseased brain and exacerbates chronic neurodegeneration. Brain, behavior, and immunity 24:996-1007.

Field RH, Gossen A, Cunningham C (2012) Prior pathology in the basal forebrain cholinergic system predisposes to inflammation-induced working memory deficits: reconciling inflammatory and cholinergic hypotheses of delirium. The Journal of neuroscience : the official journal of the Society for Neuroscience 32:6288-6294.

Fisher Y, Nemirovsky A, Baron R, Monsonego A (2010) T cells specifically targeted to amyloid plaques enhance plaque clearance in a mouse model of Alzheimer's disease. PloS one 5:e10830.

Fitzpatrick AL, Kuller LH, Lopez OL, Diehr P, O'Meara ES, Longstreth WT, Jr., Luchsinger JA (2009) Midlife and late-life obesity and the risk of dementia: cardiovascular health study. Archives of neurology 66:336-342.

Fong TG, Jones RN, Shi P, Marcantonio ER, Yap L, Rudolph JL, Yang FM, Kiely DK, Inouye SK (2009) Delirium accelerates cognitive decline in Alzheimer disease. Neurology 72:1570-1575.

Forlenza OV, Diniz BS, Talib LL, Mendonca VA, Ojopi EB, Gattaz WF, Teixeira AL (2009) Increased serum IL-1beta level in Alzheimer's disease and mild cognitive impairment. Dementia and geriatric cognitive disorders 28:507-512.

Fouillet A, Mawson J, Suliman O, Sharrack B, Romero IA, Woodroofe MN (2012) CCL2 binding is CCR2 independent in primary adult human astrocytes. Brain research 1437:115-126.

Fraker DL, Stovroff MC, Merino MJ, Norton JA (1988) Tolerance to tumor necrosis factor in rats and the relationship to endotoxin tolerance and toxicity. The Journal of experimental medicine 168:95-105.

Frank MG, Thompson BM, Watkins LR, Maier SF (2012) Glucocorticoids mediate stress-induced priming of microglial pro-inflammatory responses. Brain, behavior, and immunity 26:337-345.

Frank MG, Barrientos RM, Hein AM, Biedenkapp JC, Watkins LR, Maier SF (2010) IL-1RA blocks E. coli-induced suppression of Arc and long-term memory in aged F344xBN F1 rats. Brain, behavior, and immunity 24:254-262.

Fu X, Kassim SY, Parks WC, Heinecke JW (2001) Hypochlorous acid oxygenates the cysteine switch domain of pro-matrilysin (MMP-7). A mechanism for matrix metalloproteinase activation and atherosclerotic plaque rupture by myeloperoxidase. The Journal of biological chemistry 276:41279-41287.

Fuller S, Munch G, Steele M (2009) Activated astrocytes: a therapeutic target in Alzheimer's disease? Expert review of neurotherapeutics 9:1585-1594.

Galea I, Bechmann I, Perry VH (2007) What is immune privilege (not)? Trends in immunology 28:12-18.

Gao Y, Ottaway N, Schriever SC, Legutko B, Garcia-Caceres C, de la Fuente E, Mergen C, Bour S, Thaler JP, Seeley RJ, Filosa J, Stern JE, Perez-Tilve D,

Schwartz MW, Tschop MH, Yi CX (2014) Hormones and diet, but not body weight, control hypothalamic microglial activity. Glia 62:17-25.

Garcia I, Olleros ML, Quesniaux VF, Jacobs M, Allie N, Nedospasov SA, Szymkowski DE, Ryffel B (2011) Roles of soluble and membrane TNF and related ligands in mycobacterial infections: effects of selective and non-selective TNF inhibitors during infection. Advances in experimental medicine and biology 691:187-201.

Gardam MA, Keystone EC, Menzies R, Manners S, Skamene E, Long R, Vinh DC (2003) Anti-tumour necrosis factor agents and tuberculosis risk: mechanisms of action and clinical management. The Lancet infectious diseases 3:148-155.

Gaykema RP, Goehler LE (2011) Ascending caudal medullary catecholamine pathways drive sickness-induced deficits in exploratory behavior: brain substrates for fatigue? Brain, behavior, and immunity 25:443-460.

Gaykema RP, Balachandran MK, Godbout JP, Johnson RW, Goehler LE (2007) Enhanced neuronal activation in central autonomic network nuclei in aged mice following acute peripheral immune challenge. Autonomic neuroscience : basic & clinical 131:137-142.

Gentleman SM, Nash MJ, Sweeting CJ, Graham DI, Roberts GW (1993) Beta-amyloid precursor protein (beta APP) as a marker for axonal injury after head injury. Neuroscience letters 160:139-144.

Gerszten RE, Garcia-Zepeda EA, Lim YC, Yoshida M, Ding HA, Gimbrone MA, Jr., Luster AD, Luscinskas FW, Rosenzweig A (1999) MCP-1 and IL-8 trigger firm adhesion of monocytes to vascular endothelium under flow conditions. Nature 398:718-723.

Gibson RM, Rothwell NJ, Le Feuvre RA (2004) CNS injury: the role of the cytokine IL-1. Vet J 168:230-237.

Giulian D, Young DG, Woodward J, Brown DC, Lachman LB (1988) Interleukin-1 is an astroglial growth factor in the developing brain. The Journal of neuroscience : the official journal of the Society for Neuroscience 8:709-714.

Giuliani F, Vernay A, Leuba G, Schenk F (2009) Decreased behavioral impairments in an Alzheimer mice model by interfering with TNF-alpha metabolism. Brain research bulletin 80:302-308.

Glass CK, Saijo K, Winner B, Marchetto MC, Gage FH (2010) Mechanisms underlying inflammation in neurodegeneration. Cell 140:918-934.

Godbout JP, Chen J, Abraham J, Richwine AF, Berg BM, Kelley KW, Johnson RW (2005) Exaggerated neuroinflammation and sickness behavior in aged mice following activation of the peripheral innate immune system. FASEB journal : official publication of the Federation of American Societies for Experimental Biology 19:1329-1331.

Gomez-Nicola D, Fransen NL, Suzzi S, Perry VH (2013) Regulation of microglial proliferation during chronic neurodegeneration. The Journal of neuroscience : the official journal of the Society for Neuroscience 33:2481-2493.

Gorina R, Lyck R, Vestweber D, Engelhardt B (2014) beta2 integrin-mediated crawling on endothelial ICAM-1 and ICAM-2 is a prerequisite for transcellular neutrophil diapedesis across the inflamed blood-brain barrier. J Immunol 192:324-337.

Grainger DJ, Reckless J, McKilligin E (2004) Apolipoprotein E modulates clearance of apoptotic bodies in vitro and in vivo, resulting in a systemic

proinflammatory state in apolipoprotein E-deficient mice. Journal of immunology 173:6366-6375.
Granger JI, Ratti PL, Datta SC, Raymond RM, Opp MR (2013) Sepsis-induced morbidity in mice: effects on body temperature, body weight, cage activity, social behavior and cytokines in brain. Psychoneuroendocrinology 38:1047-1057.
Gray BC, Siskova Z, Perry VH, O'Connor V (2009) Selective presynaptic degeneration in the synaptopathy associated with ME7-induced hippocampal pathology. Neurobiol Dis 35:63-74.
Gregor MF, Hotamisligil GS (2011) Inflammatory mechanisms in obesity. Annual review of immunology 29:415-445.
Griffin EW, Skelly DT, Murray CL, Cunningham C (2013) Cyclooxygenase-1-dependent prostaglandins mediate susceptibility to systemic inflammation-induced acute cognitive dysfunction. The Journal of neuroscience : the official journal of the Society for Neuroscience 33:15248-15258.
Grunfeld C, Wilking H, Neese R, Gavin LA, Moser AH, Gulli R, Serio MK, Feingold KR (1989) Persistence of the hypertriglyceridemic effect of tumor necrosis factor despite development of tachyphylaxis to its anorectic/cachectic effects in rats. Cancer research 49:2554-2560.
Gupta S (2002) A Decision between Life and Death during

TNF-α-Induced Signaling. Journal of clinical immunology 22:185-194.
Gupta S, Agrawal A, Agrawal S, Su H, Gollapudi S (2006) A paradox of immunodeficiency and inflammation in human aging: lessons learned from apoptosis. Immunity & ageing : I & A 3:5.
Gutierrez EG, Banks WA, Kastin AJ (1993) Murine tumor necrosis factor alpha is transported from blood to brain in the mouse. Journal of neuroimmunology 47:169-176.
Haas J, Storch-Hagenlocher B, Biessmann A, Wildemann B (2002) Inducible nitric oxide synthase and argininosuccinate synthetase: co-induction in brain tissue of patients with Alzheimer's dementia and following stimulation with beta-amyloid 1-42 in vitro. Neuroscience letters 322:121-125.
Hafner-Bratkovic I, Bencina M, Fitzgerald KA, Golenbock D, Jerala R (2012) NLRP3 inflammasome activation in macrophage cell lines by prion protein fibrils as the source of IL-1beta and neuronal toxicity. Cellular and molecular life sciences : CMLS 69:4215-4228.
Hamilton CD (2004) Infectious complications of treatment with biologic agents. Current opinion in rheumatology 16:393-398.
Hanada R et al. (2009) Central control of fever and female body temperature by RANKL/RANK. Nature 462:505-509.
Hao S, Baltimore D (2009) The stability of mRNA influences the temporal order of the induction of genes encoding inflammatory molecules. Nature immunology 10:281-288.
Haruda FD (1995) Nonsteroidal anti-inflammatory drugs in Alzheimer's disease. Neurology 45:2116.
Hayakata T, Shiozaki T, Tasaki O, Ikegawa H, Inoue Y, Toshiyuki F, Hosotubo H, Kieko F, Yamashita T, Tanaka H, Shimazu T, Sugimoto H (2004) Changes in CSF S100B and cytokine concentrations in early-phase severe traumatic brain injury. Shock 22:102-107.
He P, Zhong Z, Lindholm K, Berning L, Lee W, Lemere C, Staufenbiel M, Li R, Shen Y (2007) Deletion of tumor necrosis factor death receptor inhibits amyloid

beta generation and prevents learning and memory deficits in Alzheimer's mice. The Journal of cell biology 178:829-841.

Hehlgans T, Mannel DN (2002) The TNF-TNF receptor system. Biological chemistry 383:1581-1585.

Hehlgans T, Pfeffer K (2005) The intriguing biology of the tumour necrosis factor/tumour necrosis factor receptor superfamily: players, rules and the games. Immunology 115:1-20.

Hein AM, Stasko MR, Matousek SB, Scott-McKean JJ, Maier SF, Olschowka JA, Costa AC, O'Banion MK (2010) Sustained hippocampal IL-1beta overexpression impairs contextual and spatial memory in transgenic mice. Brain, behavior, and immunity 24:243-253.

Helmy A, Guilfoyle MR, Carpenter KL, Pickard JD, Menon DK, Hutchinson PJ (2014) Recombinant human interleukin-1 receptor antagonist in severe traumatic brain injury: a phase II randomized control trial. Journal of cerebral blood flow and metabolism : official journal of the International Society of Cerebral Blood Flow and Metabolism 34:845-851.

Heneka MT, Kummer MP, Stutz A, Delekate A, Schwartz S, Vieira-Saecker A, Griep A, Axt D, Remus A, Tzeng TC, Gelpi E, Halle A, Korte M, Latz E, Golenbock DT (2013) NLRP3 is activated in Alzheimer's disease and contributes to pathology in APP/PS1 mice. Nature 493:674-678.

Henn A, Kirner S, Leist M (2011) TLR2 hypersensitivity of astrocytes as functional consequence of previous inflammatory episodes. J Immunol 186:3237-3247.

Hennessy E, Griffin EW, Cunningham C (2015) Astrocytes are primed by chronic neurodegeneration to produce exaggerated chemokine and cell infiltration responses to acute stimulation with the cytokines IL-1β and TNF-α. . Journal of Neuroscience.

Herber DL, Roth LM, Wilson D, Wilson N, Mason JE, Morgan D, Gordon MN (2004) Time-dependent reduction in Abeta levels after intracranial LPS administration in APP transgenic mice. Exp Neurol 190:245-253.

Herber DL, Mercer M, Roth LM, Symmonds K, Maloney J, Wilson N, Freeman MJ, Morgan D, Gordon MN (2007) Microglial activation is required for Abeta clearance after intracranial injection of lipopolysaccharide in APP transgenic mice. Journal of neuroimmune pharmacology : the official journal of the Society on NeuroImmune Pharmacology 2:222-231.

Higuchi M, Hatta K, Honma T, Hitomi YH, Kambayashi Y, Hibino Y, Matsuzaki I, Sasahara S, Nakamura H (2010) Association between altered systemic inflammatory interleukin-1beta and natural killer cell activity and subsequently agitation in patients with Alzheimer disease. International journal of geriatric psychiatry 25:604-611.

Higuma M, Sanjo N, Satoh K, Shiga Y, Sakai K, Nozaki I, Hamaguchi T, Nakamura Y, Kitamoto T, Shirabe S, Murayama S, Yamada M, Tateishi J, Mizusawa H (2013) Relationships between clinicopathological features and cerebrospinal fluid biomarkers in Japanese patients with genetic prion diseases. PloS one 8:e60003.

Hilton KJ, Cunningham C, Reynolds RA, Perry VH (2013) Early Hippocampal Synaptic Loss Precedes Neuronal Loss and Associates with Early Behavioural Deficits in Three Distinct Strains of Prion Disease. PloS one 8:e68062.

Himmelstein DS, Ward SM, Lancia JK, Patterson KR, Binder LI (2012) Tau as a therapeutic target in neurodegenerative disease. Pharmacology & therapeutics 136:8-22.

Ho AW, Wong CK, Lam CW (2008) Tumor necrosis factor-alpha up-regulates the expression of CCL2 and adhesion molecules of human proximal tubular epithelial cells through MAPK signaling pathways. Immunobiology 213:533-544.

Hofman A, Ott A, Breteler MM, Bots ML, Slooter AJ, van Harskamp F, van Duijn CN, Van Broeckhoven C, Grobbee DE (1997) Atherosclerosis, apolipoprotein E, and prevalence of dementia and Alzheimer's disease in the Rotterdam Study. Lancet 349:151-154.

Holm TH, Draeby D, Owens T (2012) Microglia are required for astroglial Toll-like receptor 4 response and for optimal TLR2 and TLR3 response. Glia 60:630-638.

Holmes C, Cunningham C, Zotova E, Culliford D, Perry VH (2011) Proinflammatory cytokines, sickness behavior, and Alzheimer disease. Neurology 77:212-218.

Holmes C, El-Okl M, Williams AL, Cunningham C, Wilcockson D, Perry VH (2003) Systemic infection, interleukin 1beta, and cognitive decline in Alzheimer's disease. Journal of neurology, neurosurgery, and psychiatry 74:788-789.

Holmes C, Cunningham C, Zotova E, Woolford J, Dean C, Kerr S, Culliford D, Perry VH (2009a) Systemic inflammation and disease progression in Alzheimer disease. Neurology 73:768-774.

Holmes C, Cunningham C, Zotova E, Woolford J, Dean C, Kerr S, Culliford D, Perry VH (2009b) Systemic inflammation and disease progression in Alzheimer's disease. Neurology 73:768-774.

Holmes C, Boche D, Wilkinson D, Yadegarfar G, Hopkins V, Bayer A, Jones RW, Bullock R, Love S, Neal JW, Zotova E, Nicoll JA (2008) Long-term effects of Abeta42 immunisation in Alzheimer's disease: follow-up of a randomised, placebo-controlled phase I trial. Lancet 372:216-223.

Holmes C, Butchart J, Wolfe L, Davies L, Dodge S, Lewsey I, McFarlan B, Nicholls M, Perry H, Rayner C, Sheram S, Sharples R, Sussams R, Stevens A, Teeling J (2014) THE SAFETYAND TOLERABILITY OF ETANERCEPT IN ALZHEIMER'S DISEASE (STEADI-09): A PHASE II DOUBLE BLIND RANDOMISED PLACEBO CONTROLLED TRIAL. In: Alzheimer's Association International Conference, p 273. Copenhagen, Denmark: Alzheimer's & Dementia.

Holscher C (2014) Insulin, incretins and other growth factors as potential novel treatments for Alzheimer's and Parkinson's diseases. Biochemical Society transactions 42:593-599.

Honma T, Hatta K, Hitomi Y, Kambayashi Y, Hibino Y, Konoshita T, Nakamura H (2013) Increased systemic inflammatory interleukin-1ss and interleukin-6 during agitation as predictors of Alzheimer's disease. International journal of geriatric psychiatry 28:233-241.

Hopp SC, Royer S, Brothers HM, Kaercher RM, D'Angelo H, Bardou I, Wenk GL (2014) Age-associated alterations in the time-dependent profile of pro- and anti-inflammatory proteins within the hippocampus in response to acute exposure to interleukin-1beta. Journal of neuroimmunology 267:86-91.

Hortobagyi T, Wise S, Hunt N, Cary N, Djurovic V, Fegan-Earl A, Shorrock K, Rouse D, Al-Sarraj S (2007) Traumatic axonal damage in the brain can be detected

using beta-APP immunohistochemistry within 35 min after head injury to human adults. Neuropathology and applied neurobiology 33:226-237.
Hsieh CL, Niemi EC, Wang SH, Lee CC, Bingham D, Zhang J, Cozen ML, Charo I, Huang EJ, Liu J, Nakamura MC (2014) CCR2 deficiency impairs macrophage infiltration and improves cognitive function after traumatic brain injury. Journal of neurotrauma 31:1677-1688.
Hu J, Van Eldik LJ (1999) Glial-derived proteins activate cultured astrocytes and enhance beta amyloid-induced glial activation. Brain research 842:46-54.
Hughes MM, Field RH, Perry VH, Murray CL, Cunningham C (2010) Microglia in the degenerating brain are capable of phagocytosis of beads and of apoptotic cells, but do not efficiently remove PrPSc, even upon LPS stimulation. Glia 58:2017-2030.
Hutchinson PJ, O'Connell MT, Rothwell NJ, Hopkins SJ, Nortje J, Carpenter KL, Timofeev I, Al-Rawi PG, Menon DK, Pickard JD (2007) Inflammation in human brain injury: intracerebral concentrations of IL-1alpha, IL-1beta, and their endogenous inhibitor IL-1ra. Journal of neurotrauma 24:1545-1557.
Inouye SK (2006) Delirium in older persons. N Engl J Med 354:1157-1165.
Ishii M, Wang G, Racchumi G, Dyke JP, Iadecola C (2014) Transgenic mice overexpressing amyloid precursor protein exhibit early metabolic deficits and a pathologically low leptin state associated with hypothalamic dysfunction in arcuate neuropeptide Y neurons. The Journal of neuroscience : the official journal of the Society for Neuroscience 34:9096-9106.
Iwashyna TJ, Ely EW, Smith DM, Langa KM (2010) Long-term cognitive impairment and functional disability among survivors of severe sepsis. JAMA : the journal of the American Medical Association 304:1787-1794.
Jackson JC, Gordon SM, Hart RP, Hopkins RO, Ely EW (2004) The association between delirium and cognitive decline: a review of the empirical literature. Neuropsychology review 14:87-98.
Jefferson AL, Massaro JM, Wolf PA, Seshadri S, Au R, Vasan RS, Larson MG, Meigs JB, Keaney JF, Jr., Lipinska I, Kathiresan S, Benjamin EJ, DeCarli C (2007) Inflammatory biomarkers are associated with total brain volume: the Framingham Heart Study. Neurology 68:1032-1038.
Jeffrey M, Halliday WG, Bell J, Johnston AR, MacLeod NK, Ingham C, Sayers AR, Brown DA, Fraser JR (2000) Synapse loss associated with abnormal PrP precedes neuronal degeneration in the scrapie-infected murine hippocampus. Neuropathol Appl Neurobiol 26:41-54.
Jimenez S, Baglietto-Vargas D, Caballero C, Moreno-Gonzalez I, Torres M, Sanchez-Varo R, Ruano D, Vizuete M, Gutierrez A, Vitorica J (2008) Inflammatory response in the hippocampus of PS1M146L/APP751SL mouse model of Alzheimer's disease: age-dependent switch in the microglial phenotype from alternative to classic. The Journal of neuroscience : the official journal of the Society for Neuroscience 28:11650-11661.
Jin R, Yang G, Li G (2010) Inflammatory mechanisms in ischemic stroke: role of inflammatory cells. Journal of leukocyte biology 87:779-789.
Jing T, Wu L, Borgmann K, Surendran S, Ghorpade A, Liu J, Xiong H (2010) Soluble factors from IL-1beta-stimulated astrocytes activate NR1a/NR2B receptors: implications for HIV-1-induced neurodegeneration. Biochemical and biophysical research communications 402:241-246.

Johnson M, Huyn S, Burton J, Sato M, Wu L (2006) Differential biodistribution of adenoviral vector in vivo as monitored by bioluminescence imaging and quantitative polymerase chain reaction. Human gene therapy 17:1262-1269.

Jun G et al. (2010) Meta-analysis confirms CR1, CLU, and PICALM as alzheimer disease risk loci and reveals interactions with APOE genotypes. Archives of neurology 67:1473-1484.

Karakas M, Koenig W (2012) Myeloperoxidase production by macrophage and risk of atherosclerosis. Current atherosclerosis reports 14:277-283.

Kawabori M, Kacimi R, Kauppinen T, Calosing C, Kim JY, Hsieh CL, Nakamura MC, Yenari MA (2015) Triggering Receptor Expressed on Myeloid Cells 2 (TREM2) Deficiency Attenuates Phagocytic Activities of Microglia and Exacerbates Ischemic Damage in Experimental Stroke. The Journal of neuroscience : the official journal of the Society for Neuroscience 35:3384-3396.

Kelley KW, O'Connor JC, Lawson MA, Dantzer R, Rodriguez-Zas SL, McCusker RH (2013) Aging leads to prolonged duration of inflammation-induced depression-like behavior caused by Bacillus Calmette-Guerin. Brain, behavior, and immunity 32:63-69.

Kelly KA, Li X, Tan Z, VanGilder RL, Rosen CL, Huber JD (2009) NOX2 inhibition with apocynin worsens stroke outcome in aged rats. Brain research 1292:165-172.

Kenne E, Erlandsson A, Lindbom L, Hillered L, Clausen F (2012) Neutrophil depletion reduces edema formation and tissue loss following traumatic brain injury in mice. Journal of neuroinflammation 9:17.

Kesner RP, Lee I, Gilbert P (2004) A behavioral assessment of hippocampal function based on a subregional analysis. Reviews in the neurosciences 15:333-351.

Kettelhut IC, Goldberg AL (1988) Tumor necrosis factor can induce fever in rats without activating protein breakdown in muscle or lipolysis in adipose tissue. The Journal of clinical investigation 81:1384-1389.

Khandelwal PJ, Herman AM, Moussa CE (2011) Inflammation in the early stages of neurodegenerative pathology. Journal of neuroimmunology 238:1-11.

Khorooshi R, Babcock AA, Owens T (2008) NF-kappaB-driven STAT2 and CCL2 expression in astrocytes in response to brain injury. Journal of immunology 181:7284-7291.

Kim JM, Oh YK, Lee JH, Im DY, Kim YJ, Youn J, Lee CH, Son H, Lee YS, Park JY, Choi IH (2005) Induction of proinflammatory mediators requires activation of the TRAF, NIK, IKK and NF-kappaB signal transduction pathway in astrocytes infected with Escherichia coli. Clinical and experimental immunology 140:450-460.

Kim MS, Yan J, Wu W, Zhang G, Zhang Y, Cai D (2015) Rapid linkage of innate immunological signals to adaptive immunity by the brain-fat axis. Nature immunology 16:525-533.

King MD, Alleyne CH, Jr., Dhandapani KM (2013) TNF-alpha receptor antagonist, R-7050, improves neurological outcomes following intracerebral hemorrhage in mice. Neuroscience letters 542:92-96.

Kitazawa M, Oddo S, Yamasaki TR, Green KN, LaFerla FM (2005) Lipopolysaccharide-induced inflammation exacerbates tau pathology by a cyclin-dependent kinase 5-mediated pathway in a transgenic model of

Alzheimer's disease. The Journal of neuroscience : the official journal of the Society for Neuroscience 25:8843-8853.
Kitazawa M, Cheng D, Tsukamoto MR, Koike MA, Wes PD, Vasilevko V, Cribbs DH, LaFerla FM (2011) Blocking IL-1 signaling rescues cognition, attenuates tau pathology, and restores neuronal beta-catenin pathway function in an Alzheimer's disease model. J Immunol 187:6539-6549.
Kiyota T, Gendelman HE, Weir RA, Higgins EE, Zhang G, Jain M (2013) CCL2 affects beta-amyloidosis and progressive neurocognitive dysfunction in a mouse model of Alzheimer's disease. Neurobiology of aging 34:1060-1068.
Kiyota T, Yamamoto M, Xiong H, Lambert MP, Klein WL, Gendelman HE, Ransohoff RM, Ikezu T (2009) CCL2 accelerates microglia-mediated Abeta oligomer formation and progression of neurocognitive dysfunction. PloS one 4:e6197.
Knight EM, Martins IV, Gumusgoz S, Allan SM, Lawrence CB (2014) High-fat diet-induced memory impairment in triple-transgenic Alzheimer's disease (3xTgAD) mice is independent of changes in amyloid and tau pathology. Neurobiology of aging 35:1821-1832.
Kong LY, Lai C, Wilson BC, Simpson JN, Hong JS (1997) Protein tyrosine kinase inhibitors decrease lipopolysaccharide-induced proinflammatory cytokine production in mixed glia, microglia-enriched or astrocyte-enriched cultures. Neurochemistry international 30:491-497.
Konofagou EE (2012) Optimization of the ultrasound-induced blood-brain barrier opening. Theranostics 2:1223-1237.
Kostulas N, Pelidou SH, Kivisakk P, Kostulas V, Link H (1999) Increased IL-1beta, IL-8, and IL-17 mRNA expression in blood mononuclear cells observed in a prospective ischemic stroke study. Stroke; a journal of cerebral circulation 30:2174-2179.
Koyama Y, Kotani M, Sawamura T, Kuribayashi M, Konishi R, Michinaga S (2013) Different actions of endothelin-1 on chemokine production in rat cultured astrocytes: reduction of CX3CL1/fractalkine and an increase in CCL2/MCP-1 and CXCL1/CINC-1. Journal of neuroinflammation 10:51.
Kozak W, Conn CA, Klir JJ, Wong GH, Kluger MJ (1995) TNF soluble receptor and antiserum against TNF enhance lipopolysaccharide fever in mice. The American journal of physiology 269:R23-29.
Krstic D, Knuesel I (2013) Deciphering the mechanism underlying late-onset Alzheimer disease. Nat Rev Neurol 9:25-34.
Krstic D, Madhusudan A, Doehner J, Vogel P, Notter T, Imhof C, Manalastas A, Hilfiker M, Pfister S, Schwerdel C, Riether C, Meyer U, Knuesel I (2012) Systemic immune challenges trigger and drive Alzheimer-like neuropathology in mice. Journal of neuroinflammation 9:151.
Kummer MP, Hermes M, Delekarte A, Hammerschmidt T, Kumar S, Terwel D, Walter J, Pape HC, Konig S, Roeber S, Jessen F, Klockgether T, Korte M, Heneka MT (2011) Nitration of tyrosine 10 critically enhances amyloid beta aggregation and plaque formation. Neuron 71:833-844.
Kurata T, Kawai H, Miyazaki K, Kozuki M, Morimoto N, Ohta Y, Ikeda Y, Abe K (2012) Statins have therapeutic potential for the treatment of Alzheimer's disease, likely via protection of the neurovascular unit in the AD brain. Journal of the neurological sciences 322:59-63.
Kyrkanides S, Olschowka JA, Williams JP, Hansen JT, O'Banion MK (1999) TNF alpha and IL-1beta mediate intercellular adhesion molecule-1 induction via

microglia-astrocyte interaction in CNS radiation injury. Journal of neuroimmunology 95:95-106.
Kyrkanides S, Tallents RH, Miller JN, Olschowka ME, Johnson R, Yang M, Olschowka JA, Brouxhon SM, O'Banion MK (2011) Osteoarthritis accelerates and exacerbates Alzheimer's disease pathology in mice. Journal of neuroinflammation 8:112.
Laflamme N, Lacroix S, Rivest S (1999) An essential role of interleukin-1beta in mediating NF-kappaB activity and COX-2 transcription in cells of the blood-brain barrier in response to a systemic and localized inflammation but not during endotoxemia. The Journal of neuroscience : the official journal of the Society for Neuroscience 19:10923-10930.
Lahiri DK, Chen D, Vivien D, Ge YW, Greig NH, Rogers JT (2003) Role of cytokines in the gene expression of amyloid beta-protein precursor: identification of a 5'-UTR-binding nuclear factor and its implications in Alzheimer's disease. Journal of Alzheimer's disease : JAD 5:81-90.
Larochelle A, Bellavance MA, Rivest S (2015) Role of adaptor protein MyD88 in TLR-mediated preconditioning and neuroprotection after acute excitotoxicity. Brain, behavior, and immunity 46:221-231.
Le Dreau G, Kular L, Nicot AB, Calmel C, Melik-Parsadaniantz S, Kitabgi P, Laurent M, Martinerie C (2010) NOV/CCN3 upregulates CCL2 and CXCL1 expression in astrocytes through beta1 and beta5 integrins. Glia 58:1510-1521.
Lee DC, Rizer J, Selenica ML, Reid P, Kraft C, Johnson A, Blair L, Gordon MN, Dickey CA, Morgan D (2010) LPS- induced inflammation exacerbates phospho-tau pathology in rTg4510 mice. Journal of neuroinflammation 7:56.
Lee JW, Lee YK, Yuk DY, Choi DY, Ban SB, Oh KW, Hong JT (2008) Neuro-inflammation induced by lipopolysaccharide causes cognitive impairment through enhancement of beta-amyloid generation. Journal of neuroinflammation 5:37.
Lee SC, Liu W, Dickson DW, Brosnan CF, Berman JW (1993) Cytokine production by human fetal microglia and astrocytes. Differential induction by lipopolysaccharide and IL-1 beta. Journal of immunology 150:2659-2667.
Lee TH, Avraham H, Lee SH, Avraham S (2002) Vascular endothelial growth factor modulates neutrophil transendothelial migration via up-regulation of interleukin-8 in human brain microvascular endothelial cells. The Journal of biological chemistry 277:10445-10451.
Lee YH, Kim SH, Kim Y, Lim Y, Ha K, Shin SY (2012) Inhibitory effect of the antidepressant imipramine on NF-kappaB-dependent CXCL1 expression in TNFalpha-exposed astrocytes. International immunopharmacology 12:547-555.
Lei B, Dawson HN, Roulhac-Wilson B, Wang H, Laskowitz DT, James ML (2013) Tumor necrosis factor alpha antagonism improves neurological recovery in murine intracerebral hemorrhage. Journal of neuroinflammation 10:103.
Lennox R, Porter DW, Flatt PR, Holscher C, Irwin N, Gault VA (2014) Comparison of the independent and combined effects of sub-chronic therapy with metformin and a stable GLP-1 receptor agonist on cognitive function, hippocampal synaptic plasticity and metabolic control in high-fat fed mice. Neuropharmacology.
Leung R, Proitsi P, Simmons A, Lunnon K, Guntert A, Kronenberg D, Pritchard M, Tsolaki M, Mecocci P, Kloszewska I, Vellas B, Soininen H, Wahlund LO,

Lovestone S (2013) Inflammatory proteins in plasma are associated with severity of Alzheimer's disease. PloS one 8:e64971.
Li L, Cao D, Garber DW, Kim H, Fukuchi K (2003) Association of aortic atherosclerosis with cerebral beta-amyloidosis and learning deficits in a mouse model of Alzheimer's disease. The American journal of pathology 163:2155-2164.
Libby P, Lichtman AH, Hansson GK (2013) Immune effector mechanisms implicated in atherosclerosis: from mice to humans. Immunity 38:1092-1104.
Licastro F, Pedrini S, Caputo L, Annoni G, Davis LJ, Ferri C, Casadei V, Grimaldi LM (2000) Increased plasma levels of interleukin-1, interleukin-6 and alpha-1-antichymotrypsin in patients with Alzheimer's disease: peripheral inflammation or signals from the brain? Journal of neuroimmunology 103:97-102.
Lipowski ZJ (1989) Delirium in the elderly patient. N Engl J Med 320:578-582.
Liu S, Zhang L, Wu Q, Wang T (2013) Chemokine CCL2 Induces Apoptosis in Cortex Following Traumatic Brain Injury. Journal of molecular neuroscience : MN.
Liu T, McDonnell PC, Young PR, White RF, Siren AL, Hallenbeck JM, Barone FC, Feurestein GZ (1993) Interleukin-1 beta mRNA expression in ischemic rat cortex. Stroke; a journal of cerebral circulation 24:1746-1750; discussion 1750-1741.
Loskutova N, Honea RA, Brooks WM, Burns JM (2010) Reduced limbic and hypothalamic volumes correlate with bone density in early Alzheimer's disease. Journal of Alzheimer's disease : JAD 20:313-322.
Louveau A, Smirnov I, Keyes TJ, Eccles JD, Rouhani SJ, Peske JD, Derecki NC, Castle D, Mandell JW, Lee KS, Harris TH, Kipnis J (2015) Structural and functional features of central nervous system lymphatic vessels. Nature 523:337-341.
Lowe J, Hand N, Mayer RJ (2005) Application of ubiquitin immunohistochemistry to the diagnosis of disease. Methods Enzymol 399:86-119.
Lue LF, Brachova L, Civin WH, Rogers J (1996) Inflammation, A beta deposition, and neurofibrillary tangle formation as correlates of Alzheimer's disease neurodegeneration. Journal of neuropathology and experimental neurology 55:1083-1088.
Ma L, Li XW, Zhang SJ, Yang F, Zhu GM, Yuan XB, Jiang W (2014) Interleukin-1 beta guides the migration of cortical neurons. Journal of neuroinflammation 11:114.
Maarouf CL, Daugs ID, Kokjohn TA, Walker DG, Hunter JM, Kruchowsky JC, Woltjer R, Kaye J, Castano EM, Sabbagh MN, Beach TG, Roher AE (2011) Alzheimer's disease and non-demented high pathology control nonagenarians: comparing and contrasting the biochemistry of cognitively successful aging. PloS one 6:e27291.
Maclullich AM, Ferguson KJ, Miller T, de Rooij SE, Cunningham C (2008) Unravelling the pathophysiology of delirium: a focus on the role of aberrant stress responses. Journal of psychosomatic research 65:229-238.
Maesako M, Uemura K, Kubota M, Kuzuya A, Sasaki K, Asada M, Watanabe K, Hayashida N, Ihara M, Ito H, Shimohama S, Kihara T, Kinoshita A (2012) Environmental enrichment ameliorated high-fat diet-induced Abeta deposition and memory deficit in APP transgenic mice. Neurobiology of aging 33:1011 e1011-1023.
Mallucci GR, White MD, Farmer M, Dickinson A, Khatun H, Powell AD, Brandner S, Jefferys JG, Collinge J (2007) Targeting cellular prion protein reverses early

cognitive deficits and neurophysiological dysfunction in prion-infected mice. Neuron 53:325-335.
Marchesi VT (2012) Alzheimer's disease 2012: the great amyloid gamble. The American journal of pathology 180:1762-1767.
Martin BK, Szekely C, Brandt J, Piantadosi S, Breitner JC, Craft S, Evans D, Green R, Mullan M (2008) Cognitive function over time in the Alzheimer's Disease Anti-inflammatory Prevention Trial (ADAPT): results of a randomized, controlled trial of naproxen and celecoxib. Archives of neurology 65:896-905.
Masters SL et al. (2010) Activation of the NLRP3 inflammasome by islet amyloid polypeptide provides a mechanism for enhanced IL-1beta in type 2 diabetes. Nature immunology 11:897-904.
Mathiesen T, Edner G, Ulfarsson E, Andersson B (1997) Cerebrospinal fluid interleukin-1 receptor antagonist and tumor necrosis factor-alpha following subarachnoid hemorrhage. Journal of neurosurgery 87:215-220.
McAfoose J, Koerner H, Baune BT (2009) The effects of TNF deficiency on age-related cognitive performance. Psychoneuroendocrinology 34:615-619.
McAlpine FE, Lee JK, Harms AS, Ruhn KA, Blurton-Jones M, Hong J, Das P, Golde TE, LaFerla FM, Oddo S, Blesch A, Tansey MG (2009) Inhibition of soluble TNF signaling in a mouse model of Alzheimer's disease prevents pre-plaque amyloid-associated neuropathology. Neurobiology of disease 34:163-177.
McColl BW, Rothwell NJ, Allan SM (2007) Systemic inflammatory stimulus potentiates the acute phase and CXC chemokine responses to experimental stroke and exacerbates brain damage via interleukin-1- and neutrophil-dependent mechanisms. The Journal of neuroscience : the official journal of the Society for Neuroscience 27:4403-4412.
McGeer EG, McGeer PL (2003) Inflammatory processes in Alzheimer's disease. Progress in neuro-psychopharmacology & biological psychiatry 27:741-749.
McGeer PL, McGeer EG (1995) The inflammatory response system of brain: implications for therapy of Alzheimer and other neurodegenerative diseases. Brain research Brain research reviews 21:195-218.
McGeer PL, McGeer E, Rogers J, Sibley J (1990) Anti-inflammatory drugs and Alzheimer disease. Lancet 335:1037.
McKhann GM, Knopman DS, Chertkow H, Hyman BT, Jack CR, Jr., Kawas CH, Klunk WE, Koroshetz WJ, Manly JJ, Mayeux R, Mohs RC, Morris JC, Rossor MN, Scheltens P, Carrillo MC, Thies B, Weintraub S, Phelps CH (2011) The diagnosis of dementia due to Alzheimer's disease: recommendations from the National Institute on Aging-Alzheimer's Association workgroups on diagnostic guidelines for Alzheimer's disease. Alzheimer's & dementia : the journal of the Alzheimer's Association 7:263-269.
McKimmie CS, Graham GJ (2010) Astrocytes modulate the chemokine network in a pathogen-specific manner. Biochemical and biophysical research communications 394:1006-1011.
McManus RM, Higgins SC, Mills KH, Lynch MA (2014) Respiratory infection promotes T cell infiltration and amyloid-beta deposition in APP/PS1 mice. Neurobiology of aging 35:109-121.
Medeiros R, Figueiredo CP, Pandolfo P, Duarte FS, Prediger RD, Passos GF, Calixto JB (2010) The role of TNF-alpha signaling pathway on COX-2 upregulation and cognitive decline induced by beta-amyloid peptide. Behavioural brain research 209:165-173.

Medeiros R, Prediger RD, Passos GF, Pandolfo P, Duarte FS, Franco JL, Dafre AL, Di Giunta G, Figueiredo CP, Takahashi RN, Campos MM, Calixto JB (2007) Connecting TNF-alpha signaling pathways to iNOS expression in a mouse model of Alzheimer's disease: relevance for the behavioral and synaptic deficits induced by amyloid beta protein. The Journal of neuroscience : the official journal of the Society for Neuroscience 27:5394-5404.

Medeiros RL, F. (2013) Astrocytes: Conductors of the Alzheimer disease neuroinflammatory symphony. Experimental neurology 239:133-138.

Meerschaert J, Furie MB (1995) The adhesion molecules used by monocytes for migration across endothelium include CD11a/CD18, CD11b/CD18, and VLA-4 on monocytes and ICAM-1, VCAM-1, and other ligands on endothelium. J Immunol 154:4099-4112.

Migheli A, Attanasio A, Pezzulo T, Gullotta F, Giordana MT, Schiffer D (1992) Age-related ubiquitin deposits in dystrophic neurites: an immunoelectron microscopic study. Neuropathol Appl Neurobiol 18:3-11.

Miller AA, Spencer SJ (2014) Obesity and neuroinflammation: A pathway to cognitive impairment. Brain, behavior, and immunity.

Milner E, Zhou ML, Johnson AW, Vellimana AK, Greenberg JK, Holtzman DM, Han BH, Zipfel GJ (2014) Cerebral amyloid angiopathy increases susceptibility to infarction after focal cerebral ischemia in Tg2576 mice. Stroke; a journal of cerebral circulation 45:3064-3069.

Montgomery SL, Bowers WJ (2012) Tumor necrosis factor-alpha and the roles it plays in homeostatic and degenerative processes within the central nervous system. Journal of neuroimmune pharmacology : the official journal of the Society on NeuroImmune Pharmacology 7:42-59.

Montgomery SL, Mastrangelo MA, Habib D, Narrow WC, Knowlden SA, Wright TW, Bowers WJ (2011) Ablation of TNF-RI/RII expression in Alzheimer's disease mice leads to an unexpected enhancement of pathology: implications for chronic pan-TNF-alpha suppressive therapeutic strategies in the brain. The American journal of pathology 179:2053-2070.

Moore AH, Olschowka JA, O'Banion MK (2004) Intraparenchymal administration of interleukin-1beta induces cyclooxygenase-2-mediated expression of membrane- and cytosolic-associated prostaglandin E synthases in mouse brain. Journal of neuroimmunology 148:32-40.

Moore AH, Wu M, Shaftel SS, Graham KA, O'Banion MK (2009) Sustained expression of interleukin-1beta in mouse hippocampus impairs spatial memory. Neuroscience 164:1484-1495.

Moreno M, Bannerman P, Ma J, Guo F, Miers L, Soulika AM, Pleasure D (2014) Conditional Ablation of Astroglial CCL2 Suppresses CNS Accumulation of M1 Macrophages and Preserves Axons in Mice with MOG Peptide EAE. The Journal of neuroscience : the official journal of the Society for Neuroscience 34:8175-8185.

Morganti JM, Jopson TD, Liu S, Riparip LK, Guandique CK, Gupta N, Ferguson AR, Rosi S (2015) CCR2 Antagonism Alters Brain Macrophage Polarization and Ameliorates Cognitive Dysfunction Induced by Traumatic Brain Injury. The Journal of neuroscience : the official journal of the Society for Neuroscience 35:748-760.

Morimoto K, Horio J, Satoh H, Sue L, Beach T, Arita S, Tooyama I, Konishi Y (2011) Expression profiles of cytokines in the brains of Alzheimer's disease (AD) patients compared to the brains of non-demented patients with and

without increasing AD pathology. Journal of Alzheimer's disease : JAD 25:59-76.
Morrison CD, Pistell PJ, Ingram DK, Johnson WD, Liu Y, Fernandez-Kim SO, White CL, Purpera MN, Uranga RM, Bruce-Keller AJ, Keller JN (2010) High fat diet increases hippocampal oxidative stress and cognitive impairment in aged mice: implications for decreased Nrf2 signaling. Journal of neurochemistry 114:1581-1589.
Moschetti K, Cummings PL, Sorvillo F, Kuo T (2012) Burden of Alzheimer's Disease-Related Mortality in the United States, 1999-2008. Journal of the American Geriatrics Society.
Murphy KM (2011) Janeway's Immunobiology 8th edition: Garland Science.
Murray C, Sanderson DJ, Barkus C, Deacon RM, Rawlins JN, Bannerman DM, Cunningham C (2010) Systemic inflammation induces acute working memory deficits in the primed brain: relevance for delirium. Neurobiology of aging.
Murray C, Sanderson DJ, Barkus C, Deacon RM, Rawlins JN, Bannerman DM, Cunningham C (2012) Systemic inflammation induces acute working memory deficits in the primed brain: relevance for delirium. Neurobiology of aging 33:603-616 e603.
Murray CL, Skelly DT, Cunningham C (2011) Exacerbation of CNS inflammation and neurodegeneration by systemic LPS treatment is independent of circulating IL-1beta and IL-6. Journal of neuroinflammation 8:50.
Nacci F, Matucci-Cerinic M (2011) Tuberculosis and other infections in the anti-tumour necrosis factor-alpha (anti-TNF-alpha) era. Best practice & research Clinical rheumatology 25:375-388.
Naert G, Rivest S (2011) CC chemokine receptor 2 deficiency aggravates cognitive impairments and amyloid pathology in a transgenic mouse model of Alzheimer's disease. The Journal of neuroscience : the official journal of the Society for Neuroscience 31:6208-6220.
Napoli C, Palinski W (2005) Neurodegenerative diseases: insights into pathogenic mechanisms from atherosclerosis. Neurobiology of aging 26:293-302.
Nashleanas M, Kanaly S, Scott P (1998) Control of Leishmania major infection in mice lacking TNF receptors. J Immunol 160:5506-5513.
Nelson TE, Hao C, Manos J, Ransohoff RM, Gruol DL (2011) Altered hippocampal synaptic transmission in transgenic mice with astrocyte-targeted enhanced CCL2 expression. Brain, behavior, and immunity 25 Suppl 1:S106-119.
Neumann H, Daly MJ (2013) Variant TREM2 as risk factor for Alzheimer's disease. N Engl J Med 368:182-184.
Nicoll JA, Mrak RE, Graham DI, Stewart J, Wilcock G, MacGowan S, Esiri MM, Murray LS, Dewar D, Love S, Moss T, Griffin WS (2000) Association of interleukin-1 gene polymorphisms with Alzheimer's disease. Annals of neurology 47:365-368.
Niedowicz DM, Reeves VL, Platt TL, Kohler K, Beckett TL, Powell DK, Lee TL, Sexton TR, Song ES, Brewer LD, Latimer CS, Kraner SD, Larson KL, Ozcan S, Norris CM, Hersh LB, Porter NM, Wilcock DM, Murphy MP (2014) Obesity and diabetes cause cognitive dysfunction in the absence of accelerated beta-amyloid deposition in a novel murine model of mixed or vascular dementia. Acta neuropathologica communications 2:64.
Niessner A, Steiner S, Speidl WS, Pleiner J, Seidinger D, Maurer G, Goronzy JJ, Weyand CM, Kopp CW, Huber K, Wolzt M, Wojta J (2006) Simvastatin

suppresses endotoxin-induced upregulation of toll-like receptors 4 and 2 in vivo. Atherosclerosis 189:408-413.
Nimmerjahn A, Kirchhoff F, Helmchen F (2005) Resting microglial cells are highly dynamic surveillants of brain parenchyma in vivo. Science 308:1314-1318.
Norton S, Matthews FE, Barnes DE, Yaffe K, Brayne C (2014) Potential for primary prevention of Alzheimer's disease: an analysis of population-based data. Lancet neurology 13:788-794.
O'Connor JJ, Coogan AN (1999) Actions of the pro-inflammatory cytokine IL-1 beta on central synaptic transmission. Experimental physiology 84:601-614.
Oh JW, Schwiebert LM, Benveniste EN (1999) Cytokine regulation of CC and CXC chemokine expression by human astrocytes. Journal of neurovirology 5:82-94.
Olleros ML, Vesin D, Fotio AL, Santiago-Raber ML, Tauzin S, Szymkowski DE, Garcia I (2010) Soluble TNF, but not membrane TNF, is critical in LPS-induced hepatitis. Journal of hepatology 53:1059-1068.
Olleros ML, Vesin D, Lambou AF, Janssens JP, Ryffel B, Rose S, Fremond C, Quesniaux VF, Szymkowski DE, Garcia I (2009) Dominant-negative tumor necrosis factor protects from Mycobacterium bovis Bacillus Calmette Guerin (BCG) and endotoxin-induced liver injury without compromising host immunity to BCG and Mycobacterium tuberculosis. The Journal of infectious diseases 199:1053-1063.
Onyszchuk G, He YY, Berman NE, Brooks WM (2008) Detrimental effects of aging on outcome from traumatic brain injury: a behavioral, magnetic resonance imaging, and histological study in mice. Journal of neurotrauma 25:153-171.
Ott A, Stolk RP, van Harskamp F, Pols HA, Hofman A, Breteler MM (1999) Diabetes mellitus and the risk of dementia: The Rotterdam Study. Neurology 53:1937-1942.
Pace JL, Russell SW, Torres BA, Johnson HM, Gray PW (1983) Recombinant mouse gamma interferon induces the priming step in macrophage activation for tumor cell killing. Journal of immunology 130:2011-2013.
Paganelli R, Di Iorio A, Patricelli L, Ripani F, Sparvieri E, Faricelli R, Iarlori C, Porreca E, Di Gioacchino M, Abate G (2002) Proinflammatory cytokines in sera of elderly patients with dementia: levels in vascular injury are higher than those of mild-moderate Alzheimer's disease patients. Experimental gerontology 37:257-263.
Palin K, Cunningham C, Forse P, Perry VH, Platt N (2008) Systemic inflammation switches the inflammatory cytokine profile in CNS Wallerian degeneration. Neurobiology of disease 30:19-29.
Palin K, Bluthe RM, Verrier D, Tridon V, Dantzer R, Lestage J (2004) Interleukin-1beta mediates the memory impairment associated with a delayed type hypersensitivity response to bacillus Calmette-Guerin in the rat hippocampus. Brain, behavior, and immunity 18:223-230.
Palin K, Bluthe RM, McCusker RH, Levade T, Moos F, Dantzer R, Kelley KW (2009) The type 1 TNF receptor and its associated adapter protein, FAN, are required for TNFalpha-induced sickness behavior. Psychopharmacology 201:549-556.
Pang Y, Zheng B, Campbell LR, Fan LW, Cai Z, Rhodes PG (2010) IGF-1 can either protect against or increase LPS-induced damage in the developing rat brain. Pediatric research 67:579-584.

Parajuli B, Sonobe Y, Horiuchi H, Takeuchi H, Mizuno T, Suzumura A (2013) Oligomeric amyloid beta induces IL-1beta processing via production of ROS: implication in Alzheimer's disease. Cell death & disease 4:e975.

Park SM, Shin JH, Moon GJ, Cho SI, Lee YB, Gwag BJ (2011) Effects of collagen-induced rheumatoid arthritis on amyloidosis and microvascular pathology in APP/PS1 mice. BMC Neurosci 12:106.

Parpura V, Zorec R (2010) Gliotransmission: Exocytotic release from astrocytes. Brain research reviews 63:83-92.

Patel JR, Brewer GJ (2008) Age-related differences in NFkappaB translocation and Bcl-2/Bax ratio caused by TNFalpha and Abeta42 promote survival in middle-age neurons and death in old neurons. Experimental neurology 213:93-100.

Perry VH (2010) Contribution of systemic inflammation to chronic neurodegeneration. Acta neuropathologica 120:277-286.

Pfeffer K, Matsuyama T, Kundig TM, Wakeham A, Kishihara K, Shahinian A, Wiegmann K, Ohashi PS, Kronke M, Mak TW (1993) Mice deficient for the 55 kd tumor necrosis factor receptor are resistant to endotoxic shock, yet succumb to L. monocytogenes infection. Cell 73:457-467.

Piguet PF, Vesin C, Guo J, Donati Y, Barazzone C (1998) TNF-induced enterocyte apoptosis in mice is mediated by the TNF receptor 1 and does not require p53. European journal of immunology 28:3499-3505.

Pineau I, Sun L, Bastien D, Lacroix S (2010) Astrocytes initiate inflammation in the injured mouse spinal cord by promoting the entry of neutrophils and inflammatory monocytes in an IL-1 receptor/MyD88-dependent fashion. Brain, behavior, and immunity 24:540-553.

Plata-Salaman CR, Oomura Y, Kai Y (1988) Tumor necrosis factor and interleukin-1 beta: suppression of food intake by direct action in the central nervous system. Brain research 448:106-114.

Porter MH, Arnold M, Langhans W (1998) TNF-alpha tolerance blocks LPS-induced hypophagia but LPS tolerance fails to prevent TNF-alpha-induced hypophagia. The American journal of physiology 274:R741-745.

Pott Godoy MC, Tarelli R, Ferrari CC, Sarchi MI, Pitossi FJ (2008) Central and systemic IL-1 exacerbates neurodegeneration and motor symptoms in a model of Parkinson's disease. Brain : a journal of neurology 131:1880-1894.

Probst A, Herzig MC, Mistl C, Ipsen S, Tolnay M (2001) Perisomatic granules (non-plaque dystrophic dendrites) of hippocampal CA1 neurons in Alzheimer's disease and Pick's disease: a lesion distinct from granulovacuolar degeneration. Acta Neuropathol 102:636-644.

Prokopowicz Z, Marcinkiewicz J, Katz DR, Chain BM (2012) Neutrophil myeloperoxidase: soldier and statesman. Archivum immunologiae et therapiae experimentalis 60:43-54.

Puntener U, Booth SG, Perry VH, Teeling JL (2012) Long-term impact of systemic bacterial infection on the cerebral vasculature and microglia. Journal of neuroinflammation 9:146.

Quagliarello VJ, Wispelwey B, Long WJ, Jr., Scheld WM (1991) Recombinant human interleukin-1 induces meningitis and blood-brain barrier injury in the rat. Characterization and comparison with tumor necrosis factor. The Journal of clinical investigation 87:1360-1366.

Quan N (2008) Immune-to-brain signaling: how important are the blood-brain barrier-independent pathways? Molecular neurobiology 37:142-152.

Quan N, Banks WA (2007) Brain-immune communication pathways. Brain, behavior, and immunity 21:727-735.

Ramos-Rodriguez JJ, Ortiz O, Jimenez-Palomares M, Kay KR, Berrocoso E, Murillo-Carretero MI, Perdomo G, Spires-Jones T, Cozar-Castellano I, Lechuga-Sancho AM, Garcia-Alloza M (2013) Differential central pathology and cognitive impairment in pre-diabetic and diabetic mice. Psychoneuroendocrinology 38:2462-2475.

Rauert H, Wicovsky A, Muller N, Siegmund D, Spindler V, Waschke J, Kneitz C, Wajant H (2010) Membrane tumor necrosis factor (TNF) induces p100 processing via TNF receptor-2 (TNFR2). The Journal of biological chemistry 285:7394-7404.

Ravizza T, Moneta D, Bottazzi B, Peri G, Garlanda C, Hirsch E, Richards GJ, Mantovani A, Vezzani A (2001) Dynamic induction of the long pentraxin PTX3 in the CNS after limbic seizures: evidence for a protective role in seizure-induced neurodegeneration. Neuroscience 105:43-53.

Reijerkerk A, Lakeman KA, Drexhage JA, van Het Hof B, van Wijck Y, van der Pol SM, Kooij G, Geerts D, de Vries HE (2012) Brain endothelial barrier passage by monocytes is controlled by the endothelin system. Journal of neurochemistry 121:730-737.

Reis R, Hennessy E, Murray C, Griffin EW, Cunningham C (2015) At the centre of neuronal, synaptic and axonal pathology in murine prion disease: degeneration of neuroanatomically linked thalamic and brainstem nuclei. Neuropathology and applied neurobiology.

Relton JK, Rothwell NJ (1992) Interleukin-1 receptor antagonist inhibits ischaemic and excitotoxic neuronal damage in the rat. Brain Res Bull 29:243-246.

Ribaux P, Ehses JA, Lin-Marq N, Carrozzino F, Boni-Schnetzler M, Hammar E, Irminger JC, Donath MY, Halban PA (2007) Induction of CXCL1 by extracellular matrix and autocrine enhancement by interleukin-1 in rat pancreatic beta-cells. Endocrinology 148:5582-5590.

Rich JB, Rasmusson DX, Folstein MF, Carson KA, Kawas C, Brandt J (1995) Nonsteroidal anti-inflammatory drugs in Alzheimer's disease. Neurology 45:51-55.

Richwine AF, Sparkman NL, Dilger RN, Buchanan JB, Johnson RW (2009) Cognitive deficits in interleukin-10-deficient mice after peripheral injection of lipopolysaccharide. Brain, behavior, and immunity 23:794-802.

Richwine AF, Parkin AO, Buchanan JB, Chen J, Markham JA, Juraska JM, Johnson RW (2008) Architectural changes to CA1 pyramidal neurons in adult and aged mice after peripheral immune stimulation. Psychoneuroendocrinology 33:1369-1377.

Roach DR, Bean AG, Demangel C, France MP, Briscoe H, Britton WJ (2002) TNF regulates chemokine induction essential for cell recruitment, granuloma formation, and clearance of mycobacterial infection. J Immunol 168:4620-4627.

Rodrigues Vilela V, de Castro Ruiz Marques A, Schamber CR, Bazotte RB (2014) Hypoglycemia induced by insulin as a triggering factor of cognitive deficit in diabetic children. TheScientificWorldJournal 2014:616534.

Sadowski M, Pankiewicz J, Scholtzova H, Ji Y, Quartermain D, Jensen CH, Duff K, Nixon RA, Gruen RJ, Wisniewski T (2004) Amyloid-beta deposition is associated with decreased hippocampal glucose metabolism and spatial memory impairment in APP/PS1 mice. Journal of neuropathology and experimental neurology 63:418-428.

Sairanen T, Carpen O, Karjalainen-Lindsberg ML, Paetau A, Turpeinen U, Kaste M, Lindsberg PJ (2001) Evolution of cerebral tumor necrosis factor-alpha production during human ischemic stroke. Stroke; a journal of cerebral circulation 32:1750-1758.

Salloway S et al. (2014) Two phase 3 trials of bapineuzumab in mild-to-moderate Alzheimer's disease. The New England journal of medicine 370:322-333.

Sandhir R, Onyszchuk G, Berman NE (2008) Exacerbated glial response in the aged mouse hippocampus following controlled cortical impact injury. Exp Neurol 213:372-380.

Sanz AB, Sanchez-Nino MD, Izquierdo MC, Gonzalez-Espinoza L, Ucero AC, Poveda J, Ruiz-Andres O, Ruiz-Ortega M, Selgas R, Egido J, Ortiz A (2014) Macrophages and recently identified forms of cell death. International reviews of immunology 33:9-22.

Satlin A, Volicer L, Stopa EG, Harper D (1995) Circadian locomotor activity and core-body temperature rhythms in Alzheimer's disease. Neurobiology of aging 16:765-771.

Schmitz C, Rutten BP, Pielen A, Schafer S, Wirths O, Tremp G, Czech C, Blanchard V, Multhaup G, Rezaie P, Korr H, Steinbusch HW, Pradier L, Bayer TA (2004) Hippocampal neuron loss exceeds amyloid plaque load in a transgenic mouse model of Alzheimer's disease. The American journal of pathology 164:1495-1502.

Schnell L, Fearn S, Schwab ME, Perry VH, Anthony DC (1999a) Cytokine-induced acute inflammation in the brain and spinal cord. Journal of neuropathology and experimental neurology 58:245-254.

Schnell L, Fearn S, Klassen H, Schwab ME, Perry VH (1999b) Acute inflammatory responses to mechanical lesions in the CNS: differences between brain and spinal cord. The European journal of neuroscience 11:3648-3658.

Schultz J, Schwarz A, Neidhold S, Burwinkel M, Riemer C, Simon D, Kopf M, Otto M, Baier M (2004) Role of interleukin-1 in prion disease-associated astrocyte activation. The American journal of pathology 165:671-678.

Scott JR, Davies D, Fraser H (1992) Scrapie in the central nervous system: neuroanatomical spread of infection and Sinc control of pathogenesis. J Gen Virol 73:1637-1644.

Seabrook TJ, Hay JB (2001) Intracerebroventricular infusions of TNF-alpha preferentially recruit blood lymphocytes and induce a perivascular leukocyte infiltrate. Journal of neuroimmunology 113:81-88.

Segev Y, Michaelson DM, Rosenblum K (2013) ApoE epsilon4 is associated with eIF2alpha phosphorylation and impaired learning in young mice. Neurobiology of aging 34:863-872.

Semple BD, Bye N, Ziebell JM, Morganti-Kossmann MC (2010a) Deficiency of the chemokine receptor CXCR2 attenuates neutrophil infiltration and cortical damage following closed head injury. Neurobiology of disease 40:394-403.

Semple BD, Bye N, Rancan M, Ziebell JM, Morganti-Kossmann MC (2010b) Role of CCL2 (MCP-1) in traumatic brain injury (TBI): evidence from severe TBI patients and CCL2-/- mice. Journal of cerebral blood flow and metabolism : official journal of the International Society of Cerebral Blood Flow and Metabolism 30:769-782.

Shaftel SS, Kyrkanides S, Olschowka JA, Miller JN, Johnson RE, O'Banion MK (2007) Sustained hippocampal IL-1 beta overexpression mediates chronic neuroinflammation and ameliorates Alzheimer plaque pathology. The Journal of clinical investigation 117:1595-1604.

Sheedy FJ, Grebe A, Rayner KJ, Kalantari P, Ramkhelawon B, Carpenter SB, Becker CE, Ediriweera HN, Mullick AE, Golenbock DT, Stuart LM, Latz E, Fitzgerald KA, Moore KJ (2013) CD36 coordinates NLRP3 inflammasome activation by facilitating intracellular nucleation of soluble ligands into particulate ligands in sterile inflammation. Nature immunology 14:812-820.

Sheehan JJ, Zhou C, Gravanis I, Rogove AD, Wu YP, Bogenhagen DF, Tsirka SE (2007) Proteolytic activation of monocyte chemoattractant protein-1 by plasmin underlies excitotoxic neurodegeneration in mice. The Journal of neuroscience : the official journal of the Society for Neuroscience 27:1738-1745.

Sheng JG, Bora SH, Xu G, Borchelt DR, Price DL, Koliatsos VE (2003) Lipopolysaccharide-induced-neuroinflammation increases intracellular accumulation of amyloid precursor protein and amyloid beta peptide in APPswe transgenic mice. Neurobiology of disease 14:133-145.

Shi JQ, Shen W, Chen J, Wang BR, Zhong LL, Zhu YW, Zhu HQ, Zhang QQ, Zhang YD, Xu J (2011) Anti-TNF-alpha reduces amyloid plaques and tau phosphorylation and induces CD11c-positive dendritic-like cell in the APP/PS1 transgenic mouse brains. Brain research 1368:239-247.

Shoelson SE, Lee J, Goldfine AB (2006) Inflammation and insulin resistance. The Journal of clinical investigation 116:1793-1801.

Shoham S, Davenne D, Cady AB, Dinarello CA, Krueger JM (1987) Recombinant tumor necrosis factor and interleukin 1 enhance slow-wave sleep. The American journal of physiology 253:R142-149.

Shultz SR, Bao F, Weaver LC, Cain DP, Brown A (2013) Treatment with an anti-CD11d integrin antibody reduces neuroinflammation and improves outcome in a rat model of repeated concussion. Journal of neuroinflammation 10:26.

Simi A, Tsakiri N, Wang P, Rothwell NJ (2007) Interleukin-1 and inflammatory neurodegeneration. Biochemical Society transactions 35:1122-1126.

Singh AK, Jiang Y (2004) How does peripheral lipopolysaccharide induce gene expression in the brain of rats? Toxicology 201:197-207.

Singh AK, Jiang Y, Gupta S (2007) Effects of bacterial toxins on endothelial tight junction in vitro: a mechanism-based investigation. Toxicology mechanisms and methods 17:331-347.

Singh N, Hopkins SJ, Hulme S, Galea JP, Hoadley M, Vail A, Hutchinson PJ, Grainger S, Rothwell NJ, King AT, Tyrrell PJ (2014) The effect of intravenous interleukin-1 receptor antagonist on inflammatory mediators in cerebrospinal fluid after subarachnoid haemorrhage: a phase II randomised controlled trial. Journal of neuroinflammation 11:1.

Siskova Z, Reynolds RA, O'Connor V, Perry VH (2013) Brain region specific pre-synaptic and post-synaptic degeneration are early components of neuropathology in prion disease. PLoS One 8:e55004.

Sjogren M, Folkesson S, Blennow K, Tarkowski E (2004) Increased intrathecal inflammatory activity in frontotemporal dementia: pathophysiological implications. Journal of neurology, neurosurgery, and psychiatry 75:1107-1111.

Skelly DT, Hennessy E, Dansereau MA, Cunningham C (2013a) A systematic analysis of the peripheral and CNS effects of systemic LPS, IL-1Beta, TNF-alpha and IL-6 challenges in C57BL/6 mice. PloS one 8:e69123.

Skelly DT, Hennessy E, Dansereau MA, Cunningham C (2013b) A systematic analysis of the peripheral and CNS effects of systemic LPS, IL-1beta,

[corrected] TNF-alpha and IL-6 challenges in C57BL/6 mice. PloS one 8:e69123.

Sly LM, Krzesicki RF, Brashler JR, Buhl AE, McKinley DD, Carter DB, Chin JE (2001) Endogenous brain cytokine mRNA and inflammatory responses to lipopolysaccharide are elevated in the Tg2576 transgenic mouse model of Alzheimer's disease. Brain research bulletin 56:581-588.

Song Y, Nie H, Xu Y, Zhang L, Wu Y (2013) Association of statin use with risk of dementia: a meta-analysis of prospective cohort studies. Geriatr Gerontol Int 13:817-824.

Sonti G, Flynn MC, Plata-Salaman CR (1997) Interleukin-1 (IL-1) receptor type I mediates anorexia but not adipsia induced by centrally administered IL-1beta. Physiology & behavior 62:1179-1183.

Souza DG, Vieira AT, Pinho V, Sousa LP, Andrade AA, Bonjardim CA, McMillan M, Kahn M, Teixeira MM (2005) NF-kappaB plays a major role during the systemic and local acute inflammatory response following intestinal reperfusion injury. British journal of pharmacology 145:246-254.

Spadaro F, Dunn AJ (1990) Intracerebroventricular administration of interleukin-1 to mice alters investigation of stimuli in a novel environment. Brain, behavior, and immunity 4:308-322.

Stamatovic SM, Dimitrijevic OB, Keep RF, Andjelkovic AV (2006) Protein kinase Calpha-RhoA cross-talk in CCL2-induced alterations in brain endothelial permeability. The Journal of biological chemistry 281:8379-8388.

Stamatovic SM, Shakui P, Keep RF, Moore BB, Kunkel SL, Van Rooijen N, Andjelkovic AV (2005) Monocyte chemoattractant protein-1 regulation of blood-brain barrier permeability. Journal of cerebral blood flow and metabolism : official journal of the International Society of Cerebral Blood Flow and Metabolism 25:593-606.

Steed PM et al. (2003) Inactivation of TNF signaling by rationally designed dominant-negative TNF variants. Science 301:1895-1898.

Stefanova N, Georgievska B, Eriksson H, Poewe W, Wenning GK (2012) Myeloperoxidase inhibition ameliorates multiple system atrophy-like degeneration in a transgenic mouse model. Neurotoxicity research 21:393-404.

Stein TD, Johnson JA (2002) Lack of neurodegeneration in transgenic mice overexpressing mutant amyloid precursor protein is associated with increased levels of transthyretin and the activation of cell survival pathways. The Journal of neuroscience : the official journal of the Society for Neuroscience 22:7380-7388.

Stellwagen D, Malenka RC (2006) Synaptic scaling mediated by glial TNF-alpha. Nature 440:1054-1059.

Stowe AM, Adair-Kirk TL, Gonzales ER, Perez RS, Shah AR, Park TS, Gidday JM (2009) Neutrophil elastase and neurovascular injury following focal stroke and reperfusion. Neurobiology of disease 35:82-90.

Stranahan AM, Arumugam TV, Cutler RG, Lee K, Egan JM, Mattson MP (2008) Diabetes impairs hippocampal function through glucocorticoid-mediated effects on new and mature neurons. Nature neuroscience 11:309-317.

Sugiyama S, Okada Y, Sukhova GK, Virmani R, Heinecke JW, Libby P (2001) Macrophage myeloperoxidase regulation by granulocyte macrophage colony-stimulating factor in human atherosclerosis and implications in acute coronary syndromes. The American journal of pathology 158:879-891.

Sugiyama S, Kugiyama K, Aikawa M, Nakamura S, Ogawa H, Libby P (2004) Hypochlorous acid, a macrophage product, induces endothelial apoptosis and tissue factor expression: involvement of myeloperoxidase-mediated oxidant in plaque erosion and thrombogenesis. Arteriosclerosis, thrombosis, and vascular biology 24:1309-1314.

Sumagin R, Prizant H, Lomakina E, Waugh RE, Sarelius IH (2010) LFA-1 and Mac-1 define characteristically different intralumenal crawling and emigration patterns for monocytes and neutrophils in situ. J Immunol 185:7057-7066.

Swaroop JJ, Rajarajeswari D, Naidu JN (2012) Association of TNF-alpha with insulin resistance in type 2 diabetes mellitus. The Indian journal of medical research 135:127-130.

Swiergiel AH, Dunn AJ (1999) The roles of IL-1, IL-6, and TNFalpha in the feeding responses to endotoxin and influenza virus infection in mice. Brain, behavior, and immunity 13:252-265.

Sy M, Kitazawa M, Medeiros R, Whitman L, Cheng D, Lane TE, Laferla FM (2011) Inflammation induced by infection potentiates tau pathological features in transgenic mice. The American journal of pathology 178:2811-2822.

Takeda S, Sato N, Ikimura K, Nishino H, Rakugi H, Morishita R (2013) Increased blood-brain barrier vulnerability to systemic inflammation in an Alzheimer disease mouse model. Neurobiology of aging 34:2064-2070.

Takeda S, Sato N, Uchio-Yamada K, Sawada K, Kunieda T, Takeuchi D, Kurinami H, Shinohara M, Rakugi H, Morishita R (2010) Diabetes-accelerated memory dysfunction via cerebrovascular inflammation and Abeta deposition in an Alzheimer mouse model with diabetes. Proceedings of the National Academy of Sciences of the United States of America 107:7036-7041.

Tan ZS, Beiser AS, Vasan RS, Roubenoff R, Dinarello CA, Harris TB, Benjamin EJ, Au R, Kiel DP, Wolf PA, Seshadri S (2007) Inflammatory markers and the risk of Alzheimer disease: the Framingham Study. Neurology 68:1902-1908.

Tarkowski E, Blennow K, Wallin A, Tarkowski A (1999) Intracerebral production of tumor necrosis factor-alpha, a local neuroprotective agent, in Alzheimer disease and vascular dementia. Journal of clinical immunology 19:223-230.

Tarkowski E, Andreasen N, Tarkowski A, Blennow K (2003) Intrathecal inflammation precedes development of Alzheimer's disease. Journal of neurology, neurosurgery, and psychiatry 74:1200-1205.

Tehranian R, Andell-Jonsson S, Beni SM, Yatsiv I, Shohami E, Bartfai T, Lundkvist J, Iverfeldt K (2002) Improved recovery and delayed cytokine induction after closed head injury in mice with central overexpression of the secreted isoform of the interleukin-1 receptor antagonist. Journal of neurotrauma 19:939-951.

ten Hagen TL, Seynhaeve AL, van Tiel ST, Ruiter DJ, Eggermont AM (2002) Pegylated liposomal tumor necrosis factor-alpha results in reduced toxicity and synergistic antitumor activity after systemic administration in combination with liposomal doxorubicin (Doxil) in soft tissue sarcoma-bearing rats. International journal of cancer Journal international du cancer 97:115-120.

Terrando N, Monaco C, Ma D, Foxwell BM, Feldmann M, Maze M (2010) Tumor necrosis factor-alpha triggers a cytokine cascade yielding postoperative cognitive decline. Proceedings of the National Academy of Sciences of the United States of America 107:20518-20522.

Thaler JP, Yi CX, Schur EA, Guyenet SJ, Hwang BH, Dietrich MO, Zhao X, Sarruf DA, Izgur V, Maravilla KR, Nguyen HT, Fischer JD, Matsen ME, Wisse BE, Morton

GJ, Horvath TL, Baskin DG, Tschop MH, Schwartz MW (2012) Obesity is associated with hypothalamic injury in rodents and humans. The Journal of clinical investigation 122:153-162.

Thies W, Bleiler L (2011) 2011 Alzheimer's disease facts and figures. Alzheimer's & dementia : the journal of the Alzheimer's Association 7:208-244.

Thompson WL, Van Eldik LJ (2009) Inflammatory cytokines stimulate the chemokines CCL2/MCP-1 and CCL7/MCP-3 through NFkB and MAPK dependent pathways in rat astrocytes [corrected]. Brain research 1287:47-57.

Thornton P, McColl BW, Greenhalgh A, Denes A, Allan SM, Rothwell NJ (2010) Platelet interleukin-1alpha drives cerebrovascular inflammation. Blood 115:3632-3639.

Tibolla G, Norata GD, Meda C, Arnaboldi L, Uboldi P, Piazza F, Ferrarese C, Corsini A, Maggi A, Vegeto E, Catapano AL (2010) Increased atherosclerosis and vascular inflammation in APP transgenic mice with apolipoprotein E deficiency. Atherosclerosis 210:78-87.

Tobinick E, Kim NM, Reyzin G, Rodriguez-Romanacce H, DePuy V (2012) Selective TNF inhibition for chronic stroke and traumatic brain injury: an observational study involving 629 consecutive patients treated with perispinal etanercept. CNS drugs 26:1051-1070.

Touitou Y, Reinberg A, Bogdan A, Auzeby A, Beck H, Touitou C (1986) Age-related changes in both circadian and seasonal rhythms of rectal temperature with special reference to senile dementia of Alzheimer type. Gerontology 32:110-118.

Toulmond S, Rothwell NJ (1995) Interleukin-1 receptor antagonist inhibits neuronal damage caused by fluid percussion injury in the rat. Brain research 671:261-266.

Towfighi A, Skolasky RL, St Hillaire C, Conant K, McArthur JC (2004) CSF soluble Fas correlates with the severity of HIV-associated dementia. Neurology 62:654-656.

Toyooka T, Nawashiro H, Shinomiya N, Shima K (2011) Down-regulation of glial fibrillary acidic protein and vimentin by RNA interference improves acute urinary dysfunction associated with spinal cord injury in rats. Journal of neurotrauma 28:607-618.

Tucsek Z, Toth P, Sosnowska D, Gautam T, Mitschelen M, Koller A, Szalai G, Sonntag WE, Ungvari Z, Csiszar A (2013) Obesity in Aging Exacerbates Blood-Brain Barrier Disruption, Neuroinflammation, and Oxidative Stress in the Mouse Hippocampus: Effects on Expression of Genes Involved in Beta-Amyloid Generation and Alzheimer's Disease. The journals of gerontology Series A, Biological sciences and medical sciences.

Tucsek Z, Toth P, Tarantini S, Sosnowska D, Gautam T, Warrington JP, Giles CB, Wren JD, Koller A, Ballabh P, Sonntag WE, Ungvari Z, Csiszar A (2014) Aging Exacerbates Obesity-induced Cerebromicrovascular Rarefaction, Neurovascular Uncoupling, and Cognitive Decline in Mice. The journals of gerontology Series A, Biological sciences and medical sciences.

van Neerven S, Regen T, Wolf D, Nemes A, Johann S, Beyer C, Hanisch UK, Mey J (2010) Inflammatory chemokine release of astrocytes in vitro is reduced by all-trans retinoic acid. Journal of neurochemistry 114:1511-1526.

Varfolomeev EE, Ashkenazi A (2004) Tumor necrosis factor: an apoptosis JuNKie? Cell 116:491-497.

Verret L, Jankowsky JL, Xu GM, Borchelt DR, Rampon C (2007) Alzheimer's-type amyloidosis in transgenic mice impairs survival of newborn neurons derived from adult hippocampal neurogenesis. The Journal of neuroscience : the official journal of the Society for Neuroscience 27:6771-6780.

Veryard L, Jones E, Weaving G, Smith E, Cheek L, Wickramasinghe A, Tabet N (2013) Pro-inflammatory cytokines IL-1beta and TNF-alpha are not associated with plasma homocysteine concentration in Alzheimer's disease. Current Alzheimer research 10:174-179.

Vezzani A, Moneta D, Conti M, Richichi C, Ravizza T, De Luigi A, De Simoni MG, Sperk G, Andell-Jonsson S, Lundkvist J, Iverfeldt K, Bartfai T (2000) Powerful anticonvulsant action of IL-1 receptor antagonist on intracerebral injection and astrocytic overexpression in mice. Proceedings of the National Academy of Sciences of the United States of America 97:11534-11539.

Vigano M, Degasperi E, Aghemo A, Lampertico P, Colombo M (2012) Anti-TNF drugs in patients with hepatitis B or C virus infection: safety and clinical management. Expert opinion on biological therapy 12:193-207.

Villeda SA et al. (2011) The ageing systemic milieu negatively regulates neurogenesis and cognitive function. Nature 477:90-94.

Wallin K, Solomon A, Kareholt I, Tuomilehto J, Soininen H, Kivipelto M (2012) Midlife Rheumatoid Arthritis Increases the Risk of Cognitive Impairment Two Decades Later: A Population-Based Study. Journal of Alzheimer's disease : JAD.

Wallis RS, Broder MS, Wong JY, Hanson ME, Beenhouwer DO (2004) Granulomatous infectious diseases associated with tumor necrosis factor antagonists. Clinical infectious diseases : an official publication of the Infectious Diseases Society of America 38:1261-1265.

Wang GR, Shi S, Gao C, Zhang BY, Tian C, Dong CF, Zhou RM, Li XL, Chen C, Han J, Dong XP (2010) Changes of tau profiles in brains of the hamsters infected with scrapie strains 263 K or 139 A possibly associated with the alteration of phosphate kinases. BMC infectious diseases 10:86.

Wang J, Ando T, Dunn AJ (1997) Effect of homologous interleukin-1, interleukin-6 and tumor necrosis factor-alpha on the core body temperature of mice. Neuroimmunomodulation 4:230-236.

Wang S, Voisin MB, Larbi KY, Dangerfield J, Scheiermann C, Tran M, Maxwell PH, Sorokin L, Nourshargh S (2006a) Venular basement membranes contain specific matrix protein low expression regions that act as exit points for emigrating neutrophils. The Journal of experimental medicine 203:1519-1532.

Wang Y, Luo W, Reiser G (2007) The role of calcium in protease-activated receptor-induced secretion of chemokine GRO/CINC-1 in rat brain astrocytes. Journal of neurochemistry 103:814-819.

Wang Y, Luo W, Stricker R, Reiser G (2006b) Protease-activated receptor-1 protects rat astrocytes from apoptotic cell death via JNK-mediated release of the chemokine GRO/CINC-1. Journal of neurochemistry 98:1046-1060.

Warren EJ, Finck BN, Arkins S, Kelley KW, Scamurra RW, Murtaugh MP, Johnson RW (1997) Coincidental changes in behavior and plasma cortisol in unrestrained pigs after intracerebroventricular injection of tumor necrosis factor-alpha. Endocrinology 138:2365-2371.

Weaver KD, Branch CA, Hernandez L, Miller CH, Quattrocchi KB (2000) Effect of leukocyte-endothelial adhesion antagonism on neutrophil migration and

neurologic outcome after cortical trauma. The Journal of trauma 48:1081-1090.

Webster SJ, Van Eldik LJ, Watterson DM, Bachstetter AD (2015) Closed head injury in an age-related Alzheimer mouse model leads to an altered neuroinflammatory response and persistent cognitive impairment. The Journal of neuroscience : the official journal of the Society for Neuroscience 35:6554-6569.

Wharton SB, Brayne C, Savva GM, Matthews FE, Forster G, Simpson J, Lace G, Ince PG (2011) Epidemiological neuropathology: the MRC Cognitive Function and Aging Study experience. Journal of Alzheimer's disease : JAD 25:359-372.

White H, Pieper C, Schmader K (1998) The association of weight change in Alzheimer's disease with severity of disease and mortality: a longitudinal analysis. Journal of the American Geriatrics Society 46:1223-1227.

Whitmer RA, Sidney S, Selby J, Johnston SC, Yaffe K (2005) Midlife cardiovascular risk factors and risk of dementia in late life. Neurology 64:277-281.

Williams JG, Jurkovich GJ, Hahnel GB, Maier RV (1992) Macrophage priming by interferon gamma: a selective process with potentially harmful effects. Journal of leukocyte biology 52:579-584.

Wirths O, Bayer TA (2010) Neuron loss in transgenic mouse models of Alzheimer's disease. International journal of Alzheimer's disease 2010.

Witlox J, Eurelings LS, de Jonghe JF, Kalisvaart KJ, Eikelenboom P, van Gool WA (2010) Delirium in elderly patients and the risk of postdischarge mortality, institutionalization, and dementia: a meta-analysis. JAMA : the journal of the American Medical Association 304:443-451.

Wlodarczyk A, Lobner M, Cedile O, Owens T (2014) Comparison of microglia and infiltrating CD11c(+) cells as antigen presenting cells for T cell proliferation and cytokine response. Journal of neuroinflammation 11:57.

Wong A, Luth HJ, Deuther-Conrad W, Dukic-Stefanovic S, Gasic-Milenkovic J, Arendt T, Munch G (2001) Advanced glycation endproducts co-localize with inducible nitric oxide synthase in Alzheimer's disease. Brain research 920:32-40.

Wu H, Lozano G (1994) NF-kappa B activation of p53. A potential mechanism for suppressing cell growth in response to stress. The Journal of biological chemistry 269:20067-20074.

Wyss-Coray T, Mucke L (2002) Inflammation in neurodegenerative disease--a double-edged sword. Neuron 35:419-432.

Yaffe K, Kanaya A, Lindquist K, Simonsick EM, Harris T, Shorr RI, Tylavsky FA, Newman AB (2004) The metabolic syndrome, inflammation, and risk of cognitive decline. JAMA : the journal of the American Medical Association 292:2237-2242.

Yamasaki Y, Matsuura N, Shozuhara H, Onodera H, Itoyama Y, Kogure K (1995) Interleukin-1 as a pathogenetic mediator of ischemic brain damage in rats. Stroke; a journal of cerebral circulation 26:676-680; discussion 681.

Yang GY, Liu XH, Kadoya C, Zhao YJ, Mao Y, Davidson BL, Betz AL (1998) Attenuation of ischemic inflammatory response in mouse brain using an adenoviral vector to induce overexpression of interleukin-1 receptor antagonist. Journal of cerebral blood flow and metabolism : official journal of the International Society of Cerebral Blood Flow and Metabolism 18:840-847.

Yao Y, Tsirka SE (2011) Truncation of monocyte chemoattractant protein 1 by plasmin promotes blood-brain barrier disruption. Journal of cell science 124:1486-1495.

Yin XM (2000) Bid, a critical mediator for apoptosis induced by the activation of Fas/TNF-R1 death receptors in hepatocytes. J Mol Med (Berl) 78:203-211.

Yona S, Kim KW, Wolf Y, Mildner A, Varol D, Breker M, Strauss-Ayali D, Viukov S, Guilliams M, Misharin A, Hume DA, Perlman H, Malissen B, Zelzer E, Jung S (2013) Fate mapping reveals origins and dynamics of monocytes and tissue macrophages under homeostasis. Immunity 38:79-91.

Yoshida S, Yoshizumi T, Kamei H, Ozaki K, Yahara T, Tajiri T, Yamasaki K, Shirouzu K (1999) Effect of intracerebroventricular injection of tumor necrosis factor alpha on gut mucosal protein turnover in mice fed enterally. The Journal of surgical research 87:73-76.

You C, Zhu K, Liu X, Xi C, Zhang Z, Xu G, Yan J (2013) Tumor necrosis factor-alpha-dependent infiltration of macrophages into the dorsal root ganglion in a rat disc herniation model. Spine 38:2003-2007.

Youm YH, Grant RW, McCabe LR, Albarado DC, Nguyen KY, Ravussin A, Pistell P, Newman S, Carter R, Laque A, Munzberg H, Rosen CJ, Ingram DK, Salbaum JM, Dixit VD (2013) Canonical Nlrp3 inflammasome links systemic low-grade inflammation to functional decline in aging. Cell metabolism 18:519-532.

Youmans KL, Tai LM, Kanekiyo T, Stine WB, Jr., Michon SC, Nwabuisi-Heath E, Manelli AM, Fu Y, Riordan S, Eimer WA, Binder L, Bu G, Yu C, Hartley DM, LaDu MJ (2012) Intraneuronal Abeta detection in 5xFAD mice by a new Abeta-specific antibody. Molecular neurodegeneration 7:8.

Yu N, Zhang X, Magistretti PJ, Bloom FE (1998) IL-1-alpha and TNF-alpha differentially regulate CD4 and Mac-1 expression in mouse microglia. Neuroimmunomodulation 5:42-52.

Yu Y, He J, Zhang Y, Luo H, Zhu S, Yang Y, Zhao T, Wu J, Huang Y, Kong J, Tan Q, Li XM (2009) Increased hippocampal neurogenesis in the progressive stage of Alzheimer's disease phenotype in an APP/PS1 double transgenic mouse model. Hippocampus 19:1247-1253.

Zalevsky J, Secher T, Ezhevsky SA, Janot L, Steed PM, O'Brien C, Eivazi A, Kung J, Nguyen DH, Doberstein SK, Erard F, Ryffel B, Szymkowski DE (2007) Dominant-negative inhibitors of soluble TNF attenuate experimental arthritis without suppressing innate immunity to infection. J Immunol 179:1872-1883.

Zamanian JL, Xu L, Foo LC, Nouri N, Zhou L, Giffard RG, Barres BA (2012) Genomic analysis of reactive astrogliosis. The Journal of neuroscience : the official journal of the Society for Neuroscience 32:6391-6410.

Zera T, Ufnal M, Szczepanska-Sadowska E (2008) Central TNF-alpha elevates blood pressure and sensitizes to central pressor action of angiotensin II in the infarcted rats. Journal of physiology and pharmacology : an official journal of the Polish Physiological Society 59 Suppl 8:117-121.

Zhang G, Li J, Purkayastha S, Tang Y, Zhang H, Yin Y, Li B, Liu G, Cai D (2013a) Hypothalamic programming of systemic ageing involving IKK-beta, NF-kappaB and GnRH. Nature 497:211-216.

Zhang X, Bo X, Anderson PN, Lieberman AR, Zhang Y (2006) Distribution and expression of tissue inhibitors of metalloproteinase in dorsal root entry zone and dorsal column after dorsal root injury. Journal of neuroscience research 84:278-290.

Zhang XW, Liu Q, Wang Y, Thorlacius H (2001) CXC chemokines, MIP-2 and KC, induce P-selectin-dependent neutrophil rolling and extravascular migration in vivo. British journal of pharmacology 133:413-421.

Zhang YW, Thompson R, Zhang H, Xu H (2011) APP processing in Alzheimer's disease. Molecular brain 4:3.

Zhang ZJ, Cao DL, Zhang X, Ji RR, Gao YJ (2013b) Chemokine contribution to neuropathic pain: respective induction of CXCL1 and CXCR2 in spinal cord astrocytes and neurons. Pain.

Zhao B, Schwartz JP (1998) Involvement of cytokines in normal CNS development and neurological diseases: recent progress and perspectives. Journal of neuroscience research 52:7-16.

Zilka N, Kazmerova Z, Jadhav S, Neradil P, Madari A, Obetkova D, Bugos O, Novak M (2012) Who fans the flames of Alzheimer's disease brains? Misfolded tau on the crossroad of neurodegenerative and inflammatory pathways. Journal of neuroinflammation 9:47.

Zou CJ, Liu JD, Zhou YC (2001) Roles of central interleukin-1 on stress-induced-hypertension and footshock-induced-analgesia in rats. Neuroscience letters 311:41-44.

Zuliani G, Ranzini M, Guerra G, Rossi L, Munari MR, Zurlo A, Volpato S, Atti AR, Ble A, Fellin R (2007) Plasma cytokines profile in older subjects with late onset Alzheimer's disease or vascular dementia. Journal of psychiatric research 41:686-693.